2016

# Quantitative Oil Source-Fingerprinting Techniques and Their Application to Differentiating Crude Oil in Coastal Marsh Sediments

Buffy Marie Meyer
*Louisiana State University and Agricultural and Mechanical College*

# QUANTITATIVE OIL SOURCE-FINGERPRINTING TECHNIQUES AND THEIR APPLICATION TO DIFFERENTIATING CRUDE OIL IN COASTAL MARSH SEDIMENTS

A Dissertation

Submitted to the Graduate Faculty of the
Louisiana State University and
Agricultural and Mechanical College
in partial fulfillment of the
requirements for the degree of
Doctor of Philosophy

in

The Department of Environmental Sciences

by
Buffy Marie Meyer
B.S., Troy University, 1996
M.S., Louisiana State University, 2000
May 2016

## ACKNOWLEDGMENTS

The feat of completing a Ph.D. is not accomplished without the support and guidance of some amazing people. A huge thank you to my committee: Drs. Vince Wilson, Ed Overton, Gene Turner, Bin Li, and Louis Thibodeaux. I really couldn't have asked for a more stellar committee. You all have such an incredible knowledge base, and I am forever appreciative of your guidance and support. Thank you Ms. Charlotte St. Romain for getting me started and helping me stick with it. There were many times that I questioned what I was doing, but you always got me back on track. My gratitude is extended to my lab family: Drs. Scott Miles, Greg Olson, and Robert Wong, and Ms. Megan Calvit and Ms. Erin Saal. Thank you for all you do and giving me the support I've needed to finish over the last several months. I am so fortunate to have such great people to learn from and work with. I also greatly appreciate the patience and guidance of Brian Rohrback and Scott Ramos of Infometrix, Inc. I would also like to thank all the awesome scientists at NOAA-ERD and USGS-NWRC that I have had the opportunity to collaborate with throughout my Ph.D. and career.

I owe much of my success to a great network of friends and family who have made this experience tolerable. But above all, I'm indebted to my mom and Dad, and to Erik and Adalie. Thank you all for keeping me focused on what is important in life. This great accomplishment is also yours. I hope that I will be an inspiration to you, Adalie, in the future. Many, many thanks to my neighbor, Karen. I cannot express how appreciated you are by me, Erik, Adalie, and Pixie.

This research was supported by grants from the Gulf of Mexico Research Initiative, the USGS-National Wetland Research Center, and NOAA-ERD.

## TABLE OF CONTENTS

ACKNOWLEDGMENTS ..... ii

LIST OF TABLES ..... v

LIST OF FIGURES ..... vi

ABSTRACT ..... x

CHAPTER 1: GENERAL INTRODUCTION ..... 1
- 1.1 Background ..... 1
- 1.2 Research Objective ..... 5
- 1.3 Rationale and Approach ..... 6
  - 1.3.1 Quantitative Oil Source-Fingerprinting Using Diagnostic Biomarker Ratio Analysis (Chapter 2) ..... 7
  - 1.3.2 Oil Source-Fingerprinting in Support of Polarimetric Radar Mapping of MC252 Oil (Chapter 3) ..... 8
  - 1.3.3 Advanced Quantitative Oil Source-Fingerprinting of Louisiana Coastal Marsh Sediments Collected from 2010-2015 (Chapter 4) ..... 9
- 1.4 Literature Cited ..... 10

CHAPTER 2: QUANTITATIVE OIL SOURCE-FINGERPRINTING USING DIAGNOSTIC BIOMARKER RATIO ANALYSIS ..... 12
- 2.1 Introduction ..... 12
- 2.2 Experimental Approach ..... 13
  - 2.2.1 Source Oil Preparation for GC/MS Analysis ..... 13
  - 2.2.2 GC/MS Instrumentation ..... 14
  - 2.2.3 MC252 Diagnostic Biomarker Ratio Calculations ..... 16
  - 2.2.4 Diagnostic Biomarker Ratios for South Louisiana Crude Oils ..... 21
- 2.3 Results and Discussion ..... 22
  - 2.3.1 MC252 Diagnostic Biomarker Ratios ..... 22
  - 2.3.2 Diagnostic Ratios of South Louisiana Crude Oils ..... 24
- 2.4 Conclusions ..... 27
- 2.5 Literature Cited ..... 29

CHAPTER 3: OIL SOURCE-FINGERPRINTING IN SUPPORT OF POLARIMETRIC RADAR MAPPING OF MC252 OIL ..... 32
- 3.1 Introduction ..... 32
- 3.2 Experimental Approach ..... 35
  - 3.2.1 UAVSAR PolSAR ..... 35
  - 3.2.2 Sediment Sample Collection ..... 35
  - 3.2.3 Sample Analysis ..... 36
  - 3.2.4 Oil Source-Fingerprinting Using Diagnostic Biomarker Ratio Analysis ..... 38

3.3 Results and Discussion ....41
3.3.1 UAVSAR ....41
3.3.2 Oil Source-Fingerprinting Using Diagnostic Biomarker Ratio Analysis ....43
3.4 Conclusions ....46
3.5 Literature Cited ....47

CHAPTER 4: ADVANCED QUANTITATIVE OIL SOURCE-FINGERPRINTING OF LOUISIANA COASTAL MARSH SEDIMENTS COLLECTED FROM 2010-2015 ....50
4.1 Introduction ....50
4.2 Experimental Approach ....52
4.2.1 Sediment Sample Collection and Analysis ....52
4.2.2 Diagnostic Biomarker Ratio Analysis ....54
4.2.3 Chemometric Analysis of South Louisiana Crude Oils ....58
4.2.4 Chemometric Analysis of Coastal Marsh Sediments ....62
4.2.5 Chemometric Differentiation of Biomarker Weathering Patterns ....62
4.3 Results and Discussion ....63
4.3.1 Diagnostic Biomarker Ratio Analysis ....63
4.3.2 Chemometric Analysis of South Louisiana Crude Oils ....66
4.3.3 Chemometric Analysis of Coastal Marsh Sediments ....72
4.3.4 Chemometric Differentiation of Biomarker Weathering Patterns ....107
4.4 Conclusions ....110
4.5 Literature Cited ....112

CHAPTER 5: OVERALL CONCLUSIONS ....116

APPENDICES ....119
A: Permission Request to Reprint ....119
B: Chromatographic Profiles of Quadruplicate Analyses of Source Oils ....120
C: Extracted Biomarker Chromatographic Profiles of Source Oils ....138
D: Permission Request to Reprint ....147
E: Cluster Details for Coastal Marsh Sediments ....148
F: *m/z* 217 Cluster Details ....156

VITA ....181

## LIST OF TABLES

Table 2.1 Petroleum Biomarkers Used For Calculating MC252 Diagnostic Ratios .....18

Table 2.2 Average Diagnostic Ratios for MC252 Source Oil .....23

Table 2.3 Average Diagnostic Ratios for South Louisiana Crude Oils .....25

Table 3.1 Targeted Petroleum Hydrocarbon Analytes .....37

Table 3.2 Petroleum Biomarkers Used For Calculating MC252 Diagnostic Ratios .....39

Table 3.3 Average Diagnostic Ratios for MC252 Source Oil .....40

Table 3.4 Oil Source-Fingerprinting Results .....45

Table 4.1 Distribution of Coastal Marsh Sediments After Qualitative Sort .....55

Table 4.2 Diasteranes and Regular Steranes, and 14β(H)-steranes Used to Calculate New Diagnostic Biomarker Ratios .....57

Table 4.3 Average of New MC252 Diasteranes and Regular Steranes, and 14β(H)-steranes Diagnostic Biomarker Ratios .....58

## LIST OF FIGURES

Figure 1.1 Chemical structures of common oil biomarker families .....5

Figure 2.1 GC/MS fingerprint of hopanes recorded at *m/z* 191 in MC252 oil .....19

Figure 2.2 GC/MS fingerprint of diasteranes and regular steranes recorded at *m/z* 217 in MC252 oil .....19

Figure 2.3 GC/MS fingerprint of 14β(H)-steranes recorded at *m/z* 218 in MC252 oil .....20

Figure 2.4 GC/MS fingerprint of triaromatic steroids recorded at *m/z* 231 in MC252 oil .....20

Figure 3.1 2009 and 2010 flight lines of the UAVSAR used to acquire oil spill information during the *Deepwater Horizon*.....34

Figure 3.2 Pre- to post-oil spill PolSAR backscatter mechanism change, sediment sample locations, and fingerprinting results.....42

Figure 3.3 Chromatographic comparisons of the normal alkane (*m/z* 57) profiles and diasteranes and regular steranes (*m/z* 217) profiles .....44

Figure 4.1 Sediment sample collection sites.....53

Figure 4.2 Example of background and oiled sediment samples.....56

Figure 4.3 Comparison of raw and transformed peak intensity data .....60

Figure 4.4 Postulated weathering of MC252 diasteranes and regular steranes .....63

Figure 4.5 Percentage of samples exceeding the diagnostic ratio critical difference (CD) allowance .....65

Figure 4.6 The HCA and PCA plots of source oil tribes from the combined EIC peak intensity data with the similarity line at 0.400.....66

Figure 4.7 The HCA and PCA plots of source oil tribes from the *m/z* 217 peak intensity data with the similarity line at 0.400 .....67

Figure 4.8 The HCA and PCA plots of source oil families from the combined EIC peak intensity data with the similarity line at 0.700.....68

Figure 4.9 The HCA and PCA plots of source oil families from the *m/z* 217 peak intensity data with the similarity line at 0.680 .....69

Figure 4.10 The source oil cluster distances based on the combined EIC peak intensity data.....71

Figure 4.11 The source oil cluster distances based on the *m/z* 217 peak intensity data .....71

Figure 4.12 The HCA and PCA analysis of combined EIC peak intensity data for coastal marsh sediments collected in 2010 .....73

Figure 4.13 The HCA cluster distances of combined EIC peak intensity data for 2010 coastal marsh sediments .....75

Figure 4.14 The HCA and PCA analysis of *m/z* 217 peak intensity data for coastal marsh sediments collected in 2010 .....76

Figure 4.15 The HCA cluster distances of *m/z* 217 peak intensity data for 2010 coastal marsh sediments .....76

Figure 4.16 The HCA and PCA analysis of combined EIC peak intensity data for the coastal marsh sediments with LSU ID# 2011039 .....78

Figure 4.17 The HCA cluster distances of combined EIC peak intensity data for coastal marsh sediments with LSU ID# 2011039 .....78

Figure 4.18 The HCA and PCA analysis of *m/z* 217 peak intensity data for the coastal marsh sediments with LSU ID# 2011039 .....79

Figure 4.19 The HCA cluster distances of *m/z* 217 peak intensity data for coastal marsh sediments with LSU ID# 2011039 .....80

Figure 4.20 The HCA and PCA analysis of combined EIC peak intensity data for the remainder of 2011 coastal marsh sediments .....81

Figure 4.21 The HCA cluster distances of combined EIC peak intensity data for 2011 coastal marsh sediments .....83

Figure 4.22 The HCA and PCA analysis of *m/z* 217 peak intensity data for the remainder of 2011 of coastal marsh sediments .....84

Figure 4.23 The HCA cluster distances of *m/z* 217 peak intensity data for 2011 coastal marsh sediments .....84

Figure 4.24 The HCA and PCA analysis of combined EIC peak intensity data for 2012 coastal marsh sediments .....86

Figure 4.25 The HCA cluster distances of combined EIC peak intensity data for 2012 coastal marsh sediments .....87

Figure 4.26 The HCA and PCA analysis of *m/z* 217 peak intensity data for 2012 coastal marsh sediments .....88

Figure 4.27 The HCA cluster distances of *m/z* 217 peak intensity data for 2012 coastal marsh sediments....89

Figure 4.28 The HCA and PCA analysis of combined EIC peak intensity data for 2013 coastal marsh sediments analyzed on GT....90

Figure 4.29 The HCA cluster distances of combined EIC peak intensity data for 2013 coastal marsh sediments analyzed on GT....90

Figure 4.30 The HCA and PCA analysis of *m/z* 217 peak intensity data for 2013 coastal marsh sediments analyzed on GT....91

Figure 4.31 The HCA cluster distances of *m/z* 217 peak intensity data for 2013 coastal marsh sediments analyzed on GT....92

Figure 4.32 The HCA and PCA analysis of combined EIC peak intensity data for 2013 coastal marsh sediments analyzed on MU....93

Figure 4.33 The HCA cluster distances combined EIC peak intensity data for 2013 coastal marsh sediments analyzed on MU....93

Figure 4.34 The HCA and PCA analysis of *m/z* 217 peak intensity data for 2013 coastal marsh sediments analyzed on MU....94

Figure 4.35 The HCA cluster distances of *m/z* 217 peak intensity data for 2013 coastal marsh sediments analyzed on MU....95

Figure 4.36 The HCA and PCA analysis of combined EIC peak intensity data for 2014 coastal marsh sediments analyzed on GT....96

Figure 4.37 The HCA cluster distances of combined EIC peak intensity data for 2014 coastal marsh sediments analyzed on GT....96

Figure 4.38 The HCA and PCA analysis of *m/z* 217 peak intensity data for 2014 coastal marsh sediments analyzed on GT....97

Figure 4.39 The HCA cluster distances of *m/z* 217 peak intensity data for coastal marsh sediment samples analyzed on GT....98

Figure 4.40 The HCA and PCA analysis of combined EIC peak intensity data for 2014 coastal marsh sediments analyzed on MU....99

Figure 4.41 The HCA cluster distances of combined EIC peak intensity data for 2014 coastal marsh sediments analyzed on MU....99

Figure 4.42 The HCA and PCA analysis of *m/z* 217 EIC data for 2014 coastal marsh sediments analyzed on MU ..... 100

Figure 4.43 The HCA cluster distances of *m/z* 217 peak intensity data for 2014 coastal marsh sediments analyzed on MU ..... 101

Figure 4.44 The HCA and PCA analysis of combined EIC peak intensity data for 2015 coastal marsh sediments analyzed on GT ..... 102

Figure 4.45 The HCA cluster distances of combined EIC peak intensity data for 2015 coastal marsh sediments analyzed on GT ..... 102

Figure 4.46 The HCA and PCA analysis of *m/z* 217 peak intensity data for 2015 coastal marsh sediments analyzed on GT ..... 103

Figure 4.47 The HCA cluster distances of *m/z* 217 peak intensity data for 2015 coastal marsh sediments analyzed on GT ..... 104

Figure 4.48 The HCA and PCA analysis of combined EIC peak intensity data for 2015 coastal marsh sediments analyzed on MU ..... 105

Figure 4.49 The HCA cluster distances of combined EIC peak intensity data for 2015 coastal marsh sediments analyzed on MU ..... 105

Figure 4.50 The HCA and PCA analysis of *m/z* 217 peak intensity data for 2015 coastal marsh sediments analyzed on MU ..... 106

Figure 4.51 The HCA cluster distances of *m/z* 217 peak intensity data for 2015 coastal marsh sediments analyzed on MU ..... 107

Figure 4.52 The weathering pattern distribution for all oiled coastal marsh samples collected in 2010 – 2015 ..... 108

Figure 4.53 The pattern distribution for 51 sediment samples determined to be genetically similar to MC252 through chemometric analysis of *m/z* 217 peak intensity data ..... 109

## ABSTRACT

Oil source-fingerprinting is an environmental forensics technique that uses analytical chemistry to determine the origin of oil residues in environmental samples by comparison to a known or suspected source oil. Currently, the only standardized method for oil source fingerprinting is a qualitative approach that is very effective in almost every oil spill response situation. However, the need for quantitative oil source-fingerprinting methods to complement the qualitative determinations is extremely desired. The research herein aims to utilize data generated by gas chromatography/mass spectrometry (GC/MS) methodologies to test two different quantitative techniques: diagnostic biomarker ratio analysis and chemometrics.

The most common crude oil constituents used for oil source-fingerprinting are the oil biomarker compounds. Oil biomarkers are polycyclic aliphatic hydrocarbon molecules typically resistant to environmental weathering (i.e., biological and physiochemical transformations). They are universal in crude oils and most petroleum products, and impart unique ratios in oils of different maturities and geographic sources. Diagnostic biomarker ratio analysis will be used to establish a suite of diagnostic biomarker ratios with statistical limitations that can differentiate oil from the *Deepwater Horizon* oil spill, or Macondo 252 (MC252) oil, from other South Louisiana crude oils. This technique is not limited to MC252 oil. Diagnostic ratios can be determined and tested for any source oil.

Current published research has documented weathering of several of the biomarker compounds used for oil source-fingerprinting. Any weathering of MC252 oil residues in the environment will adversely affect the diagnostic biomarker ratio analysis. Therefore, a more advanced quantitative technique, chemometrics, will use pattern recognition algorithms to determine the innate similarity of environmental oil residues to MC252 oil.

# CHAPTER 1: GENERAL INTRODUCTION

## 1.1 BACKGROUND

Oil spills into marine environments have been recognized as major environmental insults for more than 40 years (NOAA-ERD, 2012; Stout and Wang, 2007; Wang and Fingas, 2003; Wang et al., 2006). The 1968 *Torrey Canyon* oil spill off the southwest coast of the United Kingdom accentuated the potential environmental threat posed by large volumes of oil spilled by accidents involving the then newly introduced "supertanker." A production well blow-out in 1969 off the California coastal city of Santa Barbara caused another major spill in the marine environment further highlighting environmental concerns of oil pollution. There have been numerous spills around the world since the 1960s, including the infamous *Amoco Cadiz* (Brittany, France) and *Exxon Valdez* (Prince William Sound, Alaska) spills, which resulted in considerable media attention. Media attention and public outrage during the *Exxon Valdez* incident lead to the passage of the Oil Pollution Act of 1990 that put liability on the responsible parties (i.e., spiller or spillers) to clean-up major oil spills. The most notable oil spill to date is the *Deepwater Horizon* (DWH) disaster, now considered to be one of the greatest natural disasters in the United States. The accidental spill occurred in the Macondo Prospect region located in the Mississippi Canyon Block 252 (MC252) of the northern Gulf of Mexico, and about 41 miles off the coast of Louisiana. Eleven people lost their lives and an estimated 4.9 million barrels of crude oil and gas were released into the Gulf of Mexico between April 20 and July 15, 2010 (US DOI 2010).

The foremost questions asked about spilled oil are its source, quantity in various compartments (i.e., air, water, sediment, biosphere, etc.) of the environment, and the risk and consequences associated with various hydrocarbon concentrations within these compartments.

The key to answering these questions is the chemical composition of the spilled oil. Crude oil is a complex mixture of organic compounds derived from the partial decomposition of animals and plants that have been long dead. In geological time scales, the process of oil formation (e.g., diagenesis, catagenesis, and metagenesis) occurs very slowly and produces "simple" organic molecules (petroleum) from more complex organic structures (organic biomass) (Peters et al., 2005). These processes contribute to the formation of petroleum-type hydrocarbons which can exist as a gas (natural gas), a solid (tar, bitumen), and, as a liquid (crude oil), the latter being the focus of this research.

In general, all crude oils tend to be composed of the same hydrocarbon compounds, but the relative abundance of these compounds can vary significantly between oils of different origins. Oil constituents commonly targeted by analysis techniques like gas chromatography/mass spectrometry (GC/MS) can be classified into four general groups: (1) individual saturated hydrocarbons (the normal alkanes and isoprenoids); (2) polycyclic aromatic hydrocarbons (PAHs) including their dominant alkylated homologs; (3) sulfur heterocyclic aromatic hydrocarbons and related alkylated homologs; and (4) oil biomarkers that are polycyclic aliphatics. The physical and chemical properties of crude oil vary with regions of production and reservoir zones within these regions because of differing geographic conditions and organic matter assemblages (Peters et al., 2005). As a result, there is no single definition for all crude oils. However, these differences in composition are important from an environmental chemistry perspective because they are useful to determine the possible origins of the oil and to predict how the oil will behave if spilled in the environment.

The major factor affecting spilled oil is an inherently heterogeneous distribution in the impacted environment. This is particularly true when referring to smaller scale oil spills, and

may not be an issue with large scale spills like the DWH where large areas of coastline were blanketed with crude oil. The phase separation of crude oil in water can mobilize pockets of crude oil beyond the initial shoreline impacts and into the nearshore and interior bodies of water, extending the potential environmental impacts of the spilled oil. Weathering of spilled oil is the combined effects of different biological and physiochemical processes on its original composition. Weathering includes evaporation, spreading, dispersion, dissolution, emulsification, oxidation, sedimentation, aggregation, and both microbial and photo-oxidation. These processes individually and in combination continually alter oil composition and affect its distribution into different compartments of the environment. Weathering, by changing the composition of the original spilled oil, changes the oil's physical and toxic properties, as well as its appearance. Once oil is stranded on a beach or shoreline, weathering is modified by the microenvironment in which the oil is entrapped; therefore, the degree of weathering is very site specific. An important component of the microenvironment is the microorganism assemblage and their ability to biodegrade oil. How biodegradation affects the composition of oil in the environment is highly dependent on the physical properties and amount of oil spilled, as well as the factors like redox conditions, nutrient availability, temperature and salinity. All of these factors will greatly influence the microbial ecology and petroleum hydrocarbon degradation dynamics (Atlas et al., 2015).

Crude oil spilled into the environment undergoes varying degrees of environmental weathering that affect its composition. As weathering proceeds, certain groups of oil constituents are lost in a predictable sequence. The first compounds to be depleted are the n-alkanes and isoprenoids, followed by the lighter PAHs, then the remaining PAHs and their alkyl homologs (Prince and Walters, 2007; Stout and Wang, 2007; Wang and Fingas, 2003). As a

result, unique identification of source oil may be difficult when relying on PAHs because of the variable loss of these oil constituents and the remaining distribution patterns due to the degree of weathering. Multiple or chronic petroleum releases are a particularly important factor in Louisiana complicating the ability to analytically identify and quantify trace amounts of oil residues in environmental samples. All things considered, the heterogeneous distribution of oil, a continually changing composition, and the presence of many oil sources causes considerable uncertainty in detecting and assessing the impacts of oil spills.

Oil-source fingerprinting is an environmental forensics technique that was adapted from the field of petroleum geochemistry. It is a procedure that compares oil constituents, primarily the oil biomarkers, in a sample to a known oil source. Oil biomarkers have structures of repeating subunits composed of carbon, hydrogen, and other elements, indicating that their precursors were living organisms. Steranes in petroleum originate from sterols in the cell membranes of eukaryotes. Prokaryotes use hopanoids rather than steroids in their cell structures which, in turn, accounts for the presence of hopanes in petroleum (Peters et al., 2005). Distributions of oil biomarkers are unique for different types and blends of petroleum products and source oils and represent an oil-specific fingerprint for oil source correlations (Daling et al., 2002; Wang et al., 2006; Hansen et al., 2007). Therefore, oil biomarkers can be used to distinguish one oil from another, including oils with similar geographic origins (Wang and Fingas, 1995; Stout et al., 2002; Wang and Fingas, 2003; Peters et al., 2005).

Three classes of oil biomarkers commonly referred to in the literature are: 1) the triterpanes (hopanes); 2) the steranes, including the diasteranes and regular steranes, and 14β(H)-steranes; and 3) the triaromatic steriods (Figure 1.1). Oil biomarkers are important to oil source-fingerprinting because their relatively recalcitrant nature and high molecular weights tend to

make them more resistant to environmental weathering processes. As a result, the concentration of biomarkers should increase relative to other oil constituents (Wang and Fingas, 1995) and used as internal markers to quantify the loss of the less stable oil components.

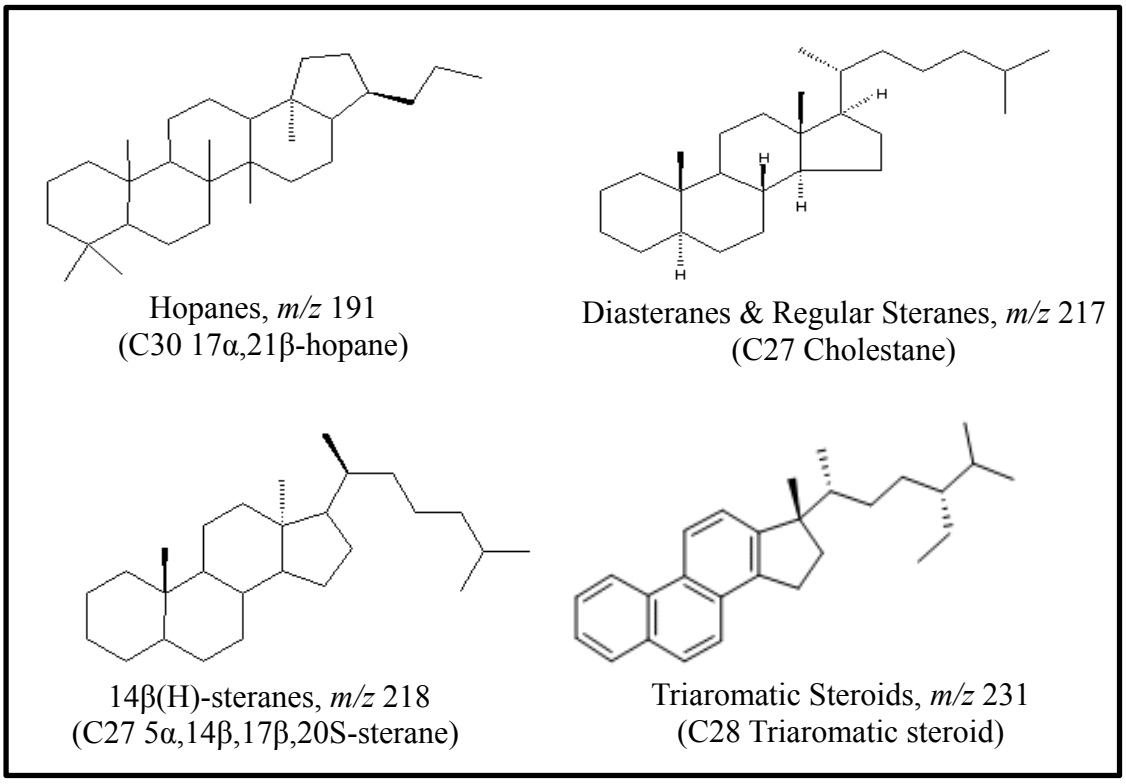


Figure 1.1 Chemical structures of common oil biomarker families. (Peters et al., 2005)

## 1.2 RESEARCH OBJECTIVE

The objective of this research is to refine the use of biomarkers as tools for identifying the source of spilled oil in both laboratory and field samples. This research aims to utilize data generated by gas chromatography/mass spectrometry (GC/MS) methodologies to test quantitative oil source-fingerprinting techniques to better identify and quantify spilled oil, to document its weathered residues, and to assess the physical/chemical transformations caused by various types of weathering. One quantitative oil source-fingerprinting technique will establish a

suite of diagnostic biomarker ratios using statistical limitations. These ratios can be used to determine whether or not oil residues in environmental samples originate from a particular source oil. For this research, Macondo 252 (MC252) from the DWH is the source oil. The technique will be further applied to coastal marsh sediments to determine its effectiveness in discriminating MC252 source oil from other possible sources. The weathering of oil residues in the environment has the potential to adversely affect the final suite of MC252 diagnostic biomarker ratios. To overcome this problem, an advanced quantitative oil source-fingerprinting technique, termed chemometrics, will be tested. Chemometrics is a multivariate statistics approach and for this research is another adaptation from petroleum geochemistry (Peters et al., 2007; Peters et al., 2008; Lorenson et al., 2011; Peters et al., 2013).

## 1.3 RATIONALE AND APPROACH

The unprecedented circumstances of the DWH disaster gave scientists very unique opportunities to identify and characterize the after effects of a large-scale oil spill in Louisiana's coastal marshes. The cumulative effects of many small detrimental impacts resulting from this disaster may not yet be readily observable and other impacts may not be observable for years to come. Developing analytical and statistical tools to aid in detecting and characterizing oil in the environment will be very important to assess these impacts.

Hypothesis: Quantitative diagnostic biomarker ratios will show little or no change over time because oil biomarker compounds are typically more resistant to environmental weathering. Diagnostic biomarker ratios of an oil residue found in the environment should match the same diagnostic biomarker ratios of a suspected source oil. Calculating diagnostic ratios under specific statistical constraints will allow for estimating a quantitative probability for making a match or a non-match determination. Furthermore, any changes in the diagnostic biomarker

ratios can be used to determine if the biomarker compounds are as resistant to degradation as they are thought to be. If the diagnostic biomarker ratios of a source oil begin to change then it can be assumed that the biomarker compounds are weathering, and more advanced oil source-fingerprinting techniques (i.e, the application of chemometrics) may be necessary.

Three research questions are posed to test the hypothesis:

1. Can a suite of diagnostic biomarker ratios be determined and used to statistically differentiate MC252 oil from other South Louisiana crude oils?
2. Can diagnostic biomarker ratio analysis, a quantitative approach, be applied to real-world environmental samples and match oil biomarkers in the MC252 oil residues?
3. Oil biomarkers are generally accepted to be resistant to weathering. However, it is known that over time that they eventually start to weather. Since this will affect the diagnostic biomarker ratios analysis, is there a more advanced quantitative oil source-fingerprinting technique that can be employed?

### 1.3.1 Quantitative Oil Source-Fingerprinting Using Diagnostic Biomarker Ratio Analysis (Chapter 2)

An oil source-fingerprinting methodology using GC/MS and specific hopane, sterane, and triaromatic steroid ratios in MC252 source oil will be developed and tested. The foundation and statistical criteria of the methodology will be adapted from the 2007 edition of *Oil Spill Environmental Forensics: Fingerprinting and Source Identification* edited by Zhendi Wang and Scott Stout, Chapter 7, "Emerging CEN Methodology for Oil Spill Identification", A.B Hansen, P.S. Daling, L. Faksness, K.R. Sorheim, P. Kienhuis, and R. Duus.

The statistical comparison of diagnostic biomarker ratios of an unknown sample to the same diagnostic biomarker ratios of MC252 source oil will allow samples with crude oil residues to be classified into one of four oil source-fingerprinting categories: match, probable match, inconclusive, or non-match to MC252. An important benefit of comparing diagnostic ratios of spilled oil and suspected source oils is that concentration effects are minimized, and the use of ratios tends to induce a self-normalizing effect on the data (Hansen et al., 2007).

The first step of this process will be to isolate specific diagnostic biomarker ratios from the chromatographic profiles of the hopanes, the steranes (diasteranes and regular steranes, and 14β(H)-steranes), and the triaromatic steroids. A minimum of 30 MC252 source oil analyses will be used to determine the diagnostic biomarker ratios to be tested. The MC252 diagnostic biomarker ratios to be tested will be chosen by using many published combinations of ratios and a few new ratios using similar guidelines as the other ratios. A fixed relative standard deviation (RSD) of 5% will be applied to determine the final suite of diagnostic biomarker ratios. Once the final suite of MC252 diagnostic biomarker ratios is established, the same ratios will be calculated for different South Louisiana crude oils and statistically compared to the MC252 ratios. The results of the comparison will determine how effective the diagnostic ratio approach is in discriminating among unweathered crude oils from a similar geographic production zone.

### 1.3.2 Oil Source-Fingerprinting in Support of Polarimetric Radar Mapping of MC252 Oil (Chapter 3)

Working in collaboration with the United States Geological Survey, National Wetlands Research Center (USGS-NWRC), the quantitative oil-source fingerprinting technique developed in Section 1.3.1 (i.e., diagnostic biomarker ratio analysis) will be used to determine if oil detected by the National Aeronautics and Space Administration's airborne Uninhabited Aerial

Vehicle Synthetic Aperture Radar (UAVSAR) is from the DWH oil spill (i.e., MC252 oil); therefore, quantitative oil source-fingerprinting will be used to link changes in remotely sensed data to oil from the DWH oil spill (i.e., MC252 oil). Sediment samples collected from Barataria Bay, Louisiana will be extracted and analyzed by GC/MS. The final suite of biomarker ratios determined from Section 1.3.1 will be calculated and sediments will be classified into one of four oil source-fingerprinting categories: match, probable match, inconclusive, and non-match. Quantitative oil source-fingerprinting will play a crucial role in demonstrating the oil tracking capabilities of the UAVSAR. Therefore, it is imperative that the quantitative oil source-fingerprinting corroborates with the changes detected in the PolSAR.

### 1.3.3 Advanced Quantitative Oil Source-Fingerprinting of Louisiana Coastal Marsh Sediments Collected from 2010-2015 (Chapter 4)

It is commonly believed that biomarkers suffer little interference from weathering and degradation effects because of their high molecular weights. What if they begin to weather and lose their effectiveness as chemical markers? The data synthesis of over 500 coastal marsh sediments collected from areas known to be impacted by the DWH spill will provide an indication as to whether or not MC252 oil biomarkers are affected by environmental weathering. The potential for oil biomarker weathering will profoundly affect the calculation and subsequent critical difference analysis of diagnostic ratios used for oil source-fingerprinting. As a result, a more robust quantitative oil source-fingerprinting approach may be necessary. Chemometrics, an exploratory data analysis technique that recognizes patterns using multivariate pattern recognition algorithms, will be tested as an additional, more advanced oil source-fingerprinting technique. The same crude oils in Section 1.3.1 will be tested again using chemometrics to determine if crude oils from a common geographic area (e.g., south Louisiana crude oils) can be

differentiated and to assess the capabilities of chemometrics as an oil source-fingerprinting technique. Chemometric analysis will then be used to determine if any of the sediment samples cluster with MC252 oil, indicating a genetic similarity in their biomarker compounds. Finally, chemometrics will be used to determine a postulated weathering pattern of MC252 diasteranes and regular steranes observed from qualitative observations.

## 1.4 LITERATURE CITED


Atlas, R.M., Stoeckel, D.M., Faith, S.A. Minard-Smith, A., Thorn, J.R., and Benotti, M.J. 2015. Oil biodegradation and oil-degrading microbial populations in marsh sediments impacted by oil from the Deepwater Horizon well blowout. Environmental Science and Technology, 49(14):8356-8366.

Daling, P.S., Faksness, L., Hansen, A.B., and Stout, S.A. 2002. Improved and standardized methodology for oil spill fingerprinting. Environmental Forensics, 3:263-278.

Hansen, A.B, Daling, P.S., Faksness, L., Sorheim, K.R., Kienhuis, P., and Duus, R. 2007. Emerging CEN Methodology for Oil Spill Identification. In: Zhendi Wang and Scott Stout, eds., *Oil Spill Environmental Forensics: Fingerprinting and Source Identification*. Burlington, MA: Academic Press, pp. 229-256.

Lorenson, T.D., Leifer, I., Wong, F.L., Rosenbauer, R.J., Campbell, P.L., Lam, A., Hostettler, F.D., Greinert, J., Finlayson, D.P., Bradley, E.S., and Luyendyk, B.P. 2011. Biomarker chemistry and flux quantification methods for natural petroleum seeps and produced oils, offshore southern California: U.S. Geological Survey Scientific Investigations Report 2011-5210, 45 p. and OCS Study BOEM 2011-016.

NOAA-ERD. 2012. Responding to environmental catastrophes: an evolving history of NOAA's involvement in oil spill response. [Online] Available from: http://celebrating200years.noaa.gov/transformations/spill_response/welcome.html#tech.

Peters, K.E., Coutrot, D., Nouvelle, X., Ramos, L.S., Rohrback, B.G., Magoon, L.B., and Zumberge, J.E. 2013. Chemometric differentiation of crude oil families in the San Joaquin Basin, California. The American Association of Petroleum Geologists Bulletin, 97(1):103-143.

Peters, K.E., Hostettler, F.D., Lorenson, T.D., and Rosenbauer, R.J. 2008. Families of Miocene Monterey crude oil, seep, and tarball samples, coastal California. The American Association of Petroleum Geologist Bulletin, 92(9):1131-1152.

Peters, K.E., Ramos, L.S., Zumberge, J.E., Valin, Z.C., Scotese, C.R., and Gautier, D.L. 2007. Circum-Artic petroleum systems identified using decision-tree chemometrics. The American Association of Petroleum Geologist Bulletin, 91(6):877-913.

Peters, K.E., Walters, C.C., and Moldowan, J.M. 2005. *The Biomarker Guide,* second edition. Cambridge, UK: Cambridge University Press.

Prince, R.C. and Walters, C.C. 2007. Biodegradation of oil hydrocarbons and its implications for source identification. In *Oil Spill Environmental Forensics: Fingerprinting and Source Identification*, Wang, Z. and Stout, S.A. (eds.), Burlington, MA: Academic Press, pp. 349-379.

Stout, S.A., Uhler, A.D., McCarthy, K.J., and Emsbo-Mattingly, S. 2002. Chemical fingerprinting of hydrocarbons. In: B.L. Murphy and R.D. Morrison, eds., *Introduction to Environmental Forensics*. London, UK: Academic Press, pp. 137–260.

Stout, S.A. and Wang, Z. 2007. Chemical fingerprinting of spilled or discharged petroleum – methods and factors affecting petroleum fingerprints in the environments. In *Oil Spill Environmental Forensics: Fingerprinting and Source Identification*, Wang, Z. and Stout, S.A. (eds.), Burlington, MA: Academic Press, pp. 1-54.

U.S. Department of the Interior. 2010. Press Release, August 2, 2010, "U.S. scientific teams refine estimates of oil flow from BP's well prior to capping." [Online] Available from: http://app.restorethegulf.gov/release/2010/08/02/us-scientific-teams-refine-estimates-oil-flow-bps-well-prior-capping.

Wang, Z., Stout, S.A., and Fingas, M. 2006. Forensic fingerprinting of biomarkers for oil spill characterization and source identification. Environmental Forensics, 7:105-146.

Wang, Z.D. and Fingas, M. 1995. Differentiation of the source of spilled oil and monitoring of the oil weathering process using gas chromatography-mass spectrometry. Journal of Chromatography, 712:321-343.

Wang, Z.D. and Fingas, M. 2003. Development of oil hydrocarbon fingerprinting and identification techniques. Marine Pollution Bulletin, 47(9-12):423-452.

# CHAPTER 2: QUANTITATIVE OIL SOURCE-FINGERPRINTING USING DIAGNOSTIC BIOMARKER RATIO ANALYSIS[1]

## 2.1 INTRODUCTION

Oil source-fingerprinting is an environmental forensics technique that utilizes analytical chemistry to compare samples containing spilled oil to a suspected source. It was first used by Overton et al. (1981) to evaluate the environmental impacts resulting from an oil spill and fire at the U.S. Strategic Petroleum Reserve Complex in West Hackberry, LA. Oil forensics typically uses oil biomarkers that are naturally occurring, ubiquitous, and stable hydrocarbons (Daling et al., 2002; Wang et al., 2006; Hansen et al., 2007). Biomarker compounds can be utilized as conserved reference compounds because they are more resistant to environmental weathering processes, compared to most other oil compounds including polycyclic aromatic hydrocarbons (PAHs), and the loss of less stable oil components can be quantitatively estimated by normalizing data with 17*α(H),*21*β(H)*-hopane (Prince et al., 1994; Wang and Fingas, 2003; Hansen et al., 2007). Furthermore, the distributions of oil biomarkers is unique for different types and blends of petroleum products (Wang and Fingas, 1995; Stout et al., 2002; Wang and Fingas, 2003; Peters et al., 2005); therefore, they can represent an oil-specific fingerprint to which distinct oil samples can be correlated.

The objective of this research was to utilize gas chromatography/mass spectrometry (GC/MS) to determine a suite of diagnostic biomarker ratios with statistical limitations that can determine whether or not oil residues are a match to Macondo 252 (MC252) oil released during the *Deepwater Horizon* (DWH) tragedy in April 2010. The diagnostic biomarker ratios should

[1] Portions of this chapter previously appeared as: Meyer, B.M., Overton, E.B., and Turner, R.E. 2014. Oil source identification using diagnostic biomarker ratio analyses. Proceedings of the 2014 International Oil Spill Conference, 2014(1): 2064-2073. It is reprinted by permission of IOSC (see Appendix A).

show little or no change over time because oil biomarkers are typically more resistant to environmental weathering (Wang and Fingas, 1995; Wang et al., 2006; Hansen et al., 2007). An important benefit of comparing diagnostic ratios of spilled oil and suspected source oils is that concentration effects are minimized. The use of ratios tends to induce a self-normalizing effect on the data (Wang and Fingas, 2003; Hansen et al., 2007) meaning that, if instrumental analysis conditions change as a result of matrix effects, column degradation, sensitivity, or tune degradation, both integers used to calculate the ratio will be affected by the same relative degree of instrumental change. The assumption is that the integers are similar in molecular weight, chemistry, and quantitation ion. The index or ratio of the two integers should, therefore remain constant. Accordingly, the measured diagnostic ratios between any pair of compounds should also match, up to a certain statistical confidence level, in oil residues from the same source oil.

## 2.2 EXPERIMENTAL APPROACH

### 2.2.1 Source Oil Preparation for GC/MS Analysis

MC252 source oil was collected by British Petroleum (BP) from a riser pipe aboard the drillship *Discover Enterprise* connected to the damaged wellhead of the DWH drilling rig located in the Gulf of Mexico on May 20, 2010. The source oil was weighed and a proportional amount of analytical grade hexane (>99.9%, VWR International, Radnor, PA) was added (e.g., 0.10 grams of oil in 10 milliliters of hexane). Approximately 1.0 gram of pre-cleaned granular anhydrous sodium sulfate (VWR International, Radnor, PA) was added to the hexane extract to remove any water, and then the sample was sonicated for 15 minutes to settle out any particulate matter. New extracts were prepared as necessary, or if they showed any evidence of compositional change after GC/MS analysis. A 1-milliliter aliquot of the extract was analyzed

daily during routine laboratory operations as a quality control mechanism, and a total of 44 of these analyses were used to determine the final suite of diagnostic biomarker ratios.

Extracts of eight additional source oils were prepared and analyzed in addition to MC252 in the same manner described above. Seven of the eight were South Louisiana crude oils, and the last was Alaskan North Slope crude. The source oils have been preserved and archived at the Louisiana State University, Department of Environmental Sciences, Response and Chemical Assessment Team (LSU-RCAT) laboratory, and most were collected as part of LSU-RCAT's response to other oil spills throughout the years. Other source oils (e.g., EPA South Louisiana crude) were provided as standard reference materials for various oil spill related research. Each source oil extract was analyzed in quadruplicate on each analytical system described in Section 2.2.2 below. Diagnostic biomarker ratios for each additional source oil were calculated using the final suite of MC252 diagnostic ratios previously tested and determined from the forty-four MC252 analyses. Chromatographic comparisons of quadruplicate samples are provided in Appendix B.

### 2.2.2 GC/MS Instrumentation

Chemical analyses of the all oil extracts were performed using either an Agilent 7890A gas chromatograph (GC) equipped with an Agilent 5975C inert XL mass selective detector (MSD), or an Agilent 6890N GC interfaced to an Agilent 5973 MSD. Both instruments were fitted with a 5% diphenyl/95% dimethyl polysiloxane high resolution capillary column (Phenomenex ZB-5MSi, 30 m x 0.25 mm ID x 0.25 micron thick film). GC/MS acquisition methodologies were identical for both instrument systems.

The GC injection temperature was set at 280°C and only high-temperature, low thermal-bleed septa were used in the GC inlet. The carrier gas was ultrahigh purity helium delivered at a constant flow rate of 1 ml $min^{-1}$. The injection port was set at 280 °C, run in splitless mode, and was fitted with a deactivated borosilicate liner. The GC was operated in the temperature program mode with an initial column temperature of 60°C for 3 minutes, then increased to 280°C at a rate of 5°C $min^{-1}$, and held at 280°C for 3 minutes. The oven was then heated from 280°C to 300°C at a rate of 1.5°C $min^{-1}$ and held at 300°C for two minutes. The total run time was 65.33 minutes per sample.

The interface to the MS was maintained at 300°C and the MS quad and source temperatures were 140°C and 230°C, respectively. The MSD was operated in the selective ion monitoring (SIM) mode to ensure low level detection of the targeted oil analytes (i.e., each acquisition window was scanned at a rate greater than 1.4 scans $sec^{-1}$ with a dwell time of 60 milli-seconds).

The GC/MS instrumentation was tuned every 12 hours using perfluorotributylamine (PFTBA) to ensure optimum operational conditions. Septa were changed before each instrument tune and inlet liners were replaced as necessary. A daily oil analysis calibration standard and MC252 extract were injected in each analytical sequence as quality control (QC) samples to ensure accurate instrument operation. Solvent blanks and instrument blanks were also included in each sequence to check for any sample carryover. If any of these analyses indicated improper instrument conditions, then the analyses were halted until the instrument could be restored to optimum operating conditions.

### 2.2.3 MC252 Diagnostic Biomarker Ratio Calculations

A quantitative oil source-fingerprinting methodology using GC/MS and specific hopane, sterane, and triaromatic steroid ratios in MC252 source oil was adapted and tested based Hansen et al. (2007) to have the capability to determine whether oil detected in coastal Louisiana marsh sediments originated from the *Deepwater Horizon* disaster. The CEN (European Committee for Standardization, 2012) method provides the quantitative foundation and statistical criteria of the methodology utilized in this research, and has since been adapted (CEN 2012/TR 15522-2:2012) in Europe, with recent application by oil spill researchers here in the United States (Radović et al., 2014; Kolian et al., 2015).

The first step of this research process was to isolate specific diagnostic biomarker ratios from the chromatographic profiles of the hopanes, the steranes (diasteranes and regular steranes, and 14β(H)-steranes), and the triaromatic steroids. A total of 44 separate GC/MS analyses of MC252 source oil were used to determine the diagnostic biomarker ratios to be tested. The MC252 diagnostic biomarker ratios tested were chosen by using many already published combinations of ratios and a few new ratios using similar guidelines. The diagnostic ratios presented herein were calculated by using the ratio of peak heights of compounds eluting within the same mass-to-charge (*m/z*) window. Hansen et al. (2007) recommends use of peak heights for diagnostic biomarker ratios because they tend to be more robust than area responses for peaks that may be poorly resolved and have noisy baselines. All ratio calculations were done using a corrected baseline value. Peak heights not exceeding three times the noise signal were not integrated. After a corrected base line value and peak heights have been determined, the diagnostic ratios were calculated by dividing peak height "A" by peak height "B" within an ion group (e.g., *m/z* 191, 217, 218, 231) to exclude the mass spectrometer's varying response for

different ions. In addition to diagnostic ratios calculated as A/B, some diagnostic ratios were calculated using the sums of peak heights within the ion group (e.g., A/(A+B)). This calculation produces ratios with lower analytical variance and in turn, lower relative standard deviations (Hansen et al., 2007).

A fixed coefficient of variation or relative standard deviation (RSD) of 5% was applied to overcome the variation in critical differences as described in Hansen et al. (2007) and to determine the final suite of diagnostic biomarker ratios. Each MC252 ratio selected was averaged, the standard deviation ($\boldsymbol{s}$) calculated, and the %RSD determined using Equation 2.1:

$$\text{Equation 2.1} \quad \%RSD = s_{ratio} \,/\, \bar{x}_{ratio} * 100\%$$

The fixed 5% RSD limit was applied as a quality criterion, because analytical methods producing higher RSD values should not be used to analyze and compare oil samples in a forensic context (Hansen et al., 2007). Any MC252 diagnostic biomarker exceeding this limit were excluded. Table 2.1 provides the compound names and abbreviations for the tested biomarkers, as well as information regarding peak labels in Figures 2.1 – 2.4. Figures 2.1 – 2.4 also display the compounds listed in Table 2.1 in their respective GC/MS fingerprint for each ion group (e.g., *m/z* 191, 217, 218, 231).

A measure of repeatability was applied to estimate an acceptable difference between two analytical results. Repeatability (**r**) is defined as precision where independent test results were obtained with the same laboratory by the same operator using the same equipment (Ranstam et al., 2000). Repeatability fixes a percentage that is unlikely to be exceeded by the difference between two measurements under repeatability conditions. Repeatability, therefore, can be

Table 2.1 Petroleum Biomarkers Used For Calculating MC252 Diagnostic Ratios

| Abbreviation | Compound Name | *m/z* Value | Figure Reference |
|---|---|---|---|
| C27 Ts | C27 18α(H)-22,29,30-trisnorneohopane | 191 | 2.1, a |
| C27 Tm | C27 17α(H)-22,29,30-trisnorhopane | 191 | 2.1, b |
| C29 aB | C29 17α(H),21β(H)-30-norhopane | 191 | 2.1, c |
| C29 Ts | C29 18α(H)-30-norneohopane | 191 | 2.1, d |
| C30 aB | C30 17α(H),21β(H)-hopane | 191 | 2.1, e |
| C31 aB (S+R) | C31 17α(H),21β(H)-22(S+R)-homohopane | 191 | 2.1, f+g |
| C32 aB (S+R) | C32 17α(H),21β(H)-22(S+R)-bishomohopane | 191 | 2.1, h+i |
| C33 aB (S+R) | C32 17α(H),21β(H)-22(S+R)-trishomohopane | 191 | 2.1, j+k |
| C27D Ba-S | C27 13β(H),17α(H),20S-diasterane | 217 | 2.2, a |
| C27D Ba-R | C27 13β(H),17α(H),20R-diasterane | 217 | 2.2, b |
| C29D Ba-S | C29 24-ethyl-13β(H),17α(H),20S-diacholestane | 217 | 2.2, c |
| C29D Ba-R | C29 24-ethyl-13β(H),17α(H),20R-diacholestane | 217 | 2.2, d |
| C28 aaa-R | C28 24-methyl-5α(H),14α(H),17α(H), 20R-cholestane | 217 | 2.2, e |
| C29 aaa-R | C29 24-ethyl-5α(H),14α(H),17α(H), 20R-cholestane | 217 | 2.2, f |
| C27 BB (R+S) | C27 5α(H),14β(H),17β(H)-cholestane (20R+20S) | 218 | 2.3, a+b |
| C28 BB (R+S) | C28 24-methyl-5α(H),14β(H),17β(H)-cholestane (20R+20S) | 218 | 2.3, c+d |
| C29 BB (R+S) | C29 24-ethyl-5α(H),14β(H),17β(H)-cholestane (20R+20S) | 218 | 2.3, e+f |
| C20 TA | C20-triaromatic steroid (pregnane derivative) | 231 | 2.4, a |
| C21 TA | C21-triaromatic steroid (homopregnane derivative) | 231 | 2.4, b |
| C26 TA-S | C26-triaromatic steroid,20S (cholestane derivative) | 231 | 2.4, c |
| C28 TA-S | C28-triaromatic steroid,20S (ethylcholestane derivative) | 231 | 2.4, d |
| C27 TA-R | C27-triaromatic steroid,20R (methylcholestane derivative) | 231 | 2.4, e |
| C28 TA-R | C28-triaromatic steroid,20R (ethylcholestane derivative) | 231 | 2.4, f |

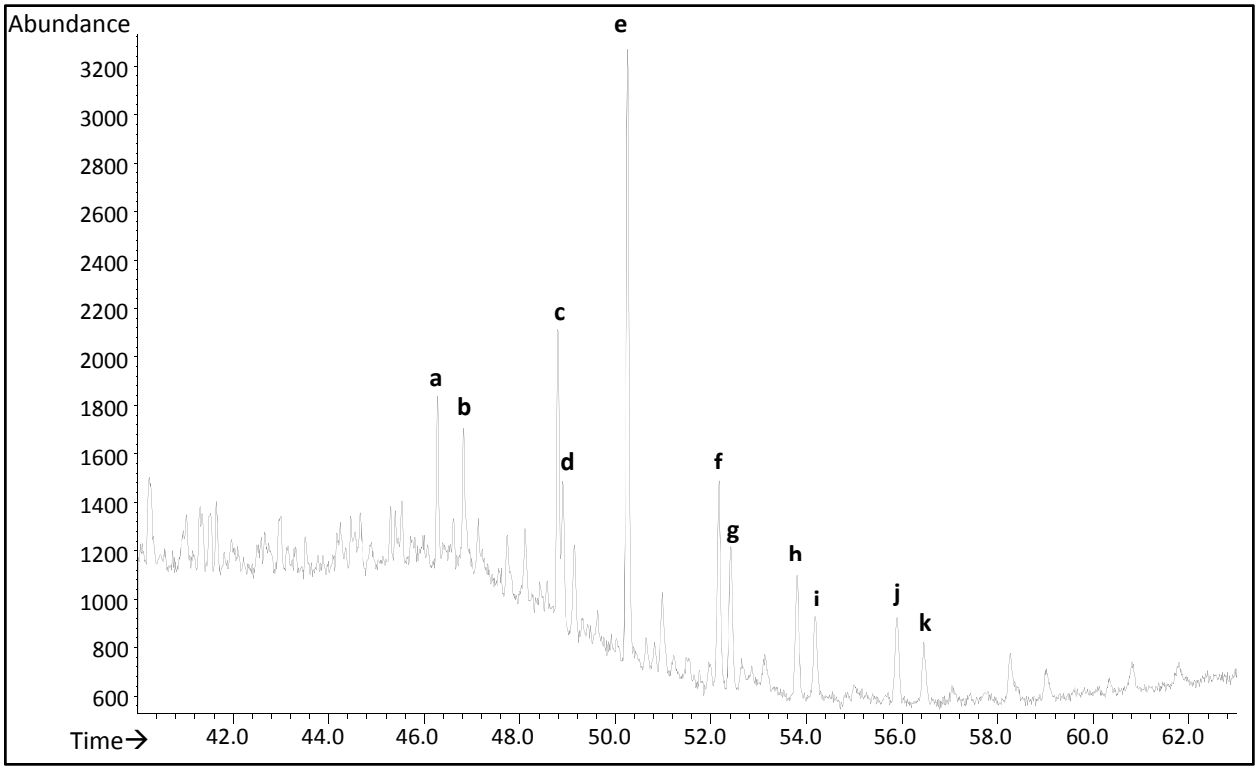


Figure 2.1 GC/MS fingerprint of hopanes recorded at *m/z* 191 in MC252 oil.

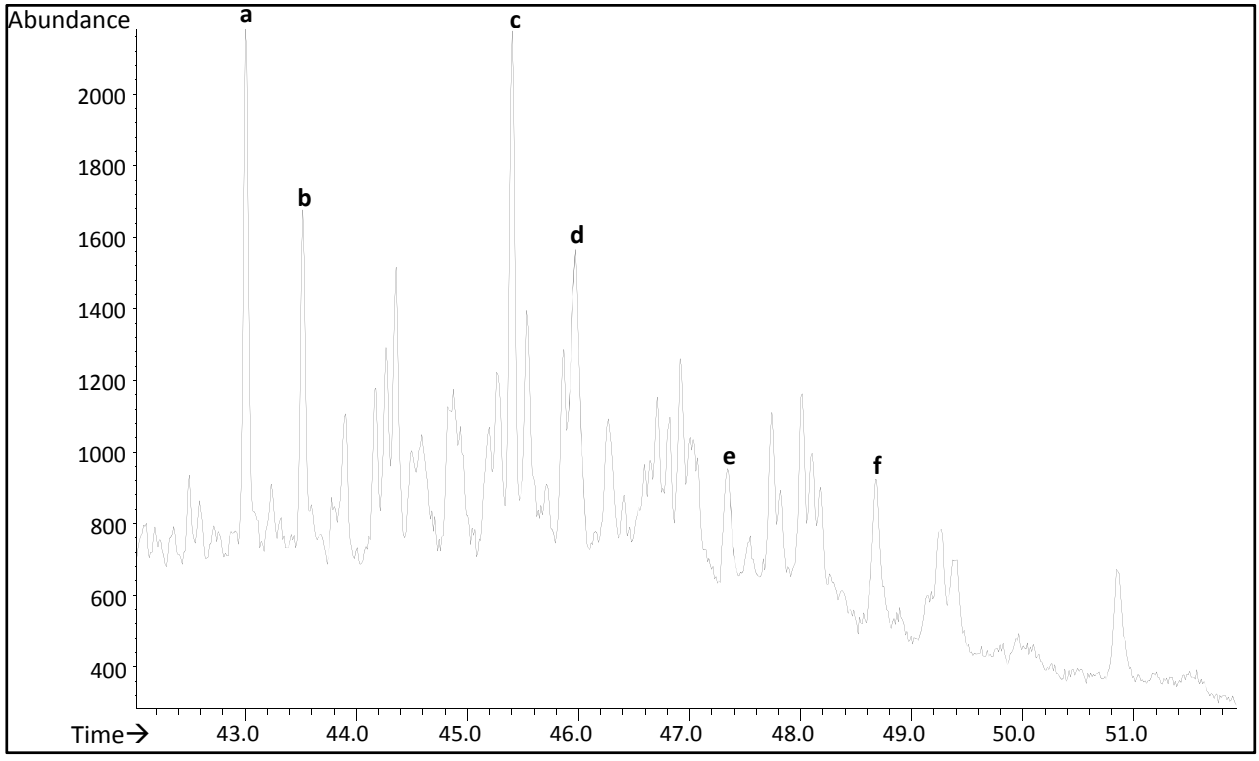


Figure 2.2 GC/MS fingerprint of diasteranes and regular steranes recorded at *m/z* 217 in MC252 oil.

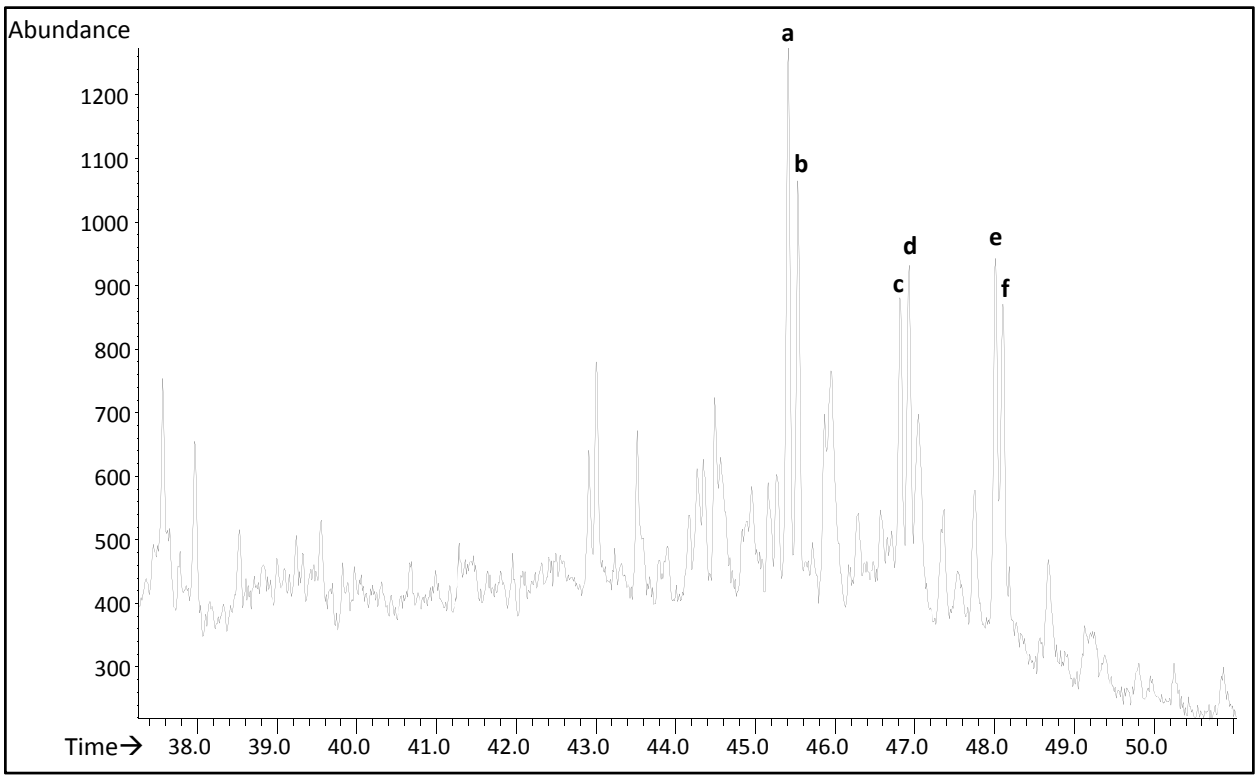


Figure 2.3 GC/MS fingerprint of 14β(H)-steranes recorded at *m/z* 218 in MC252 oil.

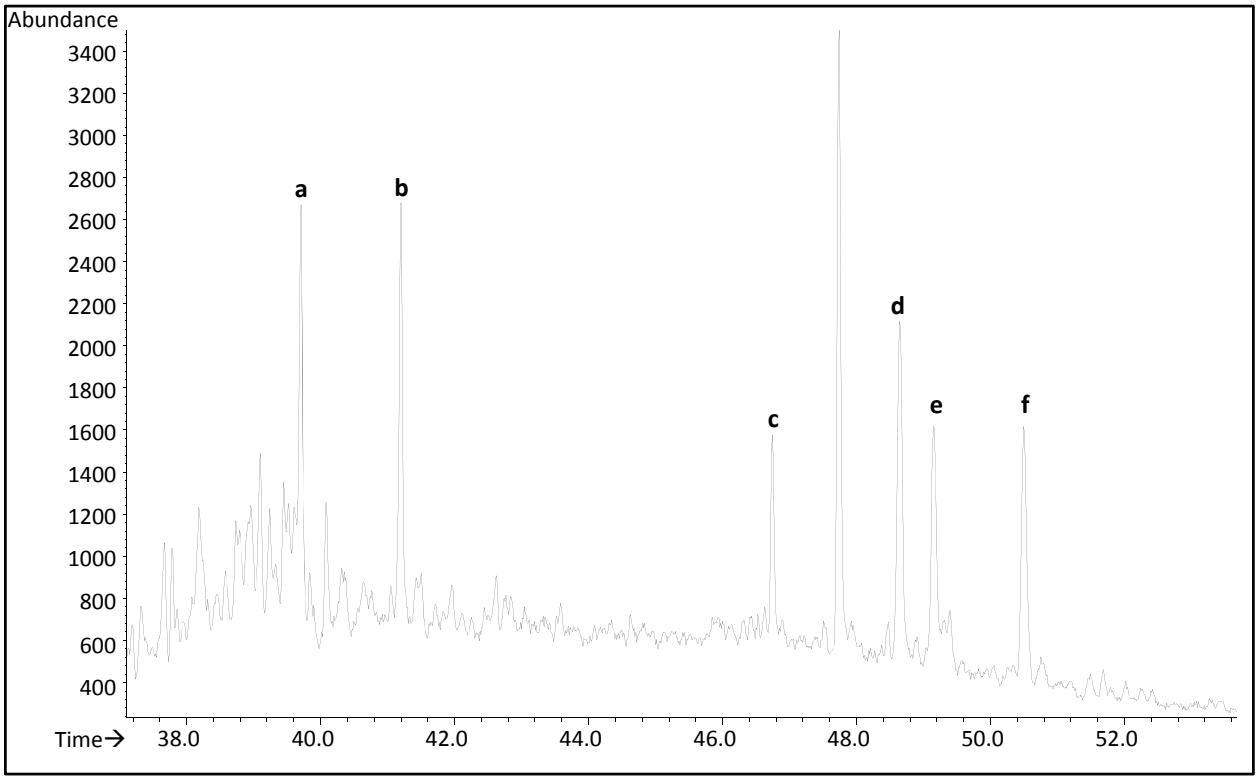


Figure 2.4 GC/MS fingerprint of triaromatic steroids recorded at *m/z* 231 in MC252 oil.

applied as a test method to compare individual diagnostic biomarker ratios with the assumption that oil in the unknown sample is the same as the source oil in question. If the repeatability limit is exceeded, then it is beyond a reasonable doubt that this assumption is not valid and that the samples originate from different sources (Hansen et al., 2007).

According to the criteria set forth by Hansen et al. (2007), the critical difference between two test results and is based on standard normal distribution with the associated standard deviation equal to $\sigma\sqrt{2}$. Critical difference (CD) examined the difference between ratios (i.e., source oil and unknown sample ratios), and equals $f*\sigma\sqrt{2}$, where $f$ = the approximate value assigned to a particular quantile of the normal distribution, and σ equals a standard deviation of the population. For a normal distribution (i.e., an assumption of approximate normality of random variable $x$ with mean of zero and standard deviation of unity) at a 95% confidence level, $f$ = 1.96 and $f*\sigma\sqrt{2}$ = 2.77, that is rounded to 2.8 because of the non-homogenous nature of oil in the environment. Therefore, the repeatability limit ($\mathbf{r}_{95\%}$) is calculated using equation 2.2:

Equation 2.2 $$\mathbf{r}_{95\%} = \%RSD * \left(f * \sigma\sqrt{2}\right) = 5\% * 2.8 = 14\%$$

This implies that any diagnostic ratio to be used for match/non-match determinations must not differ more than 14% when samples are analyzed under repeatable conditions.

### 2.2.4 Diagnostic Biomarker Ratios for South Louisiana Crude Oils

The final suite of MC252 diagnostic biomarker ratios were used to calculate the same ratios for the other South Louisiana crude oils and the Alaskan North Slope crude. The absolute and critical differences were calculated for each additional source oil and used to test whether or

not the ratio analysis had the capability to discriminate crude oils from similar productions areas. Alaskan North Slope crude oil was included as a positive control because it is from an entirely different production zone.

## 2.3 RESULTS AND DISCUSSION

### 2.3.1 MC252 Diagnostic Biomarker Ratios

A total of 15 diagnostic biomarker ratios (Table 2.2) calculated from 44 separate analyses of MC252 source oil GC/MS runs were determined. Compound names and identification within each MC252 GC/MS fingerprint for each ion group (e.g., *m/z* 191, 217, 218, and 231) are provided in Table 2.1 and Figures 2.1 – 2.4. Table 2.2 gives the 15 specific diagnostic ratios chosen, the average (n=44) MC252 source oil ratios, and their corresponding %RSD. All diagnostic ratios chosen had a %RSD less than 5%, a quality criterion, because ratio averages higher than the fixed 5% RSD should not be used to analyze and compare oil samples in a forensic context (Hansen et al., 2007).

With this suite of MC252 source oil diagnostic ratios established, the same diagnostic ratios for oil residues in environmental samples can be calculated, and the repeatability limit (**r**$_{95\%}$, Equation 2.2) applied to obtain the absolute and critical differences for match/non-match determinations. The absolute difference and critical difference for each sample ratio and corresponding MC252 source oil ratio, are calculated using equations 2.3 and 2.4, respectively.

Equation 2.3 $$Absolute\ Difference = \left|\bar{x}_{MC252ratio} - \bar{x}_{Sample\ ratio}\right|$$

Equation 2.4 $$Critical\ Difference, CD = \left(\bar{x}_{MC252ratio,sample\ ratio} * 14\right) \div 100$$

If the absolute difference of any of the 15 ratios (Table 2.2) is lower than the CD, then the unknown sample ratio is a positive match to the same MC252 ratio; if the absolute difference is higher, the unknown sample is not a match to the MC252 ratio. Comparison of the absolute and critical differences has to be performed for every diagnostic ratio.

Table 2.2 Average Diagnostic Ratios for MC252 Source Oil (n=44)

| Hopanes (m/z 191) | $\bar{x}_{MC252ratio}$ | $s_{ratio}$ | %RSD |
|---|---|---|---|
| C27 Ts/ C27 Tm | 1.26 | 0.04 | 3.1 |
| C29 aB/C29 Ts | 2.17 | 0.05 | 2.1 |
| C29 aB/C30 aB | 0.48 | 0.02 | 3.3 |
| C31 aB(S+R)/C32 aB(S+R) + C33 aB(S+R) | 0.93 | 0.02 | 2.1 |
| C32 aB(S+R)/C31 aB(S+R) + C33 aB(S+R) | 0.43 | 0.01 | 3.4 |
| C33 aB(S+R)/C31 aB(S+R) + C32 aB(S+R) | 0.28 | 0.01 | 4.2 |
| Diasteranes and Regular 14a(H)-Steranes (m/z 217) | $\bar{x}_{MC252ratio}$ | $s_{ratio}$ | %RSD |
| C27D Ba-S/C27D Ba-R | 1.61 | 0.03 | 1.8 |
| C29D Ba-S/C29D Ba-R | 1.63 | 0.05 | 2.7 |
| C28 aaa-R/C29 aaa-R | 0.74 | 0.02 | 2.2 |
| 14B(H)-Steranes (m/z 218) | $\bar{x}_{MC252ratio}$ | $s_{ratio}$ | %RSD |
| C27 BB(R+S)/C28 BB(R+S) + C29 BB(R+S) | 0.69 | 0.02 | 2.8 |
| C28 BB(R+S)/C27 BB(R+S) + C29 BB(R+S) | 0.38 | 0.01 | 3.1 |
| C29 BB(R+S)/C27 BB(R+S) + C28 BB(R+S) | 0.46 | 0.02 | 3.5 |
| Triaromatic Steriods (m/z 231) | $\bar{x}_{MC252ratio}$ | $s_{ratio}$ | %RSD |
| C20 TA/C21 TA | 1.07 | 0.03 | 2.2 |
| C26 TA-S/C28 TA-S | 0.63 | 0.02 | 2.7 |
| C27 TA-R/C28 TA-R | 0.92 | 0.02 | 2.2 |

Once the comparisons are completed for each ratio, unknown samples compared to a source oil can then be classified into one of four oil source-fingerprinting categories: positive match, probable match, inconclusive, or non-match (Hansen et al., 2007). The research presented herein expanded the categorization approach by assigning each unknown sample a final diagnostic ratio score, calculated by dividing the number of "matching" ratios by 15 and

multiplying by 100%. Oil residues in environmental samples can then be grouped according to their final diagnostic ratio score:

- 93-100 = Match (14 -15 matching ratios out of 15);
- 80-92 = Probable Match (12-13 matching ratios out of 15);
- 50-79 = Inconclusive (8-11 matching ratios out of 15); and,
- <50 = Non-match (7 or less matching ratios out of 15).

Using the $\mathbf{r}_{95\%}$ at a 95% confidence level before categorization provides a foundation for statistically viable quantitative oil source-fingerprinting, and using a final diagnostic ratio score based on the $\mathbf{r}_{95\%}$ to categorize unknown samples into the categories builds on this foundation. Therefore, using diagnostic biomarker ratios as demonstrated in this chapter will provide a statistically rigorous and quantitative evaluation of detecting and characterizing oil in the environment after oil spill events.

### 2.3.2 Diagnostic Ratios of South Louisiana Crude Oils

The average diagnostic ratios for each of the other source oils tested are in Table 2.3. The yellow highlighted cells represent ratios exceeding the CD criteria. Chromatographic profiles of each biomarker groups and oils tested are in Appendix C. The suite of MC252 diagnostic biomarker ratio analysis was able to differentiate amongst the other South Louisiana crude oils. This is especially important in environments where more than one source of petroleum contamination is entirely possible (e.g., Louisiana). Of the South Louisiana crude oils tested, BP surrogate oil and 15% weathered (by weight) BP surrogate oil were a match and a probable match, respectively, to MC252 source oil. The BP surrogate oil (South Louisiana crude

Table 2.3 Average Diagnostic Ratios for South Louisiana Crude Oils

| | ANSC | BP Surrogate | BP Surrogate 15% Weathered | Cutoff Pipeline | EPA SLC | Exxon OCS | MC252 | Pt. Coupee Pipeline | SLC Blend |
|---|---|---|---|---|---|---|---|---|---|
| Hopanes (*m/z* 191) | | | | | | | | | |
| C27 Ts/ C27 Tm | 0.07±0.01 | 1.27±0.01 | 1.34±0.12 | 0.85±0.01 | 0.76±0.01 | 0.77±0.02 | 1.26±0.04 | 0.45±0.01 | 0.92±0.02 |
| C29 aB/ C29 Ts | 3.72±0.02 | 2.18±0.01 | 2.23±0.05 | 2.20±0.03 | 3.61±0.02 | 3.66±0.03 | 2.17±0.05 | 3.97±0.03 | 3.56±0.02 |
| C29 aB/ C30 aB | 0.67±0.01 | 0.46±0.02 | 0.48±0.03 | 0.60±0.01 | 0.72±0.01 | 0.76±0.01 | 0.48±0.02 | 0.84±0.02 | 0.66±0.01 |
| C31 aB(S+R)/ C32 aB(S+R) + C33 aB(S+R) | 1.06±0.01 | 0.98±0.01 | 1.01±0.07 | 1.15±0.02 | 1.36±0.03 | 1.39±0.04 | 0.93±0.02 | 1.53±0.02 | 1.23±0.02 |
| C32 aB(S+R)/ C31 aB(S+R) + C33 aB(S+R) | 0.44±0.01 | 0.43±0.01 | 0.44±0.02 | 0.40±0.01 | 0.38±0.01 | 0.37±0.01 | 0.43±0.01 | 0.35±0.01 | 0.40±0.01 |
| C33 aB(S+R)/ C31 aB(S+R) + C32 aB(S+R) | 0.22±0.00 | 0.25±0.01 | 0.24±0.01 | 0.22±0.01 | 0.17±0.01 | 0.17±0.00 | 0.28±0.01 | 0.16±0.00 | 0.20±0.01 |
| Diasteranes and Regular 14a(H)-Steranes (*m/z* 217) | | | | | | | | | |
| C27D Ba-S/ C27D Ba-R | 1.63±0.03 | 1.64±0.02 | 1.61±0.03 | 1.73±0.03 | 1.74±0.01 | 1.60±0.03 | 1.61±0.03 | 1.66±0.02 | 1.67±0.02 |
| C29D Ba-S/ C29D Ba-R | 1.85±0.05 | 1.60±0.02 | 1.42±0.09 | 1.65±0.03 | 1.66±0.01 | 1.65±0.03 | 1.63±0.05 | 1.71±0.03 | 1.72±0.02 |
| C28 aaa-R/ C29 aaa-R | 0.95±0.01 | 0.85±0.02 | 0.81±0.05 | 0.89±0.01 | 0.81±0.02 | 0.80±0.01 | 0.74±0.02 | 0.74±0.02 | 0.80±0.02 |

Table 2.3 (continued) Average Diagnostic Ratios for South Louisiana Crude Oils

| | ANSC | BP Surrogate | BP Surrogate 15% Weathered | Cutoff Pipeline | EPA SLC | Exxon OCS | MC252 | Pt. Coupee Pipeline | SLC Blend |
|---|---|---|---|---|---|---|---|---|---|
| 14B(H)-Steranes (*m/z* 218) | | | | | | | | | |
| C27 BB(R+S)/ C28 BB(R+S) + C29 BB(R+S) | 0.65±0.02 | 0.74±0.01 | 0.75±0.03 | 0.68±0.02 | 0.63±0.01 | 0.64±0.01 | 0.69±0.02 | 0.53±0.02 | 0.68±0.01 |
| C28 BB(R+S)/ C27 BB(R+S) + C29 BB(R+S) | 0.42±0.01 | 0.35±0.01 | 0.34±0.01 | 0.39±0.01 | 0.39±0.01 | 0.39±0.01 | 0.38±0.01 | 0.43±0.01 | 0.36±0.01 |
| C29 BB(R+S)/ C27 BB(R+S) + C28 BB(R+S) | 0.45±0.01 | 0.46±0.02 | 0.47±0.01 | 0.46±0.02 | 0.50±0.01 | 0.49±0.01 | 0.46±0.02 | 0.55±0.01 | 0.49±0.01 |
| Triaromatic Steriods (*m/z* 231) | | | | | | | | | |
| C20 TA/C21 TA | 0.93±0.02 | 1.16±0.02 | 1.16±0.03 | 1.40±0.03 | 1.39±0.01 | 1.33±0.03 | 1.07±0.03 | 1.24±0.03 | 1.28±0.02 |
| C26 TA-S/ C28 TA-S | 0.89±0.01 | 0.74±0.03 | 0.71±0.04 | 0.71±0.02 | 0.73±0.01 | 0.73±0.02 | 0.63±0.02 | 0.60±0.02 | 0.71±0.01 |
| C27 TA-R/ C28 TA-R | 1.27±0.01 | 0.96±0.02 | 0.98±0.05 | 0.89±0.01 | 0.98±0.01 | 1.13±0.02 | 0.92±0.01 | 0.80±0.01 | 1.13±0.02 |
| | (n=8) | (n=8) | (n=8) | (n=5) | (n=8) | (n=8) | (n=44) | (n=4) | (n=8) |
| Diagnostic Ratio Analysis Score | 7/15<br>47%<br>Non-match | 14/15<br>93%<br>Match | 13/15<br>87%<br>Probable Match | 9/15<br>60%<br>Inconclusive | 8/15<br>53%<br>Non-match | 7/15<br>47%<br>Non-match | --<br>--<br>-- | 6/15<br>40%<br>Non-match | 8/15<br>53%<br>Non-match |

oil from the Marlin platform in the Dorado field, VK915) was distributed for research purposes by British Petroleum once availability of MC252 was limited. The Marlin oil was chosen as a surrogate oil due to its similarity to MC252 (BP, 2014). The remaining South Louisiana crude oils were either inconclusive (i.e., sample is similar to the source oil, but differ enough that confidence level is decreased) or a non-match. The most discriminating ratios for the South Louisiana crude oils were the hopanes and triaromatic steroids. As expected, the Alaskan North Slope crude oil (ANSC) was a non-match to MC252 source oil based on diagnostic ratio analysis.

## 2.4 CONCLUSIONS

There is a critical need for a robust, quantitative method for oil source-fingerprinting in a variety of oil spill situations. The ability to match oil in an impacted area of the environment to a source oil with statistical confidence, therefore, is crucial. The necessity arises from the fact that the only standardized method for oil source-fingerprinting currently used in the United States is ASTM 5739-00 (ASTM, 2000). This method only offers a qualitative approach to oil source-fingerprinting and there would be great value in having a standardized quantitative/statistical approach to complement it. The CEN (2012) method, which is the method this research is based, fills the void by providing a standardized quantitative approach that can span from the response phase to source oil correlations after spill events.

Furthermore, the diagnostic biomarker ratio process outlined here is not restricted to use on the analysis of just one source oil. A suite of diagnostic biomarker ratios can be calculated for any source oil as long as the ratios tested do not vary more than 5% RSD. A unique set of diagnostic biomarker ratios can be established for that particular source oil after integration of multiple analyses of the source oil in question (i.e., statistically, at least 30 analyses).

Another advantage of using diagnostic biomarker ratios is that the process can be applied to data previously generated if the petroleum biomarker ions are included in the GC/MS instrument acquisition phase. In most situations, samples are already extracted and analyzed in order to quantitate a targeted list of petroleum related normal alkanes, isoprenoids, and PAHs, and most acquisition methods include petroleum biomarker ions in the same analytical method. Therefore, one analysis results in multi-dimensional data interpretation and saves instrument time and analysis costs.

The statistical comparison of diagnostic ratios provides a quantitative oil fingerprinting technique; however, it is important that other quantitative and qualitative evaluations corroborate with the diagnostic ratio analysis results. Qualitative evaluations of all chromatograms (i.e., PAH alkyl homologs in addition to petroleum biomarkers) of samples in question should be done before any final conclusions are made, and other metrics, like calculation of the biodegradation ranking (Peters et al., 2005), should be performed. Low petrogenic content, which will translate into low instrument responses, may affect the calculation of the diagnostic ratios, and is an important consideration when making all conclusions.

Diagnostic biomarker ratios are most robust in the early stages of a spill and its impacts (beginning of spill to up to 1 year after). The environmental conditions where oil is deposited, however, will greatly alter its weathering path, and therefore, its chemical composition. The eventual degradation of petroleum biomarkers has been documented by Wang et al. (2001), Aeppli et al. (2014), and Radović et al. (2014). Degradation greatly depends on whether or not oil residues remain at the surface or if they are buried in anoxic conditions. Wang et al. (2001) found that petroleum biomarkers were degraded upon exposure for 24 years in surface sediments of salt marsh. Aeppli et al. (2014) found that homohopanes and triaromatic steroids in surface

photooxidation, respectively. Radović et al. (2014) further demonstrated the profound effect of photooxidation on the degradation of triaromatic steroids with laboratory irradiation experiments. The potential weathering of the biomarkers could adversely affect the application of diagnostic ratio analysis. Additional diagnostic ratios, or more advanced oil source-fingerprinting techniques, therefore, may be necessary as the length of time the oil resides in sediment increases.

The diagnostic biomarker ratios determined in this chapter will be applied to sediment samples collected throughout Louisiana's coastal marshes from 2010 to 2015 (Chapter 4). The suite of MC252 diagnostic biomarker ratio analysis was able to differentiate amongst the other South Louisiana crude oils. This is especially important in environments where more than one source of petroleum contamination is entirely possible (e.g., Louisiana). The samples were collected from areas that were initially unimpacted prior to MC252 oil moving ashore, after which most of these sites were then documented as impacted. The diagnostic biomarker ratios calculated for oil residues detected in these sediment samples will be statistically compared to the same diagnostic biomarker ratios of MC252 source oil using the procedure in this chapter. Oil residues in the coastal marsh sediments can then be classified as either a match, probable match, inconclusive, or non-match to MC252 oil.

## 2.5 LITERATURE CITED

Aeppli, C., Nelson, R.K., Radović, J.R., Carmichael, C.A., Valentine, D.L., and Reddy, C.M. 2014. Recalcitrance and degradation of petroleum biomarkers upon abiotic and biotic natural weathering of Deepwater Horizon oil. Environmental Science and Technology, 48:6726-6734.

ASTM 5739-00. 2000. Oil spill source identification by gas chromatography and positive ion electron impact low resolution mass spectrometry. ASTM International, West Conshohocken, PA.

BP Exploration & Production Inc. and BP Gulf Coast Restoration Organization. 2014. Data Publication Summary Report: Reference oil characterization. Reference No. O-04v01-02, January 22, 2014. [Online] Available from: www.gulfsciencedata.bp.com.

CEN. 2012. CEN/TR 15522-2:2012, Oil Spill Identification – Waterborne Petroleum and Petroleum Products – Part 2: Analytical Methodology and Interpretation of Results.

Daling, P.S., Faksness, L., Hansen A.B., and Stout, S.A. 2002. Improved and standardized methodology for oil spill fingerprinting. Environmental Forensics, 3:263-278.

Hansen, A.B, Daling, P.S., Faksness, L., Sorheim, K.R., Kienhuis, P., and Duus, R. 2007. Emerging CEN Methodology for Oil Spill Identification. In: Zhendi Wang and Scott Stout, eds., *Oil Spill Environmental Forensics: Fingerprinting and Source Identification*. Burlington, MA: Academic Press, pp. 229-256.

Kolian, S.R., Porter, S.A., Sammarco, P.W., Birkholz, D., Cake Jr., E.W., and Subra, W.A. 2015. Oil in the Gulf of Mexico after the capping of the BP/Deepwater Horizon Mississippi Canyon (MC-252) well. Environmental Science and Pollution Research, 22:12073-12082.

Overton, E.B., McFall, J.A., Mascarella, S.W., Steele, C.F., Antoine, S.A., Politezer, I.R., and Laseter, J.L. 1981. Identification of petroleum residue sources after a fire and oil spill. Proceedings of the 1981 International Oil Spill Conference, 1981(1):541-546.

Peters, K.E., Walters, C.C., and Moldowan, J.M. 2005. *The Biomarker Guide, 2nd Edition*. Cambridge, UK: Cambridge University Press.

Prince, R.C., Elmendorf, D.L., Lute, J.R., Hsu, C.S., Haith, C.E., Senius, J.D., Dechert, G.J., Douglas, G.S., and Butler, E.L. 1994. 17*α(H),*21*β(H)*-hopane as a conserved internal marker for estimating the biodegradation of crude oil. Environmental Science and Technology, 28:142-145.

Radović, J.R., Aeppli C., Nelson, R.K., Jimenez, N., Reddy, C.M., Bayona, J.M., and Albaigés, J. 2014. Assessment of photochemical processes in marine oil spill fingerprinting. Marine Pollution Bulletin, 79:268-277.

Ranstam, J., Ryd, L., and Onsten, I. 2000. Accurate accuracy assessment. Acta Orthopaedica Scandinavica, 71(1):106-108.

Stout, S.A., Uhler, A.D., McCarthy, K.J., and Emsbo-Mattingly, S. 2002. Chemical fingerprinting of hydrocarbons. In: B.L. Murphy and R.D. Morrison, eds., *Introduction to Environmental Forensics*. London, UK: Academic Press, pp. 137–260.

Wang, Z., Fingas, M.F., Owens, E.H., Sigouin, L., and Brown, C.E. 2001. Long-term fate and persistence of the spilled *Metula* oil in a marine salt marsh environment: degradation of petroleum biomarkers. Journal of Chromatography A, 926:275-290.

Wang, Z., Stout, S.A., and Fingas, M. 2006. Forensic fingerprinting of biomarkers for oil spill characterization and source identification. Environmental Forensics, 7:105-146.

Wang, Z.D. and Fingas, M. 1995. Differentiation of the source of spilled oil and monitoring of the oil weathering process using gas chromatography-mass spectrometry. Journal of Chromatography, 712:321-343.

Wang, Z.D. and Fingas, M. 2003. Development of oil hydrocarbon fingerprinting and identification techniques. Marine Pollution Bulletin, 47:423-452.

# CHAPTER 3: OIL SOURCE-FINGERPRINTING IN SUPPORT OF POLARIMETRIC RADAR MAPPING OF MC252 OIL[2]

## 3.1 INTRODUCTION

Responding to and assessing the geographic extent of an oil spill presents many challenges. It relies heavily on visual observations that are an integral part of the response efforts. Determining where spilled oil has been deposited in the environment often relies on trained field personnel that are part of aerial observation teams participating in daily overflights of the impacted areas, or are part of the Shoreline Cleanup and Assessment Technique (SCAT) team. Aerial observers are trained to describe the appearance of oil floating on water based on oil or sheen color (e.g., black or brown, light, silver, or rainbow) and oil texture (e.g., streamers, mousse, tarballs, tarmats), and these descriptions are then used to assess oil movement, implement appropriate countermeasures, and assess the status of pollution distribution (NOAA, 2012; IPIECA-OGP, 2015). The SCAT teams collect data on shoreline habitats, the type and degree of shoreline oiling conditions, site-specific physical processes, and resources at risk, which is used to support cleanup guidelines and endpoints (Michel et al., 2013).

There remains several limitations in visually tracking the fate of spilled oil after an oil spill. Although these analyses are the most common oil tracking technique, visual observations can be subjective, are limited to daylight hours, can be hindered by fog, and other materials in the environment (e.g., seaweed, floating debris, vegetation) can be mistaken as oil (Fingas and Brown, 2007). Fingas and Brown (2007) point out that spilled oil is not always visible to the

[2] Portions of this chapter previously appeared as: Ramsey III, E., Meyer, B.M., Rangoonwala, A., Overton, E.B., Jones, C.E., and Bannister, T. 2014. Oil source-fingerprinting in support of polarimetric radar mapping of Macondo-252 oil in Gulf Coast marshes. Marine Pollution Bulletin, 89:85-95. It is reprinted by permission of Elsevier (see Appendix D).

human eye and can be in a very thin slick that is not evenly or uniformly dispersed throughout the environment. Other factors directly affecting visual observations may affect the visual assessment of how much oil remains, such as limited accessibility due to environmental sensitivity, a lack of access either on foot or by boat, or the alteration of oil distribution due to environmental conditions (i.e., tidal changes, inundation, oil burial, etc.). All of these factors complicate visual oil detection and may affect the subsequent evaluation of environmental impacts. The visual detection and tracking of oil after an oil spill can be supported by remote sensing technology, particularly active remote sensing techniques like synthetic aperture radar (SAR). SAR has the benefits of being deployed in all weather conditions, during the day or night, and can cover large areas in a short amount of time (Fingas and Brown, 2011).

Twenty-nine (29) sediment samples collected from Barataria Bay, Louisiana were extracted, analyzed, and oil source-fingerprinted working in collaboration with the United States Geological Survey, National Wetlands Research Center (USGS-NWRC). The overall objective of this collaboration was to validate SAR-based oil detection by linking changes in remotely sensed data to oil from the *Deepwater Horizon* (DWH) oil spill (i.e., MC252 oil). Oil source-fingerprinting was crucial in achieving this objective. The samples were chosen based on fully polarimetric synthetic aperture radar (PolSAR) data collected by the National Aeronautics and Space Administration's airborne Uninhabited Aerial Vehicle Synthetic Aperture Radar (UAVSAR) before and after the DWH oil spill (Figure 3.1). The GC/MS analysis of the sediment samples exhibiting substantial changes in PolSAR backscatter data from 2009 to 2010 would indicate whether or not oil was detected. If oil was detected, the objective of the quantitative oil source-fingerprinting (i.e., diagnostic biomarker ratio analyses) was to determine whether or not the oil was MC252 oil.

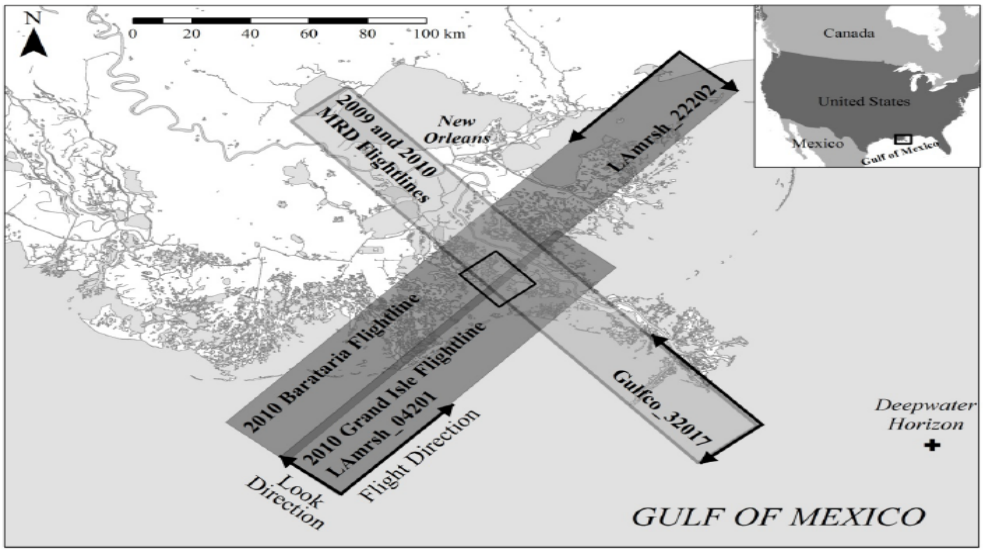


Figure 3.1 2009 and 2010 flight lines of the UAVSAR used to acquire oil spill information during the *Deepwater Horizon*. The small black rectangle indicates the Barataria Bay study area. (Ramsey et al., 2011)

Previous research by Jones et al. (2011) determined that UAVSAR was uniquely suited for imaging highly heterogeneous and spatially complex wetlands because its high spatial resolutions, low noise, L-band radar frequency, and full polarization capabilities (e.g., HH, HV, VV, VH). The L-band radar of the UAVSAR obtains backscatter intensities based on the dielectric properties of water in the natural environment. This includes the water in marsh canopies and subcanopies (Ramsey et al., 2014). The full polarization capabilities of the UAVSAR are capable of differentiating changes in marsh structure versus changes due to the presence of oil (Ramsey et al., 2011). Additionally, the precision repeat-track capability of the UAVSAR enables for direct comparisons between revisited data collections (Ramsey et al., 2011). As a result, any oil impacts should be easily identified by comparison of the pre- and post-spill UAVSAR flight line data sets.

## 3.2 EXPERIMENTAL APPROACH

### 3.2.1 UAVSAR PolSAR

In a previous investigation of the 2009 and 2010 UAVSAR data, the USGS-NWRC focused on PolSAR change-detection patterns that could be caused by oil but, at the same time, were not due to flooding or changes in water levels. Water levels in the study area were recorded and documented (Ramsey et al., 2011). The change-detection patterns derived by USGS-NWRC were then used to separate changes in PolSAR backscatter intensity caused by marsh inundation as opposed to the potential impacts caused by the oil spill. Four different classifications of PolSAR backscatter intensity changes were used to evaluate marsh impacts after the oil spill, and to select the sampling sites for oil source-fingerprinting.

### 3.2.2 Sediment Sample Collection

Ramsey et al. (2011) used a total of four Barataria Bay UAVSAR flight lines to initially detect abnormal backscatter changes from pre- and post-spill PoLSAR data that were believed to be the result of the DWH oil spill. The pre-spill flight line was completed on June 17, 2009, almost one year earlier than the DWH oil spill; and the three post-spill flight lines were performed on June 23, 2010. The 2009 flight line was replicated as one of the three 2010 flight lines in the pre- and post-spill data set.

A total of 29 (12 shoreline, 15 interior, 1 nearshore, and 1 interior/shoreline) sediment samples were collected for oil source-fingerprinting by one year after MC252 oil impacted the Barataria Bay marshes in an effort to calibrate and validate the UAVSAR detection capabilities,. The sediment sampling sites were chosen based on where the largest changes were detected in pre- and post-spill PoLSAR backscatter data collected by the UAVSAR. Surface sediments were

collected from the top 15 centimeters (cm) and stored in pre-cleaned glass jars on ice until delivery to the laboratory. Samples were logged-in at the laboratory with unique laboratory identification numbers to track them through the entire extraction, analysis, and integration process without bias. Samples were stored in a freezer until the time of extraction.

### 3.2.3 Sample Analysis

Target petrogenic compounds and oil biomarkers (Table 3.1) were extracted from the sediment samples using EPA SW-846 Soxhlet extraction method 3540C (EPA, 2000). Samples were homogenized and approximately 30 grams (g) of subsamples were weighed, spiked with recovery standards (5-alpha androstane and phenanthrene-$d_{10}$, AccuStandard, Inc., New Haven, CT) at 20 $\mu g\ g^{-1}$, and dried by mixing with pre-cleaned anhydrous sodium sulfate (Fisher Scientific, Fair Lawn, NJ) in a pre-cleaned Soxhlet extraction thimble. Samples were extracted with dichloromethane (>99.9%, Avantor Performance Materials, Inc., Center Valley, PA) for a minimum of 12 hours. At the completion of the extraction procedure, sample extracts were filtered through pre-cleaned anhydrous sodium sulfate and concentrated (unless gross oil contamination was observed) to a final volume of 1-2 milliliters (mL) using rotary evaporation and nitrogen gas blow-down.

A chemical analyses of the sediment samples used gas chromatography/mass spectrometry operated in selected ion monitoring mode (GC/MS-SIM) and as described in Meyer et al. (2014), Ramsey et al. (2014), and Turner et al. (2014a,b). Samples were analyzed in three exclusive analytical batches, and each batch included a continuing calibration standard of a commercially available oil analysis standard (Absolute Standards, Inc., Hamden, CT), solvent and instrument blanks, and an extract of unweathered MC252 source oil (collected from a riser

pipe aboard the drillship *Discoverer Enterprise*, May 20, 2010) to ensure instrument performance and response sensitivity.

Table 3.1 Targeted Petroleum Hydrocarbon Analytes

| | | |
|---|---|---|
| Anthracene | Fluoranthene | C-1 Phenanthrenes/Anthracenes |
| Benz[a]anthracene | Fluorene | C-2 Phenanthrenes/Anthracenes |
| Benzo[a]pyrene | C-1 Fluorenes | C-3 Phenanthrenes/Anthracenes |
| Benzo[b]fluoranthene | C-2 Fluorenes | C-4 Phenanthrenes/Anthracenes |
| Benzo[e]pyrene | C-3 Fluorenes | Pyrene |
| Benzo[g,h,i]perylene | Indeno[1,2,3-cd]pyrene | C-1 Fluoranthenes/Pyrenes |
| Benzo[k]fluoranthene | Naphthalene | C-2 Fluoranthenes/Pyrenes |
| Chrysene | C-1 Naphthalenes | C-3 Fluoranthenes/Pyrenes |
| C-1 Chrysenes | C-2 Naphthalenes | C-4 Fluoranthenes/Pyrenes |
| C-2 Chrysenes | C-3 Naphthalenes | Saturate Hydrocarbons: |
| C-3 Chrysenes | C-4 Naphthalenes | $nC_{10}$-$nC_{35}$ |
| C-4 Chrysenes | Naphthobenzothiophene (NBT) | Oil Biomarkers: |
| Dibenz[a,h]anthracene | C-1 NBTs | Hopanes (*m/z* 191) |
| Dibenzothiophene (DBT) | C-2 NBTs | Diasteranes & Regular Steranes (*m/z* 217) |
| C-1 DBTs | C-3 NBTS | 14β(H)-steranes (*m/z* 218) |
| C-2 DBTs | Perylene | Triaromatic Steroids (*m/z* 231) |
| C-3 DBTs | Phenanthrene | |

The GC/MS analysis of the sediment extracts was on an Agilent (Santa Clara, CA) 6890N GC fitted with a 30 m x 0.25 mm x 0.25 μm ZB5-MSi (Phenomenex, Torrance, CA) fused silica capillary column and an Agilent 5973 MSD. An Agilent 7693 autosampler made splitless injections and the injector temperature was set at 280 ºC. The oven temperature was programmed from 60 to 280 ºC at 5 ºC $min^{-1}$, held at 280 ºC for 3 min, ramped to 300 ºC at 1.5 ºC $min^{-1}$, and held at 300 ºC for 2 min. The total run time was 65 minutes per sample.

The interface to the MS was maintained at 300°C and the MS quad and source temperatures were 140°C and 230°C, respectively. The MSD was operated at an ionization energy of 70eV in the selective ion monitoring (SIM) mode to ensure low level detection of the targeted oil analytes (i.e., each acquisition window was scanned at a rate greater than 1.4 scans $sec^{-1}$ with a dwell time of 60 milli-seconds).

### 3.2.4 Oil Source-Fingerprinting Using Diagnostic Biomarker Ratio Analysis

The normal alkane chromatograms of each sediment sample were first qualitatively checked for weathering (i.e., $C_{17}$/pristane and $C_{18}$/phytane ratios were examined and compared; presence of an unresolved complex mixture, or UCM), and oil biomarker chromatograms were checked for any characteristic features or differences that could eliminate MC252 as the source oil. The oil source-fingerprinting technique using diagnostic oil biomarker ratios, previously described in Chapter 2 herein and also in Meyer et al. (2014) and Ramsey et al. (2014), was used to determine whether MC252 oil was present in any of the 29 sediment samples. This technique generates 15 quantitative ratios that can be statistically analyzed and compared using repeatability limits, and the results extended to interpret potential oil contamination detected by the UAVSAR.

Table 3.2 gives the compound names, abbreviations, and ion group (e.g., *m/z* 191, 217, 218, and 231) of the 15 MC252 diagnostic ratios to which each sediment sample was compared. Table 3.3 provides the average (n=44) for each MC252 source oil ratio, and the corresponding %RSD. All diagnostic ratios chosen had a %RSD less than 5%, which is a quality criterion, because ratio averages higher than a fixed 5% RSD should not be used to analyze and compare oil samples in a forensic context (Hansen et al., 2007).

Table 3.2 Petroleum Biomarkers Used For Calculating MC252 Diagnostic Ratios

| Abbreviation | Compound Name | *m/z* Value |
|---|---|---|
| C27 Ts | C27 18α(H)-22,29,30-trisnorneohopane | 191 |
| C27 Tm | C27 17α(H)-22,29,30-trisnorhopane | 191 |
| C29 aB | C29 17α(H),21β(H)-30-norhopane | 191 |
| C29 Ts | C29 18α(H)-30-norneohopane | 191 |
| C30 aB | C30 17α(H),21β(H)-hopane | 191 |
| C31 aB (S+R) | C31 17α(H),21β(H)-22(S+R)-homohopane | 191 |
| C32 aB (S+R) | C32 17α(H),21β(H)-22(S+R)-bishomohopane | 191 |
| C33 aB (S+R) | C32 17α(H),21β(H)-22(S+R)-trishomohopane | 191 |
| C27D Ba-S | C27 13β(H),17α(H),20S-diasterane | 217 |
| C27D Ba-R | C27 13β(H),17α(H),20R-diasterane | 217 |
| C29D Ba-S | C29 24-ethyl-13β(H),17α(H),20S-diacholestane | 217 |
| C29D Ba-R | C29 24-ethyl-13β(H),17α(H),20R-diacholestane | 217 |
| C28 aaa-R | C28 24-methyl-5α(H),14α(H),17α(H), 20R-cholestane | 217 |
| C29 aaa-R | C29 24-ethyl-5α(H),14α(H),17α(H), 20R-cholestane | 217 |
| C27 BB (R+S) | C27 5α(H),14β(H),17β(H)-cholestane (20R+20S) | 218 |
| C28 BB (R+S) | C28 24-methyl-5α(H),14β(H),17β(H)-cholestane (20R+20S) | 218 |
| C29 BB (R+S) | C29 24-ethyl-5α(H),14β(H),17β(H)-cholestane (20R+20S) | 218 |
| C20 TA | C20-triaromatic steroid (pregnane derivative) | 231 |
| C21 TA | C21-triaromatic steroid (homopregnane derivative) | 231 |
| C26 TA-S | C26-triaromatic steroid,20S (cholestane derivative) | 231 |
| C28 TA-S | C28-triaromatic steroid,20S (ethylcholestane derivative) | 231 |
| C27 TA-R | C27-triaromatic steroid,20R (methylcholestane derivative) | 231 |
| C28 TA-R | C28-triaromatic steroid,20R (ethylcholestane derivative) | 231 |

Table 3.3 Average Diagnostic Ratios for MC252 Source Oil (n=44)

| Hopanes (m/z 191) | $\bar{x}_{MC252ratio}$ | $s_{ratio}$ | %RSD |
|---|---|---|---|
| C27 Ts/ C27 Tm | 1.26 | 0.04 | 3.1 |
| C29 aB/C29 Ts | 2.17 | 0.05 | 2.1 |
| C29 aB/C30 aB | 0.48 | 0.02 | 3.3 |
| C31 aB(S+R)/C32 aB(S+R) + C33 aB(S+R) | 0.93 | 0.02 | 2.1 |
| C32 aB(S+R)/C31 aB(S+R) + C33 aB(S+R) | 0.43 | 0.01 | 3.4 |
| C33 aB(S+R)/C31 aB(S+R) + C32 aB(S+R) | 0.28 | 0.01 | 4.2 |
| **Diasteranes and Regular 14α(H)-Steranes (m/z 217)** | $\bar{x}_{MC252ratio}$ | $s_{ratio}$ | %RSD |
| C27D Ba-S/C27D Ba-R | 1.61 | 0.03 | 1.8 |
| C29D Ba-S/C29D Ba-R | 1.63 | 0.05 | 2.7 |
| C28 aaa-R/C29 aaa-R | 0.74 | 0.02 | 2.2 |
| **14β(H)-Steranes (m/z 218)** | $\bar{x}_{MC252ratio}$ | $s_{ratio}$ | %RSD |
| C27 BB(R+S)/C28 BB(R+S) + C29 BB(R+S) | 0.69 | 0.02 | 2.8 |
| C28 BB(R+S)/C27 BB(R+S) + C29 BB(R+S) | 0.38 | 0.01 | 3.1 |
| C29 BB(R+S)/C27 BB(R+S) + C28 BB(R+S) | 0.46 | 0.02 | 3.5 |
| **Triaromatic Steriods (m/z 231)** | $\bar{x}_{MC252ratio}$ | $s_{ratio}$ | %RSD |
| C20 TA/C21 TA | 1.07 | 0.03 | 2.2 |
| C26 TA-S/C28 TA-S | 0.63 | 0.02 | 2.7 |
| C27 TA-R/C28 TA-R | 0.92 | 0.02 | 2.2 |

A repeatability limit ($\mathbf{r}_{95\%}$) determined the absolute and critical difference between the MC252 oil diagnostic ratio and the sediment sample diagnostic ratio. A final score for each sediment sample was calculated based on the number of matching diagnostic ratios per sample (e.g., # of matching sample ratios/15 total MC252 ratios * 100%). The final diagnostic ratio score was used to classify each sediment sample into one of four oil source-fingerprinting categories: 93-100% = match; 80-92% = probable match; 50-79% = inconclusive; and <50% = non-match (Meyer et al., 2014; Ramsey et al., 2014).

Because of the chronic oiling of southern Louisiana marshes, including Barataria Bay, two supplemental ratios based on area responses of the $C_2$ and $C_3$ alkyl dibenzothiophene (DBTs)

and phenanthrenes (Phens), $C_2$-DBTs/$C_2$-Phens and $C_3$-DBTs/$C_3$-Phens, were applied as a secondary fingerprinting measure for samples falling into the probable match and inconclusive categories, and have been used as source specific markers of oil in sediments (Overton et al., 1981; Wang et al., 1994; Douglas et al., 1996; Wang and Fingas, 2003; Hegazi and Andersson, 2007). The samples initially categorized either as a probable match or as inconclusive could be reclassified into the match category only if they met the following criteria: DBTs/Phens ratios were within ±5% of the MC252 DBTs/Phens ratios; and, they exhibited a qualitative positive match to MC252 oil.

## 3.3 RESULTS AND DISCUSSION

### 3.3.1 UAVSAR

The change-detection patterns to delineate marsh inundation and to predict areas where oil may have impacted inland marsh areas were derived from HH-intensity data and polarimetric decomposition (Ramsey et al., 2014). This process simplified the pre- to post-spill PolSAR backscatter mechanism change according to Ramsey et al. (2014). Figure 3.2 displays the sediment sample locations, oil source-fingerprinting results, and changes in the pre- to post-spill PolSAR backscatter mechanism. The darkest areas of Barataria Bay (black) denote no change in pre- to post-spill backscatter, and the dark grey shade represents changes that were not associated with possible oil impact. The white areas depict changes in backscatter mechanism due to oil impacted shorelines, and the light grey areas are interior marshes that experienced tidal flushing of waters containing surface oil. Shorelines with prominent pre- to post-spill changes were in agreement with locations identified by the SCAT-based assessments of oil impacted areas (Ramsey et al., 2014). Furthermore, the UAVSAR data displayed anomalies in some interior

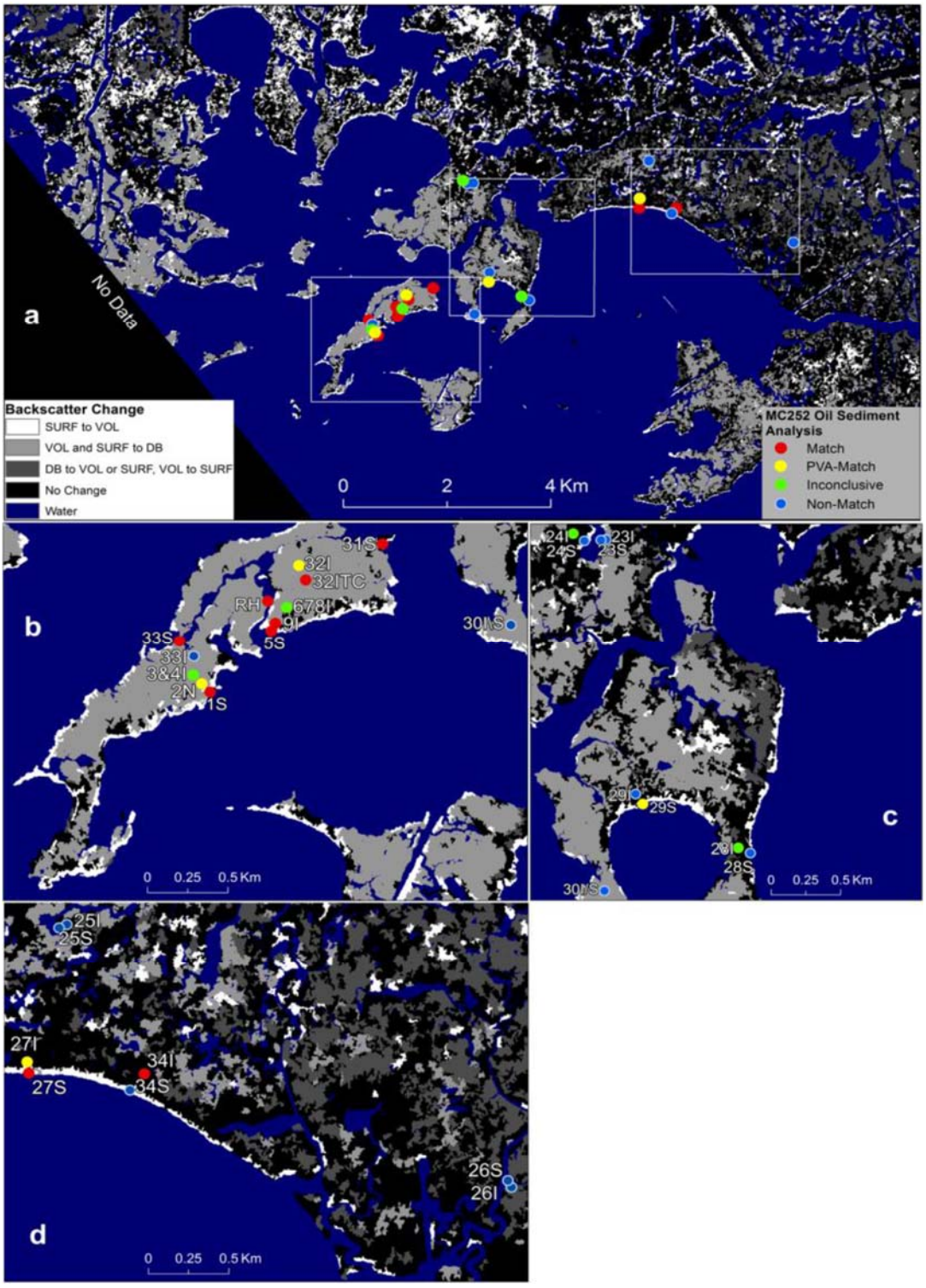


Figure 3.2 Pre- to post-oil spill PolSAR backscatter mechanism change, sediment sample locations, and fingerprinting results. Darker shades (black and dark grey) denotes no change and changes not associated with possible oil impact. White areas depict changes in backscatter associated with oil impacts, and light grey depicts marshes that experienced tidal flushing of waters containing surface oil. (Ramsey et al., 2014)

marshes up to 40 meters from the shoreline, which were concluded to be extremely low concentrations of oil brought by surface-water films and deposited onto the marsh subcanopy without any visual structural damage to the marsh vegetation (Ramsey et al., 2014).

### 3.3.2 Oil Source-Fingerprinting Using Diagnostic Biomarker Ratio Analysis

The diagnostic biomarker ratio analysis separated the 29 sediment samples into four oil source-fingerprinting categories: 7 match, 2 probable match, 8 inconclusive, and 12 non-match. The oil source-fingerprinting categories were determined by the score of each sediment sample that was calculated based on the total number of ratios that matched the MC252 ratios (i.e., critical difference did not vary more than 14%). Figure 3.3 provides a chromatographic comparisons of the normal alkane (*m/z* 57) profiles and diasteranes and regular steranes (*m/z* 217) profiles of samples in each oil source-fingerprinting category. Peak height integrations and signal-to-noise ratios were double checked for all samples that fell in the inconclusive and non-match categories. Corrections were made, if necessary, and the diagnostic ratio critical differences were re-calculated based on any corrections made. The results of the diagnostic ratio analysis (Table 3.4) were in good agreement with the pre- and post-spill PolSAR backscatter mechanism change categories depicted in Figure 3.2. The supplemental alkyl DBTs/Phens ratios moved samples 33 Shore and 34 Interior from the probable match to match category, resulting in a final total of: 9 match, 8 inconclusive, and 12 non-match.

Degradation of petroleum biomarkers has been documented by Wang et al. (2001), Aeppli et al. (2014), and Radović et al. (2014). The degree of degradation greatly depends on the environmental conditions where oil is deposited, and whether or not oil residues remain at the surface or if they are buried in anoxic conditions (i.e., coastal marsh environments). Aeppli et al.

(2014) demonstrated that the hopanes and triaromatic steranes in surface slicks and oiled samples collected on beaches were affected by biodegradation and photooxidation, respectively. Changes in the hopane and triaromatic steroid chromatographic profiles were observed in some of the sediment samples used here, particularly in samples falling in the inconclusive category. Therefore, the suite of diagnostic biomarker ratios can be expanded in future applications to include additional ratios within the diasterane and normal 14α(H)-steranes (*m/z* 217), and 14β(H)-steranes (*m/z* 218) biomarker groups.

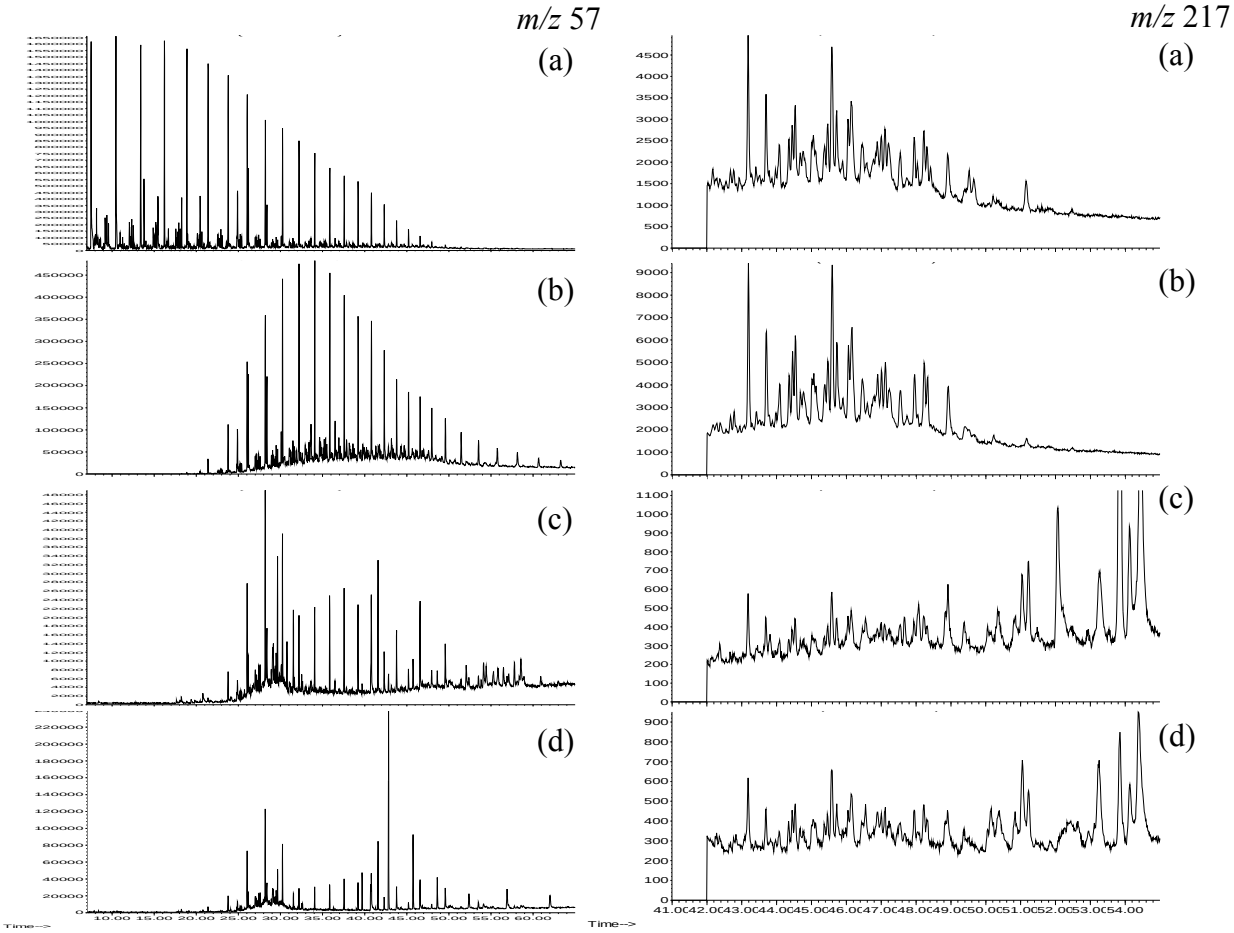


Figure 3.3 Chromatographic comparisons of the normal alkane (*m/z* 57) profiles (left) and diasteranes and regular steranes (*m/z* 217) profiles (right). (a) MC252 source oil, (b) Sample 5S, a match to MC252 source oil, (c) Sample 678I, inconclusive, and (d) Sample 26S, a non-match to MC252 oil.

Table 3.4 Oil Source-Fingerprinting Results*

| Sample | ∑Target PAHs (ng/g) | DR | Score | Oil Source-Fingerprinting Category |
|---|---|---|---|---|
| 1S | 480,000 | 15 | 100 | Match |
| 5S | 230,000 | 15 | 100 | Match |
| 9I | 5,700 | 15 | 100 | Match |
| RH-ITC | 66,000 | 15 | 100 | Match |
| 27S | 77,000 | 15 | 100 | Match |
| 31S | 470,000 | 15 | 100 | Match |
| 32ITC | 3,100 | 15 | 100 | Match |
| 33S | 2,400 | 13 | 87 | Match (Alkyl-homolog criteria met) |
| 34I | 780 | 12 | 80 | Match (Alkyl-homolog criteria met) |
| 24I | 270 | 11 | 73 | Inconclusive |
| 2N | 400 | 10 | 67 | Inconclusive (PVA-Match) |
| 32I | 910 | 10 | 67 | Inconclusive (PVA-Match) |
| 678I | 100 | 9 | 60 | Inconclusive |
| 28I | 180 | 9 | 60 | Inconclusive |
| 29S | 380 | 9 | 60 | Inconclusive (PVA-Match) |
| 3&4I | 270 | 8 | 53 | Inconclusive |
| 27I | 200 | 8 | 53 | Inconclusive (PVA-Match) |
| 25S | 110 | 7 | 47 | Non-match |
| 28S | 500 | 7 | 47 | Non-match |
| 23I | 260 | 6 | 40 | Non-match |
| 29I | 140 | 6 | 40 | Non-match |
| 33I | 78 | 4 | 27 | Non-match |
| 34S | 160 | 4 | 27 | Non-match |
| 24S | 120 | 3 | 20 | Non-match |
| 26S | 3,200 | 2 | 13 | Non-match |
| 30I\S | 60 | 2 | 13 | Non-match |
| 23S | 120 | 1 | 6.7 | Non-match |
| 26I | 81 | 1 | 6.7 | Non-match |
| 25I | 92 | 0 | 0 | Non-match |

* The sample names include designation of collection location type (e.g., S designates shore, I designates interior, ITC designates inland tidal channel, and N designates nearshore). ∑Target PAHs = the concentrations of targeted polycyclic aromatic hydrocarbons. DR = the number of diagnostic ratios that matched MC252 oil out of a possible total of 15.

The diagnostic biomarker ratios calculated herein are seemingly robust down to a concentration of ~200 parts per billion (ppb or ng $g^{-1}$) of the total target PAHs (Table 3.4). Samples with concentrations lower than this typically contained background hydrocarbon compounds. Polytopic vector analysis (PVA) was applied by USGS-NWRC after the diagnostic biomarker ratio analyses were completed to re-evaluate samples that were in the inconclusive category (Ramsey et al, 2014). The results of this multivariate analysis technique directly assessed the likelihood of each inconclusive sediment sample containing MC252 oil (Ramsey et al., 2014). Four of the eight inconclusive samples were considered to be a PVA match to MC252 oil (Table 3.4).

The statistical comparison of diagnostic ratios provided a robust quantitative evaluation of data; however, it is crucial that other qualitative (visual) evaluations and circumstantial evidence corroborate with the quantitative evaluations. It is important to note that the presence of petrogenic hydrocarbons did not necessarily mean that MC252 oil was present in the samples. These samples tended to have a bimodal profile and lacked the large unresolved complex mixture (UCM) that is indicative of weathered or degraded petroleum. The petrogenic content in the inconclusive samples were in low concentrations which could have affected the confidence level of the diagnostic ratios and, consequently, affected the oil source-fingerprinting categorization.

## 3.4 CONCLUSIONS

The oil source-fingerprinting of 29 sediment samples was essential in showing that significant changes in pre- to post-DWH oil spill PolSAR backscatter mechanisms were related to the presence of oil in Barataria Bay. Furthermore, the oil source-fingerprinting resulted in the

positive identification of MC252 oil in some of the sampled locations, demonstrating that oil-laden waters penetrated beyond visually observed shoreline oiling and into the nearshore and interior marshes (Ramsey et al., 2014).

The UAVSAR data collected during the DWH oil spill was very effective to detect and map oil spill deposited in the marsh subcanopy (Ramsey et al., 2014). What made the UAVSAR data unique and scientifically valuable was the fact that there were two data sets within one year of each other for the exact same area of the Mississippi River Delta. This allowed for the direct comparison of pre- and post-oil spill impacts on backscatter intensity within the study area and the similar timing minimized any phenological effects (Ramsey et al., 2011, 2014).

This collaborative research is an uncommon assimilation of environmental chemistry and quantitative oil source-fingerprinting, and the direct assessment of remote sensing of oil spill impacts. Application of a quantitative oil source-fingerprinting methodology was necessary to provide a quantitative assessment of the operational capabilities of the UAVSAR. On the whole, this collaborative research adds fundamental evidence that remote sensing, particularly PolSAR, can be successfully implemented in addition to visual observation techniques to detect and track oil in marshes after an oil spill (Ramsey et al., 2014).

## 3.5 LITERATURE CITED

Aeppli, C., Nelson, R.K., Radović, J.R., Carmichael, C.A., Valentine, D.L., and Reddy, C.M. 2014. Recalcitrance and degradation of petroleum biomarkers upon abiotic and biotic natural weathering of Deepwater Horizon oil. Environmental Science and Technology, 48:6726-6734.

Douglas, G.S., Bence, A.E., Prince, R.C., Mcmillen, S.J., and Butler, E.L. 1996. Environmental stability of selected petroleum hydrocarbon source and weathering ratios. Environmental Science and Technology, 30(7):2332-2339.

Fingas, M.F. and Brown, C.E. 2007. Oil spill remote sensing: a forensic approach. In: Zhendi Wang and Scott Stout, eds., *Oil Spill Environmental Forensics: Fingerprinting and Source Identification*. Burlington, MA: Academic Press, pp. 419-447.

Fingas, M.F. and Brown, C.E. 2011. Oil spill remote sensing. In: Merv Fingas, ed., *Handbook of Oil Spill Science and Technology*. Hoboken, New Jersey: John Wiley & Sons, Inc., pp. 313-356.

Hansen, A.B, Daling, P.S., Faksness, L., Sorheim, K.R., Kienhuis, P., and Duus, R. 2007. Emerging CEN Methodology for Oil Spill Identification. In: Zhendi Wang and Scott Stout, eds., *Oil Spill Environmental Forensics: Fingerprinting and Source Identification*. Burlington, MA: Academic Press, pp. 229-256.

Hegazi, A.H. and Andersson, J.T. 2007. Characterization of polycyclic aromatic sulfur heterocycles for source identification. In: Zhendi Wang and Scott Stout, eds., *Oil Spill Environmental Forensics: Fingerprinting and Source Identification*. Burlington, MA: Academic Press, pp. 147-168.

IPIECA-OGP. 2015. Aerial observation of oil spills at sea, OGP Report Number 518. [Online] Available from: http://www.ipieca.org/publication/aerial-observation-oil-spills-sea .

Jones, C.E., Minchew, B., Holt, B., and Hensley, S. 2011. Studies of the *Deepwater Horizon* oil spill with the UAVSAR radar. Monitoring and modeling the *Deepwater Horizon* oil spill: a record-breaking enterprise. Geophysical Monography Series, 195:33-50.

Meyer, B.M., Overton, E.B., and Turner, R.E. 2014. Oil source identification using diagnostic biomarker ratio analyses. Proceedings of the 2014 International Oil Spill Conference, 2014(1): 2064-2073. doi: 10.7901/2169-3358-2014.1.2064

Michel, J., Owens, E.H., Zengel, S., Graham, A., Nixon, Z., Allard, T., Holton, W., Reimer, P.D., Lamarche, A., White, M., Rutherford, N., Childs, C., Mauseth, G., Challenger, G., and Taylor, E. 2013. Extent and degree of shoreline oiling: *Deepwater Horizon* oil spill, Gulf of Mexico, 2010. PLoS ONE, 8(6):e65087. doi:10.1371/journal.pone.0065087

Overton, E.B., McFall, J.A., Mascarella, S.W., Steele, C.F., Antoine, S.A., Politezer, I.R., and Laseter, J.L. 1981. Identification of petroleum residue sources after a fire and oil spill. Proceedings of the 1981 International Oil Spill Conference, 1981(1):541-546.

Radović, J.R., Aeppli C., Nelson, R.K., Jimenez, N., Reddy, C.M., Bayona, J.M., and Albaigés, J. 2014. Assessment of photochemical processes in marine oil spill fingerprinting. Marine Pollution Bulletin, 79:268-277

Ramsey III, E., Rangoonwala, A., Suzuoki, Y., and Jones, C. 2011. Oil detection in a coastal marsh with polarimetric synthetic aperture radar (SAR). Remote Sensing, 3:2630-2662.

Ramsey III, E., Meyer, B.M., Rangoonwala, A., Overton, E., Jones, C.E., and Bannister, T. 2014. Oil source-fingerprinting in support of polarimetric radar mapping of Macondo-252 oil in Gulf Coast marshes. Marine Pollution Bulletin, 89:85-95.

Turner, R.E., Overton, E.B., Meyer, B.M., Miles, M.S., and Hooper-Bui, L. 2014a. Changes in the concentration and relative abundance of alkanes and PAHs from the *Deepwater Horizon* oiling of coastal marshes. Marine Pollution Bulletin, 86:291-297.

Turner, R.E., Overton, E.B., Meyer, B.M., Miles, M.S., McClenachan, G., Hooper-Bui, L., Summers Engle, A., Swenson, E.M., Lee, J.M., Milan, C.S., and Gao, H. 2014b. Distribution and recovery trajectory of Macondo (Mississippi Canyon 252) oil in Louisiana coastal wetlands. Marine Pollution Bulletin, 87:57-67.

U.S. Department of Commerce, National Oceanic and Atmospheric Administration, Office of Response and Restoration, Emergency Response Division. 2012. Open water oil identification job aid for aerial observation. [Online] Available from: http://response.restoration.noaa.gov/oil-and-chemical-spills/oil-spills/resources/open-water-oil-identification-job-aid.html .

U.S. Environmental Protection Agency. 2000. Test Methods for Evaluating Solid Wastes, Physical/Chemical Methods, SW-846. [Online] Available from: http://www.epa.gov/wastes/hazard/testmethods/sw846/online/index.htm . USEPA, Office of Solid Waste and Emergency Response, Washington, D.C.

Wang, Z., Fingas, M., and Sergy, G. 1994. Study of 22-year old *Arrow* oil samples using biomarker compounds by GC/MS. Environmental Science and Technology, 28(9):1733-1748.

Wang, Z., Fingas, M.F., Owens, E.H., Sigouin, L., and Brown, C.E. 2001. Long-term fate and persistence of the spilled *Metula* oil in a marine salt marsh environment: degradation of petroleum biomarkers. Journal of Chromatography A, 926:275-290.

Wang, Z.D. and Fingas, M. 2003. Development of oil hydrocarbon fingerprinting and identification techniques. Marine Pollution Bulletin, 47(9-12):423-452.

# CHAPTER 4: ADVANCED QUANTITATIVE OIL SOURCE-FINGERPRINTING OF LOUISIANA COASTAL MARSH SEDIMENTS COLLECTED FROM 2010-2015

## 4.1 INTRODUCTION

The magnitude of the *Deepwater Horizon* (DWH) oil spill has provided an opportunity to investigate quantitative oil source-fingerprinting techniques and to study the long-term effects of Gulf of Mexico coastal environments on the oil source-fingerprinting compounds, the oil biomarkers. Oil biomarkers are the compounds that typically suffer little interference from weathering and biodegradation effects because of their high molecular weights (Wang and Fingas, 1995; Peters et al., 2005; Wang et al., 2006; Hansen et al., 2007). The composition of crude oil in the environment, however, is continually being altered by a variety of biological, chemical and physical processes, and the culmination of these processes over many months to years could logically affect their usefulness.

The persistence of crude oil in some coastal salt marsh environments has been well documented (Teal et al.,1992; Reddy et al., 2002; Oudot and Chaillan, 2010; Lin and Mendelssohn, 2012; Natter et al., 2012). Coastal salt marshes tend to be low-energy and organic-rich environments with anoxic conditions, resulting in the preservation of some crude oil constituents, including the oil biomarkers. On the other hand, degradation of petroleum biomarkers in other environments was documented by Wang et al. (2001), Aeppli et al. (2014), and Radović et al. (2014). Wang et al. (2001) found that petroleum biomarkers were degraded upon exposure for 24 years in surface sediments in a salt marsh environment. Aeppli et al. (2014) found that after 4 years that homohopanes and triaromatic steroids in surface slicks and oiled samples collected on beaches were affected by biodegradation and photooxidation, respectively. Radović et al. (2014) demonstrated the profound effect of photooxidation on the

degradation of triaromatic steroids with laboratory irradiation experiments. The degradation of crude oil, therefore, greatly depends on the environmental conditions where oil is deposited and whether or not oil residues remain at the surface or if they are buried in anoxic conditions.

The differing potential for oil biomarker weathering will profoundly affect the calculation and subsequent critical difference analysis of diagnostic ratios used for oil source-fingerprinting. As a result, a more robust quantitative oil source-fingerprinting approach may be necessary. Chemometrics is an exploratory data analysis technique that recognizes patterns using multivariate pattern recognition algorithms and classifies samples into related groupings, often termed tribes and families (Peters et al., 2005; Peters et al., 2007; Peters et al., 2008; Lorenson et al., 2011; Peters et al., 2013). It is used extensively to interpret quantitative data of all varieties but is particularly common in the field of petroleum geochemistry to determine oil-oil and oil-source rock correlations (Peters et al., 2007; Peters et al., 2008; Peters et al., 2013). The field of petroleum geochemistry forms the foundation of the oil source-fingerprinting methods used currently during oil spills. The utilization of chemometrics as a quantitative oil source-fingerprinting technique is also a logical extension of this field into the realm of oil spills.

The two most common chemometric analyses are hierarchical cluster analysis (HCA) and principal component analysis (PCA). HCA groups samples based on cluster distance, which is a measure of similarity that accentuates the relationships among samples. A HCA also reveals samples that are contributing to a high variance. As a result, these samples can be excluded to improve the cluster results. A PCA simplifies a complex data matrix into a few components or factors to explain the majority of the variation in the data, while noise or irrelevant information comprises the remaining factors. A PCA also reveals samples that may be outliers. A visualization of data is a key component of chemometric analyses (Infometrix, 2014). Tribes and

families determined by a HCA are simply displayed in a dendrogram based on cluster distance and natural groupings that reveals similarities among samples. A PCA employs 2-D or 3-D scatterplots to graphically display significant differences between sample clusters and to evaluate the HCA groupings. Chemometric analysis, therefore, reduces complex data into interpretable patterns without any assumptions regarding the distribution of the data (Infometrix, 2014).

Both a diagnostic oil biomarker ratio analysis and a chemometric analysis were applied to 313 and 555 near-surface sediments, respectively, out of a total of 778 sediment samples that were collected in Louisiana coastal marshes from 2010 to 2015. The objectives of applying two different quantitative techniques were to determine which diagnostic ratios were most affected in coastal marsh sediments and to assess the effectiveness of chemometric analysis when used as a quantitative oil source-fingerprinting technique. The objectives for assessing the applicability of chemometric analysis as an oil source-fingerprinting technique included: differentiating crude oils from a common geographic origin (e.g., South Louisiana crude oils), and, determining a genetic similarity between oil residues in the sediment samples and MC252 oil. An extension of the second objective tested the ability of chemometrics to corroborate a postulated weathering pattern of MC252 diasteranes and regular steranes.

## 4.2 EXPERIMENTAL APPROACH

### 4.2.1 Sediment Sample Collection and Analysis

Sediment samples were collected throughout Louisiana coastal marshes from 2010 to 2015 and more detailed sample site information is provided in Turner et al. (2014b). Figure 4.1 shows the sediment sample collection sites through 2013, and all of these sites were sampled every year, and sometimes more than twice a year. Sediment samples were collected from the

top 5 centimeters (cm), stored in pre-cleaned amber glass jars on ice until delivery to the laboratory. At the laboratory, samples were logged-in and given unique laboratory identification numbers so that they could be tracked through the entire extraction, analysis, and integration process without bias. Samples were stored in a freezer, or refrigerator just prior to extraction.

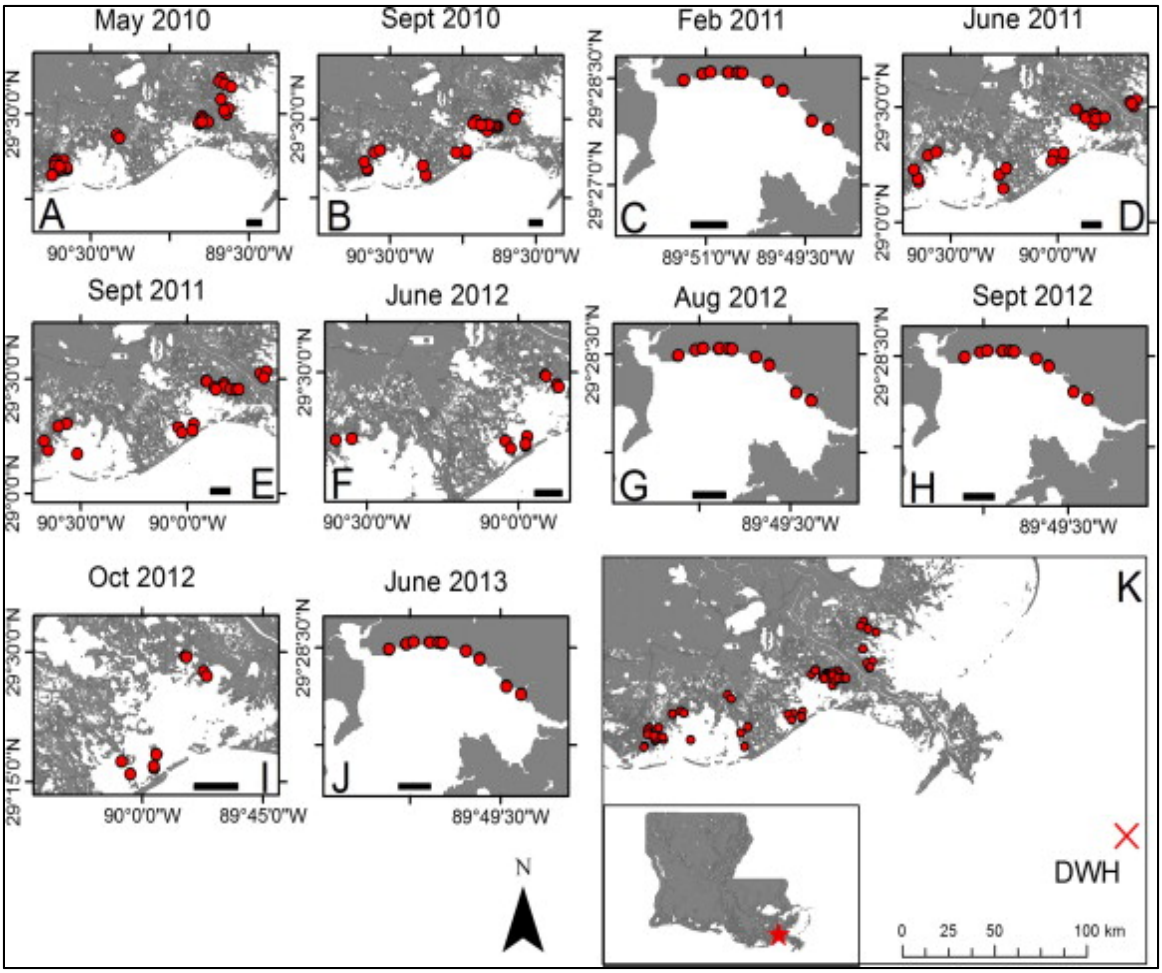


Figure 4.1 Sediment sample collection sites (Turner et al., 2014b).

Samples were extracted using either a Soxhlet or a pressurized speed extraction method. Samples from 2010 to late August 2013 were extracted using EPA SW-846 method 3540C, Soxhlet extraction (US EPA, 2000). These sediment samples were mixed with pre-cleaned

anhydrous sodium sulfate (10-60 mesh, certified ACS, Fisher Chemical, Fair Lawn, NJ), spiked with 1-mL surrogate standard, placed in a pre-cleaned extraction thimble, and Soxhlet extracted for 12-16 hours with dichloromethane (UltimAR®, Avantor Performance Materials, Center Valley, PA). At the completion of the Soxhlet extraction procedure the extraction solvent was concentrated, if necessary, to 1 to 2-mL. Samples collected after late August 2013 were extracted using a Buchi Speed Extractor E-916 (Buchi, New Castle, DE) and concentrated to 200-500 microliter (μL) final volume using a combination of a Buchi Syncore instrument and the Organomation Associates, Inc. (Berlin, MA), N-Evap 111, nitrogen evaporator.

The chemical analyses of all sediment samples was accomplished using gas chromatography/mass spectrometry operated in selected ion monitoring mode (GC/MS-SIM) Details of the GC/MS-SIM analysis are described in Meyer et al. (2014), Ramsey et al. (2014), and Turner et al. (2014a,b). The GC/MS instrumentation was tuned every 12 hours using perfluorotributylamine (PFTBA) to ensure optimum operational conditions. The inlet septa were changed prior to each instrument tune and inlet liners were replaced as necessary. Each analytical batch included a continuing calibration standard of oil analysis standard (Absolute Standards, Inc., Hamden, CT), an extract of unweathered MC252 source oil (from a riser pipe aboard the drillship *Discoverer Enterprise*, May 20, 2010), solvent blanks, and instrument blanks. All of these samples were used to ensure quality control of the instrumental acquisition process.

### 4.2.2 Diagnostic Biomarker Ratio Analysis

A total of 778 samples were qualitatively sorted into background versus oiled based on the total ion chromatogram (TIC), the normal alkanes, and oil biomarker profiles. Table 4.1

provides the results of this qualitative sort and Figure 4.2 displays the chromatographic differentiation between a background and oiled sample. The field identifications were excluded until after all data processing, including chemometric analysis, was finalized to minimize bias. After sorting, oiled samples were treated in two ways: (1) diagnostic oil biomarker ratio analysis, and (2) chemometric analysis using extracted ion chromatogram (EIC) peak intensity data. Oil biomarkers were targeted in both cases because they provide unique chemical fingerprinting information that can distinguish one oil from another, including oils with similar geographic origins (Wang and Fingas, 1995; Stout et al., 2002; Wang and Fingas, 2003; Peters et al., 2005).

Table 4.1 Distribution of Coastal Marsh Sediments After Qualitative Sort

| Year | Background | Oiled | Total |
|---|---|---|---|
| 2010 | 72 | 24 | 96 |
| 2011 | 87 | 91 | 178 |
| 2012 | 24 | 63 | 87 |
| 2013 | 85 | 64 | 149 |
| 2014 | 51 | 85 | 136 |
| 2015 | 55 | 77 | 132 |
| | | TOTAL | 778 |

Diagnostic oil biomarker ratios were calculated for a total of 313 oiled sediment samples as long as peak heights met the three times the signal-to-noise ratio criteria. Based on the qualitative sort and the evidence of homohopane and triaromatic steroid biomarker weathering (Aeppli et al., 2014; Radović et al., 2014), five new ratios within the diasteranes and regular steranes (*m/z* 217) and 14β(H)-steranes (*m/z* 218) were determined and tested using the same forty-four MC252 analyses described in Chapter 2, bringing the total number of MC252

diagnostic ratios to 20. Each of the new MC252 steranes ratios chosen were averaged and the standard deviation calculated. The %RSD had to meet the <5% relative standard deviation (%RSD) criteria.

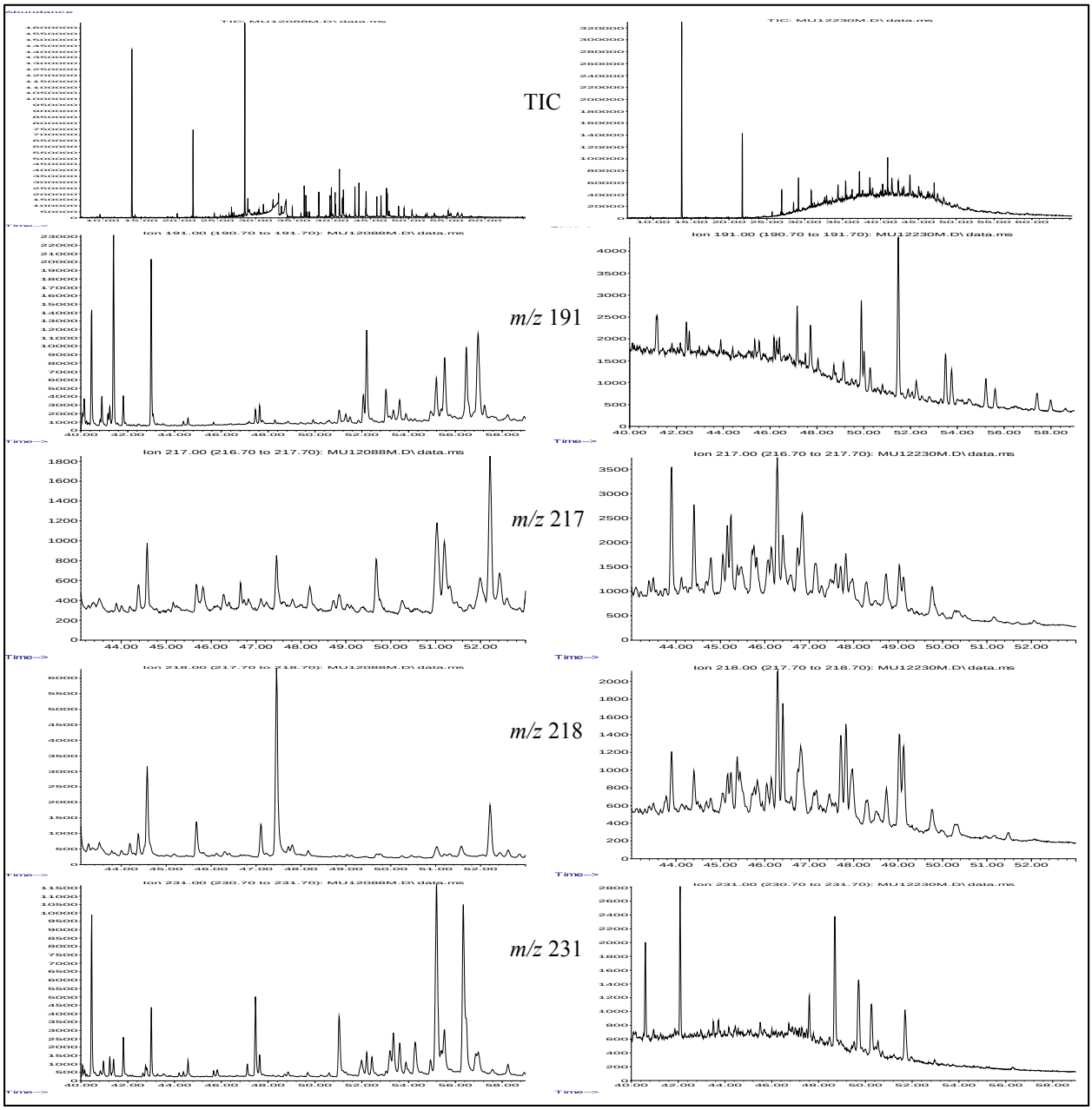


Figure 4.2 Example of background (left) and oiled (right) sediment samples.

Table 4.2 provides the compound names, abbreviations, and ion groups utilized to establish the new ratios. Only two of the compounds listed in Table 4.2 (C29 24-ethyl-5α(H),14β(H),17β(H),20R-cholestane and C29 24-ethyl-5α(H),14β(H),17β(H),20S-cholestane) are new, and the peak heights of the remaining compounds were already determined in the original 15 diagnostic biomarker ratio suite. Table 4.3 provides the averages (n=44), standard deviation, and %RSD for the five new ratios. Any diagnostic biomarker ratios exceeding the critical difference criteria were recorded and the ratios with the highest percentage of non-match to the average MC252 ratios were used to determine how the coastal marsh environment has affected the biomarker compounds.

Table 4.2 Diasteranes and Regular Steranes, and 14β(H)-steranes Used to Calculate New Diagnostic Biomarker Ratios

| Abbreviation | Compound Name | *m/z* Value |
|---|---|---|
| C29 aaa-R | C29 24-ethyl-5α(H),14α(H),17α,20R-cholestane | 217 |
| C29 aaa-S | C29 24-ethyl-5α(H),14α(H),17α,20S-cholestane | 217 |
| C29D BB-R | C29 24-ethyl-5α(H),14β(H),17β(H),20R-cholestane | 217 |
| C29D BB-S | C29 24-ethyl-5α(H),14β(H),17β(H),20S-cholestane | 217 |
| C27 BB-R | C27 5α(H),14β(H),17β(H),20R-cholestane | 218 |
| C27 BB-S | C27 5α(H),14β(H),17β(H),20S-cholestane | 218 |
| C28 BB-R | C28 24-methyl-5α(H),14β(H),17β(H),20R-cholestane | 218 |
| C28 BB-S | C28 24-methyl-5α(H),14β(H),17β(H),20S-cholestane | 218 |
| C29 BB-R | C29 24-ethyl-5α(H),14β(H),17β(H),20R-cholestane | 218 |
| C29 BB-S | C29 24-ethyl-5α(H),14β(H),17β(H),20S-cholestane | 218 |

Table 4.3 Average of New MC252 Diasteranes and Regular Steranes, and 14β(H)-steranes Diagnostic Biomarker Ratios

| Diasteranes and Regular 14a(H)-Steranes (m/z 217) | $\bar{x}_{MC252ratio}$ | $s_{ratio}$ | %RSD |
|---|---|---|---|
| C29 aaa-S/C29 aaa-R | 1.04 | 0.04 | 3.1 |
| C29D BB-R/C29D BB-S | 1.40 | 0.02 | 1.7 |
| **14B(H)-Steranes (m/z 218)** | $\bar{x}_{MC252ratio}$ | $s_{ratio}$ | %RSD |
| C27 BB-R/C27 BB-S | 1.39 | 0.04 | 3.0 |
| C28 BB-R/ C28 BB-S | 0.92 | 0.02 | 2.5 |
| C29 BB-R/C29 BB-S | 1.15 | 0.03 | 4.0 |

### 4.2.3 Chemometric Analysis of South Louisiana Crude Oils

Extracts of eight (8) different South Louisiana crude oils and one extract of Alaskan North Slope crude oil were analyzed by GC/MS and the data were converted to determine if chemometric analysis could differentiate between source oils from the same geographic origin area. The Alaskan North Slope crude, originating from a totally different geographic origin, was included as a positive control. The source oils have been preserved and archived at the Louisiana State University, Department of Environmental Sciences, Response and Chemical Assessment Team (LSU-RCAT) laboratory, and most were collected as part of LSU-RCAT's response to other oil spills throughout the years. Other source oils (e.g., EPA South Louisiana crude) were provided as standard reference materials for various oil spill related research.

After the GC/MS analysis, the ion chromatograms were then extracted for the hopanes (*m/*z 191), steranes (*m/z* 217 and 218), and triaromatic steroids (*m/z* 231) within the time range of 40 to 59 minutes. The extracted ion chromatograms (EIC) of the biomarkers were merged and exported to a spreadsheet. This resulted in peak intensity data points recorded approximately every 10 milliseconds within the 40 to 59 minute range of the instrumental data acquisition for

each EIC. The EIC peak intensity data was used after initially testing the total ion chromatogram (TIC) peak intensity data. The disadvantage of using the TIC peak intensity data was that it included not just the biomarker compounds, but also any alkanes, PAHs, and internal standards. Extracting the peak intensity data for just the biomarker compounds decreased interference from these compounds and increased the effectiveness of the chemometric analysis.

Once exported, the peak intensity data for all four biomarker EIC were summed (combined EIC = *m/z* 191 + *m/z* 217 + *m/z* 218 + *m/z* 231) for each source oil, and a separate spreadsheet was created for only the *m/z* 217 (217 only) peak intensity data. Isolating the *m/z* 217 EIC allowed for the testing the postulated weathering pattern. The original EIC time range was limited to 43 to 53 minutes for the *m/z* 217 by deleting peak intensity data that were outside of this range. The peak intensity data were transferred into the chemometric software package Pirouette ® (Infometrix, Bothell, WA) for subsequent HCA and PCA analysis.

The Pirouette® parameters included mean-center pre-processing and two data transforms (baseline correction-quadratic fit and divide by sample 1-norm). Mean-center pre-processing situates the plot origin at the center of the data. The baseline correction transform corrects offsets in the data by subtracting a profile derived from a quadratic fit of the data, while the divide sample by 1-norm transform is equivalent to area normalization. The effects of the baseline correction and area normalization are displayed in Figure 4.3. The data transforms (right side of Figure 4.3) result in a decrease in the noise and adjusts the baseline so that all peak intensity variables are similarly contributing to the distance measurements.

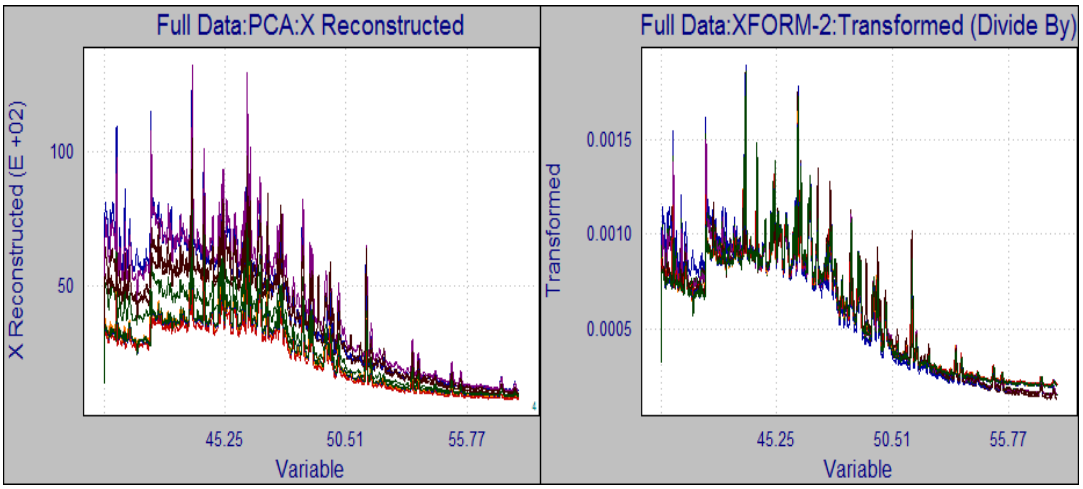

Figure 4.3 Comparison of raw (left) and transformed (right) peak intensity data.

The HCA analysis used incremental linkage and distance measure was set to Euclidean. Both the linkage and measure parameters use a sum of squares approach (i.e., a measure of deviation from the mean) in calculating inter-cluster distances. Clustering in Pirouette® is agglomerative meaning that each sample starts as its own cluster. Pirouette® calculates distances between all pairs of samples in a similarity matrix and links the 2 most similar samples. Inter-sample distances are then transformed into a scale similarity from 1 to 0 using Equation 4.1 below, where $d_{ab}$=distance between two samples and $d_{max}$=largest distance in the data set (Infometrix, 2014). Once a cluster is linked to another cluster, they form a single new cluster. The smallest inter-cluster distance is again sought and another linkage is formed (Infometrix, 2014). This process continues until all samples are part of a single cluster.

Equation 4.1 $$Similarity_{ab} = 1 - \frac{d_{ab}}{d_{max}}$$

The horizontal axis equals the distance between clusters in the HCA dendrograms to follow. The length of the horizontal lines, called branches, extending from each cluster is related to similarity. The longer the branch, the less similar the clusters are, and vice versa (Infometrix, 2014). Individual samples, called leaves, are displayed on the far left of the dendrogram, and clusters, whether they are by tribe or family, are determined by moving the similarity line (i.e., the vertical line in the dendrograms). The similarity line for each analysis was set qualitatively based on the initial clustering in the sample set and was adjusted after viewing the clustering in the 2-D PCA plot and comparing cluster distances in the dendrogram. The similarity line was adjusted to a point where there were any sudden increases (i.e., larger distance measures) among the clusters within the major tribes of samples.

The 2-D PCA plots (shown to the right of the HCA dendrograms in the figures to come) displays important relationships among samples. They were used to confirm outliers (i.e., any samples outside of the 95% sample distribution ellipse) (Infometrix, 2014). Cluster locations in any of the four quadrants of the 2-D scatterplot determines which samples are similar and which are not. For example, a cluster of samples in the top half of the 2-D PCA scatterplot is less similar to a cluster of samples that are in the bottom half of the plot; or, a cluster of samples in the top, left quadrant of the 2-D PCA scatterplot is less similar to a cluster of samples in the bottom, right quadrant of the plot. The axes in the plot represent the two principal components that have the optimal variance among inter-sample relationships (Infometrix, 2014). PCA removes irrelevant or random variation by retaining only the principal components that capture relevant information based on different linear combinations of the original variables. None of the original variables are removed from the PCA, just certain linear combinations are discarded after the relevant principal components are determined (Infometrix, 2014).

### 4.2.4 Chemometric Analysis of Coastal Marsh Sediments

The combined EIC and *m/z* 217 peak intensity data for a total of 555 coastal marsh sediment samples underwent a chemometric analysis in Pirouette®. The combined EIC peak intensity data for samples collected in 2010-2012 was generated for all samples (e.g., background and oiled samples) to validate the differentiation capabilities of the pattern recognition algorithm. Samples for these years was also processed without the background samples. Exclusion of the background samples eliminated their contribution to the variation used for calculating cluster distances. A chemometric analysis for samples collected in 2013-2015 included only oiled sediments. Two comparable instrument systems were used to analyze these samples over the six years of collection. Despite their identical acquisition methodologies, the extracted peak intensity data did not align; therefore, data from each instrument were analyzed and interpreted separately. Each analysis in Pirouette® included EIC peak intensity data for MC252 source oil extracts (a QC sample) analyzed in the same analytical batch to minimize effects of instrument variability.

### 4.2.5 Chemometric Differentiation of Biomarker Weathering Patterns

The qualitative analysis of the EIC for all the oiled sediment samples has led to a postulated weathering pattern of MC252 diasteranes and regular steranes (Figure 4.3). Having a mathematical relationship developed from a chemometric analysis would validate this proposed MC252 diasteranes and regular steranes weathering pattern. The *m/z* 217 peak intensity data previously separated from the combined EIC data was, therefore, processed separately in Pirouette®. Furthermore, data from the background samples were excluded from the *m/z* 217 analysis because the primary focus was on changes occurring within an oil fingerprinting pattern.

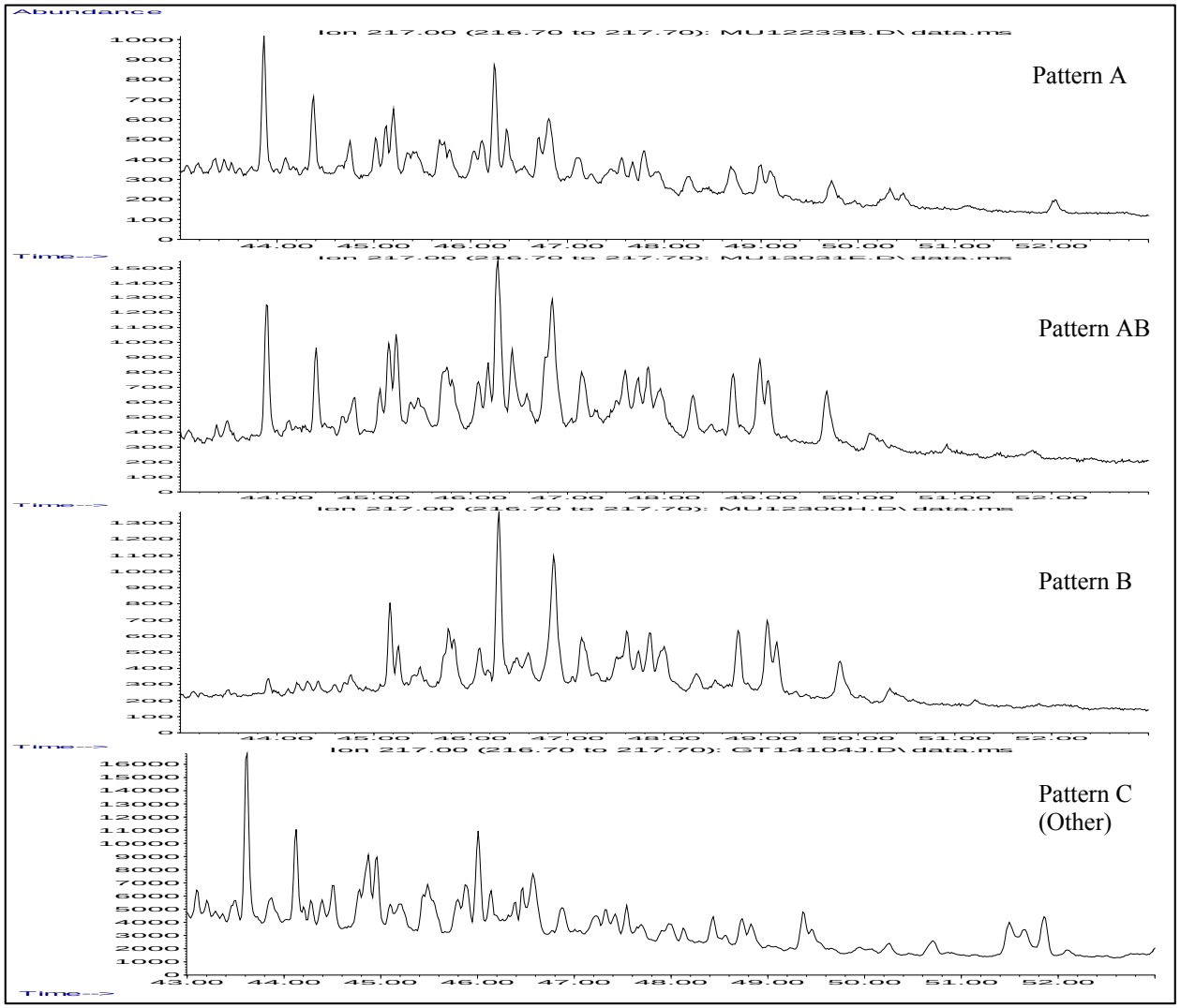


Figure 4.4 Postulated weathering of MC252 diasteranes and regular steranes. (Pattern A=fairly fresh MC252 steranes; Pattern AB=slightly weathered MC252 steranes; Pattern B=weathered MC252 steranes; and, Pattern C=other)

## 4.3 RESULTS AND DISCUSSION

### 4.3.1 Diagnostic Biomarker Ratio Analysis

Figure 4.5 displays the 20 diagnostic biomarker ratios tested by each year and by the percentage of samples that had that particular ratio exceeding the critical difference (CD) allowance stipulated by the diagnostic ratio analysis in Chapter 2. The data from 2010 and one

data set from 2011 (LSU ID# 2011039) were analyzed before the addition of *m/z* 218 or *m/z* 231 to the GC/MS acquisition methodology. Only the hopane and diasterane and regular sterane ratios are included for these data sets in the figure. The ratios in all four biomarker groups were eventually affected by weathering, assuming that any oil in the samples was MC252 oil. The fact that this particular area of Louisiana is chronically oiled cannot be ignored. However, it is not unreasonable to assume that oil detected in the sediment samples is MC252 oil because of the volume of oil spilled during the DWH spill. Furthermore, oil mitigation and/or cleanup of Louisiana marsh shorelines amounted to approximately 9% of the 1773 kilometers of Gulf of Mexico shoreline that were oiled (Michel et al., 2013). The coastal marsh sediment sample locations, therefore, were chosen because of prominent oiling after DWH (Turner et al., 2014b). Additionally, PolSAR remote sensing data presented in Chapter 3 detected oil in a post-DWH flight line that was determined to be MC252 based on diagnostic ratio analysis.

Clearly, the 14β(H)-steranes and the triaromatic steroids were the most affected ratios, with 6 of the 9 ratios between these two biomarker groups having over 50% of the samples exceeding the CD criteria (Figure 4.5). Only one of the 14β(H)-steranes ratios (C29 BB-R/C29 BB-S) remained unaffected where only 3% of samples from 2011 exceeded the CD for this ratio. The hopane ratios incorporating the homohopanes that had the highest percentage of samples exceeding the CD criteria, and corroborated the findings of Aeppli et al. (2014). Less than 20% of samples from 2010-2015 for the other hopane ratios exceeded the CD limit. Two of the diasterane and regular sterane ratios (C28 aaa-R/C29 aaa-R and C29 aaa-S/C29 aaa-R) were also affected. The average percent of samples exceeding the CD were 45% and 23%, respectively, for these two ratios.

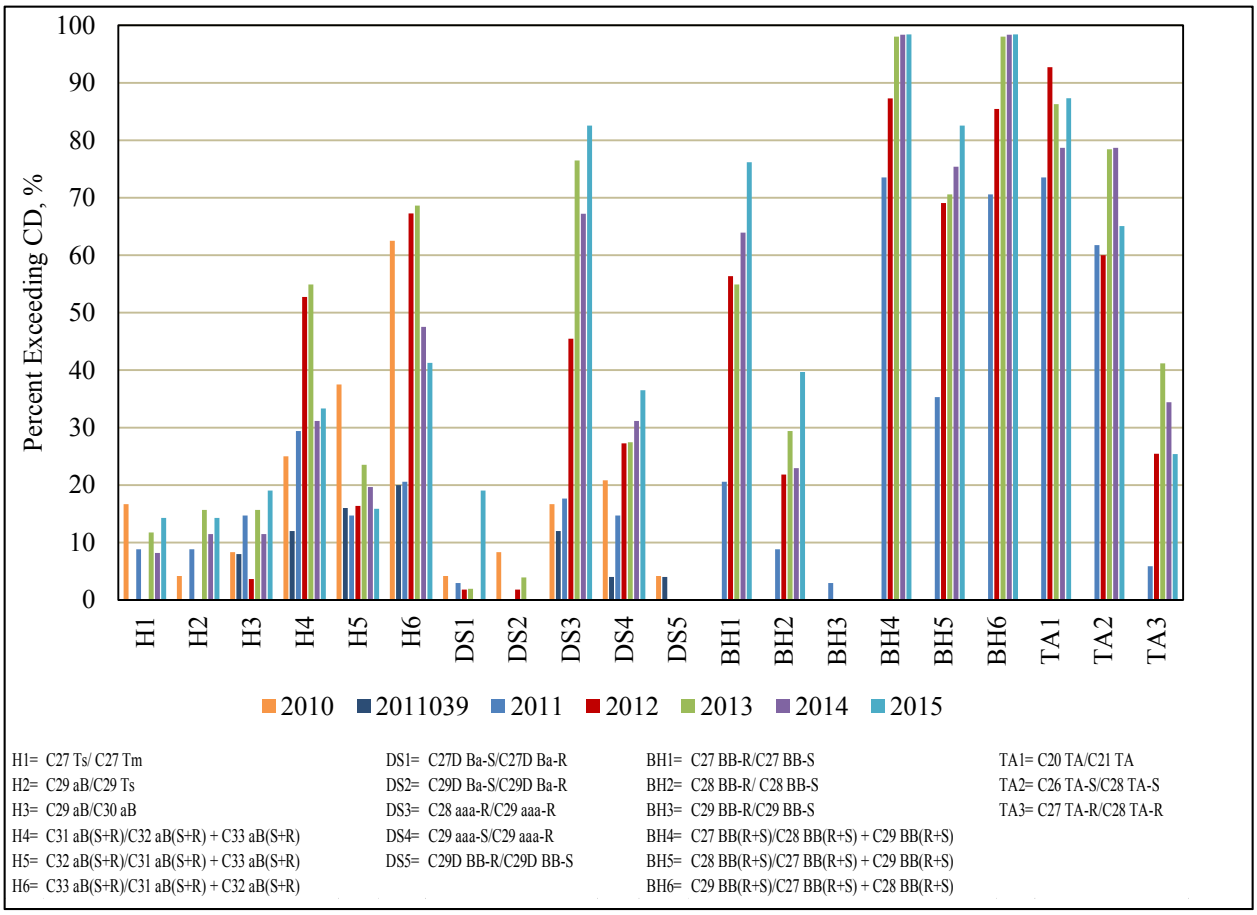


Figure 4.5 Percentage of samples exceeding the diagnostic ratio critical difference (CD) allowance.

One ratio within *m/z* 217 (29D BB-R/C29D BB-S) remained relatively unchanged for all years, where both 2010 and the data set with LSU ID# 2011039 had only 4% of samples exceeding the CD. The CD limit for this ratio was not exceeded after 2011. The second relatively stable *m/z* 217 ratio (C29D Ba-S/C29D Ba-R) had 2% of samples from 2012 and 4% of samples from 2013 exceed the critical difference limit. A third *m/z* 217 ratio (C27D Ba-S/C27D Ba-R) also remained relatively unaffected until 2015 (i.e., all years except 2015 had less than 20% of samples affected).

### 4.3.2 Chemometric Analysis of South Louisiana Crude Oils

The following four figures display the Pirouette® analysis results of the quadruplicate analyses of the eight (8) different South Louisiana crude oils, including MC252, and the Alaskan North Slope crude oil used as a positive control. The first two figures (Figures 4.6 and 4.7) display the tribes among the sample set. The tribes were the result of setting the similarity line (the dashed, vertical line) at 0.400 where 3 different tribes are visually evident in both the combined EIC peak intensities (Figure 4.6) and the *m/z* 217 only peak intensities (Figure 4.7). Clusters were more inclusive at the tribal level, and families were visually apparent within the tribes (i.e., in the HCA plot of Figure 4.6, there are 3 families within the large blue tribe).

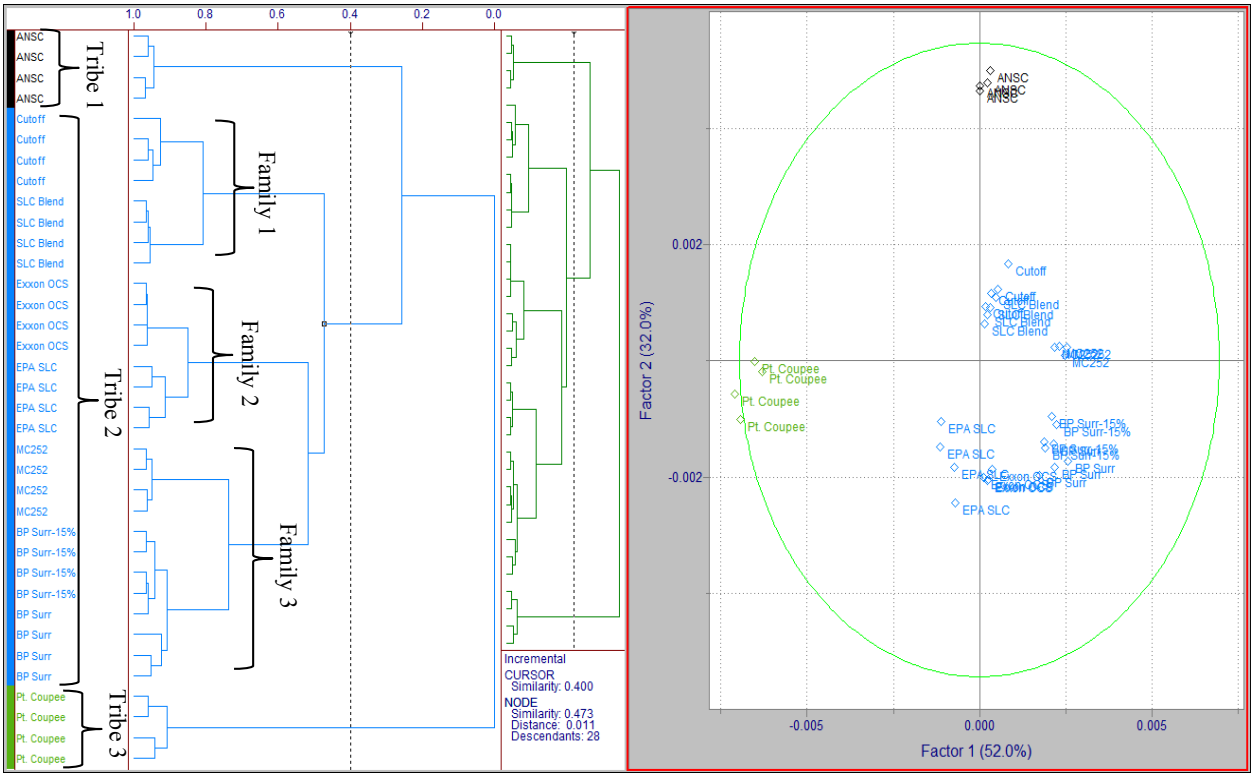


Figure 4.6 The HCA (left) and PCA (right) plots of source oil tribes from the combined EIC peak intensity data with the similarity line at 0.400.

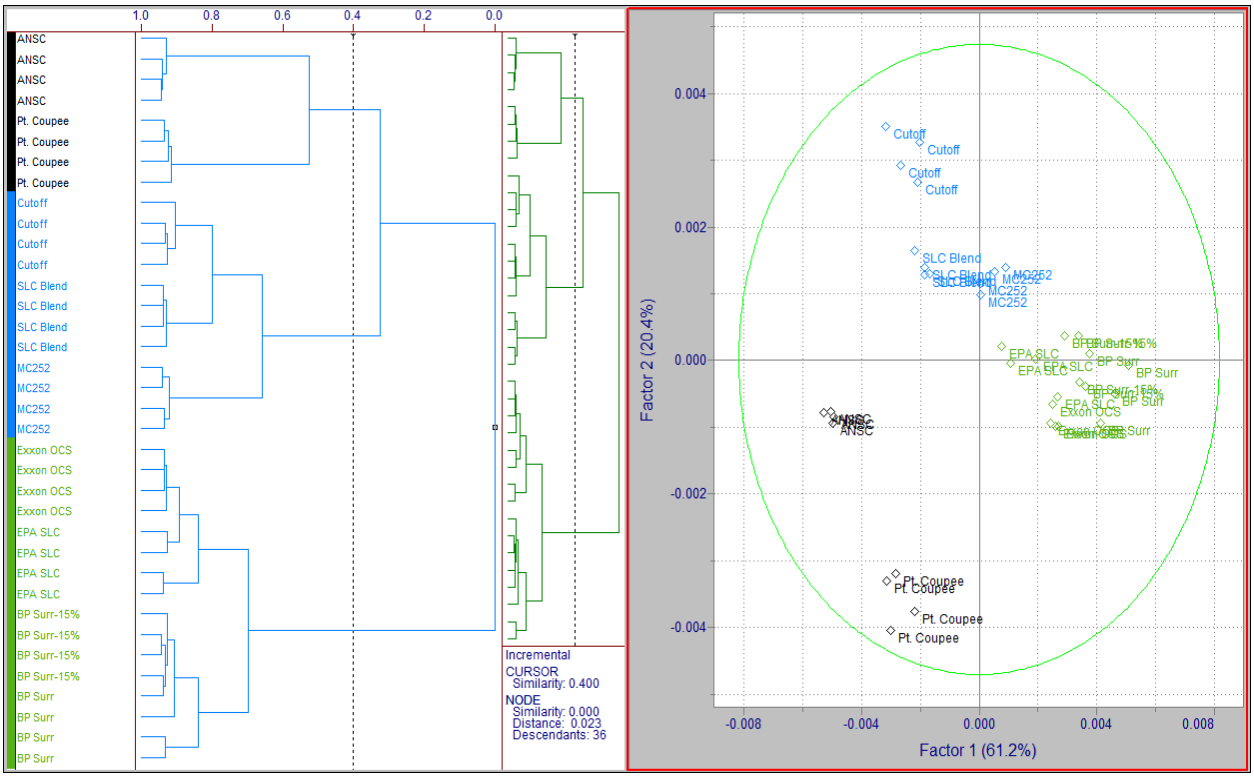


Figure 4.7 The HCA (left) and PCA (right) plots of source oil tribes from the *m/z* 217 peak intensity data with the similarity line at 0.400.

The 2-D PCA plot at the tribe level does not provide differentiation among source oils that are in different quadrants of the plot (e.g., SLC Blend and BP surrogate oil). As a result, the similarity line was moved to 0.700 and 0.701 in Figures 4.8 (combined EIC) and 4.9 (*m/z* 217), respectively. Moving the similarity line resulted in improved differentiation of source oils in the 2-D PCA plots in Figure 4.8 and 4.9. This was evident because the SLC Blend and BP surrogate oil clusters were in different families. There were five families in Figure 4.8 and six families in Figure 4.9. Branching among families was used to determine if the similarity line required adjustments. The similarity line was unadjusted if the branching among families had similar cluster distances (indicating similarity between the clusters). The similarity line was adjusted if the distance of the branching among families was long (indicating less similarity) and if the

relationship among other clusters was not compromised. For example, the green and purple clusters in Figure 4.9 are within one family. The branch for the green cluster, however, is longer than the branch of the purple cluster, indicating that even though they are in the same family, these two clusters have some dissimilarity. On the other hand, the orange cluster in Figure 4.9 has two families, but the branches are about equal, indicating that these two families are similar. A total of 1275 and 638 variables were analyzed for the combined EIC and *m/z* 217 peak intensities, respectively. The variables are the peak intensities recorded approximately every 10 milliseconds for the given EIC time range.

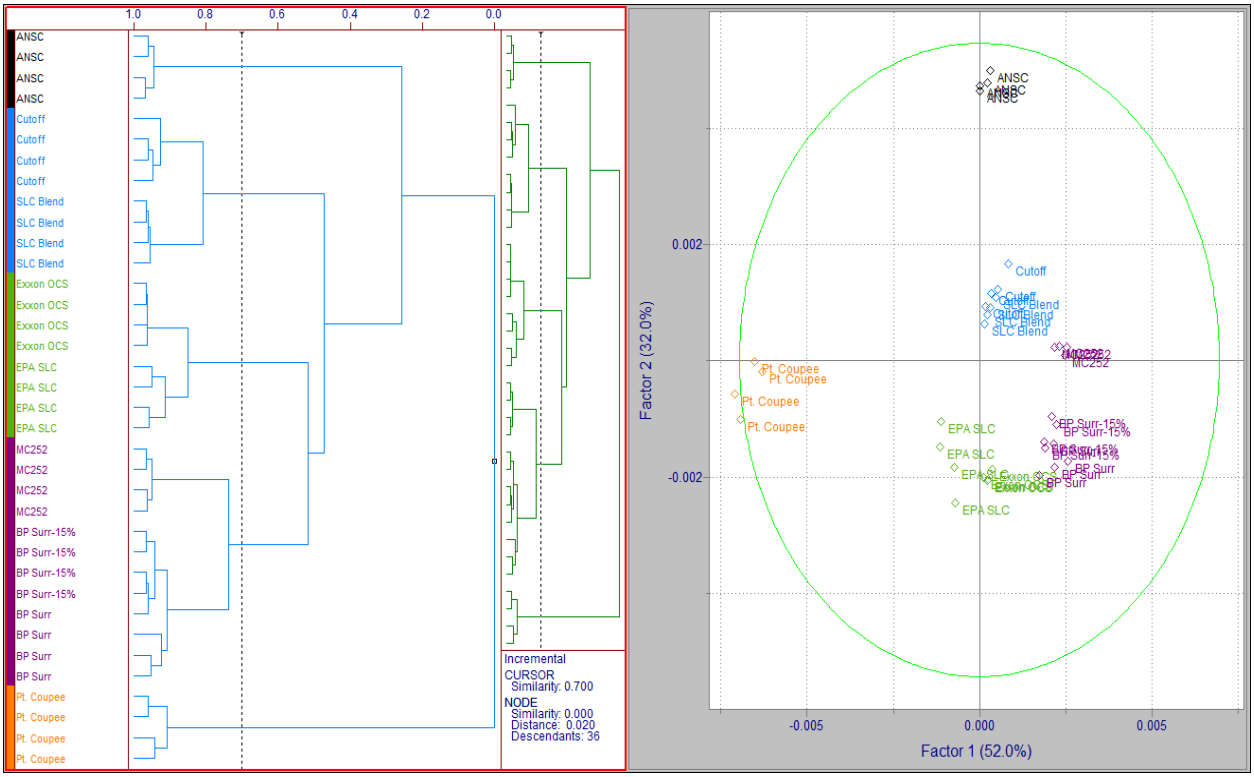


Figure 4.8 The HCA (left) and PCA (right) plots of source oil families from the combined EIC peak intensity data with the similarity line at 0.700.

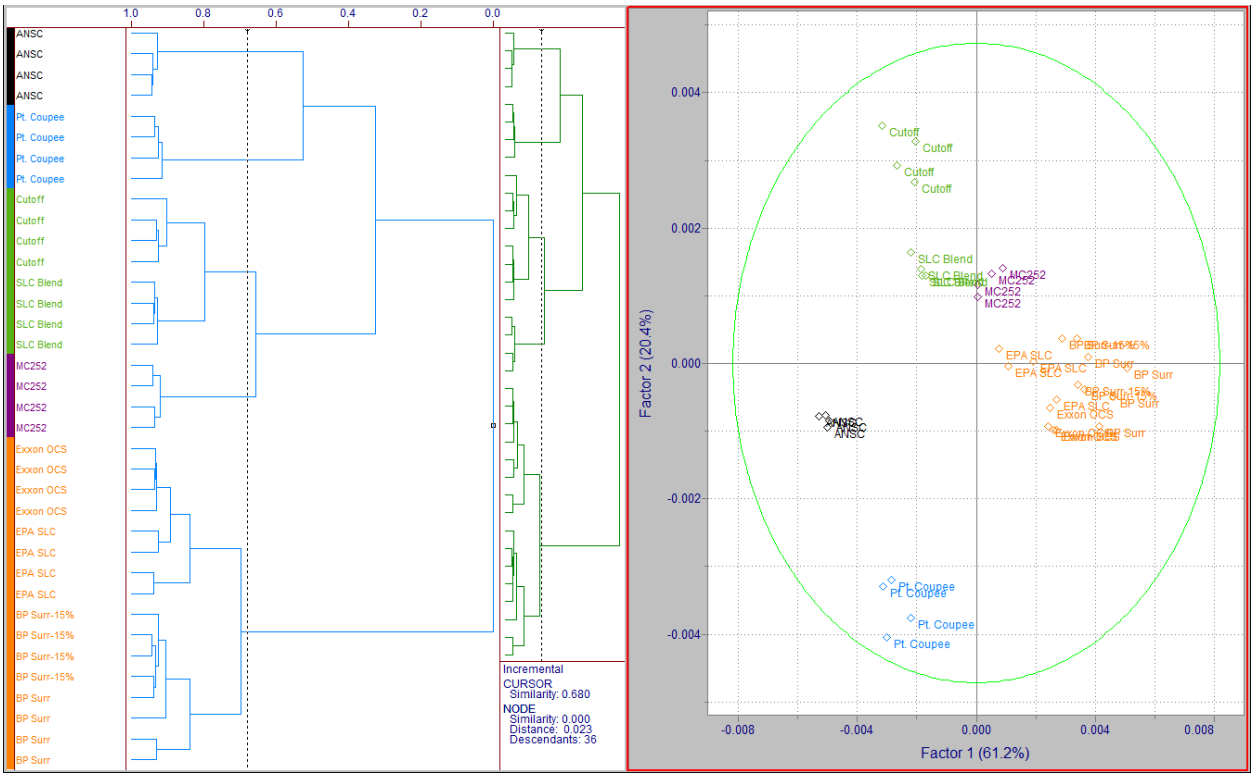


Figure 4.9 The HCA (left) and PCA (right) plots of source oil families from the *m/z* 217 peak intensity data with the similarity line at 0.680.

In Figure 4.8, MC252 source oil clusters with the Marlin Platform oil (VK915) from the Dorado field using the combined EIC peak intensity data, indicating similarity in their biomarker families. The Marlin platform oil was chosen as a surrogate oil because of its similarity to MC252, and as reported in Chapter 2, it would be considered a match to MC252 oil with a diagnostic biomarker ratio score of 14/15, or 93%. The 15% weathered (by weight) Marlin oil also clusters with MC252 source oil in Figure 4.8. This source oil was considered a probable match to MC252 source oil based on a diagnostic biomarker ratio score of 13/15, or 87%. The Point Coupee pipeline source oil was distinctly dissimilar from the other South Louisiana crude oils. It was in its own cluster in the HCA dendrogram and its cluster position was distinctly separated in the 2-D PCA plot. The Alaskan North Slope crude, the positive control, was also

distinctly dissimilar from all the South Louisiana crude oils. It was in its own cluster in the HCA dendrogram and its cluster position is also distinctly separated in the 2-D PCA plot.

The *m/z* 217 peak intensity data (Figure 4.9) displays some different clustering of the South Louisiana crude oils. The MC252 oil, at this similarity level, is in its own cluster, which is reasonable because of its cluster distance compared to other cluster in this family (i.e., the green cluster), and its position relative to the other South Louisiana crude oils in the 2-D PCA plot. The Point Coupee pipeline source oil and the Alaskan North Slope source oil were again distinctly dissimilar from all the other source oils. The biomarker EIC profiles for all source oils, including MC252, are provided in Appendix C.

Figure 4.10 is a plot of the HCA cluster distances determined from the combined EIC peak intensities of all the source oils. Cluster distance is related to similarity and is indicated by the horizontal length of the branches in the HCA dendrogram. The longer the branch linking the clusters, the less similar, and the shorter the branch, the more similar. The same is true for the branches within the clusters. The connectivity of the various branches is a function of the linkage method (Infometrix, 2014).

Clearly in Figure 4.10, the Pt. Coupee cluster is the most dissimilar of the source oils since it has the longest Euclidean distance. All of the other oils are more similar based on distance; however, are distinct enough to be in their own clusters. Figure 4.11 displays the source oil cluster distances based on the *m/z* 217 only peak intensity data. The Alaskan North Slope and the Pt. Coupee pipeline source oils have higher cluster distances and are less similar to the other source oils. The MC252 source oil has a cluster distance in Figure 4.11 that is lower (less similar) than the other South Louisiana crudes in the green and orange clusters.

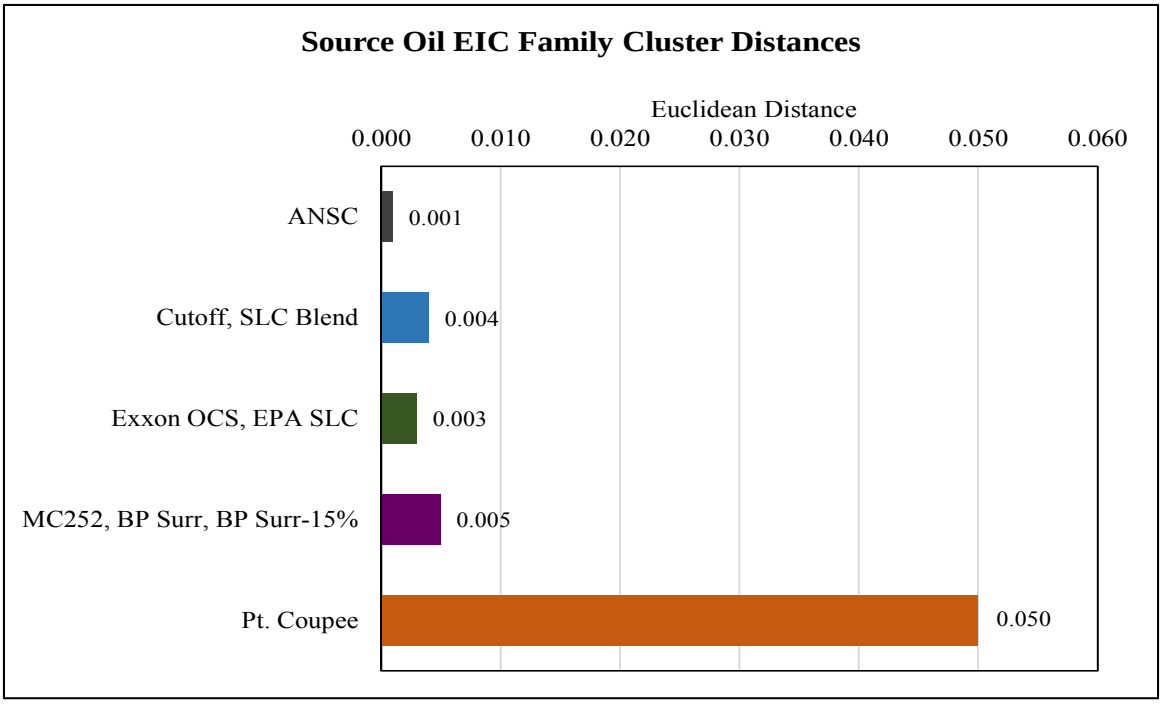


Figure 4.10 The source oil cluster distances based on the combined EIC peak intensity data.

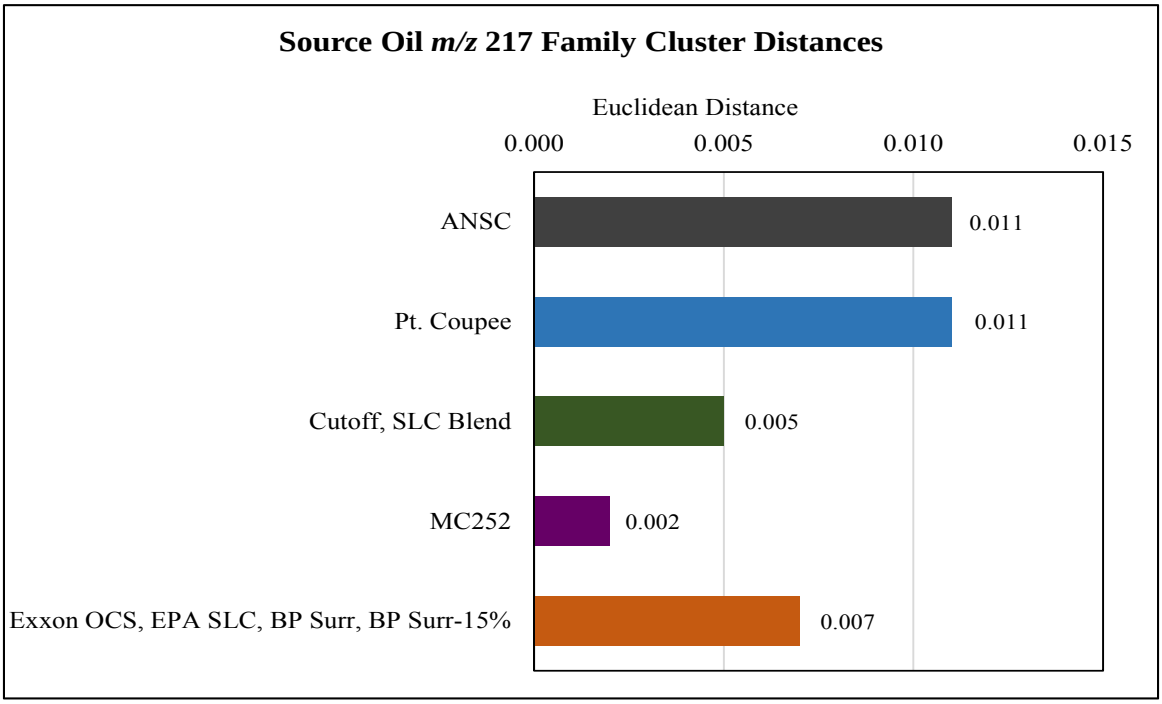


Figure 4.11 The source oil cluster distances based on the *m/z* 217 peak intensity data.

### 4.3.3 Chemometric Analysis of Coastal Marsh Sediments

The combined EIC and *m/z* 217 peak intensity data for a total of 555 coastal marsh sediments were analyzed in Pirouette® by year and by instrument as necessary. The background samples were differentiated from oiled samples for the years 2010-2012, validating the capabilities of the pattern recognition algorithm. After this validation, the chemometric analysis for 2010-2012 was performed again but excluded the background samples, and the years 2013 to 2015 included only oiled sediments. The exclusion of background samples allowed for a reduction in variance, and generally resulted in improved differentiation of oiled sediment samples. The expanded HCA cluster details of the figures with blocks of color on the left of the figure instead of sample identification numbers are provided in Appendix E. The objective of this section is to assess the effectiveness chemometric analysis when used as an oil source-fingerprinting tool. The focus of this section, therefore, is on clusters containing MC252 oil and any samples in the same cluster, indicating inherent similarity between MC252 oil and oil residues in these sediment samples.

The HCA and PCA results for sediment samples collected in July and September 2010 are shown in Figures 4.12 through 4.15. The GC/MS acquisition method did not include *m/z* 218 or 231 for samples analyzed in 2010. The combined EIC data, therefore, are the sum of just *m/z* 191 and 217 peak intensities for each 10 millisecond interval. Figure 4.12 contains two sets of the HCA and the PCA results of the combined EIC data. The top portion of the Figure 4.12 includes background and oiled samples, and the bottom portion of the figure contains only the oiled samples. The top portion of Figure 4.12 displays all background and oiled samples. The red cluster is the MC252 source oil cluster and contains 16 samples, all of which were collected in September 2010. The black, blue, green and purple clusters consist mostly of background

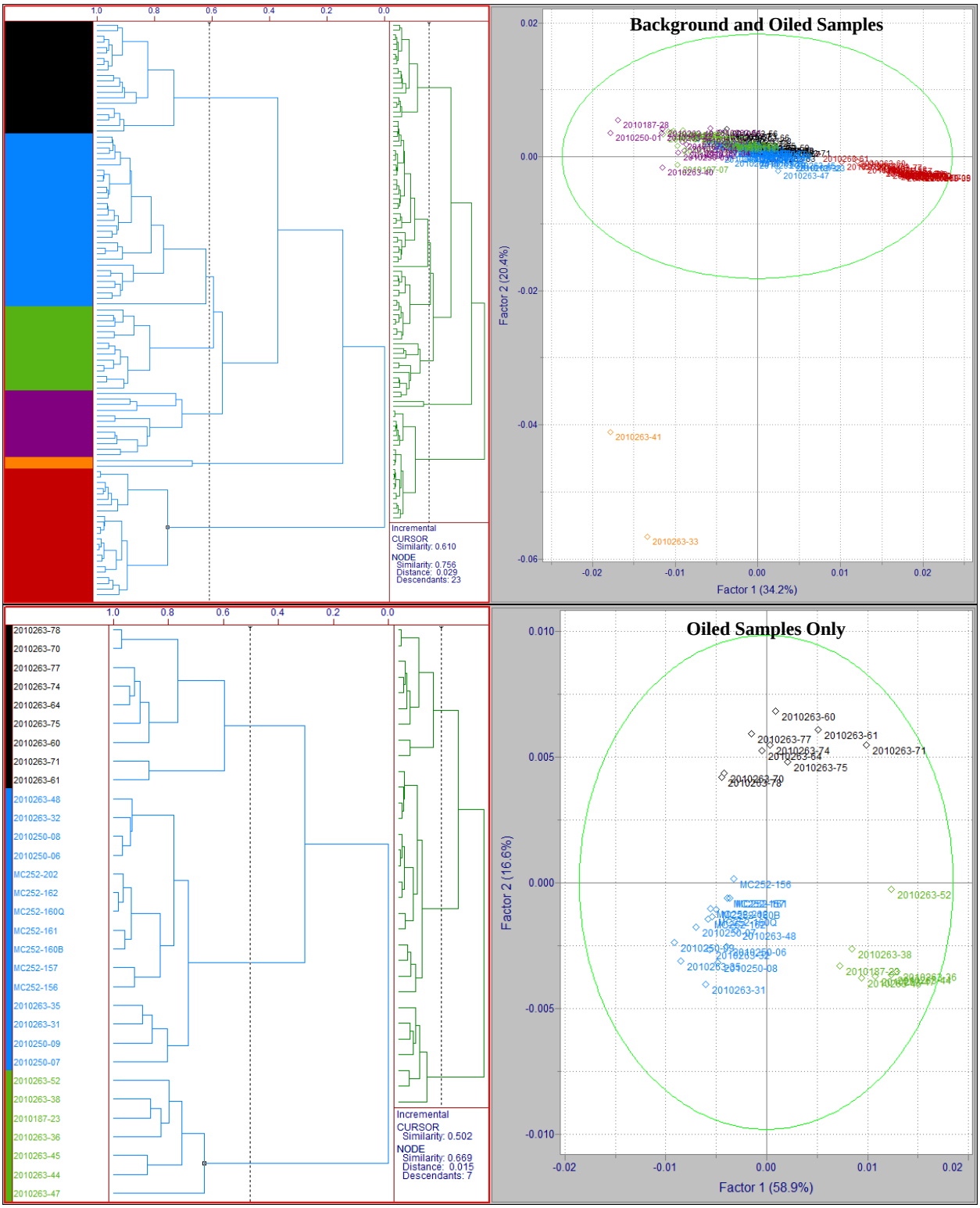


Figure 4.12 The HCA (left) and PCA (right) analysis of combined EIC peak intensity data for coastal marsh sediments collected in 2010. The top portion includes background and oiled samples (n=103, # variables=1494) and the bottom portion includes only oiled samples (n=31, # variables=1494) (See Appendix E for cluster detail)

samples, and samples that appear to be background samples based on their TIC and normal alkane chromatographic profiles, yet have quantifiable abundances of biomarker compounds. The clustering of the background and oil samples in the top 2-D PCA plot of Figure 4.12 is not differentiated. Clustering is readily apparent in the bottom portion of Figure 4.12 where the background samples have been excluded. In the bottom portion of Figure 4.12, the blue cluster contains eight samples collected in September 2010 that are similar to MC252 source oil. The black cluster in the oiled samples only consists of samples that either have a prominent oil profile that do not cluster with MC252, or background samples with quantifiable abundances of biomarker compounds. The black and blue (MC252) clusters at a tribal level would be similar (Figure 4.12, bottom). However, they are less similar to one another at the displayed family level, and based on their cluster distances in Figure 4.13 (bottom).

In Figure 4.14 (*m/z* 217 only data), the green and purple clusters contain MC252 oil and seven samples. All of the samples clustering with MC252 were collected in September 2010, but from different sampling sites. These two clusters are similar to each other despite clustering separately, and would cluster together at the tribal level. The cluster distances (Figure 4.15) for these two clusters is also similar. The blue cluster is contains eight samples that have either trace abundances of biomarkers, or have background profiles with quantifiable abundances of biomarkers. There is some variation within this cluster as indicated by spreading in the 2-D PCA plot. The variation is probably due to the samples with trace abundances of biomarker compounds. In Figure 4.15, the green (MC252), purple (MC252) and blue clusters all have fairly similar cluster distances indicating some similarity among them. Their positions in the 2-D PCA plot, however, indicate otherwise (i.e., blue is less similar to green and purple). The sample in the orange cluster is an outlier despite being a qualitative match to MC252. At the tribal level, however, it would be related to the MC252 clusters.

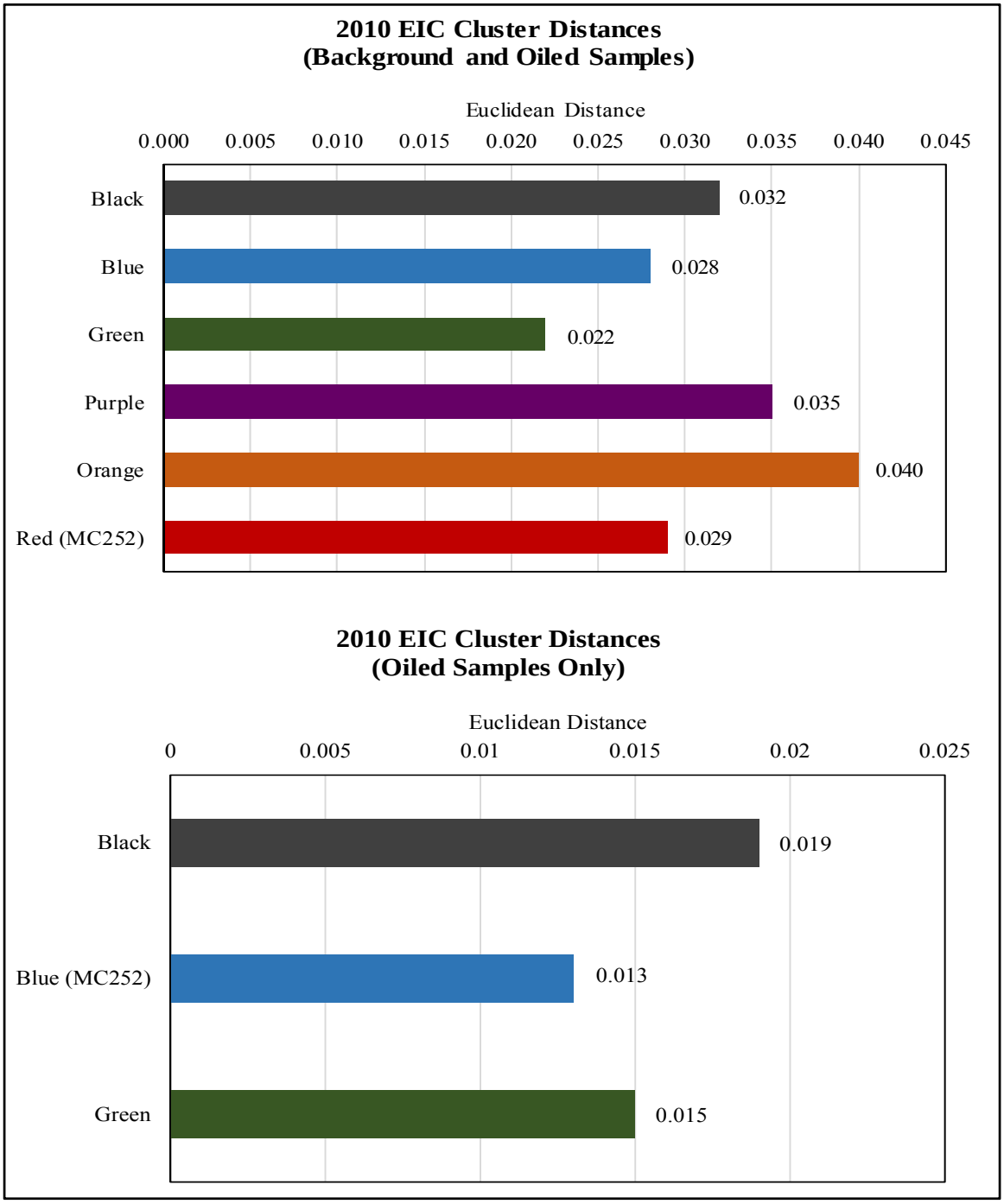


Figure 4.13 The HCA cluster distances of combined EIC peak intensity data for 2010 coastal marsh sediments. The top portion includes background and oiled samples and the bottom portion includes only oiled samples.

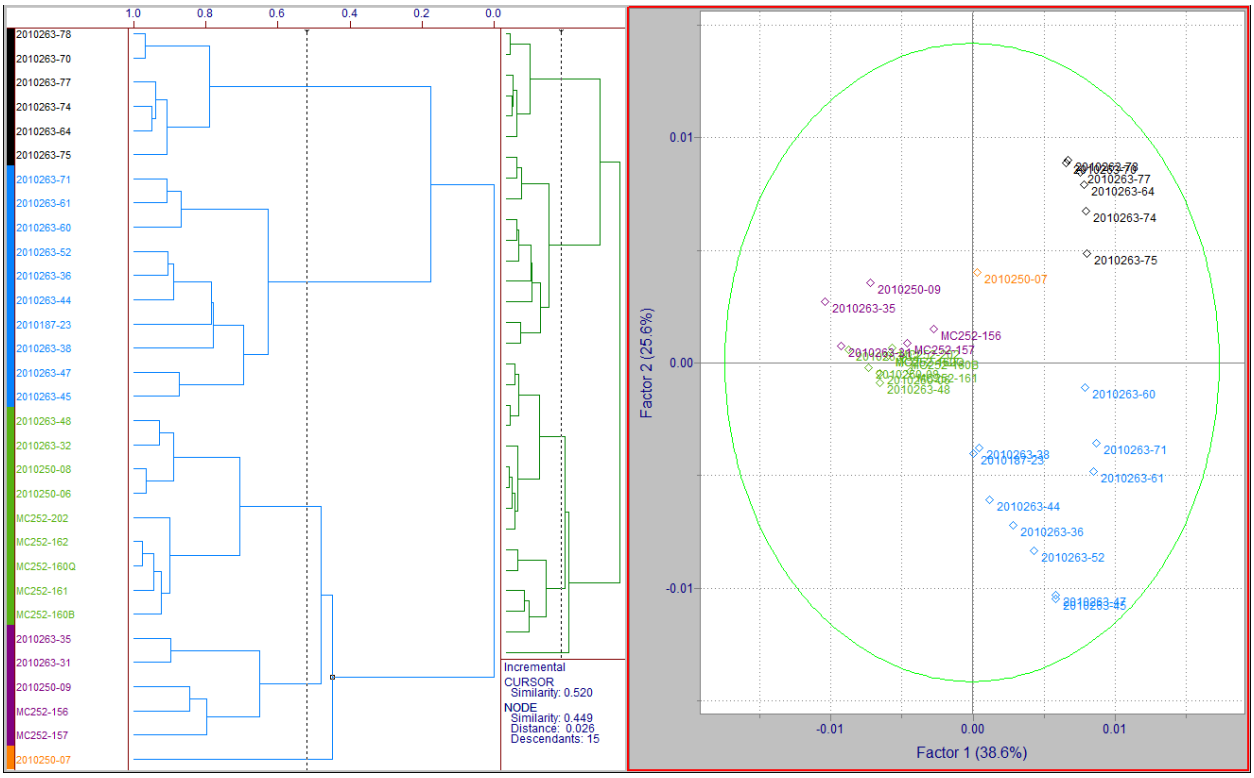


Figure 4.14 The HCA (left) and PCA (right) analysis of *m/z* 217 peak intensity data for coastal marsh sediments collected in 2010. (n=31, # variables=924)

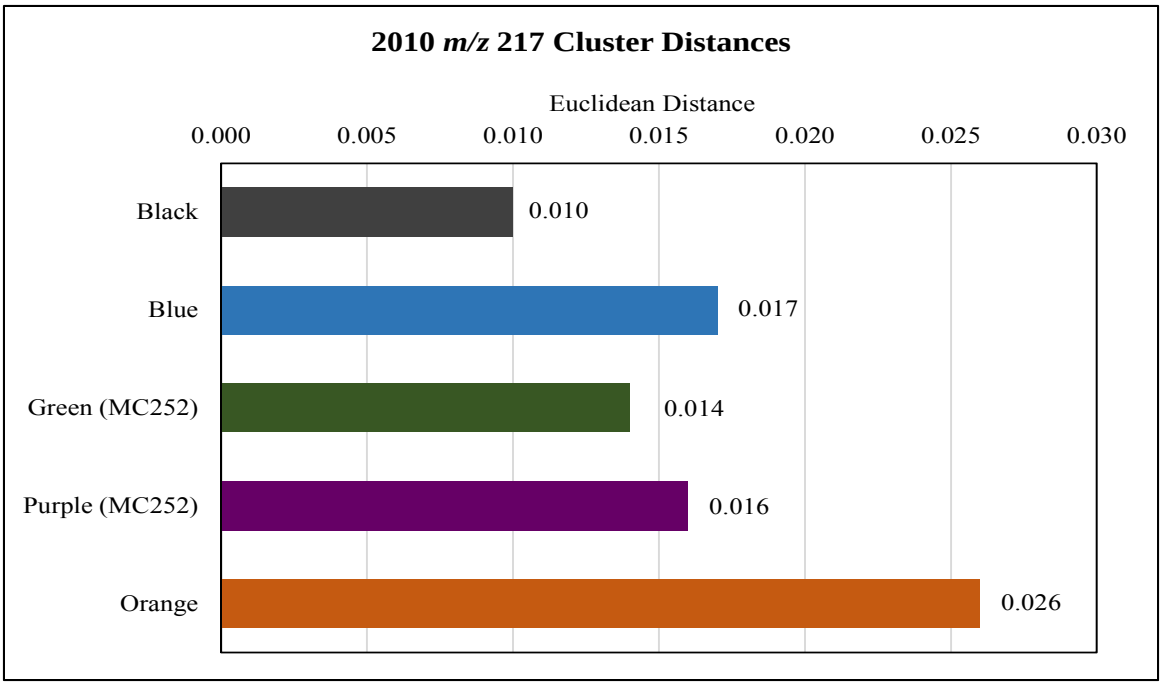


Figure 4.15 The HCA cluster distances of *m/z* 217 peak intensity data for 2010 coastal marsh sediments.

The HCA and PCA results for the 2011 coastal marsh sediments with the LSU ID# 2011039 are shown in Figures 4.16 through 4.19. Again, the GC/MS acquisition method did not include *m/z* 218 or 231 for this sample set. The combined EIC data, therefore, are the sum of just the *m/z* 191 and 217 peak intensities for each 10 millisecond interval. All 30 of the samples in this data set were collected from the same sample site in February 2011. Also, all the samples in this set were sorted as oiled. Four samples, however, were excluded because their biomarker abundances were considered to be extremely low, or they were weathered with an unidentifiable *m/z* 217 pattern.

For the combined EIC data (Figure 4.16), the green cluster contains MC252 and five samples. The purple cluster contains eight samples with significant oil profiles that, at this family level, do not cluster with MC252. The green (MC252) and purple clusters are similar based on their proximity to each other in the 2-D PCA plot. Cluster distances in Figure 4.17 also support this similarity. In the black cluster, the majority of the samples have significant oil profiles that did not cluster with MC252. The blue cluster contains four samples that based on their TIC and normal alkane chromatographic profiles would be considered background samples with measurable amounts of biomarker compounds in them. The black clusters have intra-cluster variation as indicated by spreading in the 2-D PCA plot. The green (MC252) cluster has the same cluster distance to the black cluster in Figure 4.17. The positon of the black cluster in the 2-D PCA plot, however, indicates that the two clusters are less similar to each other.

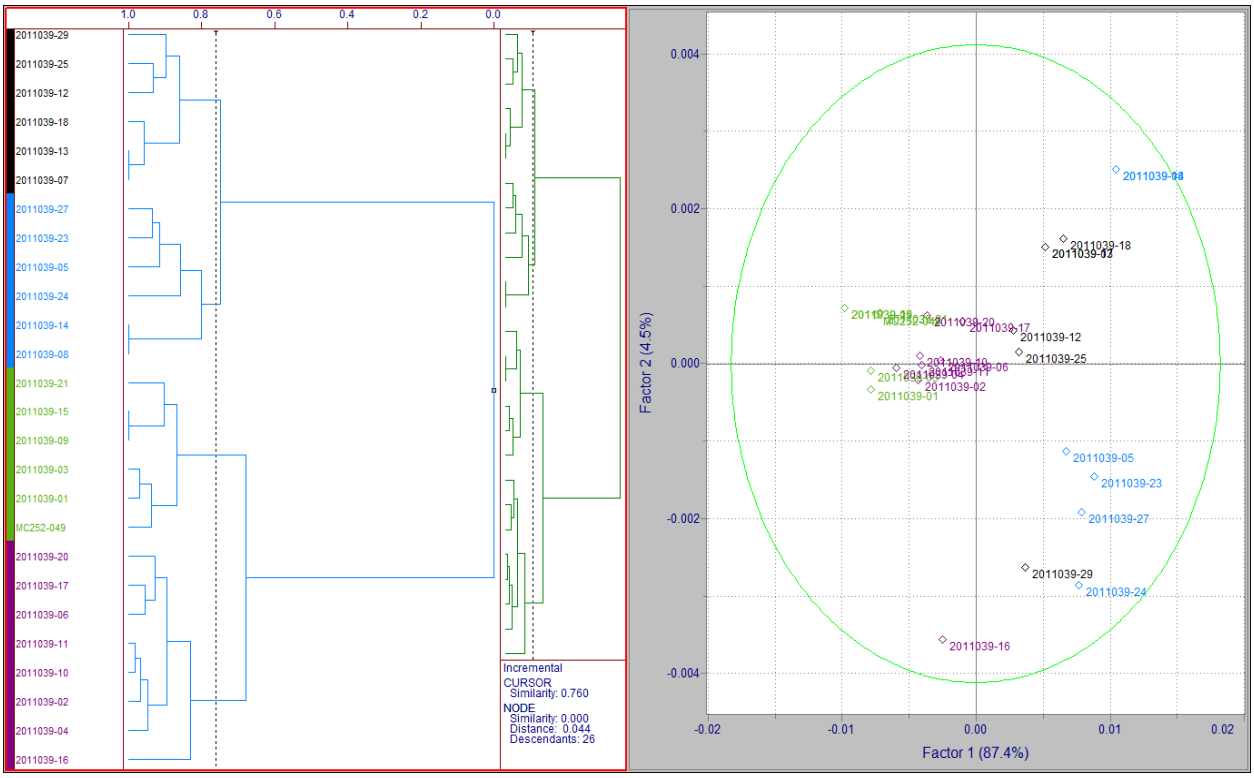


Figure 4.16 The HCA (left) and PCA (right) analysis of combined EIC peak intensity data for the coastal marsh sediments with LSU ID# 2011039. (n=26, # variables=1636)

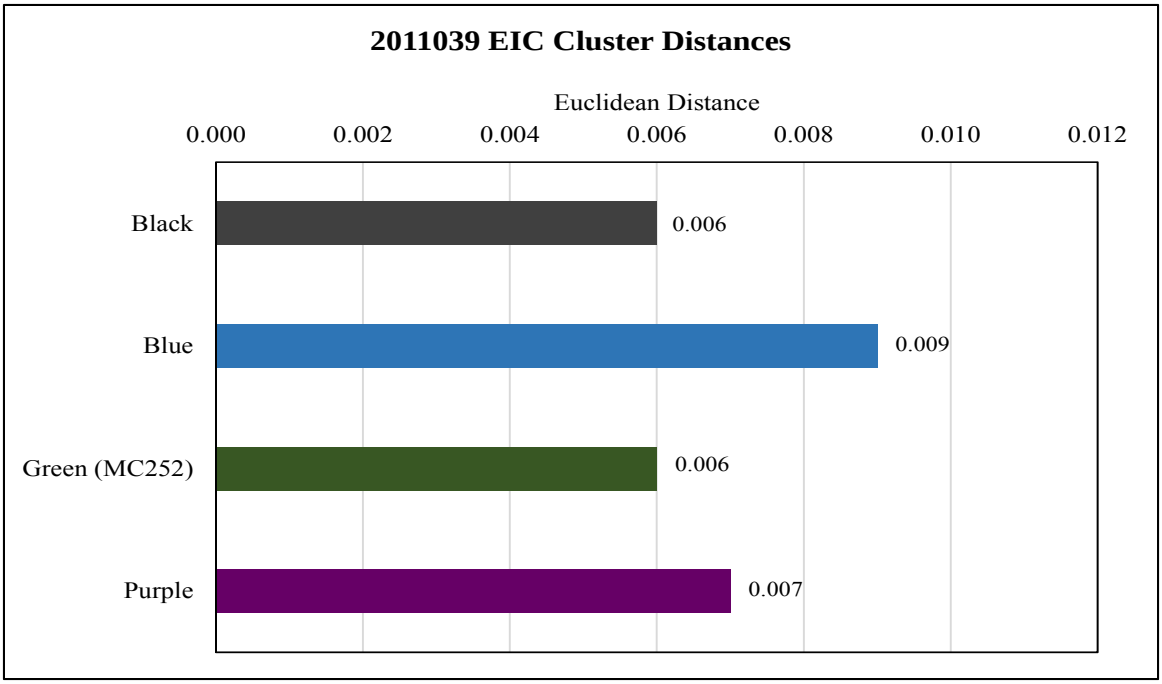


Figure 4.17 The HCA cluster distances of combined EIC peak intensity data for coastal marsh sediments with LSU ID# 2011039.

Figure 4.18 shows the HCA and PCA results of the *m/z* 217 peak intensity data for the coastal marsh sediments with LSU ID# 2011039. The purple cluster contains nine oiled samples that cluster with MC252. The purple cluster is spread out in the 2-D PCA plot perhaps due to variation in the samples above the horizontal line. The blue and green clusters have similar distances in Figure 4.19. Their positions in the 2-D PCA plot, however, are distinctly different. The purple (MC252) and orange cluster have similar cluster distances, stem from the same branch in the HCA plot, and are close to one another in the 2-D PCA plot. Therefore, there is some similarity between these two clusters.

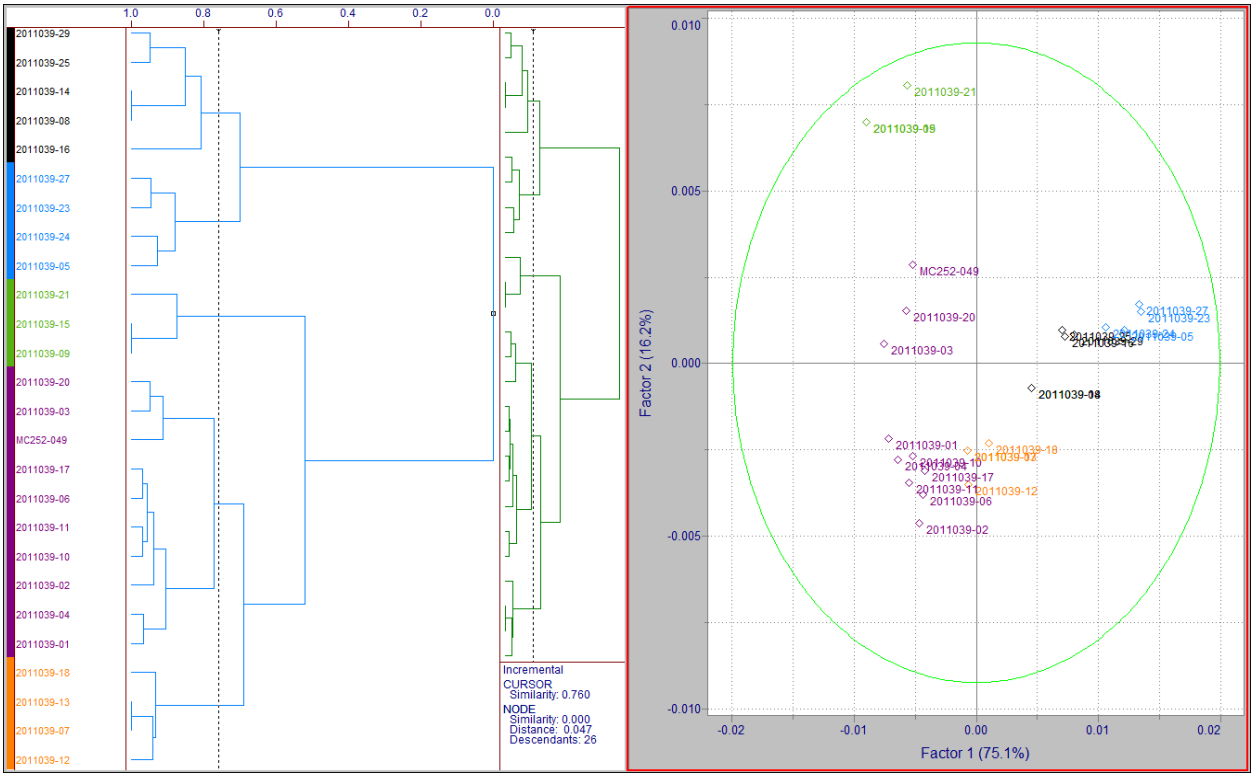

Figure 4.18 The HCA (left) and PCA (right) analysis of *m/z* 217 peak intensity data for the coastal marsh sediments with LSU ID# 2011039. (n=26, # variables = 924)

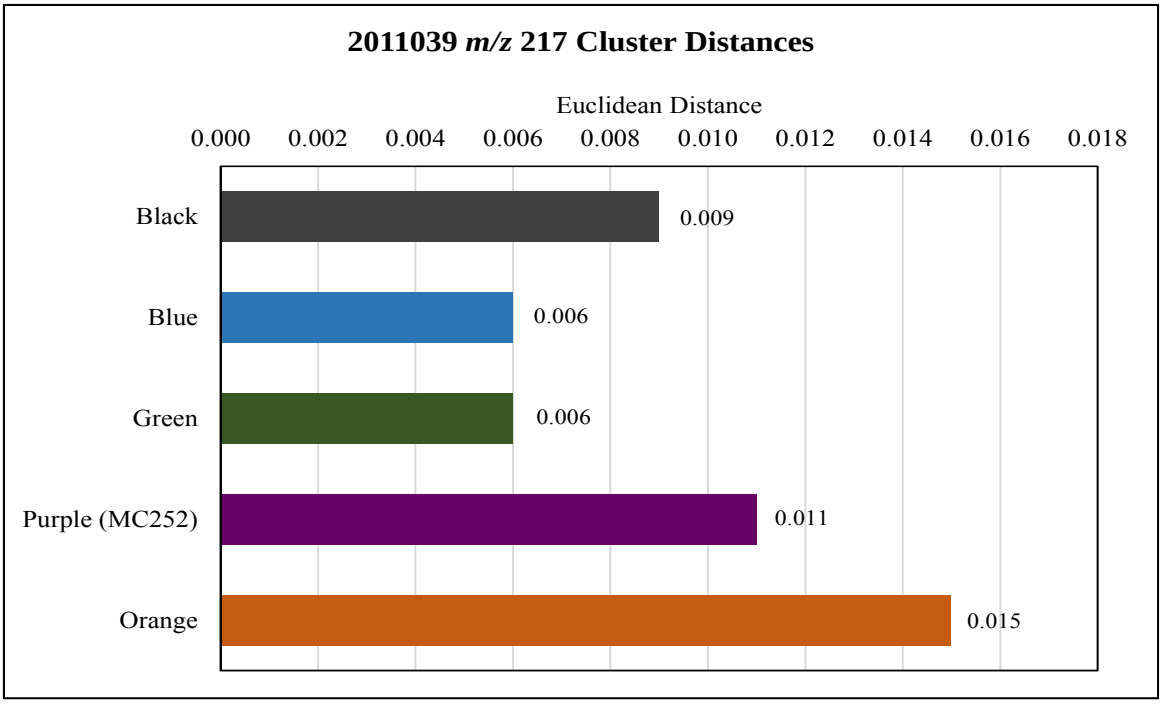


Figure 4.19 The HCA cluster distances of *m/z* 217 peak intensity data for coastal marsh sediments with LSU ID# 2011039.

Figures 4.20 through 4.23 are the HCA and PCA results for the remainder of samples collected in 2011. The GC/MS acquisition method for these samples did include *m/z* 218 and 231. The combined EIC includes peak intensity data, therefore, includes all four biomarkers. The data for years following 2011 includes peak intensity data for all four biomarker EICs. Figure 4.20 contains two sets of the HCA and PCA results. The top portion of the Figure 4.20 includes background and oiled samples and the bottom portion of the figure contains only the oiled samples. The blue cluster contains 29 oiled and 10 background samples that cluster with MC252 in the top portion of Figure 4.20 (combined EIC data). The black, green, and purple clusters mostly consist of background samples with a few oiled samples with trace abundances of biomarker compounds. The red cluster has one sample in it that has a large peak at approximately 42.80 minutes in all the biomarker EICs. This sample is an outlier. In the

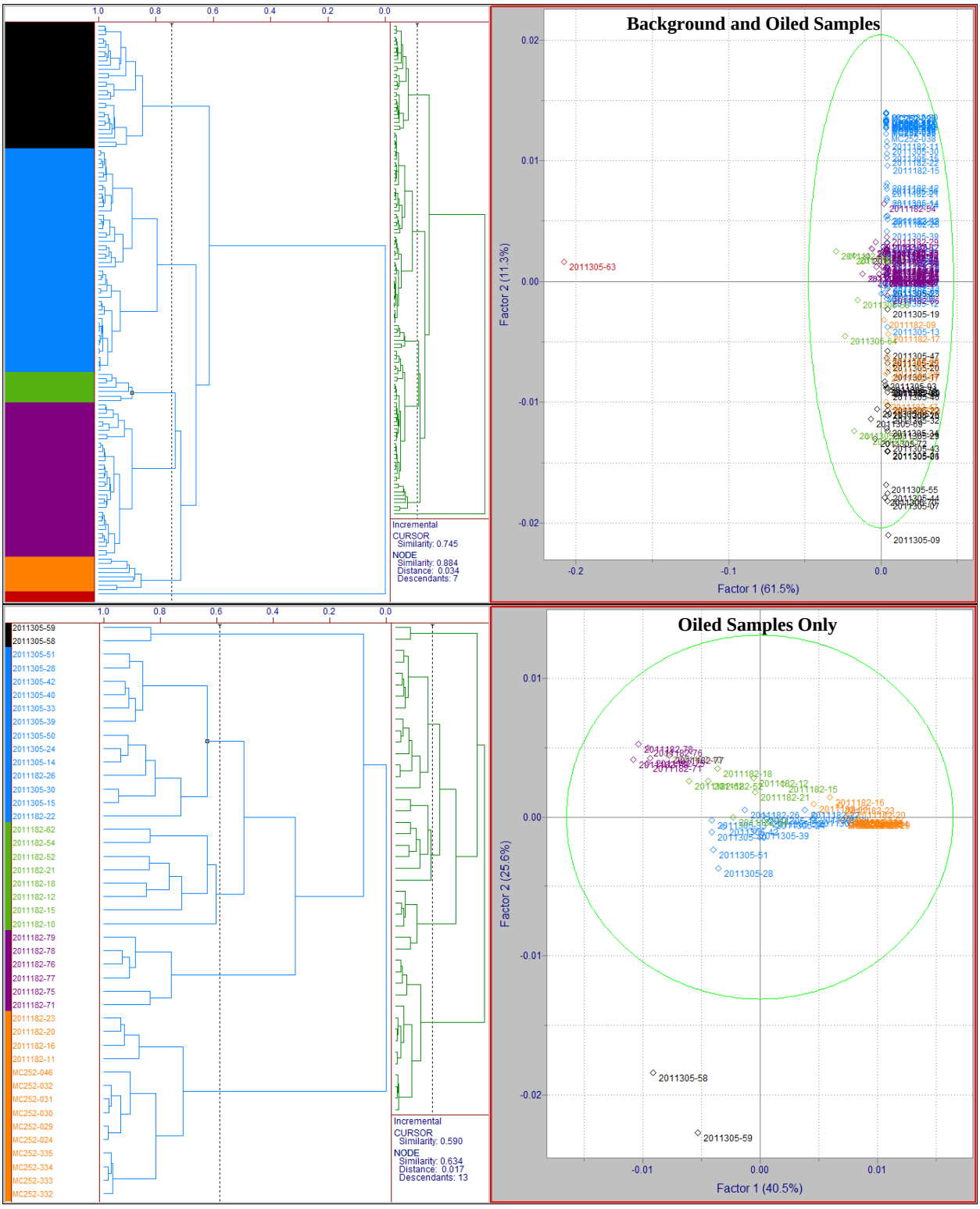


Figure 4.20 The HCA (left) and PCA (right) analysis of combined EIC peak intensity data for the remainder of 2011 coastal marsh sediments. The top portion includes background and oiled samples (n=133, # variables=1517) and the bottom portion includes only oiled samples (n=43, # variables=1517) (See Appendix E for cluster detail)

bottom portion of Figure 4.20 (oiled only samples), the green, purple, and orange (MC252) clusters in the top hemisphere of the 2-D PCA plot were all collected in July 2011. The orange (MC252) cluster has four samples in it. The blue cluster is less similar to the other clusters since it is in the bottom hemisphere. This cluster mostly consists of samples collected in September 2011. The two samples in the black cluster are background-like samples with biomarker compounds. Figure 4.21 provides combined EIC cluster distances for the background and oiled samples, and just the oiled samples. The purple and orange (MC252) clusters have similar distances. Their positions in the 2-D PCA plot, however, indicate they are less similar to each other. The same can be said for the blue and green clusters.

Figure 4.22 displays the HCA and PCA plots of the *m/z* 217 peak intensity data for the 2011 coastal marsh sediments. The black and orange clusters contain seven and one sample, respectively, that cluster with MC252 for a total of eight samples. These clusters are differentiated from each other in the 2-D PCA plot. Samples in the black cluster were collected in September 2011, and samples in the orange clusters were collected in July 2011. When comparing the MC252 cluster distances (Figure 4.23), the black and orange clusters have the same cluster distance, indicating that they are similar. Their positions in the 2-D PCA plot, however, indicate a difference between these two MC252 clusters. Perhaps this is an indication of weathering since samples in the black MC252 cluster were collected in September, and samples in the orange MC252 cluster were collected in July. The red, dark blue, and grey clusters appear to be related as indicated by their positions in the 2-D PCA plot, and by cluster distances in Figure 4.23.

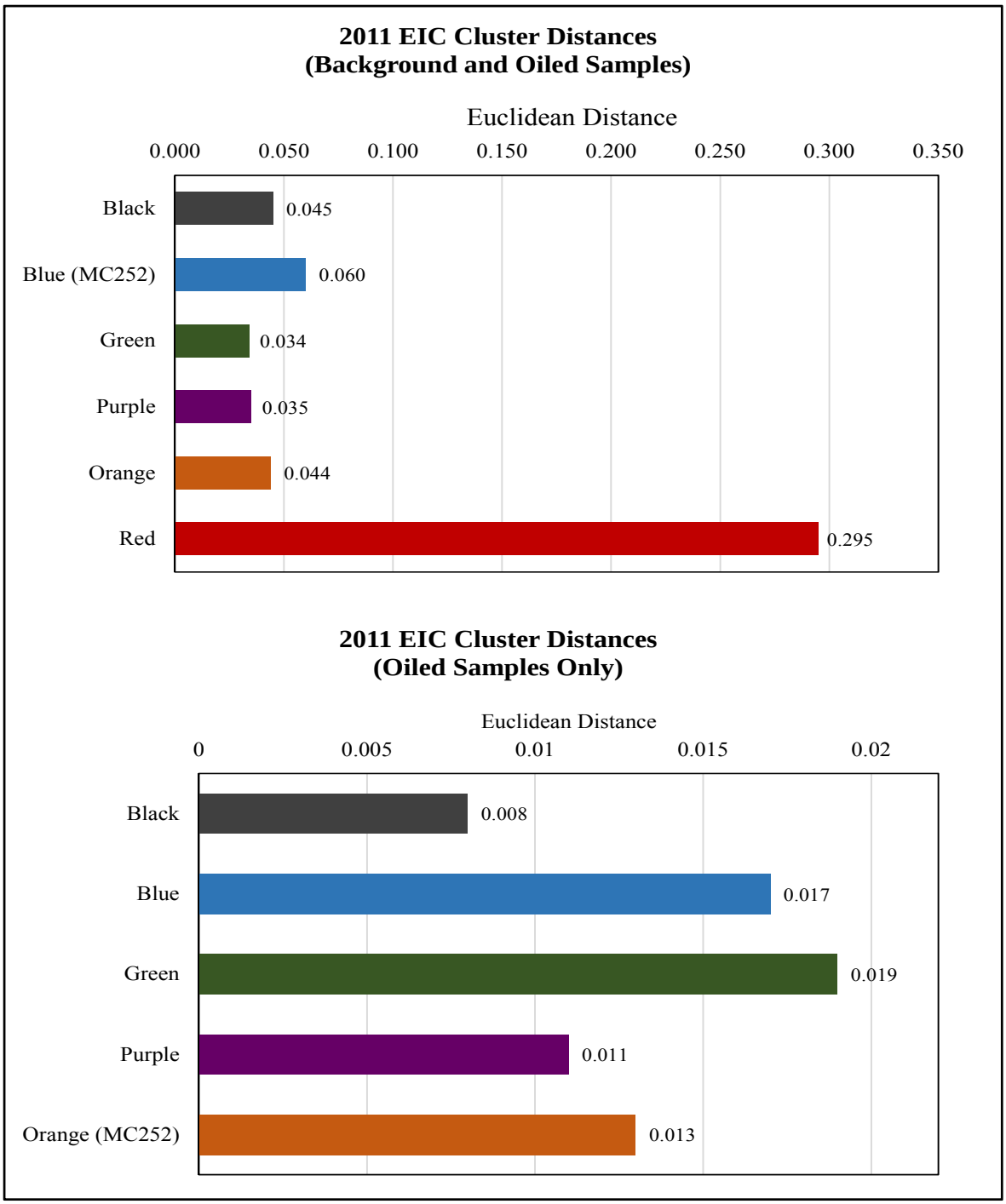


Figure 4.21 The HCA cluster distances of combined EIC peak intensity data for 2011 coastal marsh sediments. The top portion includes background and oiled samples and the bottom portion includes only oiled samples.

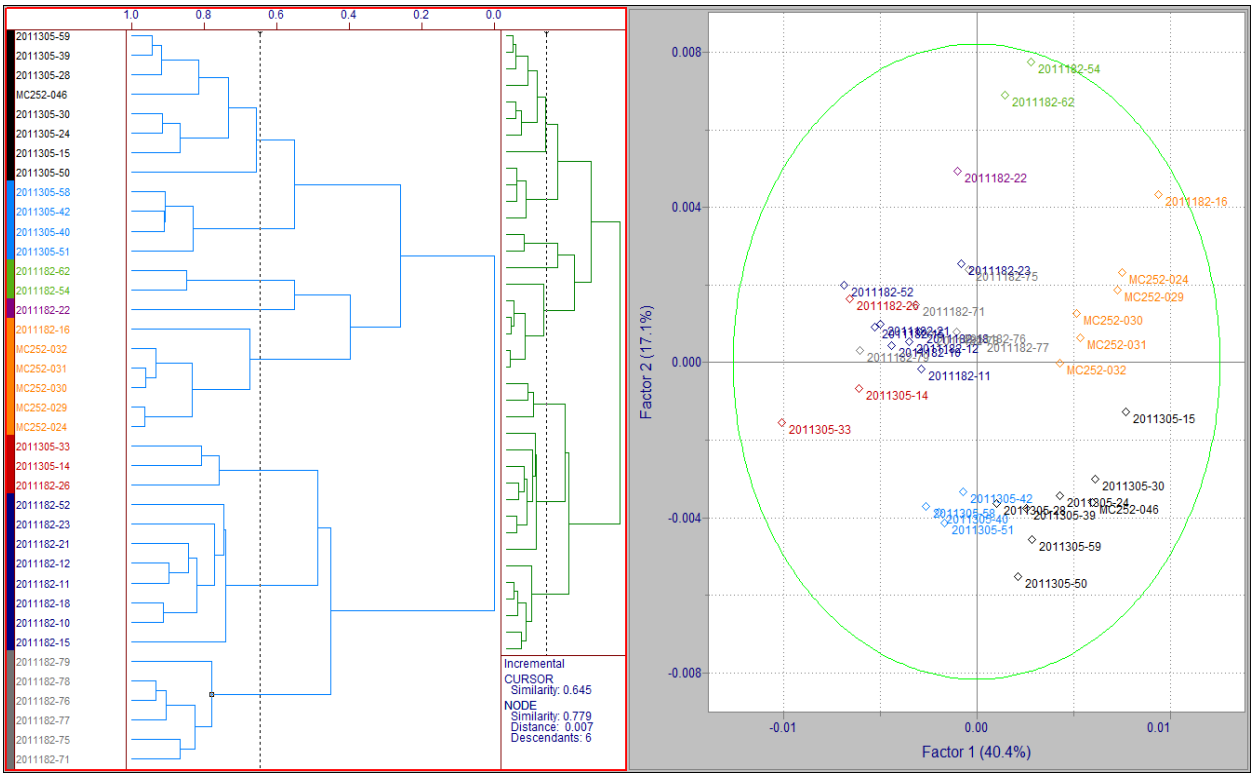


Figure 4.22 The HCA (left) and PCA (right) analysis of *m/z* 217 peak intensity data for the remainder of 2011 of coastal marsh sediments. (n=38, # variables=799)

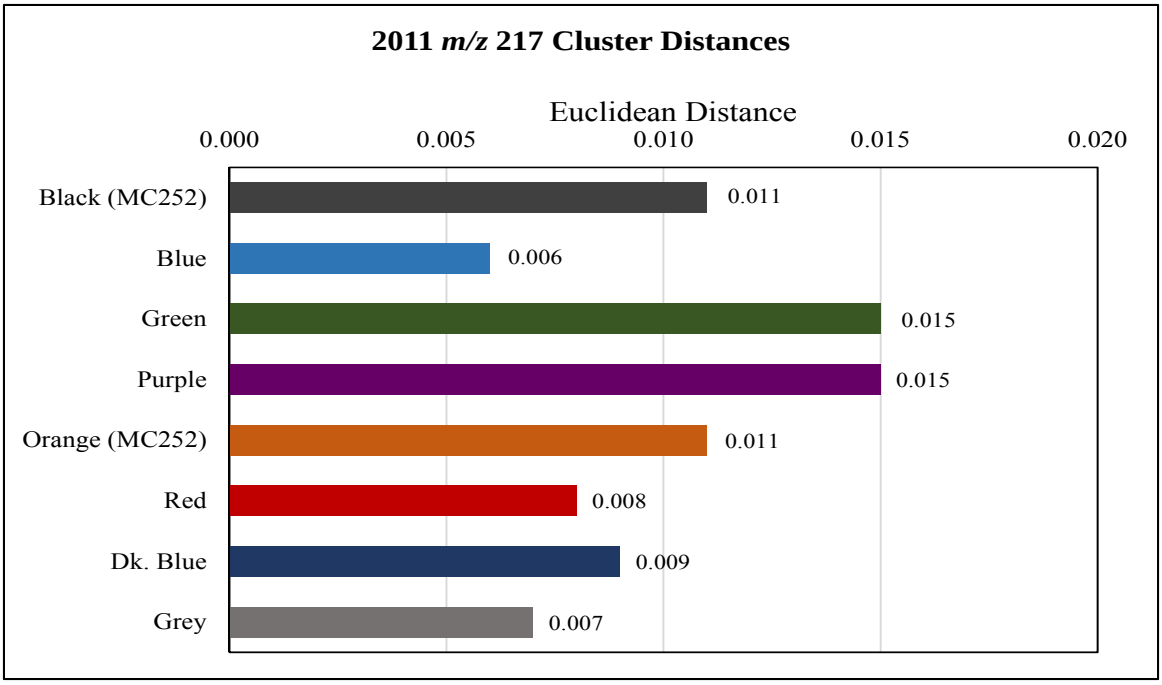


Figure 4.23 The HCA cluster distances of *m/z* 217 peak intensity data for 2011 coastal marsh sediments.

Figures 4.24 through 4.27 are the HCA and PCA results for coastal marsh sediment collected in 2012. Figure 4.24 contains two sets of the HCA and PCA results. The top portion of the Figure 4.24 includes background and oiled samples, and the bottom portion of the figure contains only the oiled samples. The black cluster in the top portion of Figure 4.24 (combined EIC data) contains 33 oiled samples and one background sample that cluster with MC252 source oil. The blue cluster contains 20 oiled samples and 10 background samples that did not cluster with MC252. The oiled samples within the blue cluster were samples with trace abundances of oil biomarkers, or samples that appeared to be background but with resolved biomarker components. The green cluster contains four (4) oiled samples with trace abundances of biomarker compounds. The orange cluster is mostly background samples with traces of oil biomarkers.

The blue cluster in the bottom portion of Figure 4.24 is the MC252 cluster. It contains 26 oiled samples: 23 samples from before Hurricane Isaac, and 3 samples after. The samples collected before and after Hurricane Isaac were all collected from Bay Batiste, LA. The black cluster contains 14 oiled samples that did not cluster with MC252. The position of this cluster in the 2-D PCA plot and cluster distances in Figure 4.25, however, indicate that the blue (MC252) and black cluster are similar to one another. The black and blue clusters would be in the same tribe if the similarity line was adjusted to a tribal level. The green cluster in Figure 4.24 (bottom) contains 10 samples with trace abundances of biomarker compounds. The five samples in the last three clusters (i.e., purple, orange, and red) are outliers. These clusters contained samples with trace abundances of biomarker compounds, or were oiled samples that did not cluster with MC252. Three of the five samples were collected in May 2012 from Cat Island, LA and the other two were collected after Hurricane Isaac in Bay Batiste.

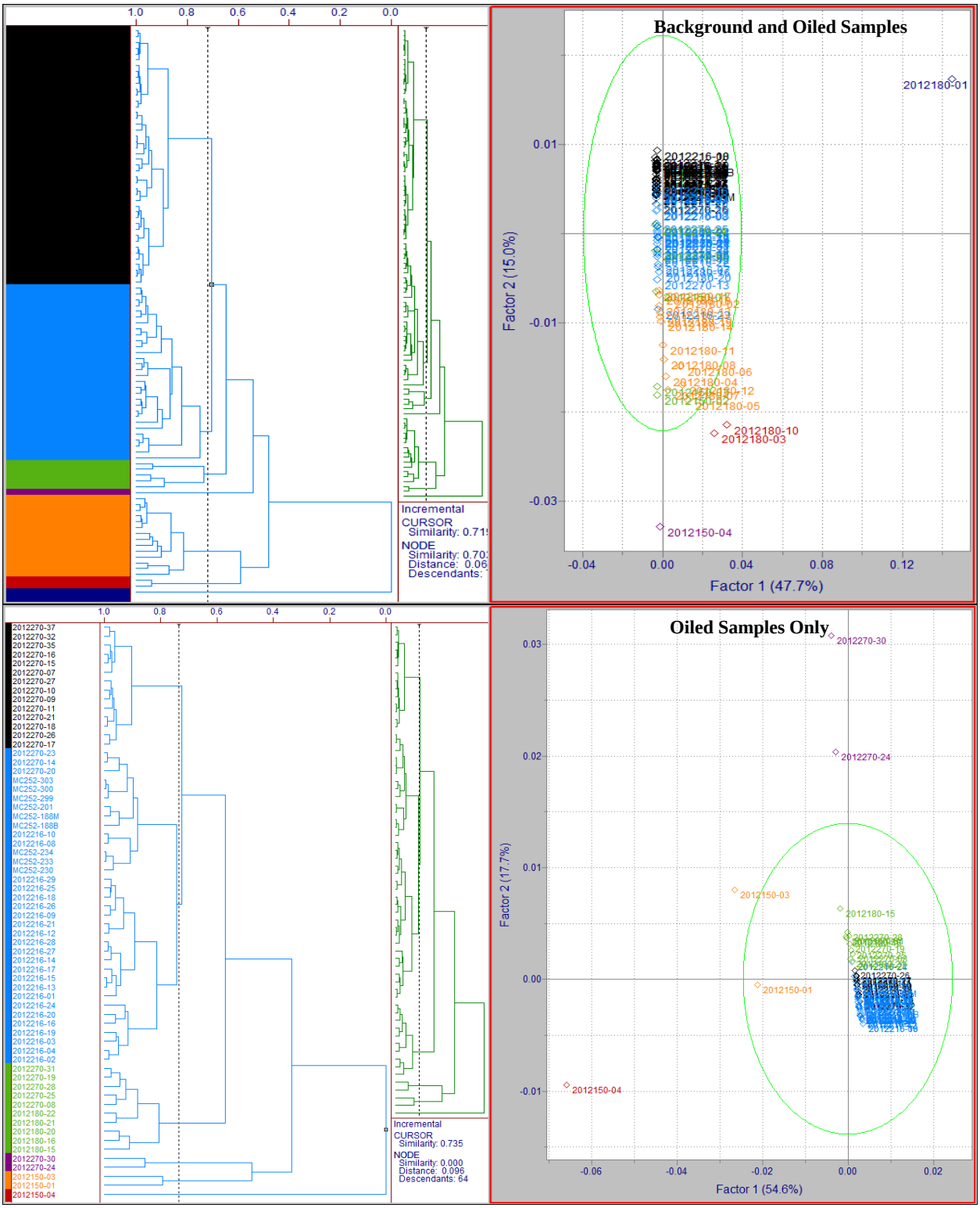


Figure 4.24 The HCA (left) and PCA (right) analysis of combined EIC peak intensity data for 2012 coastal marsh sediments. The top portion includes background and oiled samples (n=97, # variables=1517). The bottom portion includes only oiled samples (n=64, # variables=1517) (See Appendix E for HCA cluster detail)

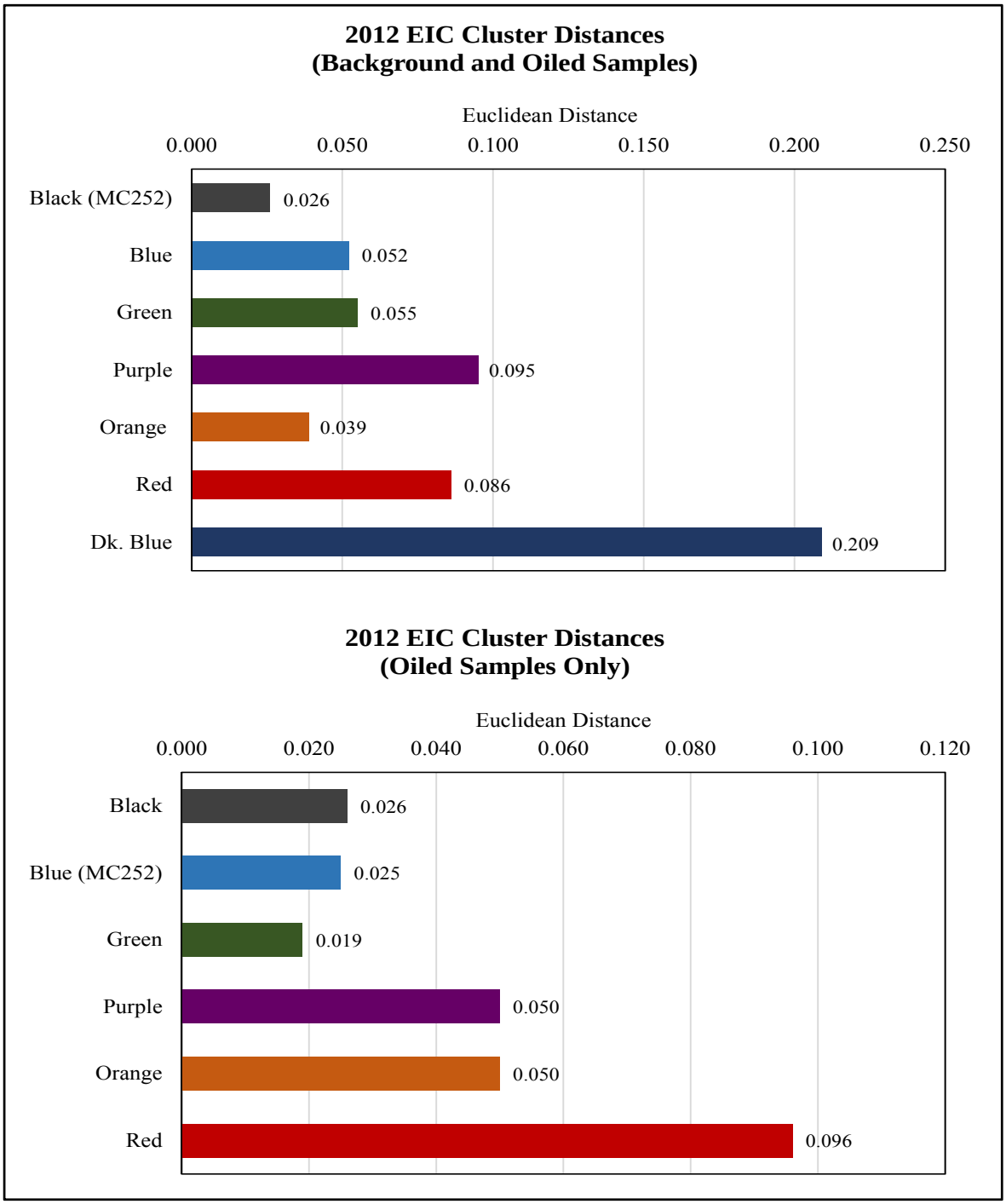


Figure 4.25 The HCA cluster distances of combined EIC peak intensity data for 2012 coastal marsh sediments. The top portion includes background and oiled samples and the bottom portion includes only oiled samples.

The black, purple, and red clusters in Figure 4.26 (peak intensity data for *m/z* 217 only) contain a total of 19 samples that cluster with MC252 source oil. The black MC252 cluster contains seven samples that were collected from Bay Batiste after Hurricane Isaac. The purple MC252 cluster contains five samples collected from CWC base sites, and one sample from Bay Batiste after Hurricane Isaac. The red MC252 cluster contains seven samples collected before Hurricane Isaac. The samples in red and black MC252 clusters have differing positions in the 2-D PCA plot and differing cluster distances in Figure 4.27. This may indicate a shift from more weathered oil before the hurricane to fresher oil after the hurricane. The TIC and normal alkane chromatographic profiles do support the fact that some of the oil after the hurricane was fresher than the oil in the samples before the hurricane. The purple MC252 cluster contains sample from another sampling site.

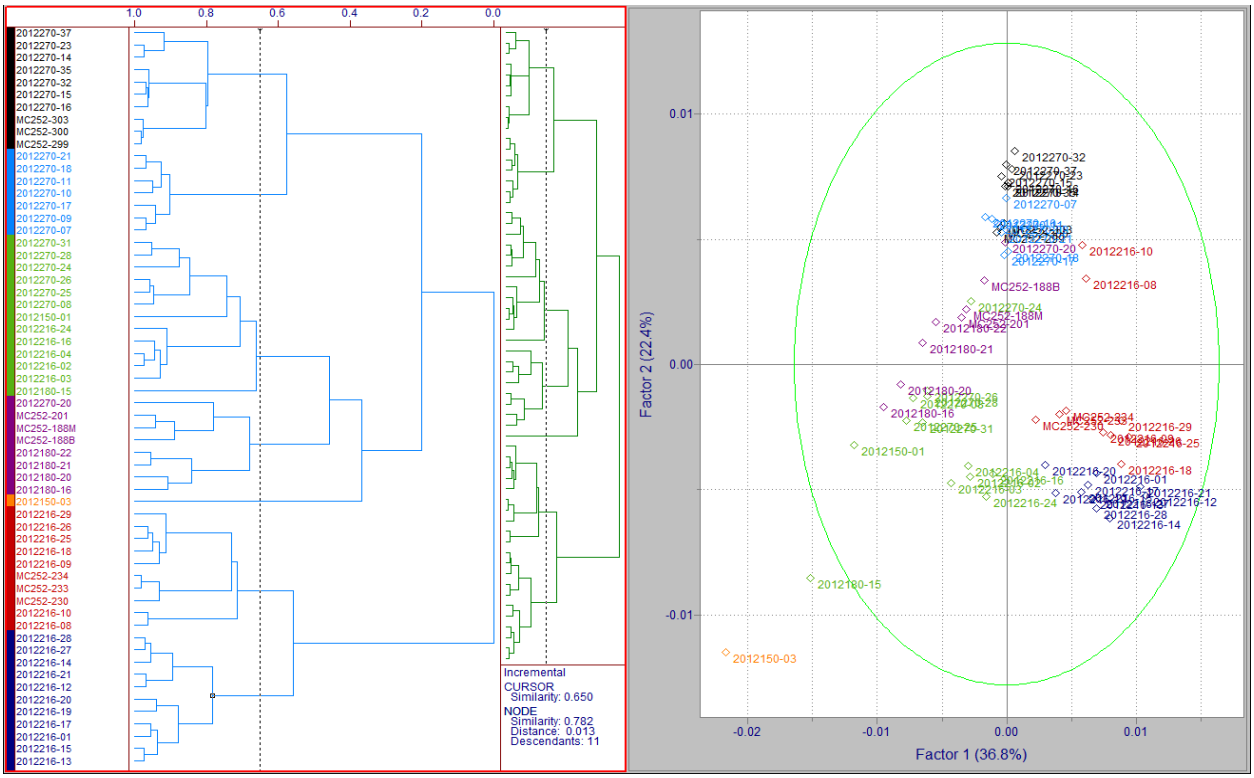


Figure 4.26 The HCA (left) and PCA (right) analysis of *m/z* 217 peak intensity data for 2012 coastal marsh sediments. (n=60, # variables=799)

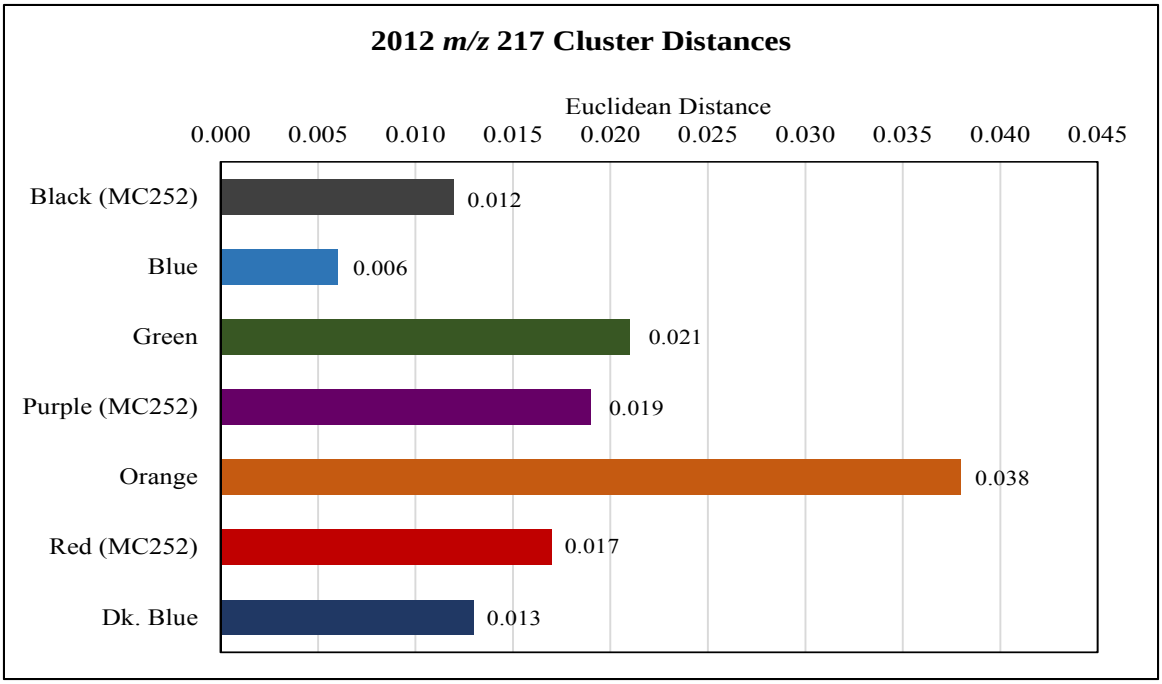


Figure 4.27 The HCA cluster distances of *m/z* 217 peak intensity data for 2012 coastal marsh sediments.

The HCA and PCA results for the 2013 sediments analyzed on the instrument system designated GT are shown in Figures 4.28 through and 4.31. Data from this point forward will be presented by year and instrument system (either GT or MU). The green cluster in Figure 4.28 (combined EIC data for instrument system GT) contains MC252 oil, and no 2013 coastal marsh sediments. The green (MC252) cluster is also differentiated from the other clusters in the 2-D PCA plot, and in Figure 4.29 cluster distance plot. The blue and black clusters appear to be similar based on the 2-D PCA plot. Variation within each of these clusters, however, is resulting in spreading. The spreading may also be an effect of a lower sample size compared to previous sample sets.

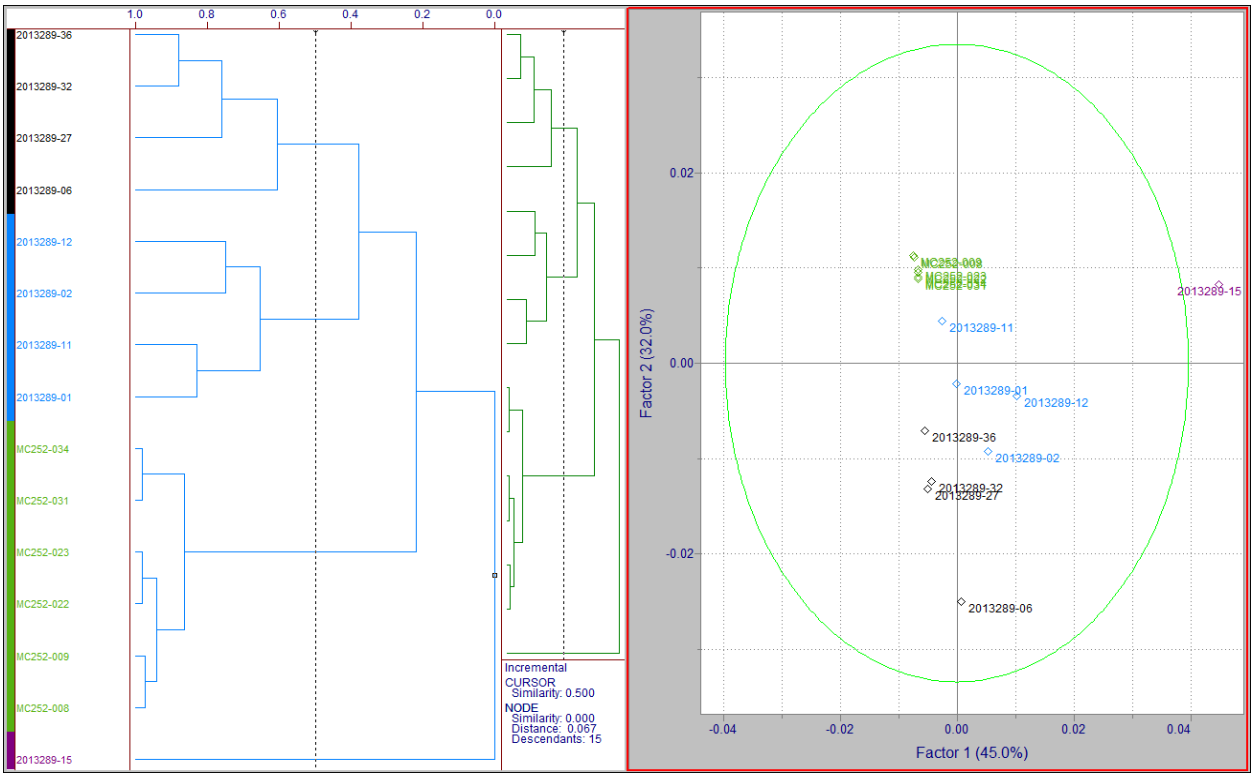


Figure 4.28 The HCA (left) and PCA (right) analysis of combined EIC peak intensity data for 2013 coastal marsh sediments analyzed on GT. (n=15, # variables=1208)

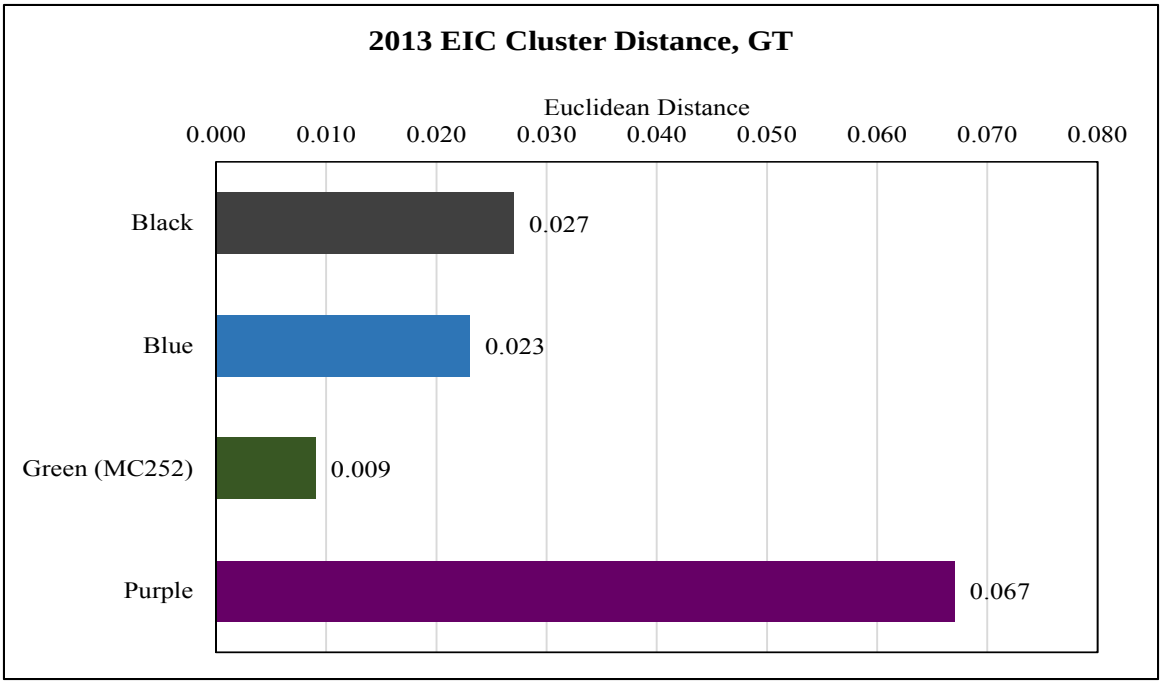


Figure 4.29 The HCA cluster distances of combined EIC peak intensity data for 2013 coastal marsh sediments analyzed on GT.

There is excellent separation of the oiled samples analyzed on GT from 2013 in the *m/z* 217 peak intensity data (Figure 4.30). The green MC252 cluster still contains no samples. Figure 4.31 also shows the clear distinction among samples based on cluster distances. All of the 2013 coastal marsh samples displayed in Figure 4.30 were collected in October from the CWC base sites. All the oiled samples collected in August 2013 from a different sampling location had trace levels of biomarker compounds; therefore, these samples were contributing more variation to the HCA and PCA and were excluded from the final analysis.

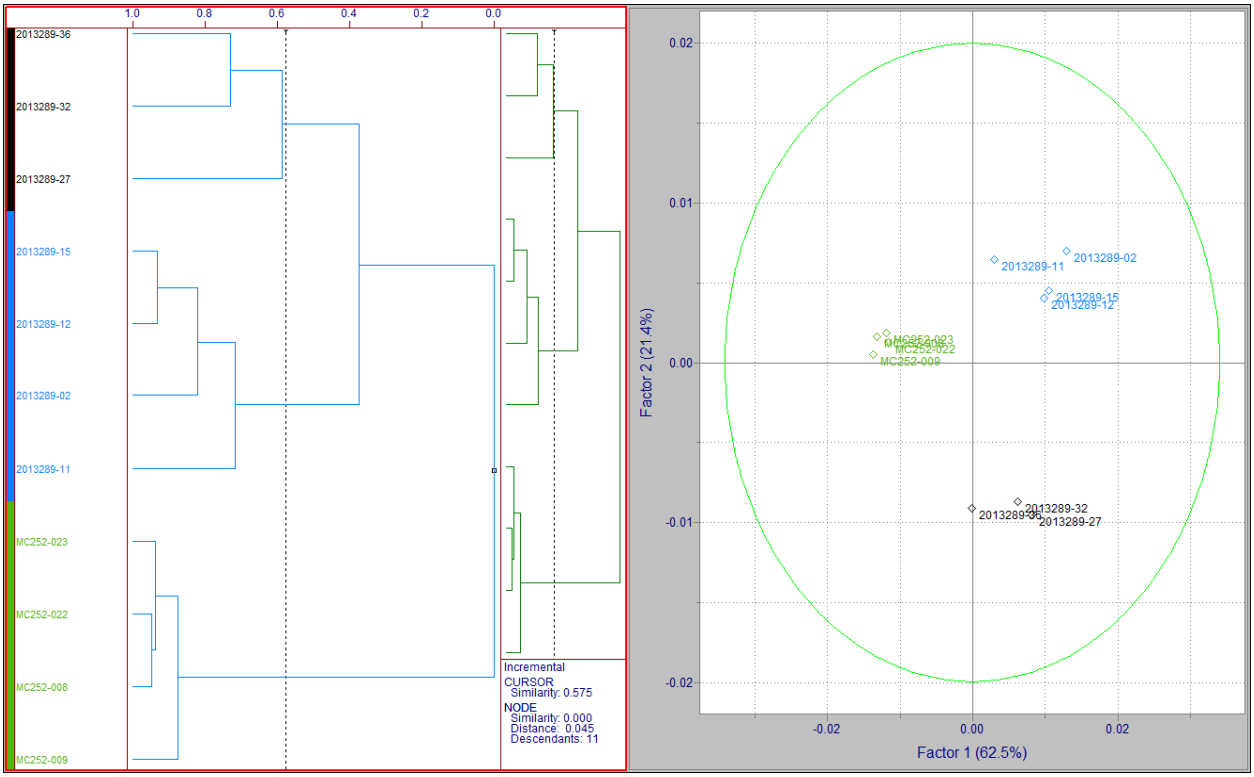


Figure 4.30 The HCA (left) and PCA (right) analysis of *m/z* 217 peak intensity data for 2013 coastal marsh sediments analyzed on GT. (n=11, # variables=672)

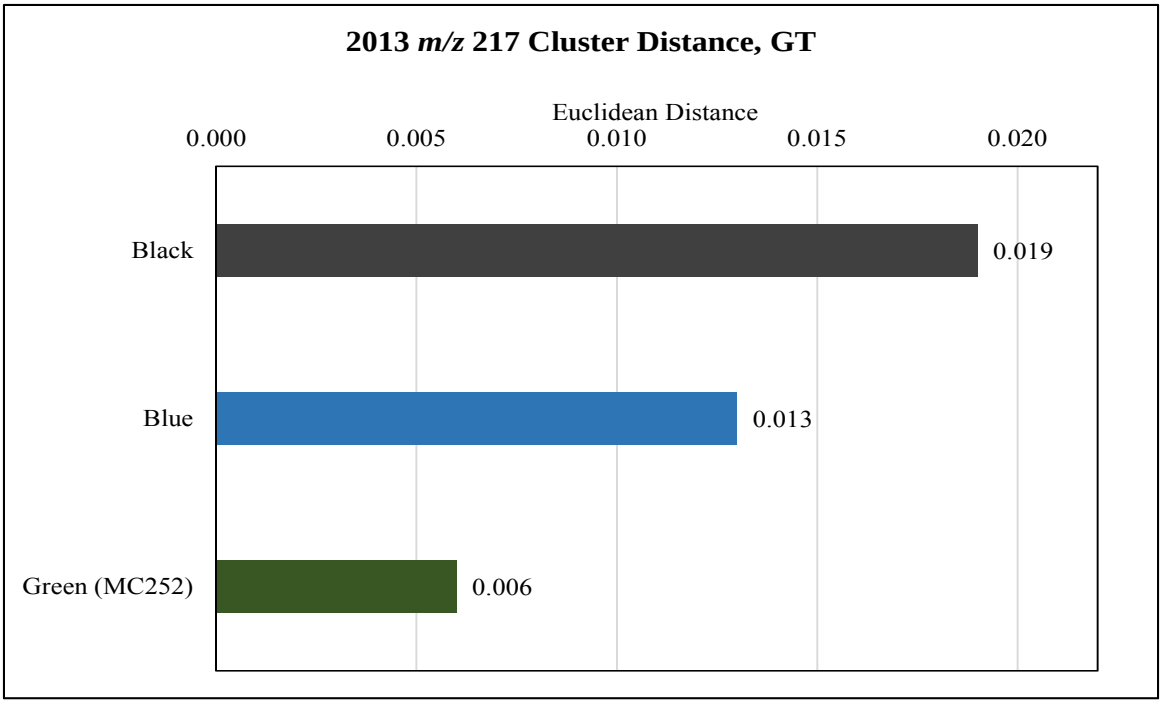


Figure 4.31 The HCA cluster distances of *m/z* 217 peak intensity data for 2013 coastal marsh sediments analyzed on GT.

The HCA and PCA results for the 2013 sediments analyzed on the instrument system designated MU are shown in Figures 4.32 through 4.35. None of the 2013 coastal marsh sediments analyzed on MU clustered with MC252, the green cluster in Figure 4.32. The blue cluster, consisting of 13 oiled samples collected in June 2013 is similar to the green (MC252) cluster based on their positions in the 2-D PCA plots. Cluster distances (Figure 4.33) support this conclusion. There is no real distinction of cluster among these samples from 2013, except for the two outliers. Cluster distances in Figure 4.33, on the other hand, do display dissimilarities among clusters with the exception of the blue and green (MC252) clusters. The blue and green (MC252) cluster have the same cluster distance and are similar to each other based on the branching in the HCA dendrogram. The green (MC252), blue, and black clusters would all be similar at the tribal level.

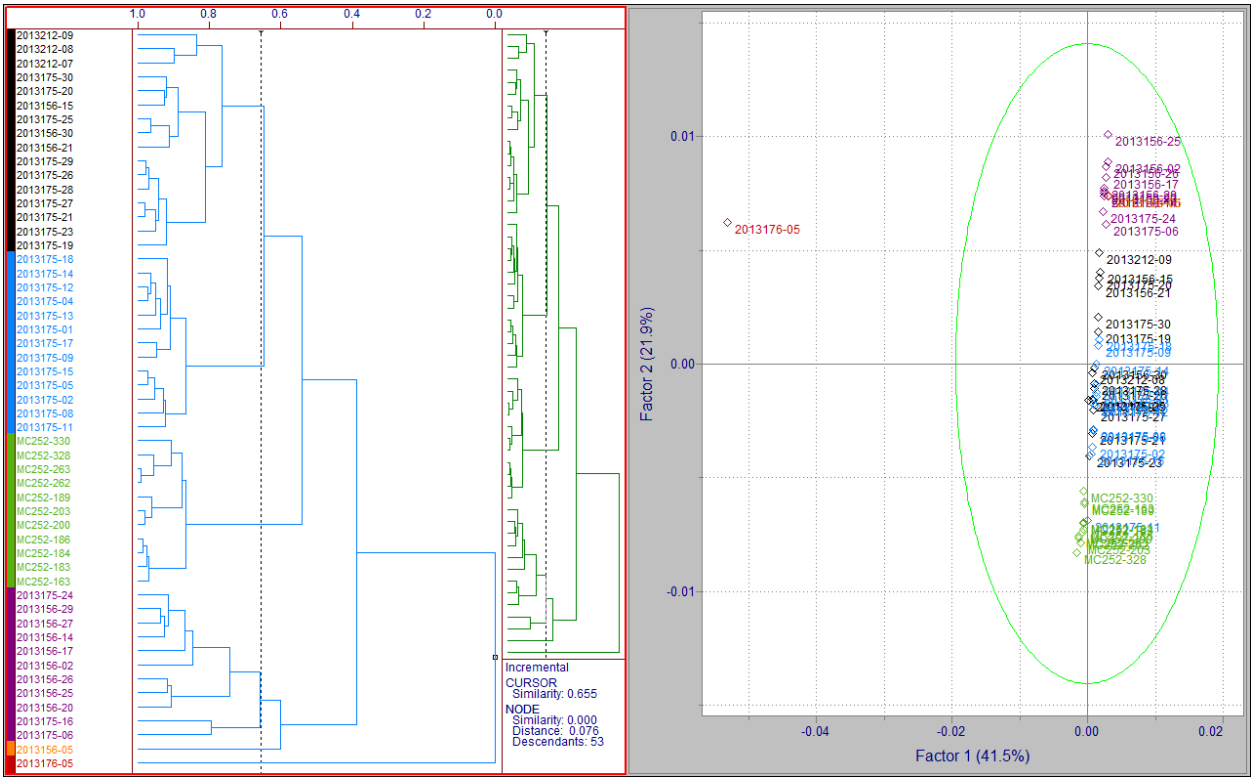


Figure 4.32 The HCA (left) and PCA (right) analysis of combined EIC peak intensity data for 2013 coastal marsh sediments analyzed on MU. (n=53, # variables=1517)

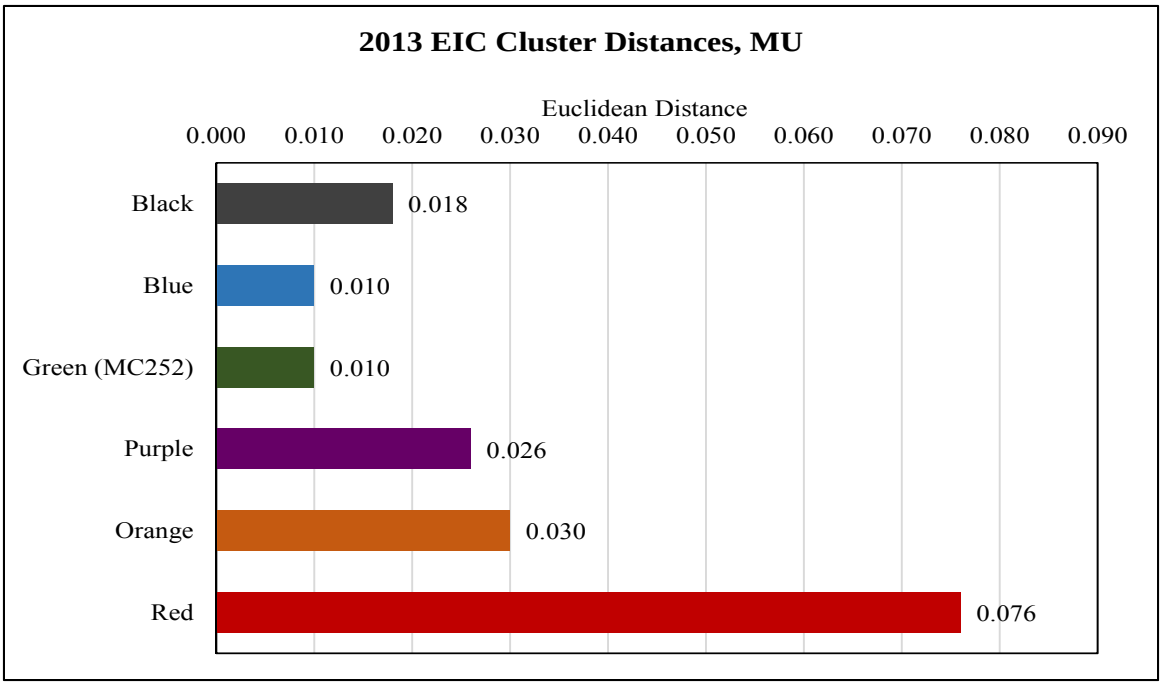


Figure 4.33 The HCA cluster distances combined EIC peak intensity data for 2013 coastal marsh sediments analyzed on MU.

Clustering is more prominent in the HCA and PCA plots for the *m/z* 217 peak intensity data (Figure 4.34). The green cluster contains MC252 and has two samples within it. These two samples were collected in June 2013. In Figure 4.35, the green (MC252) has the same cluster distance as the black cluster that contains 14 oiled samples. The position of these clusters in the 2-D PCA plot, however, indicates some dissimilarity between the two (i.e., these two clusters would be in different tribes if the similarity line was adjusted to the right). The orange, blue and purple clusters differentiated nicely in the 2-D PCA plot in Figure 4.34. All of the samples with significant oil profiles are on the right side of the 2-D PCA plot, while the samples on the left side are all background samples with biomarkers. This positioning defines the oiled samples from the weathered oil samples.

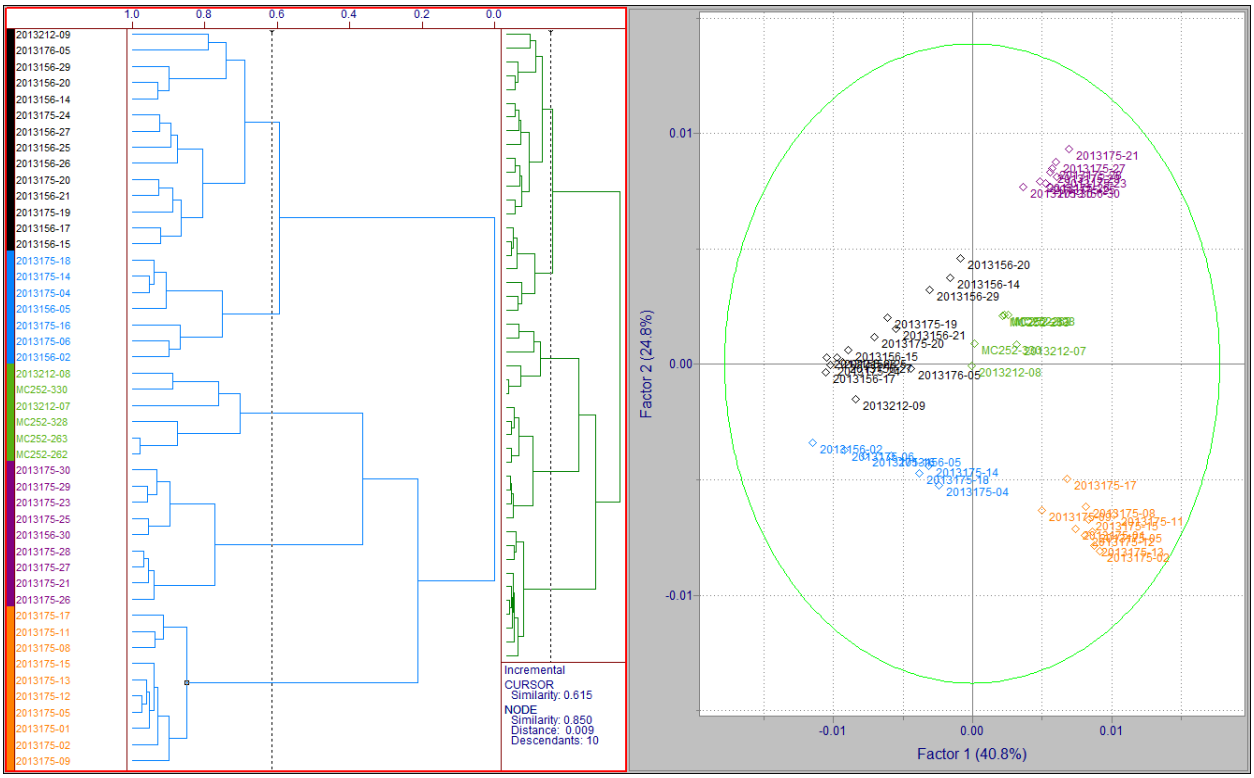


Figure 4.34 The HCA (left) and PCA (right) analysis of *m/z* 217 peak intensity data for 2013 coastal marsh sediments analyzed on MU. (n=46, # variables=799)

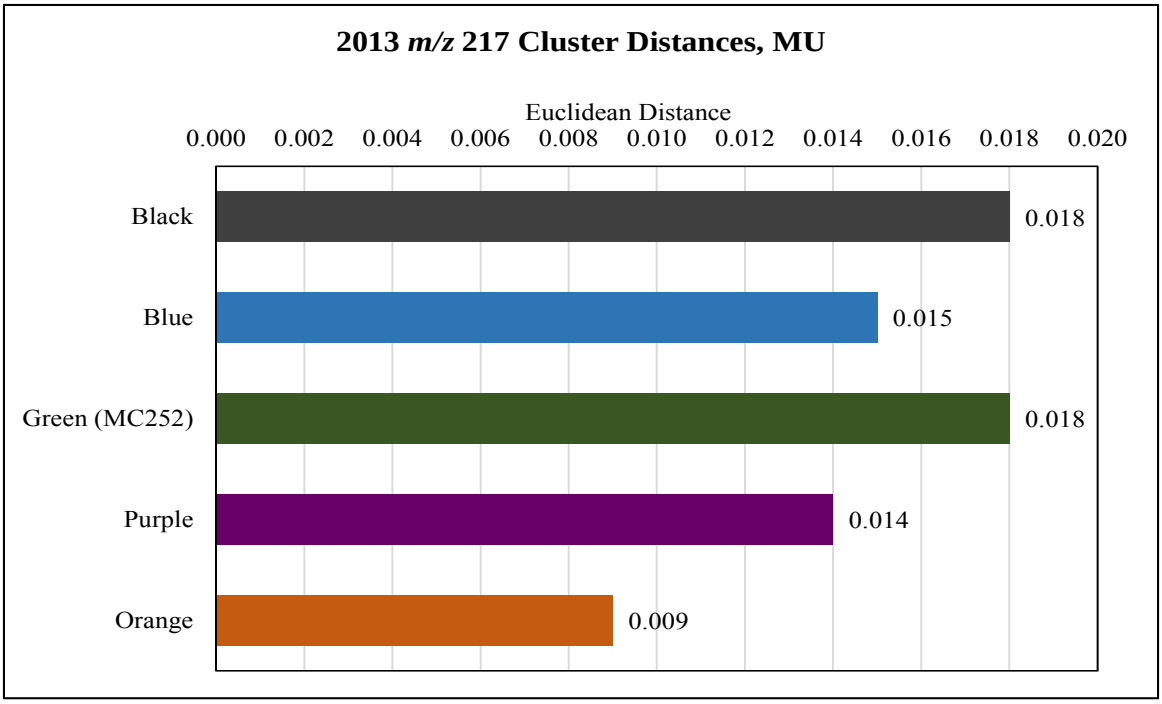


Figure 4.35 The HCA cluster distances of *m/z* 217 peak intensity data for 2013 coastal marsh sediments analyzed on MU.

Figures 4.36 through 4.39 are the HCA and PCA results for coastal marsh sediment collected in 2014 and analyzed on the instrument system GT. The clusters are differentiated to some extent in Figure 4.36. The cluster distances, however, are relatively close in Figure 4.37. The blue cluster has 15 samples that are genetically similar to MC252 based on the combined EIC peak intensity data. The green cluster is in a different branch from the blue and black clusters indicating it is less similar. The majority of the samples in the green cluster are background samples with quantifiable abundances of biomarker compounds. All samples within these three clusters were collected from Bay Batiste. All of the samples in the black cluster, however, were collected in August 2014, and the samples in the green (MC252) and blue cluster were a mixture of samples collected in February 2014 and August 2014 from the same sample sites.

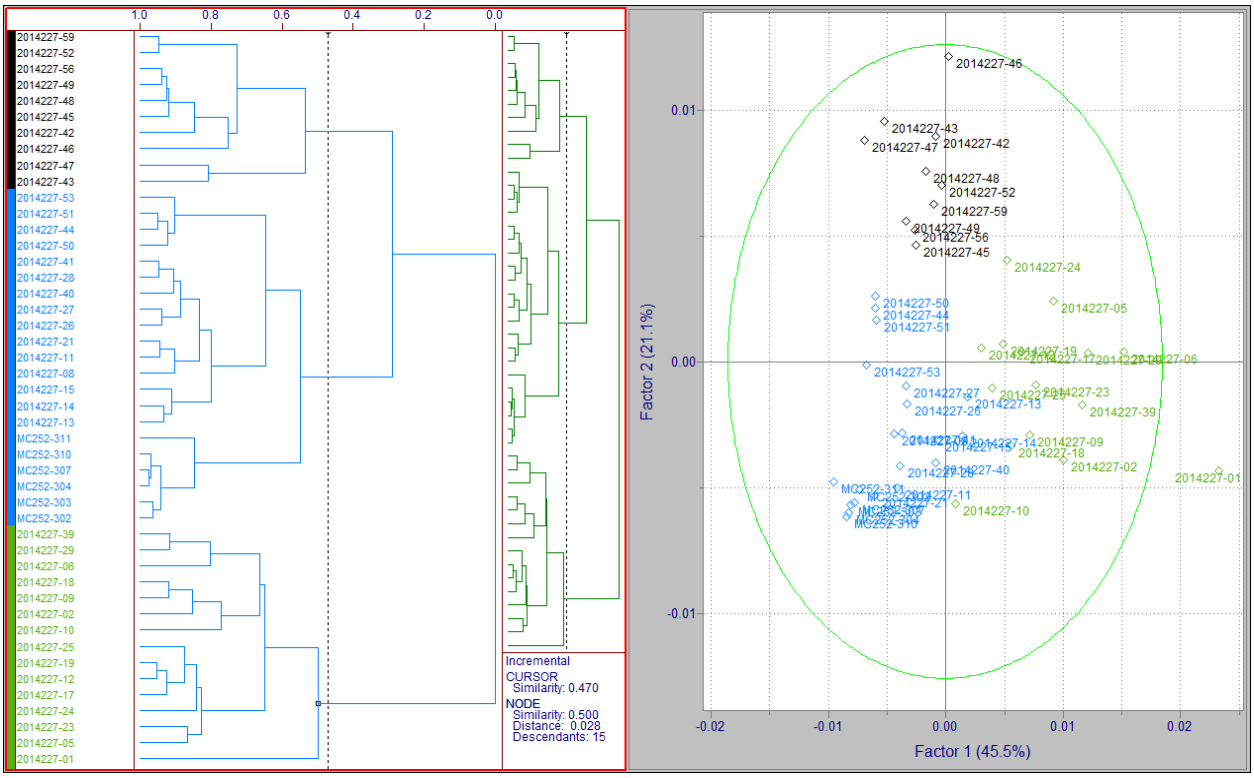


Figure 4.36 The HCA (left) and PCA (right) analysis of combined EIC peak intensity data for 2014 coastal marsh sediments analyzed on GT. (n=46, # variables=1208)

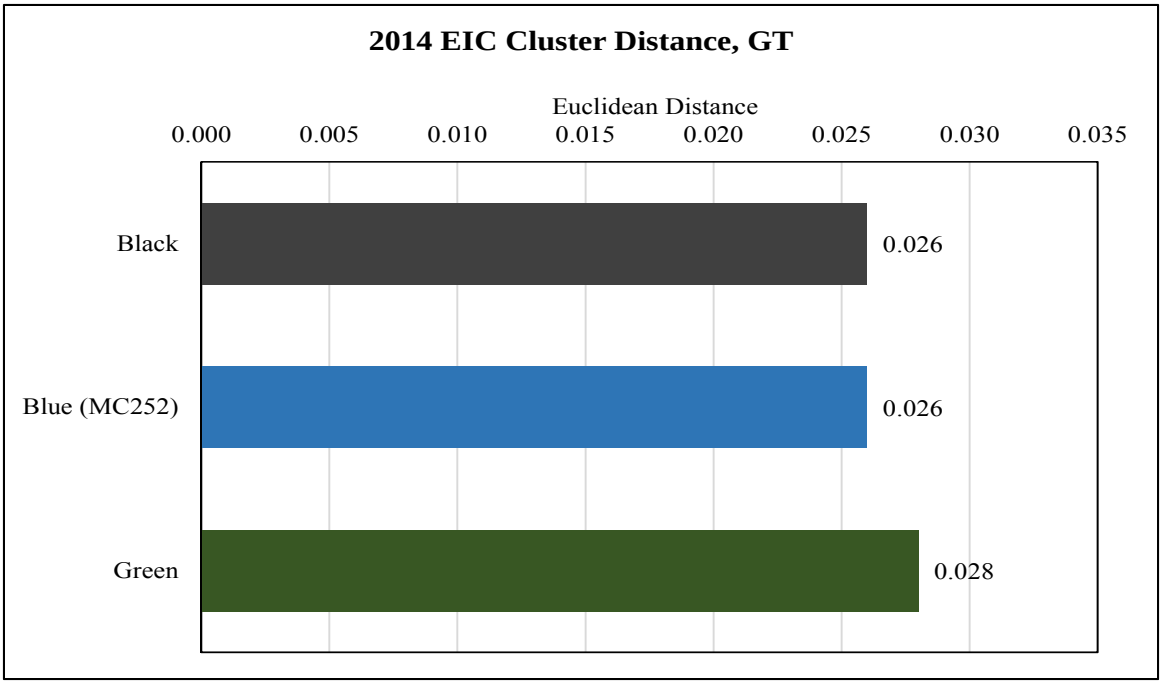


Figure 4.37 The HCA cluster distances of combined EIC peak intensity data for 2014 coastal marsh sediments analyzed on GT.

The orange cluster in Figure 4.38 (*m/z* 217 only) contains MC252 oil and one sample collected in February 2014. The orange (MC252) and purple clusters are in the same quadrant and overlapping in the 2-D PCA plot. The cluster distances in Figure 4.39 between these two clusters is quite different. The same can be said for the blue and green clusters. The black cluster is the least similar of all the clusters and contains most of the same samples that clustered in the black cluster in the combined EIC plot. All the samples in the black cluster were collected in August 2014. The majority of the samples in this cluster had unresolved complex mixture (UCM) humps in their normal alkane chromatographic profiles. All the 2014 coastal marsh sediments analyzed on GT were collected from the same sampling sites but at different times of the year.

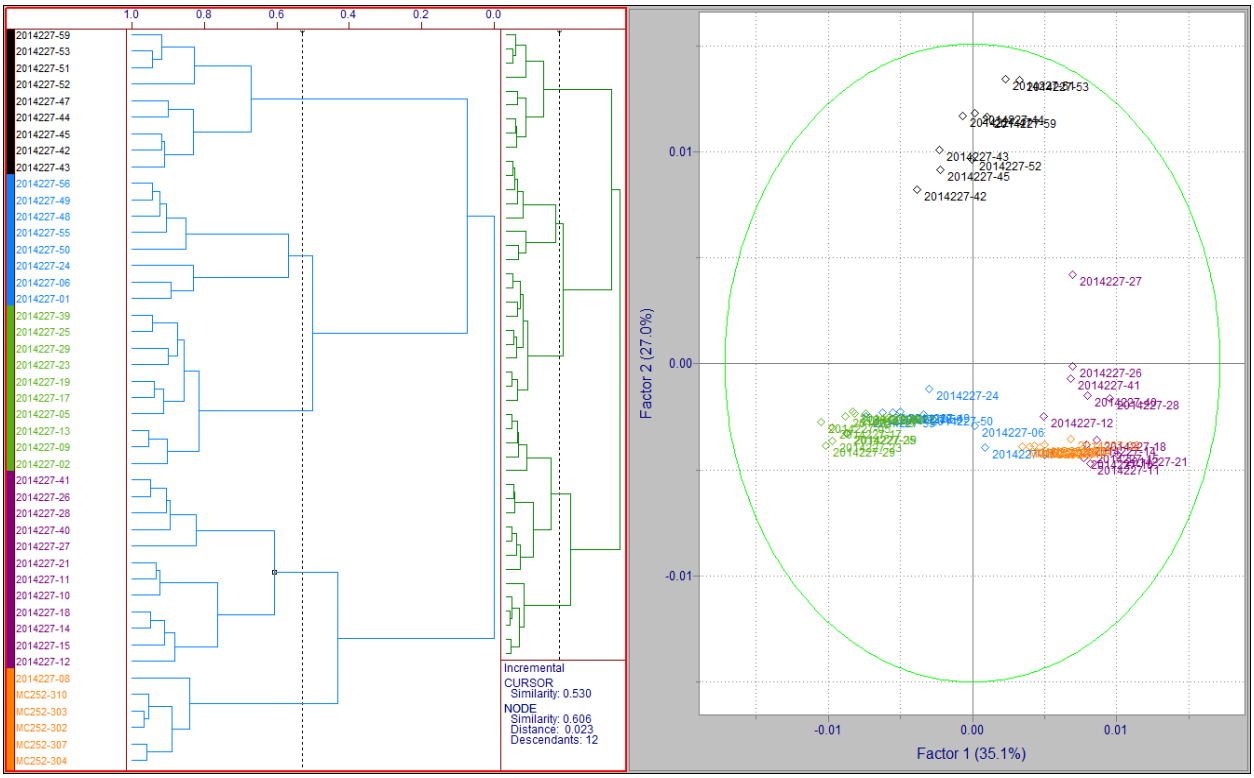


Figure 4.38 The HCA (left) and PCA (right) analysis of *m/z* 217 peak intensity data for 2014 coastal marsh sediments analyzed on GT. (n=45, # variables=671)

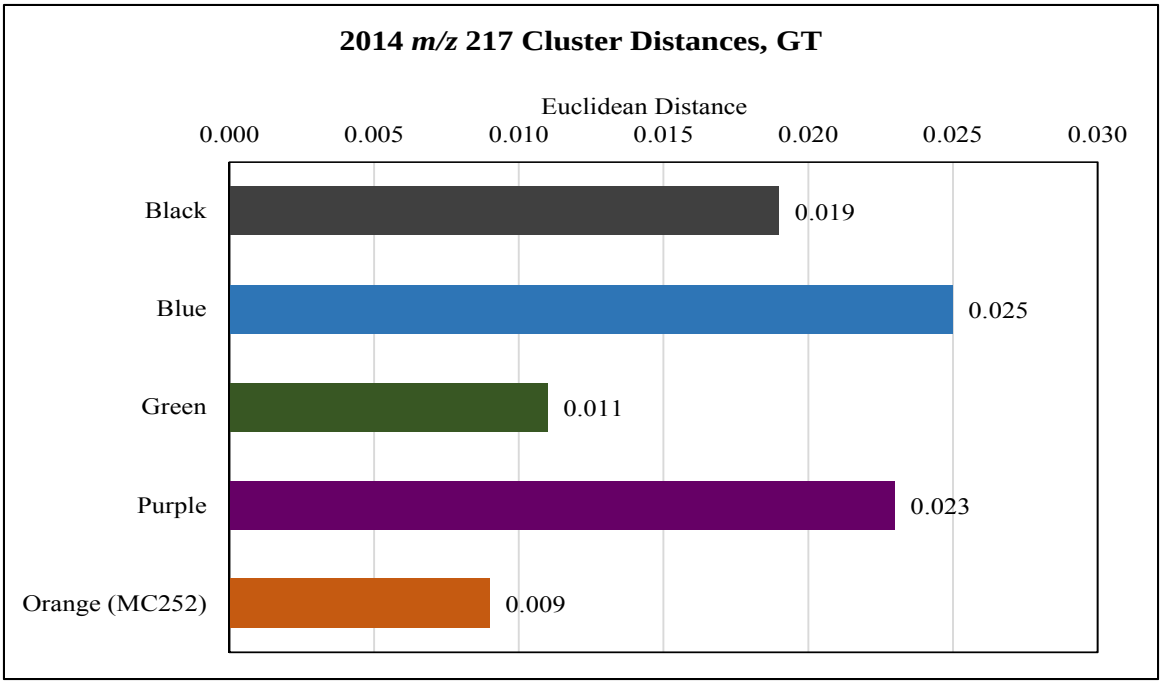


Figure 4.39 The HCA cluster distances of *m/z* 217 peak intensity data for coastal marsh sediment samples analyzed on GT.

Figures 4.40 through 4.43 are the HCA and PCA results for coastal marsh sediment collected in 2014 and analyzed on the instrument system MU. In Figure 4.40, MC252 oil is within the purple cluster and there are no samples included in the cluster. The black, blue and green clusters would be related at the tribal level; however, at the family level, cluster distances (Figure 4.41) are distinctly different. The orange and red clusters are less similar to all other clusters as indicated by their cluster distances in Figure 4.41, but also by the fact that they are in their own branch in the HCA dendrogram. Distinct differentiation of samples is not entirely evident in the 2-D PCA plot. Samples in this data set were collected from the CWC base sites in the spring and fall, and the majority of these samples had TIC and normal alkane chromatographic profiles that look like background samples but have quantifiable abundances of biomarker compounds.

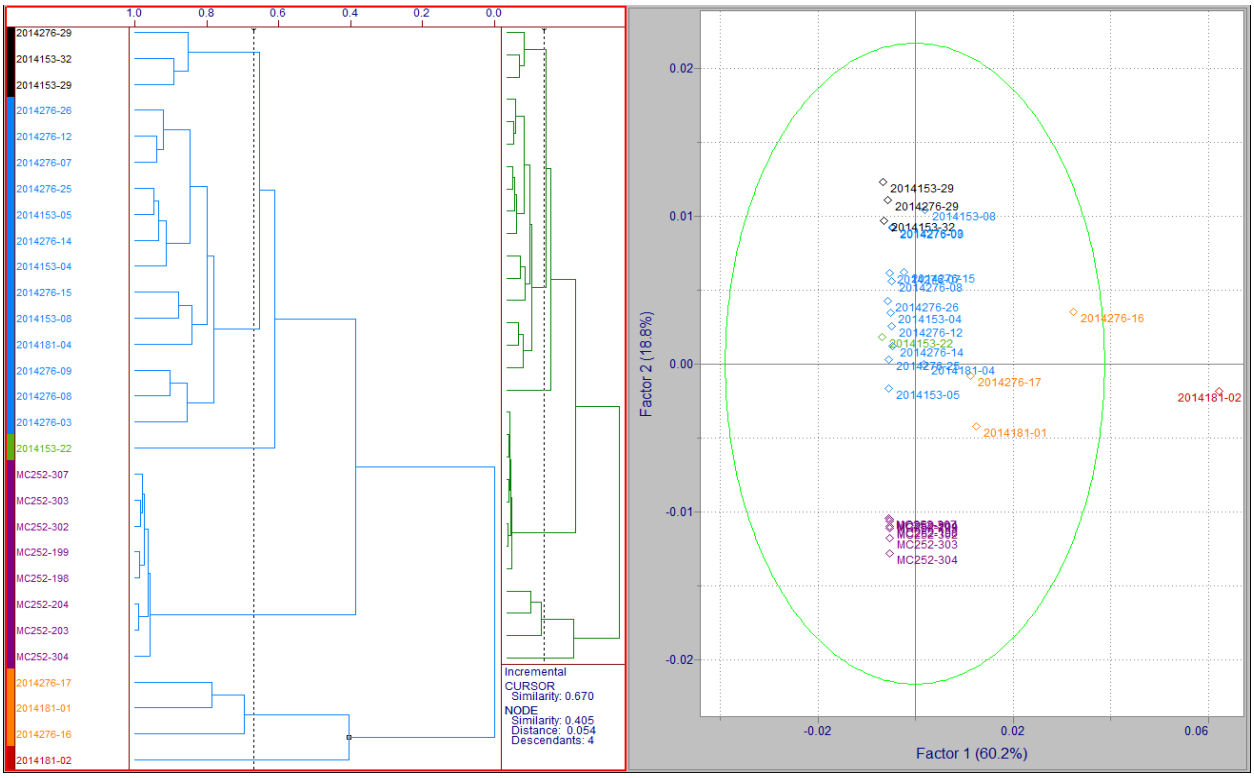


Figure 4.40 The HCA (left) and PCA (right) analysis of combined EIC peak intensity data for 2014 coastal marsh sediments analyzed on MU. (n=29, # variables=1517)

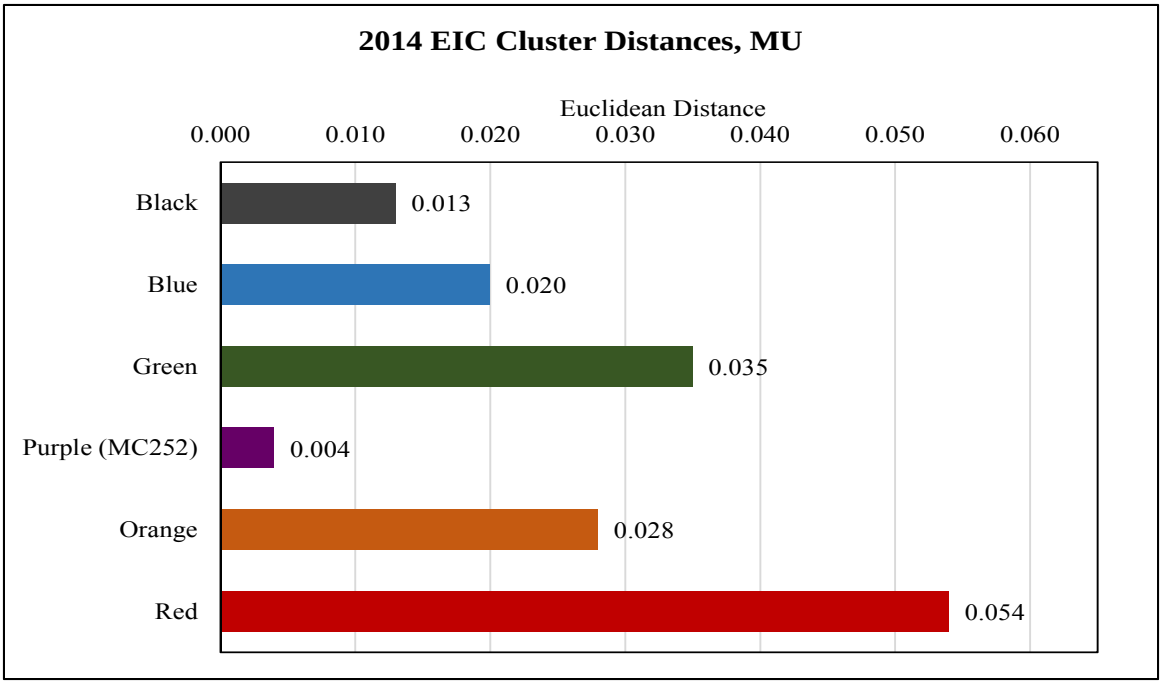


Figure 4.41 The HCA cluster distances of combined EIC peak intensity data for 2014 coastal marsh sediments analyzed on MU.

Figure 4.42 displays the results of the *m/z* 217 only EIC data for 2014 coastal marsh sediments analyzed on instrument MU. The purple cluster is the MC252 cluster and there are no samples within it at the family level displayed. The purple MC252 cluster, at a tribal level, would still be differentiated from the black, blue, and green clusters. The latter three clusters, however, would be related at the tribal level. Cluster distances are all similar in Figure 4.43. The 2-D PCA plot, however, differentiates the purple (MC252) cluster from the blue and black clusters, and green is separated from all other clusters. Almost all of the 2014 coastal marsh sediments analyzed on instrument MU had background chromatographic profile with quantifiable abundances of biomarker compounds, or were samples with trace abundances of biomarkers. There is no apparent effect of sampling time on the clustering of samples like there has been in previously discussed data sets.

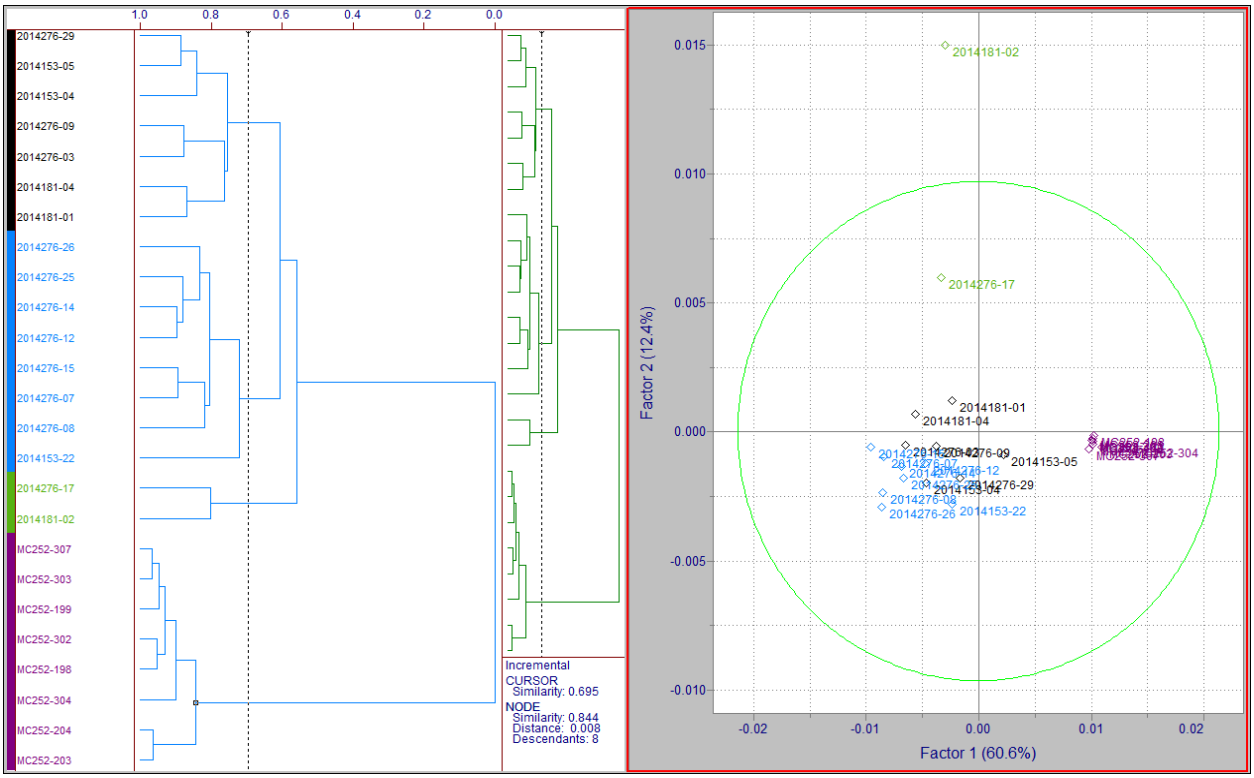


Figure 4.42 The HCA (left) and PCA (right) analysis of *m/z* 217 peak intensity data for 2014 coastal marsh sediments analyzed on MU. (n=25, # variables=799)

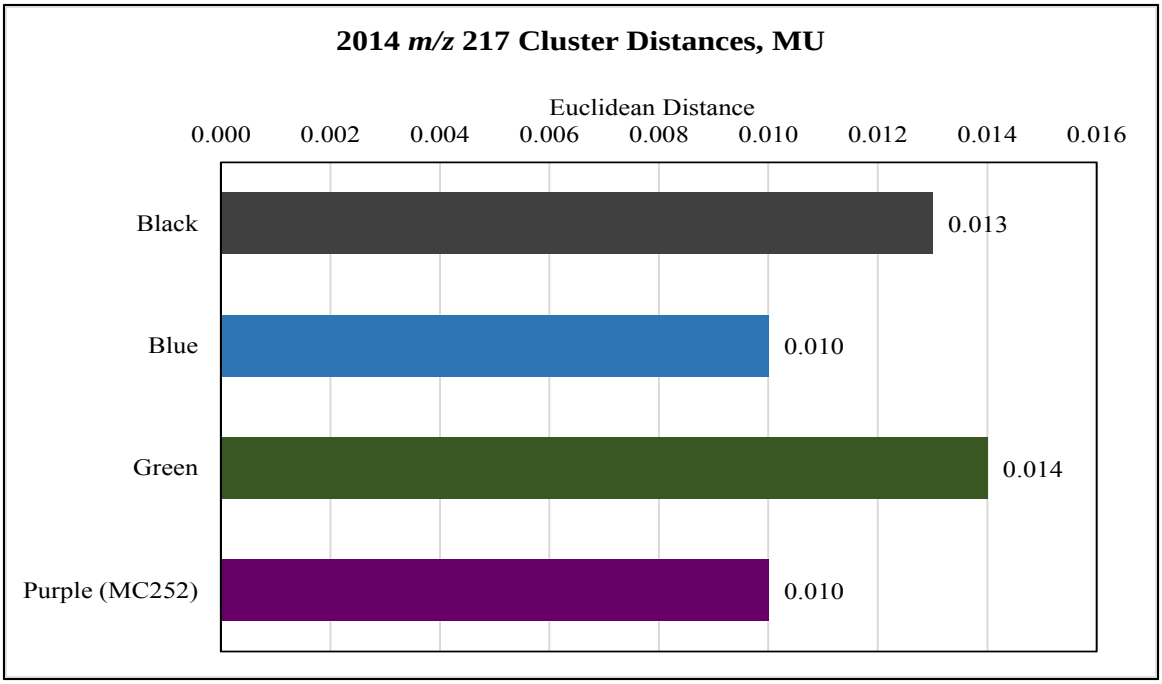


Figure 4.43 The HCA cluster distances of *m/z* 217 peak intensity data for 2014 coastal marsh sediments analyzed on MU.

Figures 4.44 through 4.47 are the HCA and PCA results for coastal marsh sediments collected in 2015 and analyzed on the instrument system GT. MC252 oil is in the red cluster in Figure 4.44, along with three samples collected in February 2015 from Bay Batiste. The red (MC252), orange, and blue clusters appear to have some similarity based on their position in the 2-D PCA plot, and their cluster distances in Figure 4.45 also seem to support this. The black cluster contains 10 oiled samples that were collected in May 2015 from the CWC base sites. The blue cluster contains 12 oiled samples collected in February 2015 from Bay Batiste. The majority of samples in the blue cluster, and the black cluster to some extent, have UCM humps in their normal alkane chromatographic profiles. The sample in the dark blue cluster was collected in February 2015 from Bay Batiste, and has a very large peak in its *m/z* 217 chromatographic profile.

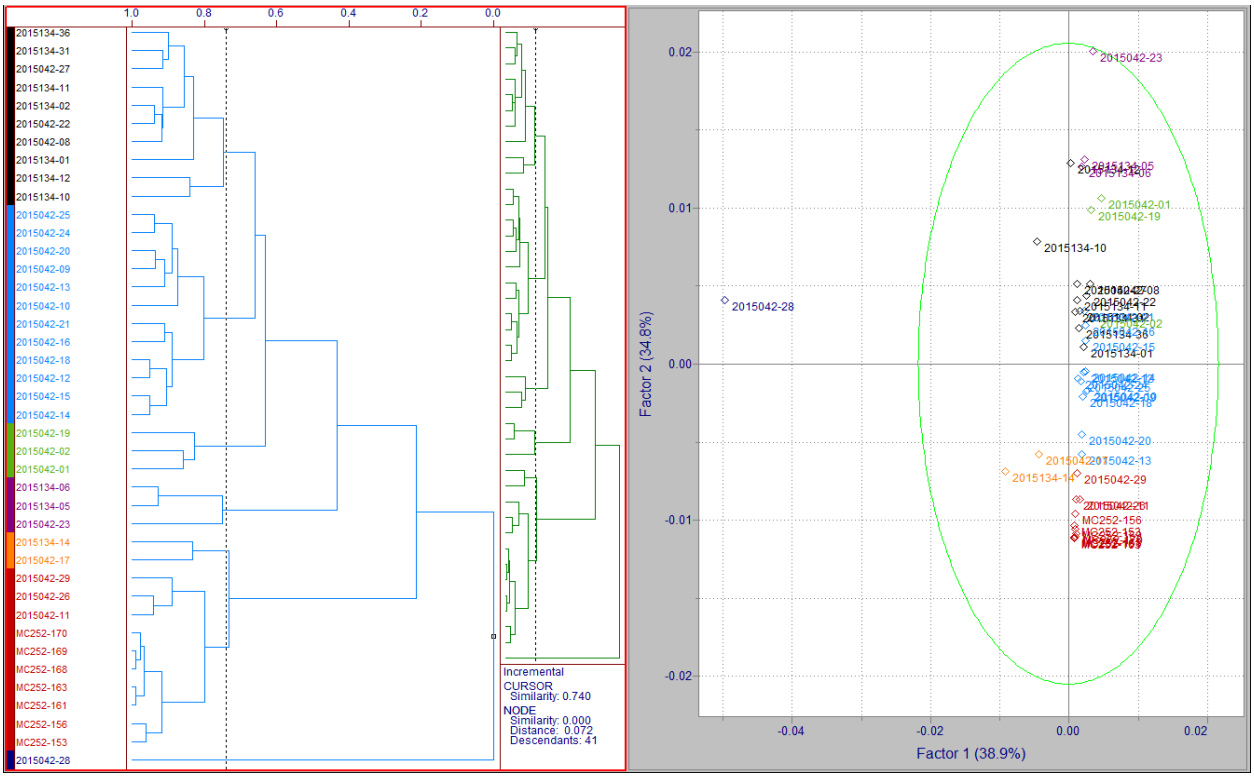


Figure 4.44 The HCA (left) and PCA (right) analysis of combined EIC peak intensity data for 2015 coastal marsh sediments analyzed on GT. (n=41, # variables=1208)

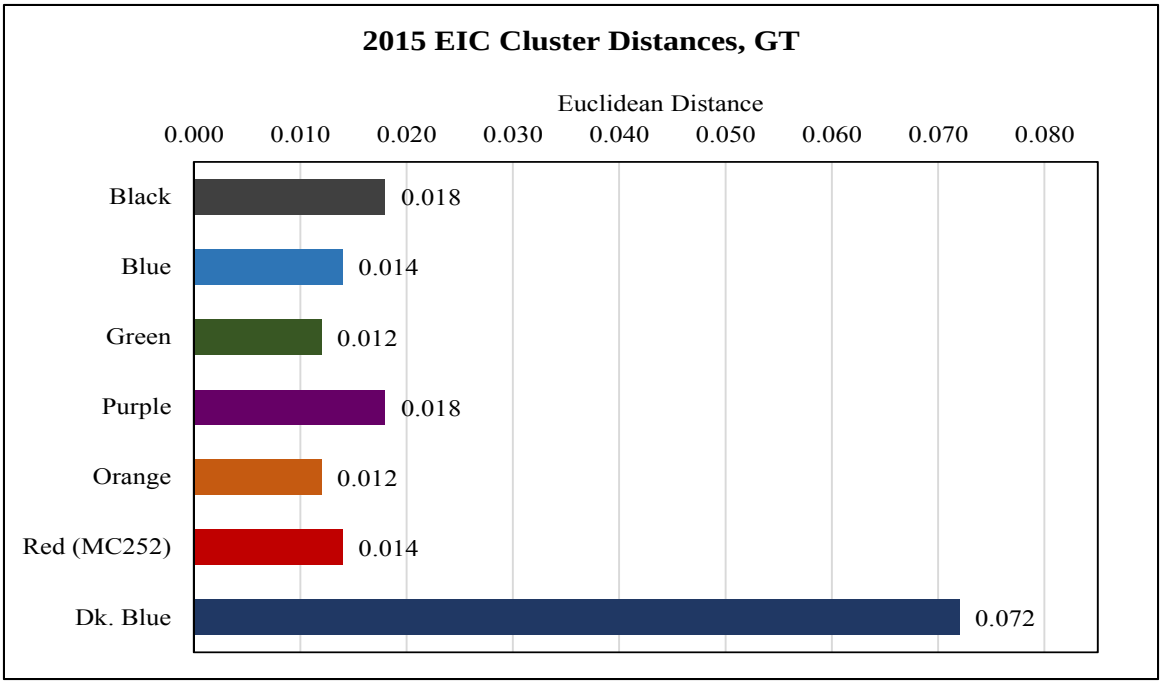


Figure 4.45 The HCA cluster distances of combined EIC peak intensity data for 2015 coastal marsh sediments analyzed on GT.

There are no samples in Figure 4.46 that cluster with MC252 (purple cluster) based on peak intensity data of *m/z* 217 only. The purple cluster, however, is more similar to the green cluster when considering proximity to each other in the 2-D PCA plot, and also cluster distances given in Figure 4.47. The green cluster contains three samples with obvious oil profiles in the TIC and normal alkane chromatograms. The blue and black clusters contain samples that have UCM humps in their normal alkane profiles. The orange cluster contains samples that would be considered background based on TIC and normal alkanes, yet these samples have quantifiable amounts of biomarker compounds in them. Samples in the red cluster (3 total) have the same large interfering peak in their *m/z* 217 profiles.

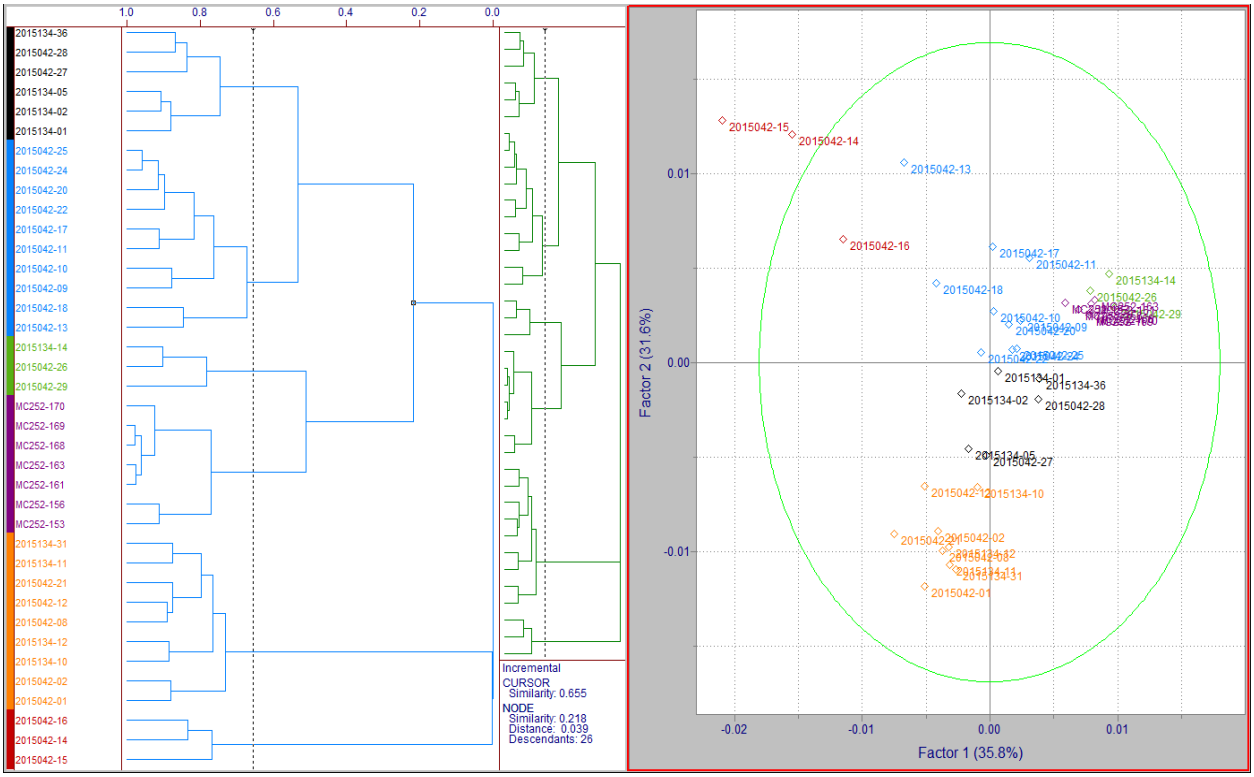

Figure 4.46 The HCA (left) and PCA (right) analysis of *m/z* 217 peak intensity data for 2015 coastal marsh sediments analyzed on GT. (n=38, # variables=671)

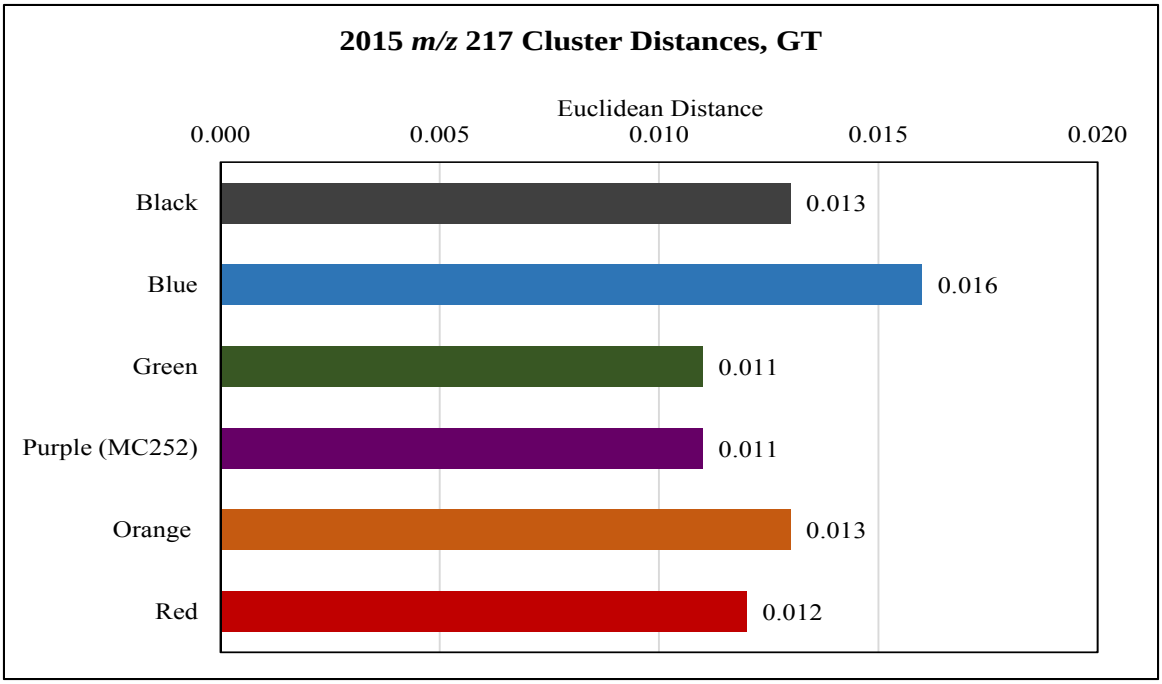


Figure 4.47 The HCA cluster distances of *m/z* 217 peak intensity data for 2015 coastal marsh sediments analyzed on GT.

Figures 4.48 through 4.51 are the HCA and PCA results for coastal marsh sediment collected in 2015 and analyzed on the instrument system MU. There are eight samples that cluster with MC252 (blue cluster) in Figure 4.48. Six of the eight samples were collected in September 2015 from Bay Batiste, and the other two samples were collected in October 2015 from the CWC base site in Cocodrie, LA. The green cluster contains samples collected in September 2015 from Bay Batiste, and most have a UCM hump. The black cluster consists of background samples with biomarkers collected from CWC base sites in either October 2015 or December 2015. This black cluster, however, has a very different cluster distance compared to the blue (MC252) and green clusters in Figure 4.49. The black, blue, and green clusters would be similar at a tribal level.

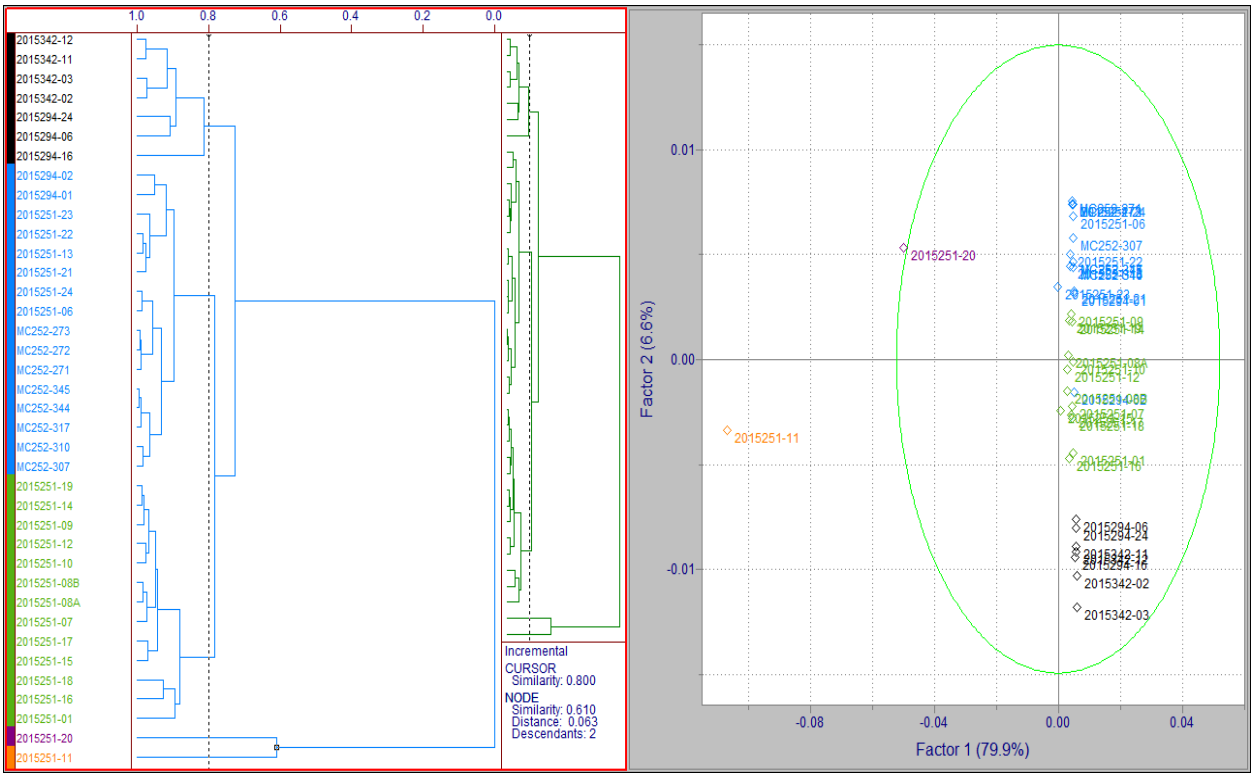


Figure 4.48 The HCA (left) and PCA (right) analysis of combined EIC peak intensity data for 2015 coastal marsh sediments analyzed on MU. (n=38, # variables=1517)

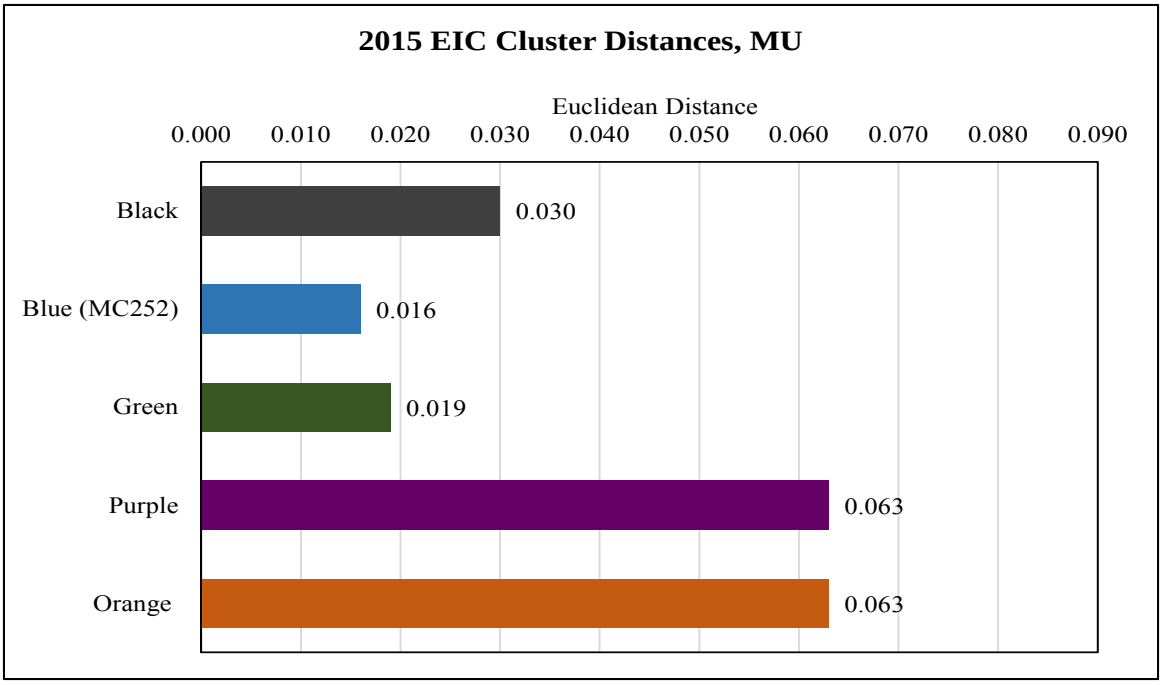


Figure 4.49 The HCA cluster distances of combined EIC peak intensity data for 2015 coastal marsh sediments analyzed on MU.

Sample differentiation is quite evident in the 2-D PCA plot of the *m/z* 217 peak intensity data for 2015 sediments analyzed on MU (Figure 4.50). The green cluster contains MC252 and three samples: two collected in September 2015 from Bay Batiste, and one sample collected in October 2015 from the CWC base site in Cocodrie, LA. These three samples also clustered with MC252 in the HCA analysis using the combined EIC peak intensities. The purple cluster contains nine samples with distinct oil profiles, or UCM humps in their TIC and normal alkane chromatographic profiles that did not cluster with MC252. The green (MC252) and purple clusters, however, have similar cluster distances in Figure 4.51, and these clusters would be similar if the HCA and PCA results were at the tribal level. The black and blue clusters would also be related at the tribal level.

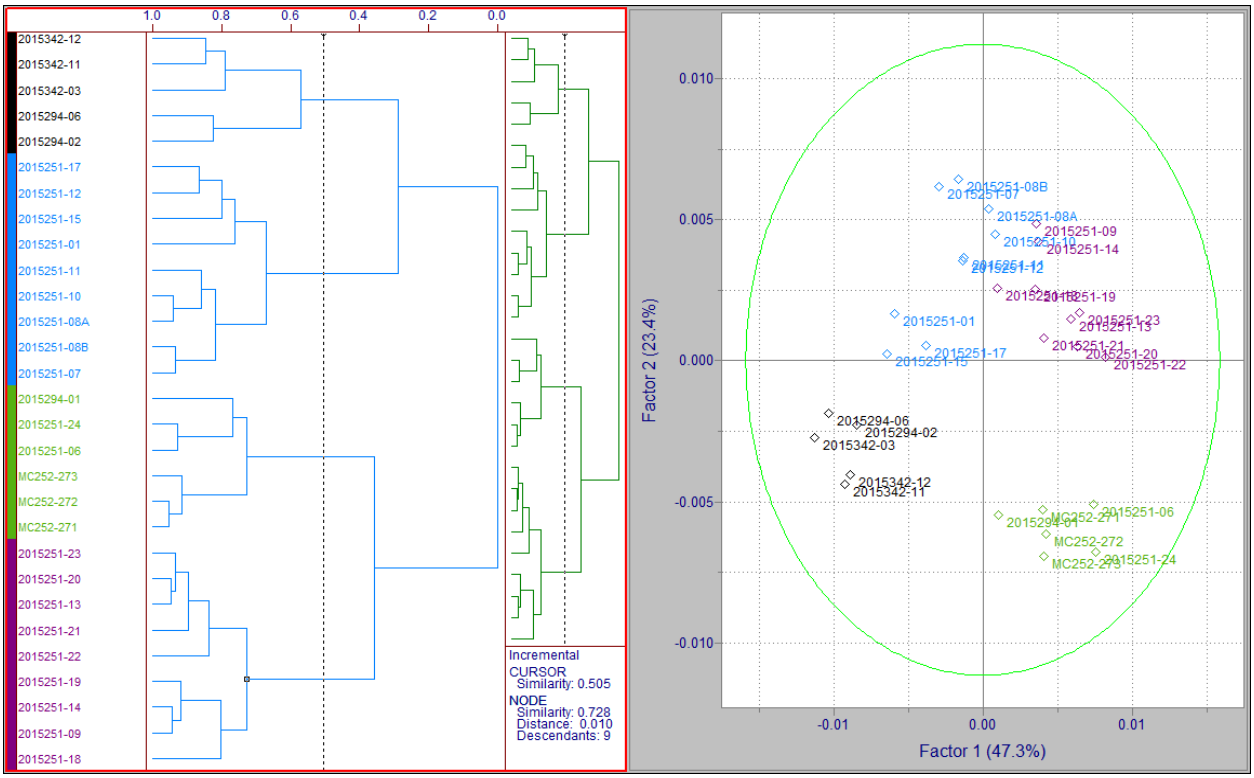


Figure 4.50 The HCA (left) and PCA (right) analysis of *m/z* 217 peak intensity data for 2015 coastal marsh sediments analyzed on MU. (n=29, # variables=799)

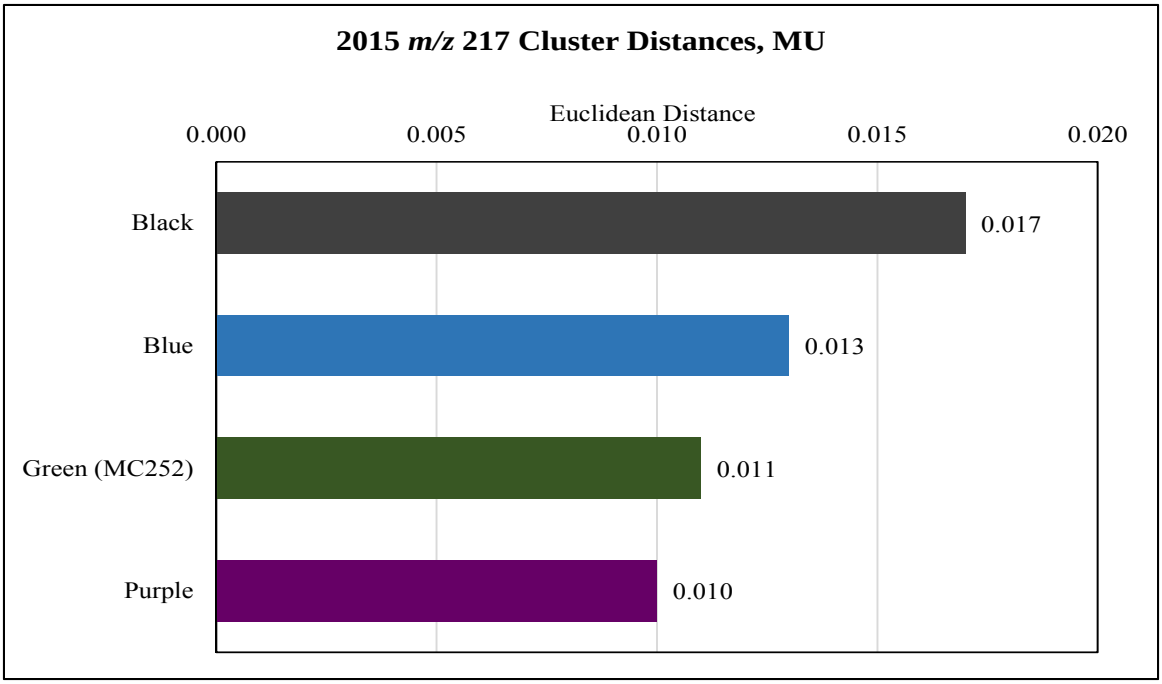


Figure 4.51 The HCA cluster distances of *m/z* 217 peak intensity data for 2015 coastal marsh sediments analyzed on MU.

### 4.3.4 Chemometric Differentiation of Biomarker Weathering Patterns

The *m/z* 217 peak intensity data for oiled coastal marsh sediments was examined and processed separately in Pirouette® to determine if the proposed weathering changes within the MC252 diasteranes and regular steranes profiles (refer back to Figure 4.4) were mathematically related. Pattern A, AB, B, or C (other) were assigned when all the sediment samples were qualitatively sorted as either background or oiled. Figure 4.52 displays the weathering pattern distribution for a total of 293 samples for the entire study time frame (i.e., 2010 through 2015). The samples that underwent Pirouette® analysis had significant abundances of diasteranes and regular steranes, and since the weathering patterns were assigned prior to the chemometric analysis of the *m/z* 217 peak intensity data, the samples could be sorted based on their cluster association after the analysis was complete.

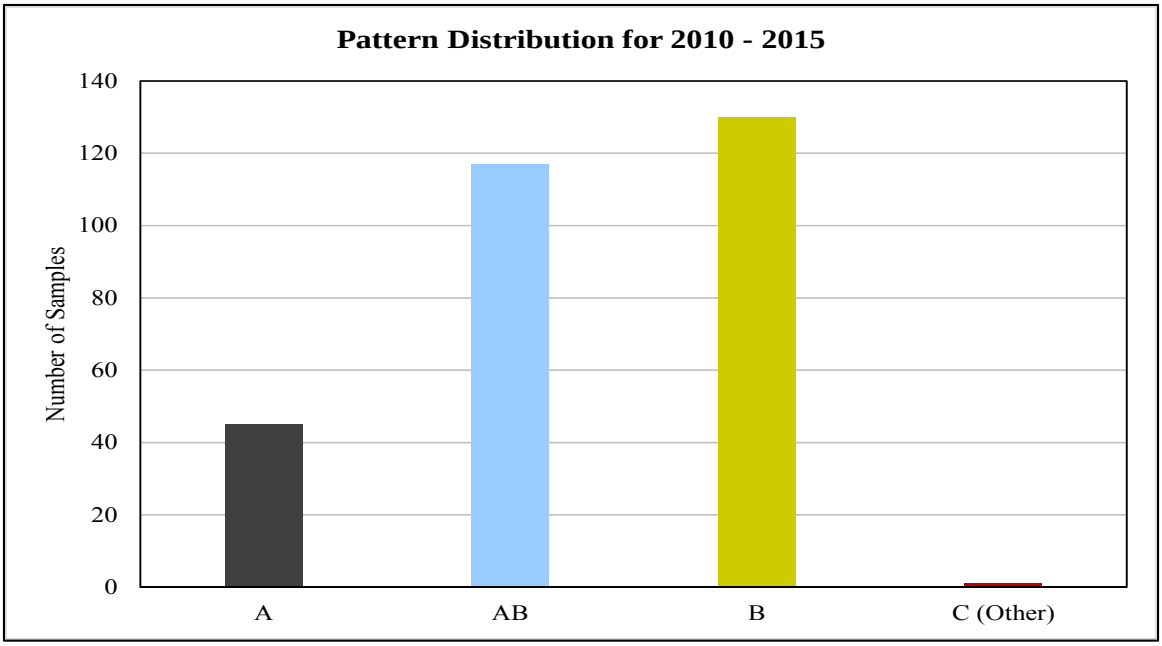


Figure 4.52 The weathering pattern distribution for all oiled coastal marsh samples collected in 2010 – 2015.

The pattern distribution for all the oiled samples increases starting from pattern A, with pattern B having the highest number of oiled samples associated with it. This is in agreement with the proposed weathering pattern where pattern A weathers to pattern AB, and pattern AB eventually weathers to pattern B. The trend in Figure 4.52 does suggest that eventually all oiled samples will have pattern B. There will be re-oiling events that will distribute less weathered oil, like Hurricane Isaac in 2012, and may interrupt the trend from time to time. On the whole, the capability of Pirouette® to separate sample patterns based on qualitative observations was demonstrated. Details for each year and cluster are provided in Appendix F.

A total of 51 of the 293 oiled samples were determined to be genetically similar to MC252 oil based on the *m/z* 217 peak intensity data. Of these 51 samples, 41% were pattern A, 51% were pattern AB, and 8% were pattern B. This distribution is depicted in Figure 4.52.

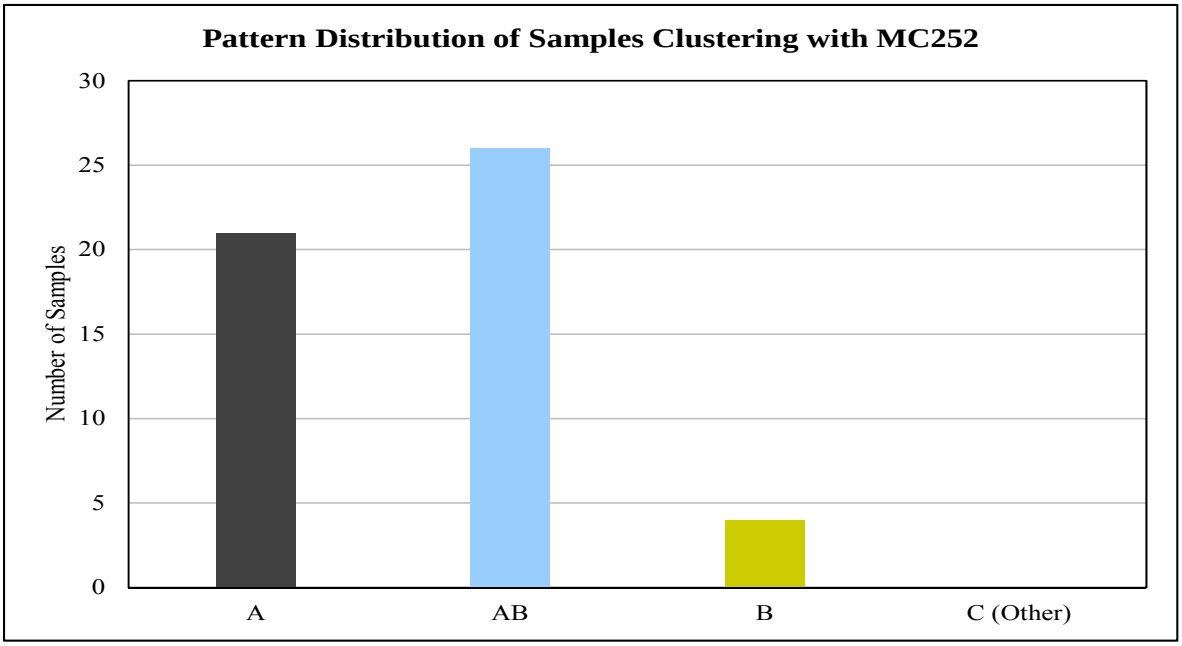


Figure 4.53 The pattern distribution for 51 sediment samples determined to be genetically similar to MC252 through chemometric analysis of *m/z* 217 peak intensity data.

The pattern distribution based on the HCA and PCA analysis of the *m/z* 217 EIC indicates that pattern AB is likely to be weathered MC252 oil; however, there are occurrences, albeit few, where pattern B does cluster with MC252. Weathering from pattern A to AB to B significantly affects the *m/z* 217 chromatographic profile, which in turn will affect the pattern recognition algorithm. Therefore, if an oiled sample has significant differences in peak intensities due to weathering, it will be in a cluster other than MC252 even if it would be qualitatively matched to MC252. This is the result of the sum of squares approach to calculating the distance measure where any changes to large peak intensity values will contribute more to the distance measure (i.e., increasing the distance and decreasing similarity) than slight changes to small peak intensity values (Infometrix, 2014). The cluster distances based on branches in the HCA dendrograms and cluster positions in the 2-D PCA plots can be used to determine if the

weathering patterns are genetically similar. Since there are no probability levels or confidence limits for exploratory HCA and PCA analysis in Pirouette®, however, it is unclear at this point as to whether or not chemometric analysis alone can answer this question.

## 4.4 CONCLUSIONS

Two different quantitative techniques, diagnostic biomarker ratio analysis and chemometric analysis, were applied to coastal Louisiana marsh samples collected from 2010 to 2015. After a qualitative sort of all samples, it was apparent that weathering affected the oil biomarkers, particularly the hopanes and the triaromatic steroids. Five new MC252 diagnostic biomarker ratios within the diasteranes and regular steranes (*m/z* 217), and 14β(H)-steranes (*m/z* 218) were determined and tested because these biomarkers appeared to be the least affected by weathering. These ratios were added to the suite of MC252 diagnostic biomarker ratios in Chapter 2. As a result, a total of 20 ratios were calculated for each oiled sample. The diagnostic biomarker ratio analysis demonstrated that oil biomarker weathering had profoundly affected the calculation, and subsequent critical difference analysis of diagnostic ratios used for MC252 oil source-fingerprinting. Since the diagnostic ratio analysis lost its effectiveness, a more robust quantitative approach, chemometrics, was tested.

Chemometric analysis is an exploratory data analysis technique that recognizes patterns using multivariate pattern recognition algorithms and classifies samples into related groupings or clusters. This type of analysis has not been used previously as a quantitative oil-source fingerprinting tool. It was important to first test the ability of the HCA and PCA differentiation of crude oils from a common geographic origin. This ability was verified by analyzing peak intensity data converted from extracted ion chromatograms of the hopanes, steranes (both

diasteranes and regular steranes, and 14β(H)-steranes), and triaromatic steroids of eight different source oils in Pirouette®. The differentiation of source oils was successful, and chemometric analysis was effectively employed to determine which oil residues detected in coastal marsh sediments were genetically related to MC252 oil. An extension of this objective used the powerful capabilities of HCA and PCA analysis to differentiate weathering patterns within the diasteranes and regular steranes EIC (*m/z* 217).

Chemometric analysis is often used to answer the questions: is the analytical data appropriate for classifying samples, and can different sample categories be determined based on chemical composition (Infometrix, 2014). In this case, both of these questions were answered affirmatively. The benefits of chemometrics is that there are no assumptions about the distribution of data and large amounts of data can be quickly processed to understand natural groupings present in the data set. Interpretation of the HCA dendrograms, however, is relatively simple, which is one of the criticisms of the technique.

Another common issue in exploratory HCA and PCA is deciding where to set the similarity line. Incorrect positioning can result in too few clusters or too many clusters. Where to set the similarity line depends on what question you are trying to answer by using HCA and PCA. For this research, there were two questions: (1) are oil biomarkers in coastal marsh sediments genetically similar to MC252 oil; and, (2) can oil residues be separated based on a proposed progression of MC252 weathering. The similarity line was placed where clusters were in families instead of tribes for better discrimination of the *m/z* 217 weathering pattern. This approach, however, caused samples that are a qualitative match to MC252 to be misclassified into non-MC252 clusters. Setting the similarity line at a tribal level would be sufficient enough to answer the first question, and would be more inclusive of samples determined to be a qualitative match to MC252.

The effect of variation is also profound on sample clustering. The heterogeneous characteristics of oil residues in the environment are very similar to the heterogeneous gene expressions in humans. The same oil residue will be affected differently in the environment just like genetic expression varies from person to person and gene to gene. Genomic microarray analysis uses a technique called biclustering to overcome the inherent variation among large heterogeneous datasets (Shamir et al., 2005; Tanay et al., 2002). The goal of biclustering is to find subgroups that are significantly similar to each other, and as different as possible to the rest of the subgroups (Kaiser and Leisch, 2008). This approach can be extended to the chemometric analysis of oil residues.

Exploratory chemometric analysis is an effective oil-source fingerprinting tool. It is especially useful after diagnostic ratio analysis loses its effectiveness because of biomarker weathering in coastal marsh sediments. Establishing a source oil training dataset to be used for discriminant chemometric techniques like K-nearest neighbor (KNN) is the future work of this research, and will result in an increase of statistical power. Unweathered and varying degrees of weathered source oils will be incorporated in the training set. The source oil training set can then be used to classify unknown oil residues into the *a priori* source oil categories based on class fit derived from the t distribution with $\alpha=0.05$ and the degrees of freedom equal to the number of samples in the class (Infometrix, 2014).

## 4.5 LITERATURE CITED

Aeppli, C., Nelson, R.K., Radović, J.R., Carmichael, C.A., Valentine, D.L., and Reddy, C.M. 2014. Recalcitrance and degradation of petroleum biomarkers upon abiotic and biotic natural weathering of Deepwater Horizon oil. Environmental Science and Technology, 48:6726-6734.

Hansen, A.B, Daling, P.S., Faksness, L., Sorheim, K.R., Kienhuis, P., and Duus, R. 2007. Emerging CEN Methodology for Oil Spill Identification. In: Zhendi Wang and Scott Stout, eds., *Oil Spill Environmental Forensics: Fingerprinting and Source Identification*. Burlington, MA: Academic Press, pp. 229-256.

Infometrix, Inc. 2014. Pirouette Multivariate Data Analysis Software, User's Guide, version 4.5. Infometrix, Inc., Bothell, WA. [Online] Available from: http://www.infometrix.com.

Kaiser, S. and Leisch, F. 2008. A toolbox for bicluster analysis in R. Department of Statistics, University of Munich, Technical Report Number 028, 2008. [Online] Available from: http://citeseerx.ist.psu.edu/viewdoc/download?doi=10.1.1.455.9770&rep=rep1&type=pdf

Lin, Q. and Mendelssohn, I.A. 2012. Impacts and recovery of the Deepwater Horizon oil spill on vegetation structure and function of coastal salt marshes in the Northern Gulf of Mexico. Environmental Science and Technology, 46:3737-3743.

Lorenson, T.D., Leifer, I., Wong, F.L., Rosenbauer, R.J., Campbell, P.L., Lam, A., Hostettler, F.D., Greinert, J., Finlayson, D.P., Bradley, E.S., and Luyendyk, B.P. 2011. Biomarker chemistry and flux quantification methods for natural petroleum seeps and produced oils, offshore southern California: U.S. Geological Survey Scientific Investigations Report 2011-5210, 45 p. and OCS Study BOEM 2011-016.

Meyer, B.M., Overton, E.B., and Turner, R.E. 2014. Oil source identification using diagnostic biomarker ratio analyses. Proceedings of the 2014 International Oil Spill Conference, 2014(1): 2064-2073. doi: 10.7901/2169-3358-2014.1.2064

Michel, J., Owens, E.H., Zengel, S., Graham, A., Nixon, Z., Allard, T., Holton, W., Reimer, P.D., Lamarche, A., White, M., Rutherford, N., Childs, C., Mauseth, G., Challenger, G., and Taylor, E. 2013. Extent and degree of shoreline oiling: *Deepwater Horizon* oil spill, Gulf of Mexico, 2010. PLoS ONE, 8(6):e65087. doi:10.1371/journal.pone.0065087

Natter, M., Keevan, J., Wang, Y., Keimowitz, A.R., Okeke, B.C., Ahjeong, S., and Ming-Kuo, L. 2012. Level and degradation of Deepwater Horizon spilled oil in coastal marsh sediments and pore-water. Environmental Science and Technology, 46:5744-5755.

Oudot, J. and Chaillan, F. 2010. Pyrolysis of asphaltenes and biomarkers for the fingerprinting of the Amoco-Cadiz spill after 23 years. Comptes Rendus Chimie, 13:548-552.

Peters, K.E., Coutrot, D., Nouvelle, X., Ramos, L.S., Rohrback, B.G., Magoon, L.B., and Zumberge, J.E. 2013. Chemometric differentiation of crude oil families in the San Joaquin Basin, California. The American Association of Petroleum Geologists Bulletin, 97(1):103-143.

Peters, K.E., Hostettler, F.D., Lorenson, T.D., and Rosenbauer, R.J. 2008. Families of Miocene Monterey crude oil, seep, and tarball samples, coastal California. The American Association of Petroleum Geologist Bulletin, 92(9):1131-1152.

Peters, K.E., Ramos, L.S., Zumberge, J.E., Valin, Z.C., Scotese, C.R., and Gautier, D.L. 2007. Circum-Artic petroleum systems identified using decision-tree chemometrics. The American Association of Petroleum Geologist Bulletin, 91(6):877-913.

Peters, K.E., Walters, C.C., and Moldowan, J.M. 2005. *The Biomarker Guide, 2nd Edition*. Cambridge, UK: Cambridge University Press.

Radović, J.R., Aeppli C., Nelson, R.K., Jimenez, N., Reddy, C.M., Bayona, J.M., and Albaigés, J. 2014. Assessment of photochemical processes in marine oil spill fingerprinting. Marine Pollution Bulletin, 79:268-277.

Ramsey III, E., Meyer, B.M., Rangoonwala, A., Overton, E., Jones, C.E., and Bannister, T. 2014. Oil source-fingerprinting in support of polarimetric radar mapping of Macondo-252 oil in Gulf Coast marshes. Marine Pollution Bulletin, 89:85-95.

Reddy, C.M., Eglinton, T.I., Hounshell, A., White, H.K., Xu, L., Gaines, R.B., and Frysinger, G.S. 2002. The West Falmouth oil spill after thirty years: the persistence of petroleum hydrocarbons in marsh sediments. Environmental Science and Technology, 36:4754-4760.

Shamir, R., Maron-Katz, A., Tanay, A., Linhart, C., Steinfeld, I., Sharan, R., Shiloh, Y., and Elkon, R. 2005. EXPANDER – an integrative program suite for microarray data analysis. BMC Bioinformatics, 6:232. [Online] Available from: http://bmcbioinformatics.biomedcentral.com/articles/10.1186/1471-2105-6-232

Stout, S.A., Uhler, A.D., McCarthy, K.J., and Emsbo-Mattingly, S. 2002. Chemical fingerprinting of hydrocarbons. In: B.L. Murphy and R.D. Morrison, eds., *Introduction to Environmental Forensics*. London, UK: Academic Press, pp. 137–260.

Tanay, A., Sharan, R., and Shamir, R. 2002. Discovering statistically significant biclusters in gene expression data. Bioinformatics, 18(S1):S136-S144. [Online] Available from: https://bi.snu.ac.kr/SEMINAR/ISMB2002/ISMB2002/S136PPT.pdf

Teal, J.M., Farrington, J.W., Burns, K.A., Stegeman, J.J., Tripp, B.W., Woodin, B., and Phinney, C. 1992. The West Falmouth oil spill after 20 years: fate of fuel oil compounds and effects on animals.

Turner, R.E., Overton, E.B., Meyer, B.M., Miles, M.S., and Hooper-Bui, L. 2014a. Changes in the concentration and relative abundance of alkanes and PAHs from the *Deepwater Horizon* oiling of coastal marshes. Marine Pollution Bulletin, 86:291-297.

Turner, R.E., Overton, E.B., Meyer, B.M., Miles, M.S., McClenachan, G., Hooper-Bui, L., Summers Engle, A., Swenson, E.M., Lee, J.M., Milan, C.S., and Gao, H. 2014b. Distribution and recovery trajectory of Macondo (Mississippi Canyon 252) oil in Louisiana coastal wetlands. Marine Pollution Bulletin, 87:57-67.

U.S. Environmental Protection Agency. 2000. Test Methods for Evaluating Solid Wastes, Physical/Chemical Methods, SW-846. [Online] Available from: http://www.epa.gov/wastes/hazard/testmethods/sw846/online/index.htm. USEPA, Office of Solid Waste and Emergency Response, Washington, D.C.

Wang, Z., Fingas, M.F., Owens, E.H., Sigouin, L., and Brown, C.E. 2001. Long-term fate and persistence of the spilled *Metula* oil in a marine salt marsh environment: degradation of petroleum biomarkers. Journal of Chromatography A, 926:275-290.

Wang, Z., Stout, S.A., and Fingas, M. 2006. Forensic fingerprinting of biomarkers for oil spill characterization and source identification. Environmental Forensics, 7:105-146.

Wang, Z.D. and Fingas, M. 1995. Differentiation of the source of spilled oil and monitoring of the oil weathering process using gas chromatography-mass spectrometry. Journal of Chromatography, 712:321-343.

Wang, Z.D. and Fingas, M. 2003. Development of oil hydrocarbon fingerprinting and identification techniques. Marine Pollution Bulletin, 47(9-12):423-452.

# CHAPTER 5: OVERALL CONCLUSIONS

This research utilized gas chromatography/mass spectrometry (GC/MS) data to test two different quantitative oil source-fingerprinting approaches. The first quantitative oil source-fingerprinting technique was the determination of a suite of diagnostic biomarker ratios with statistical considerations that could differentiate MC252 crude oils from other South Louisiana crude oils. These same ratios were used to link changes in remotely sensed data to the oil from the *Deepwater Horizon* (DWH) oil spill (i.e., MC252 oil). Oil source-fingerprinting by means of diagnostic biomarker ratios was essential in showing that dramatic changes in pre- to post-DWH oil spill PolSAR backscatter mechanisms were related to the presence of oil in the Barataria Bay region of study, and also resulted in the positive identification of MC252 oil. The application of the diagnostic ratio analysis to coastal marsh sediments collected from 2010 to 2015 further corroborated the results described in the literature documenting that the typically recalcitrant oil biomarkers used for oil fingerprinting analysis were altered by environmental weathering. The results from the diagnostic biomarker ratio analysis indicated that oil biomarker weathering had profoundly affected the calculation, and subsequent critical difference analysis, of diagnostic ratios used for MC252 oil source-fingerprinting. Therefore, the applicability of chemometric analysis as an advanced oil source-fingerprinting technique was evaluated and validated.

There are obvious pros and cons to both quantitative techniques presented herein. The diagnostic ratio analysis calculates individual ratios and statistically compares these ratios to the same ratios of a known source oil. This approach is common, but the final criteria of placing oil residues into an oil source-fingerprinting category based on the total number of matching ratios is not. The diagnostic biomarker ratio analysis is effective up to a certain degree of weathering,

which depends on when the critical difference of 14% is exceeded. Once the majority of ratios begin to exceed the critical difference, this technique loses its effectiveness. Application of chemometrics can span from the beginning of an oil spill and beyond. It doesn't concentrate on individual compounds and instead uses the entire pattern within a biomarker mass window. Exploratory chemometric analysis can quickly determine natural similarities and dissimilarities in large datasets, and even the distribution of clusters in the PCA appears to provide insight to the potential effects of weathering on oil residues from the same source oil. Current limitations to chemometrics are objectively setting the similarity line, misclassification, and deriving *p*-values and confidence limits for clusters. Other scientific fields that use similar clustering techniques, however, have overcome these issues, so it is likely that the same is true for chemometrics applied as an oil source-fingerprinting tool.

Time and again in a variety of oil spill situations the critical need for robust quantitative oil source-fingerprinting techniques to compliment qualitative oil source-fingerprinting techniques becomes a topic of discussion. Being able to place values and statistical probabilities when comparing oil residues to a suspected source oil is a huge contribution to field of environmental forensics. Two European institutions, Nordtest and CEN, have been working towards establishing a technically robust and defensible methodology for oil source-fingerprinting. Their goal is to standardized oil spill identification protocols for European countries, as well as setting a standard for potential international use. The protocol, however, is based on the correlation of diagnostic ratios. Using diagnostic ratios is not an issue during the initial stages of an oil spill because the source oil is still relatively fresh. The question arises if there is a need for oil source-fingerprinting beyond oil spill response and clean-up stages. If so, diagnostic ratios may not be the best approach because oil biomarkers weather, and ratios lose

their effectiveness. A chemometric analysis has its roots in petroleum geochemistry, much like all other methods of oil source-fingerprinting, and holds a tremendous amount of potential as an oil source-fingerprinting tool. Furthermore, the exploratory HCA and PCA process can lead to a more powerful discriminate analysis of the data. This research only scratched the surface of the capabilities of chemometrics as an oil source-fingerprinting tool. Because chemometrics is a multivariate approach, more than just variables generated from chromatographic data can be analyzed, perhaps opening new quantitative oil source-fingerprinting avenues.

## APPENDIX A: PERMISSION REQUEST TO REPRINT

From: Buffy M Meyer
Sent: Fri 2/12/2016 10:41 AM
To: gregory.hall@uscga.edu;
Subject: Permission for dx.doi.org/10.7901/2169-3358-2014.1.2064

I am the primary author on the paper titled "Oil source identification using diagnostic biomarker ratio analyses" published in the IOSC Conference Proceedings, 2014(1):2064-2073, (dx.doi.org/10.7901/2169-3358-2014.1.2064) and need to obtain permission to use this publication as part of my dissertation. My university requires that I inform publishers that my dissertation will be available for viewing on the web. Can you please advise me on how to proceed in obtaining this permission, and receiving documentation of this permission to include in an appendix of my dissertation?

Thank you in advance.

Buffy Meyer, Ph.D. Candidate
Research Associate V
Louisiana State University
Department of Environmental Sciences
1263 Energy, Coast & Environment Bldg, Baton Rouge, LA 70803

Thanks Buffy.

Permission granted.

My apologies for this informal email while we get our formal system started.

Best Regards,

**CDR Gregory J. Hall, Ph.D.**
Associate Dean of Academics
Editor, Proceedings of the International Oil Spill Conference
**United States Coast Guard Academy**
15 Mohegan Ave
New London, CT 06320
860 444 8624

Go Bears!

## APPENDIX B: CHROMATOGRAPHIC PROFILES OF QUADRUPLICATE ANALYSES OF SOURCE OILS

ANSC – *m/z* 191

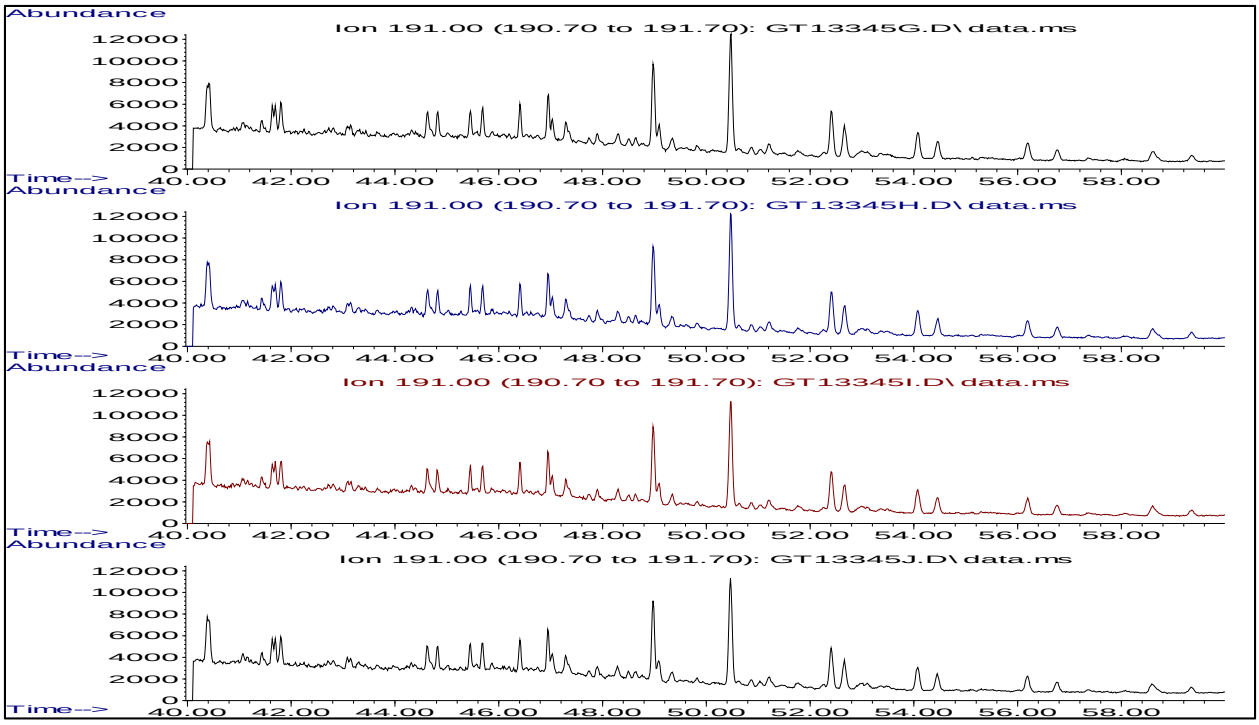


ANSC – *m/z* 217

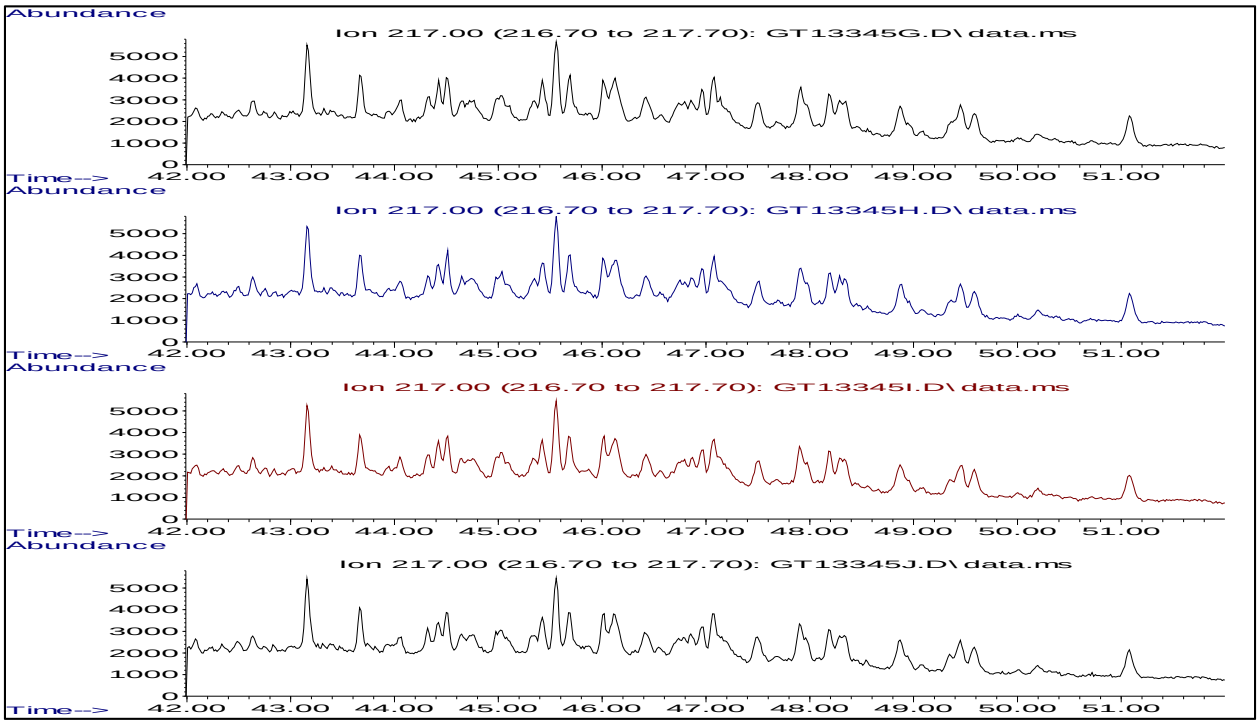

ANSC – *m/z* 218

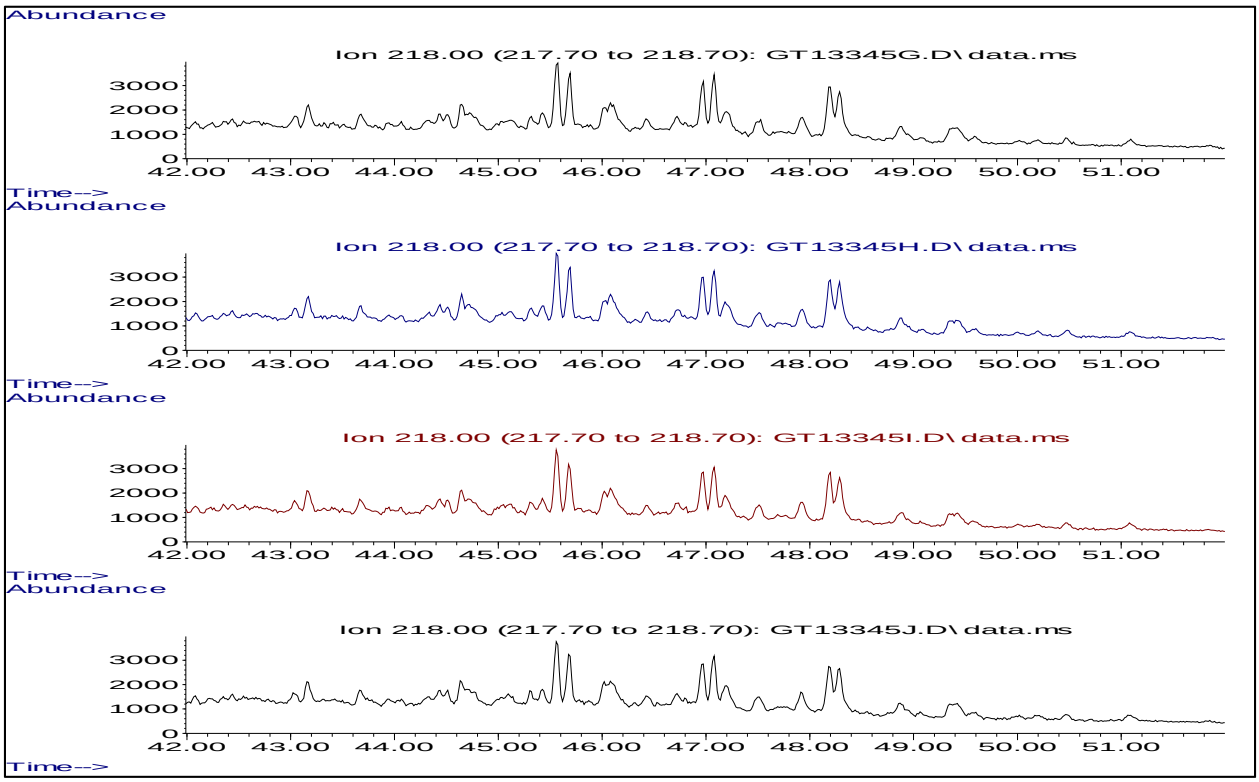


ANSC – *m/z* 231

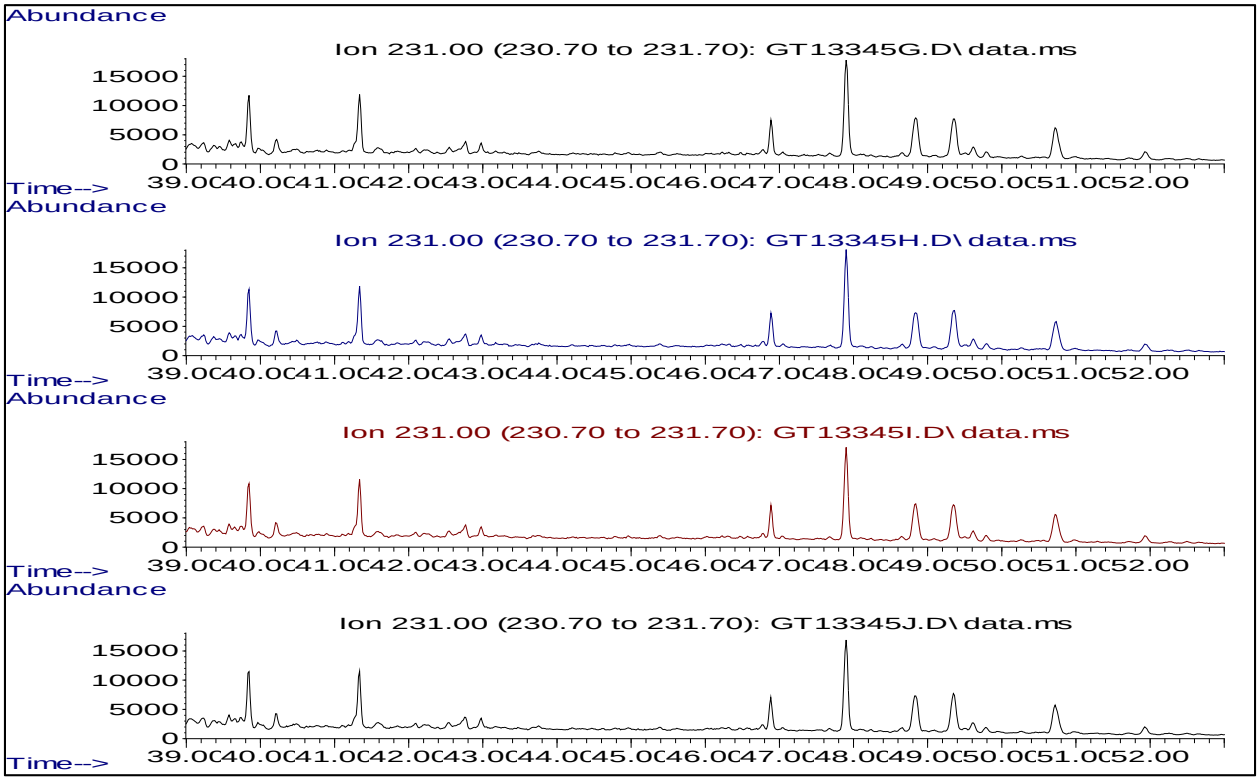

BP Surrogate Oil (Marlin Platform, VK915) – *m/z* 191

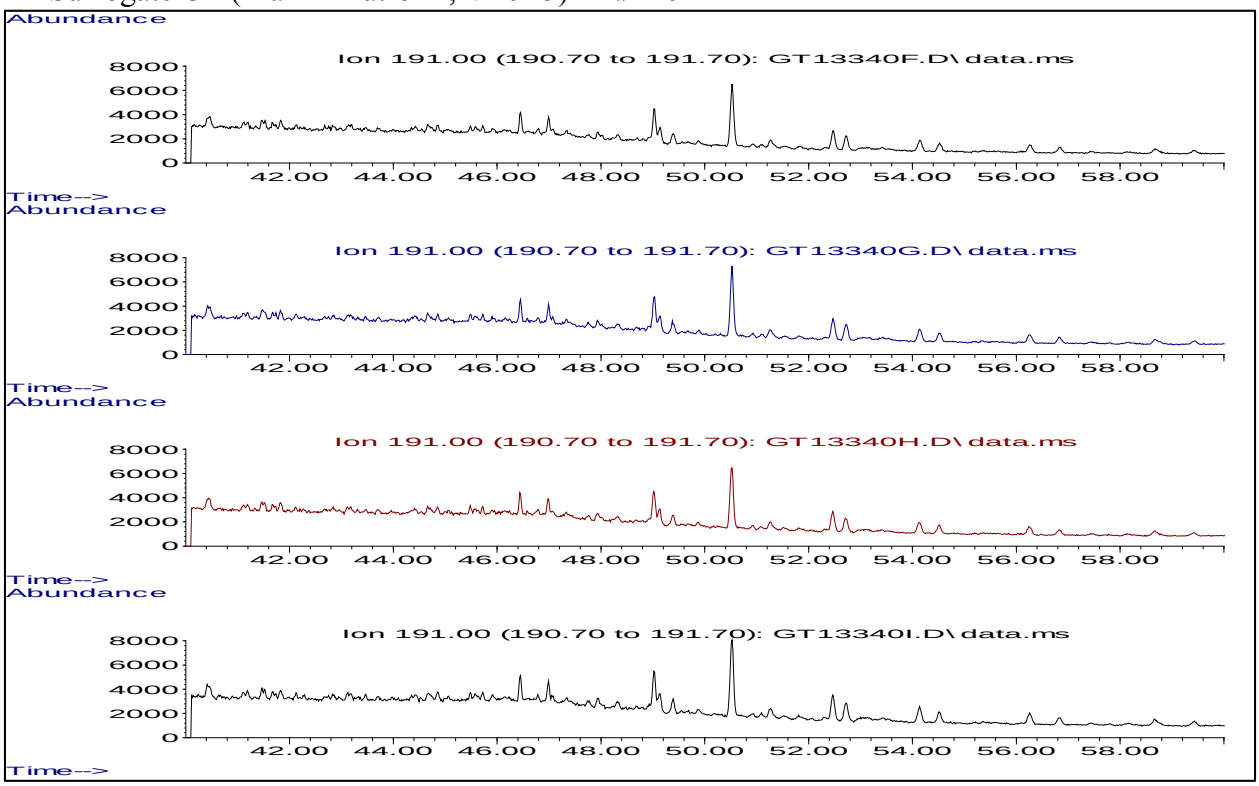


BP Surrogate Oil (Marlin Platform, VK915) – *m/z* 217

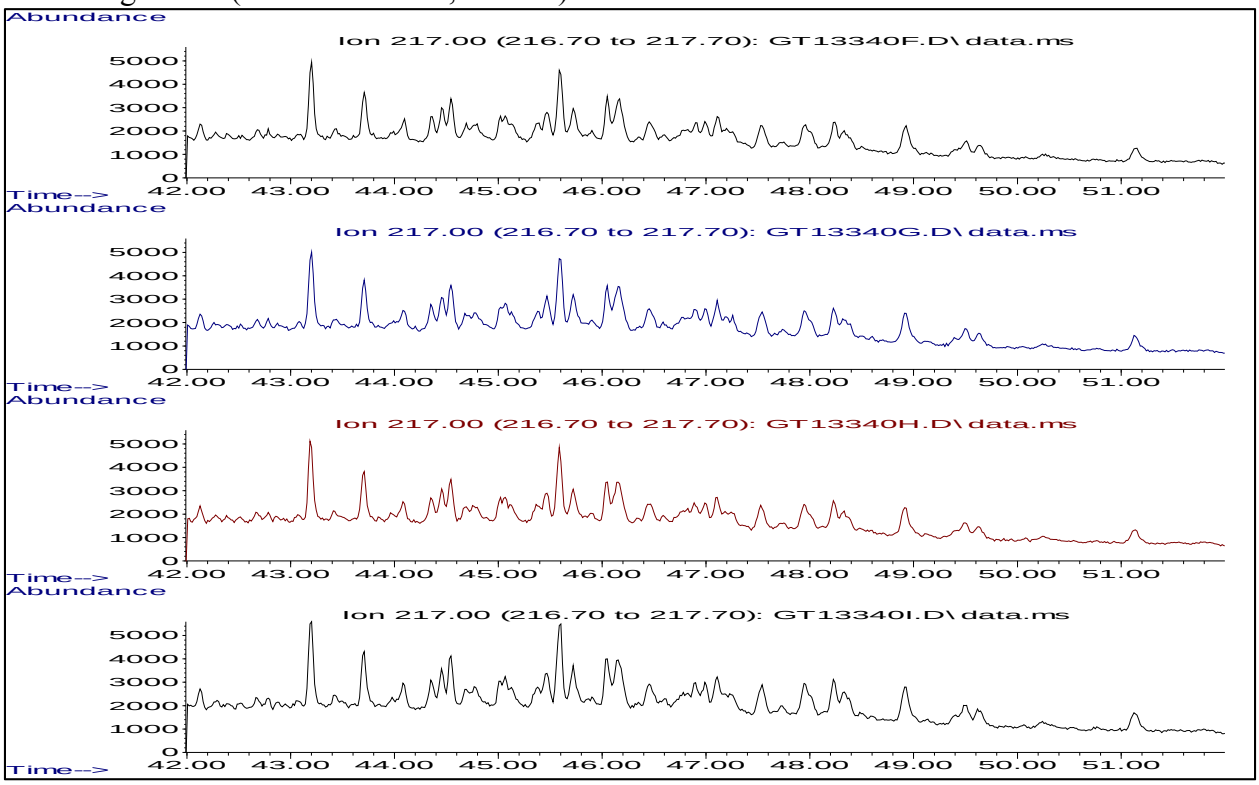

BP Surrogate Oil (Marlin Platform, VK915) – *m/z* 218

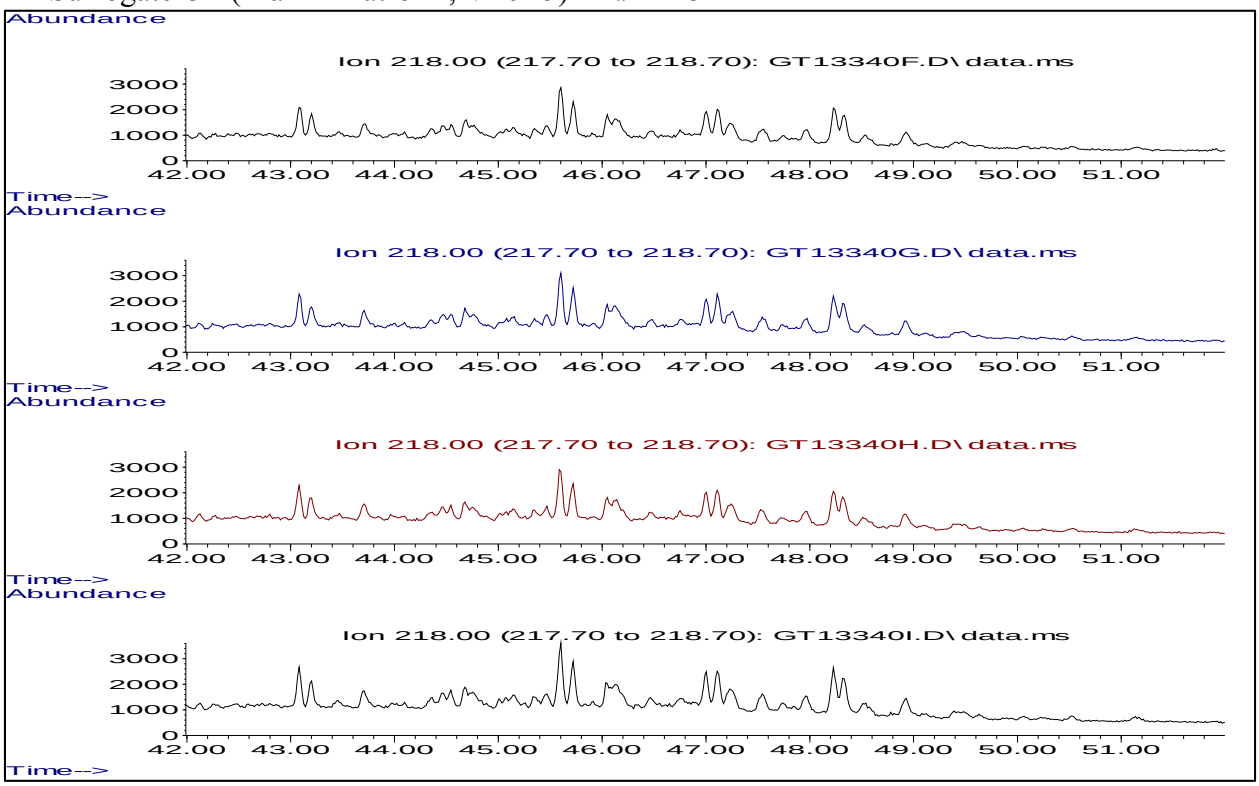


BP Surrogate Oil (Marlin Platform, VK915) – *m/z* 231

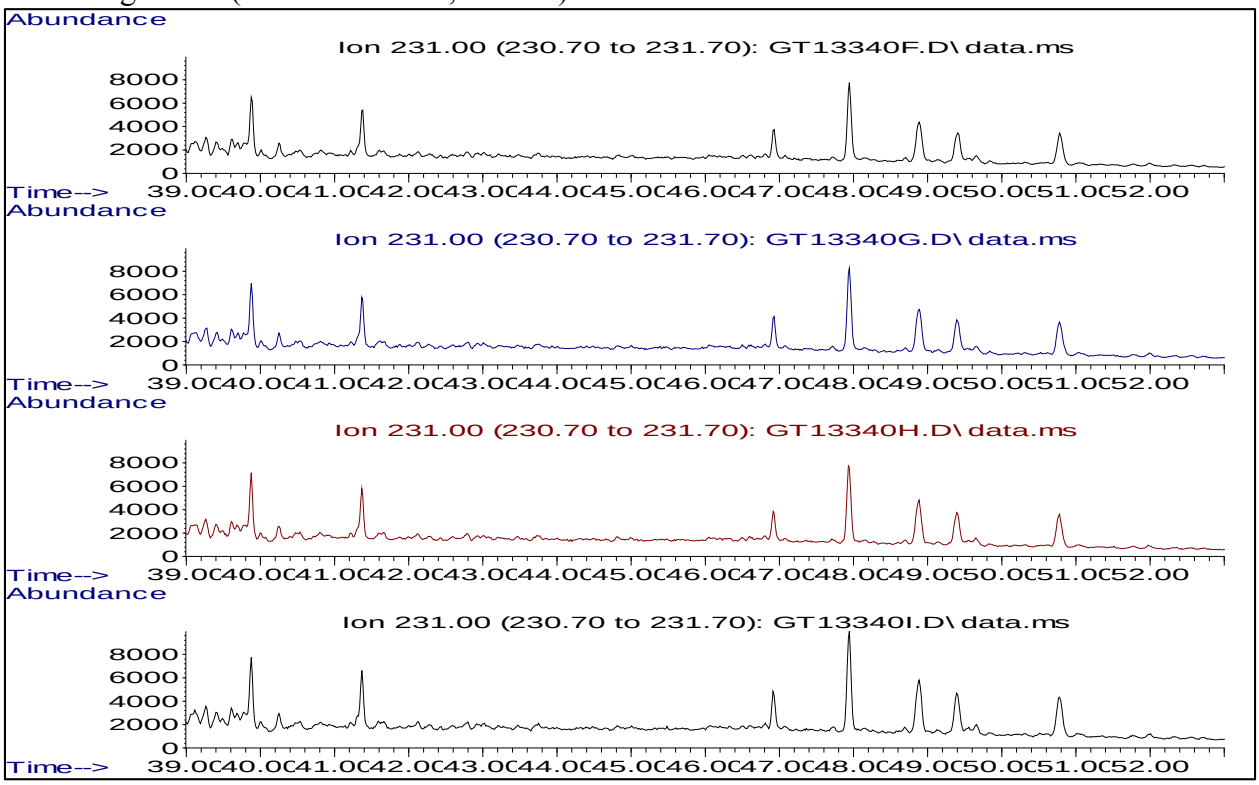

BP Surrogate Oil (Marlin Platform, VK915), 15% Weathered – *m/z* 191

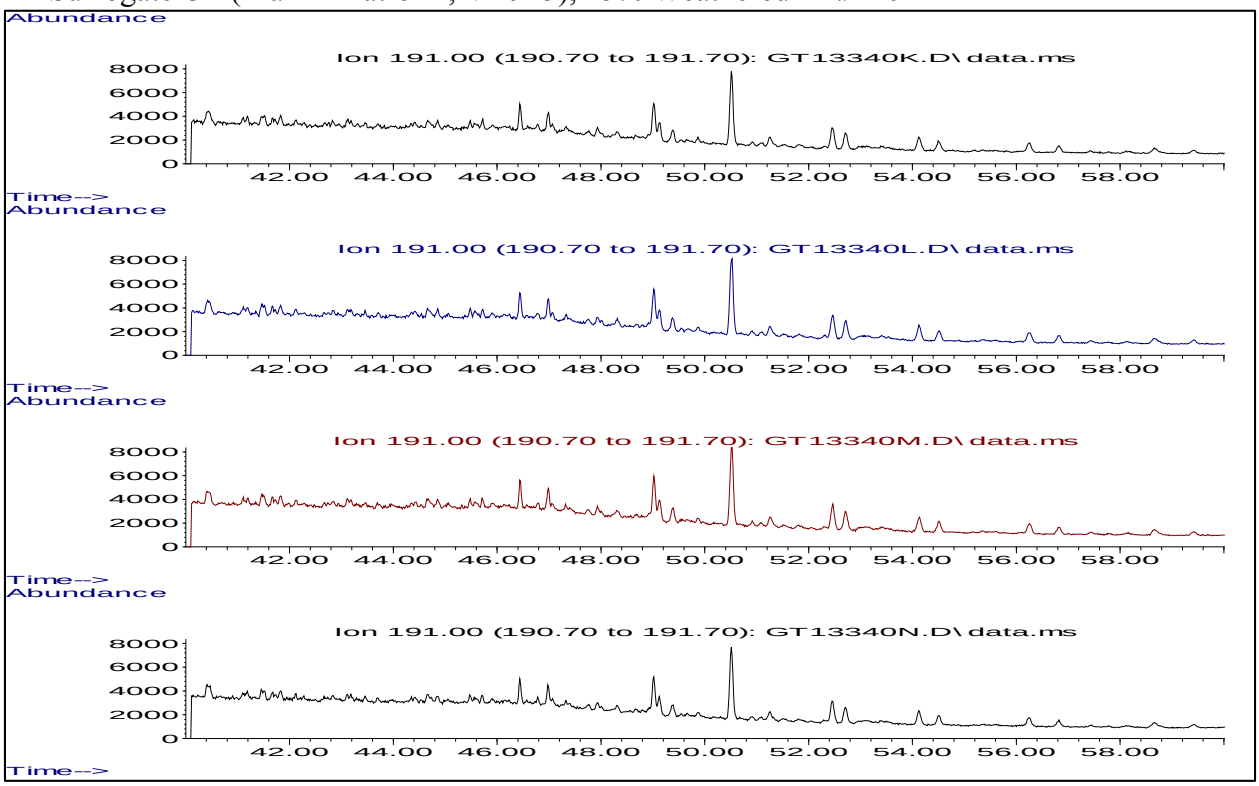


BP Surrogate Oil (Marlin Platform, VK915), 15% Weathered – *m/z* 217

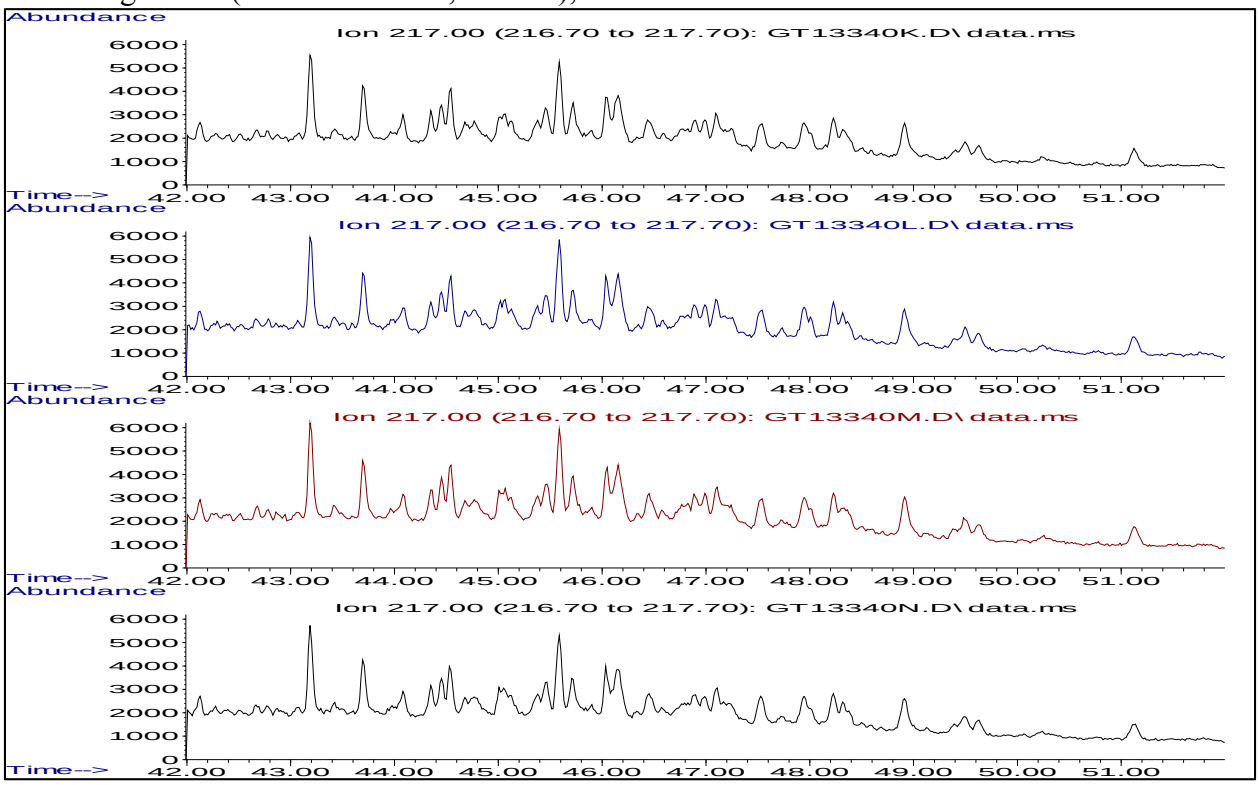

BP Surrogate Oil (Marlin Platform, VK915), 15% Weathered – *m/z* 218

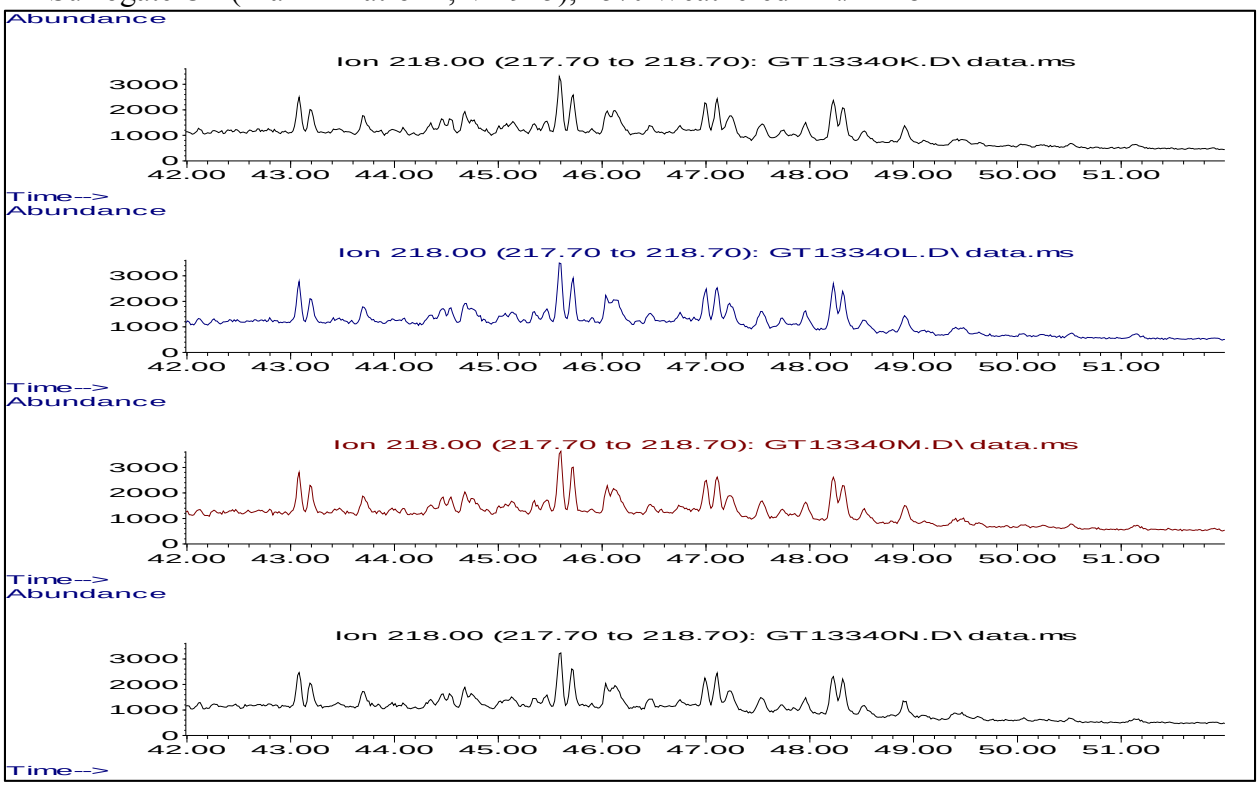


BP Surrogate Oil (Marlin Platform, VK915), 15% Weathered – *m/z* 231

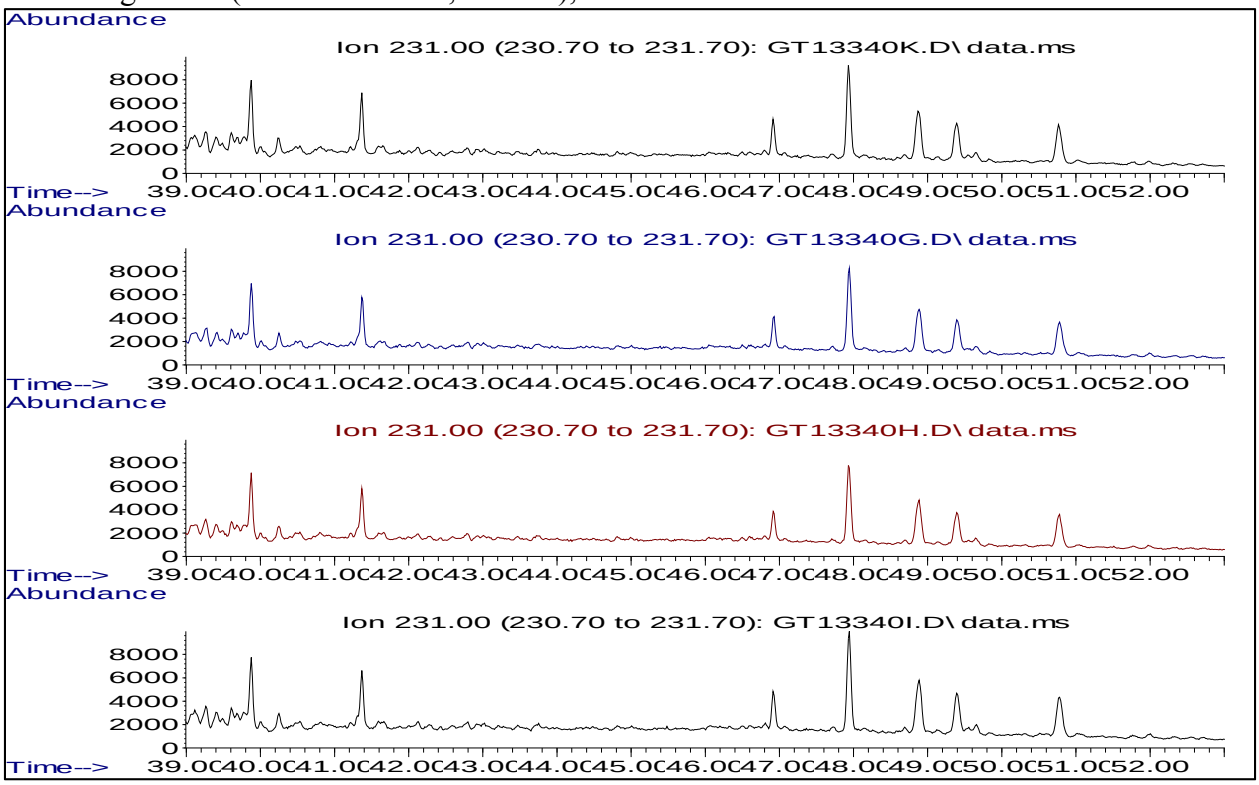

Cutoff, LA Pipeline – *m/z* 191

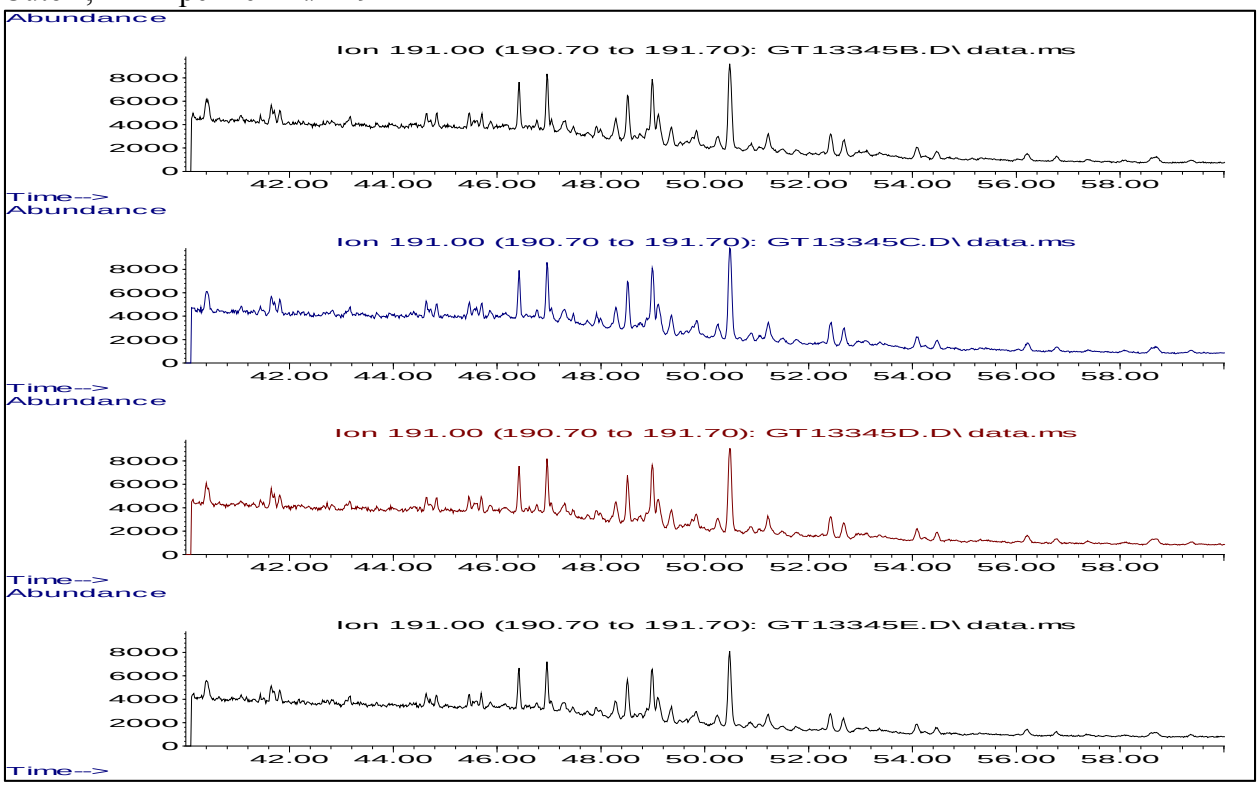


Cutoff, LA Pipeline – *m/z* 217

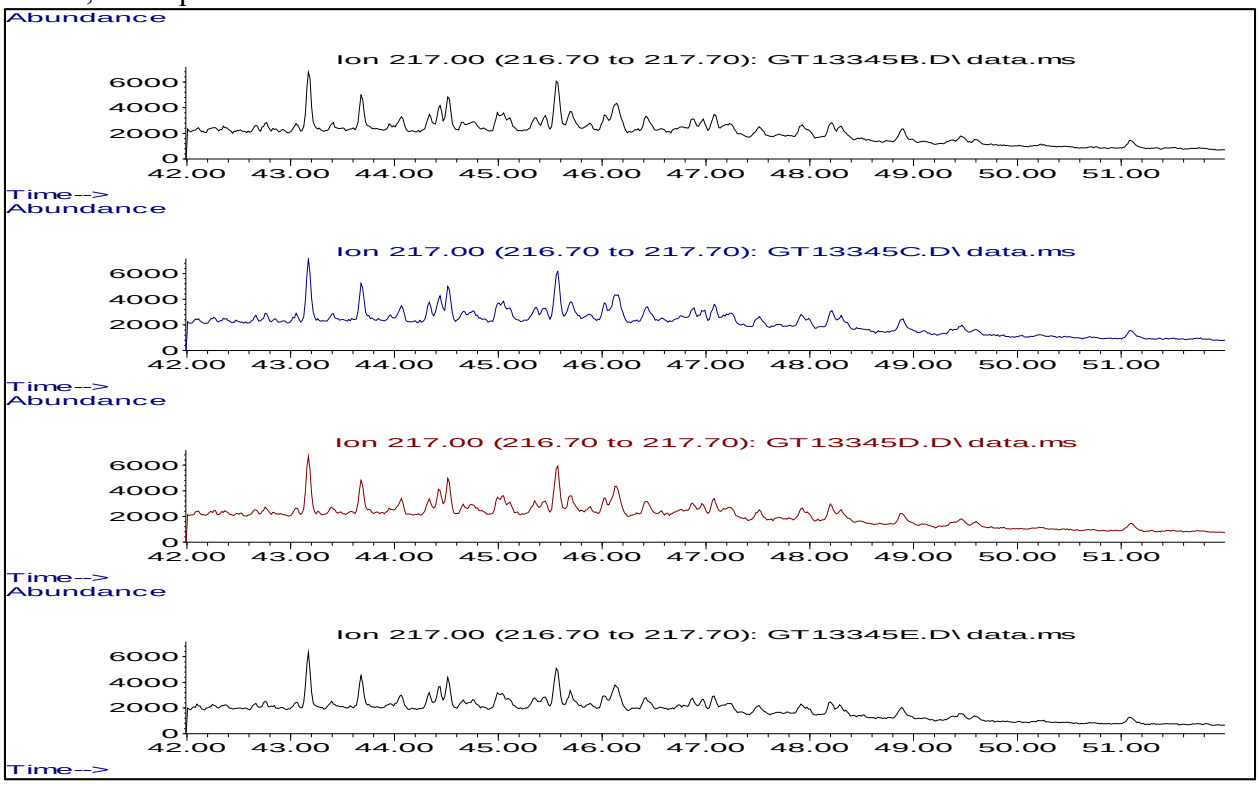

Cutoff, LA Pipeline – *m/z* 218

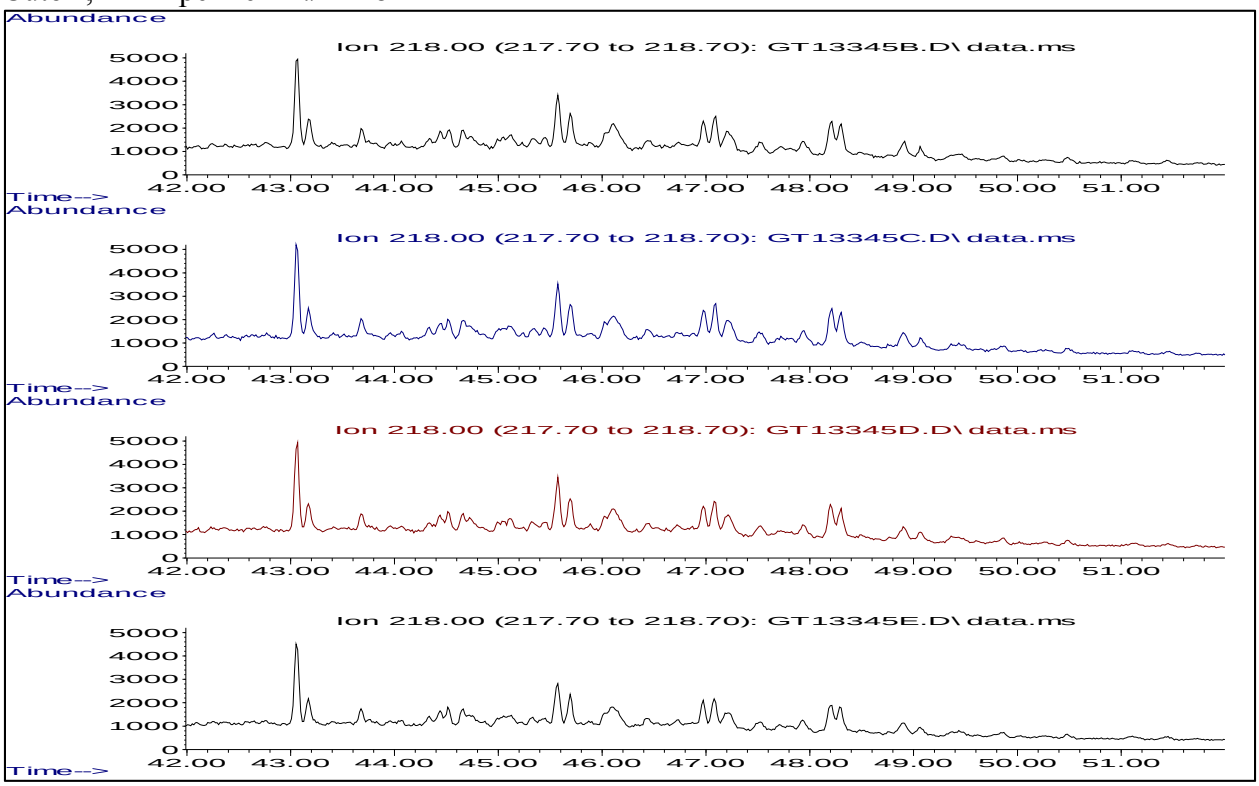


Cutoff, LA Pipeline – *m/z* 231

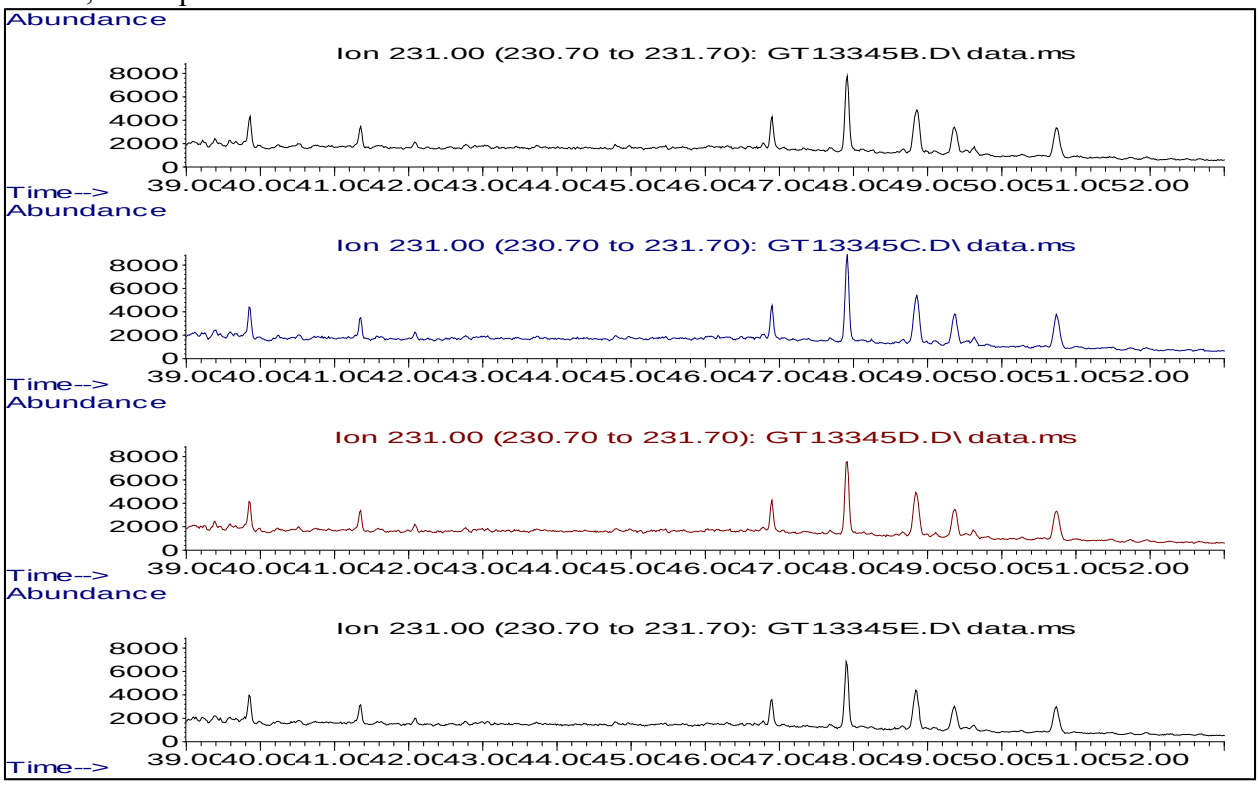

EPA South Louisiana Crude – *m/z* 191

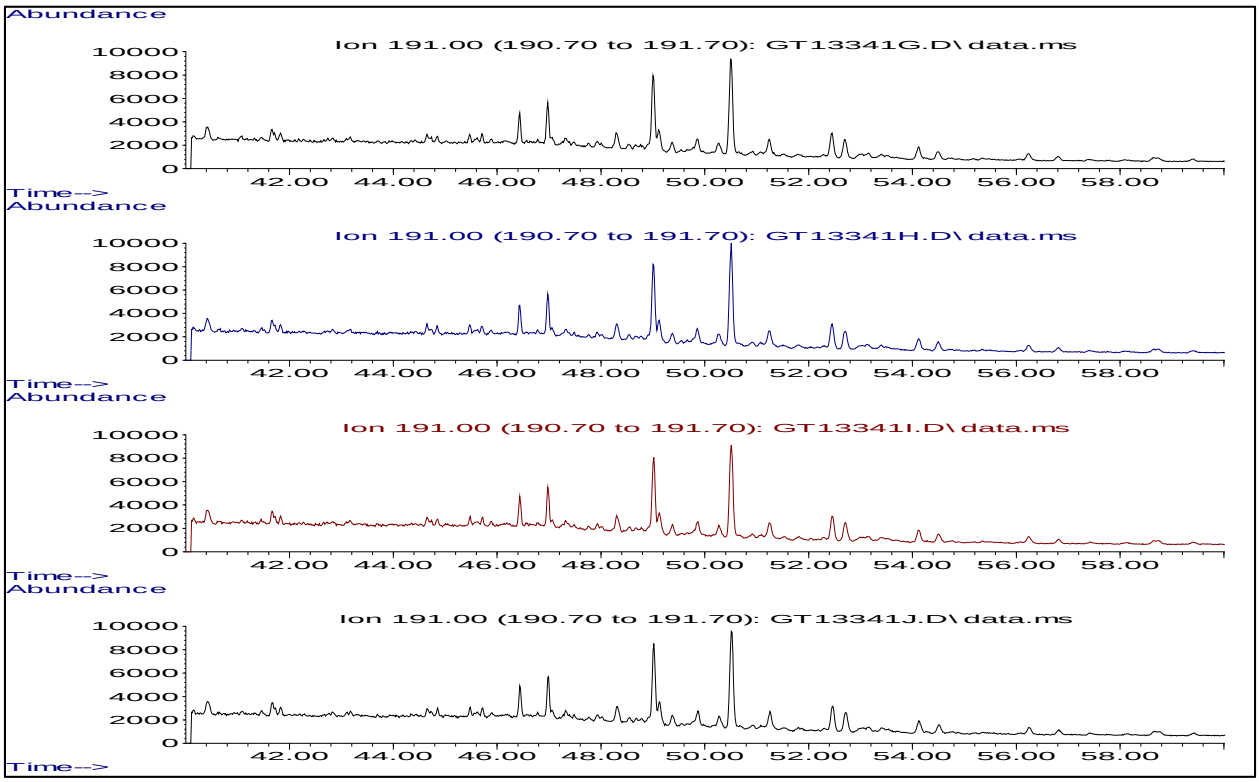


EPA South Louisiana Crude – *m/z* 217

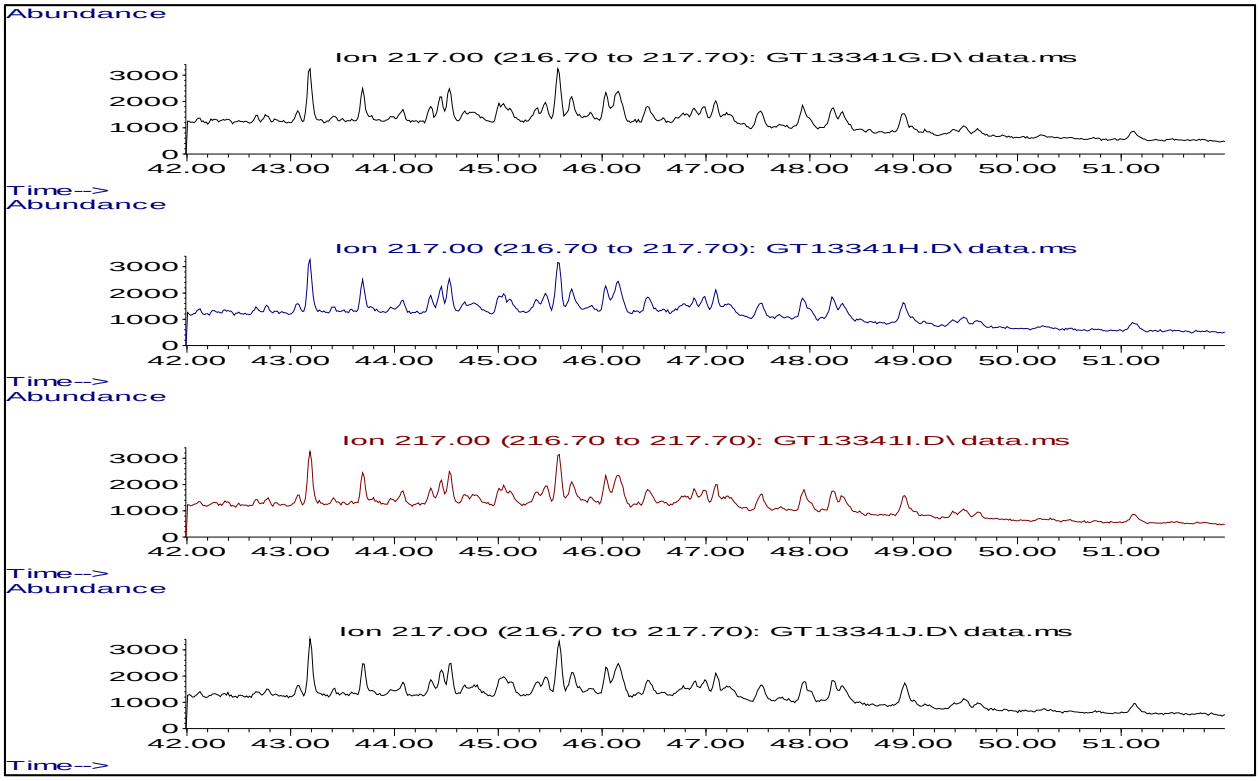

EPA South Louisiana Crude – *m/z* 218

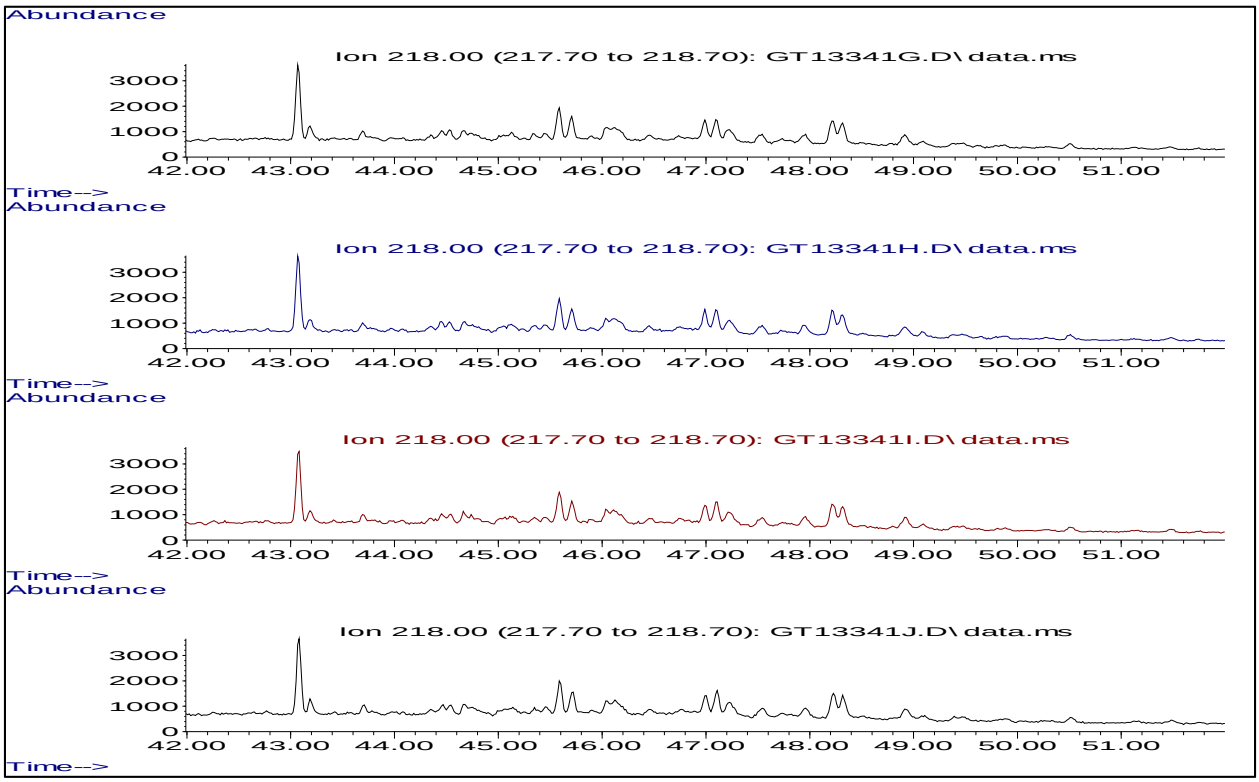


EPA South Louisiana Crude – *m/z* 231

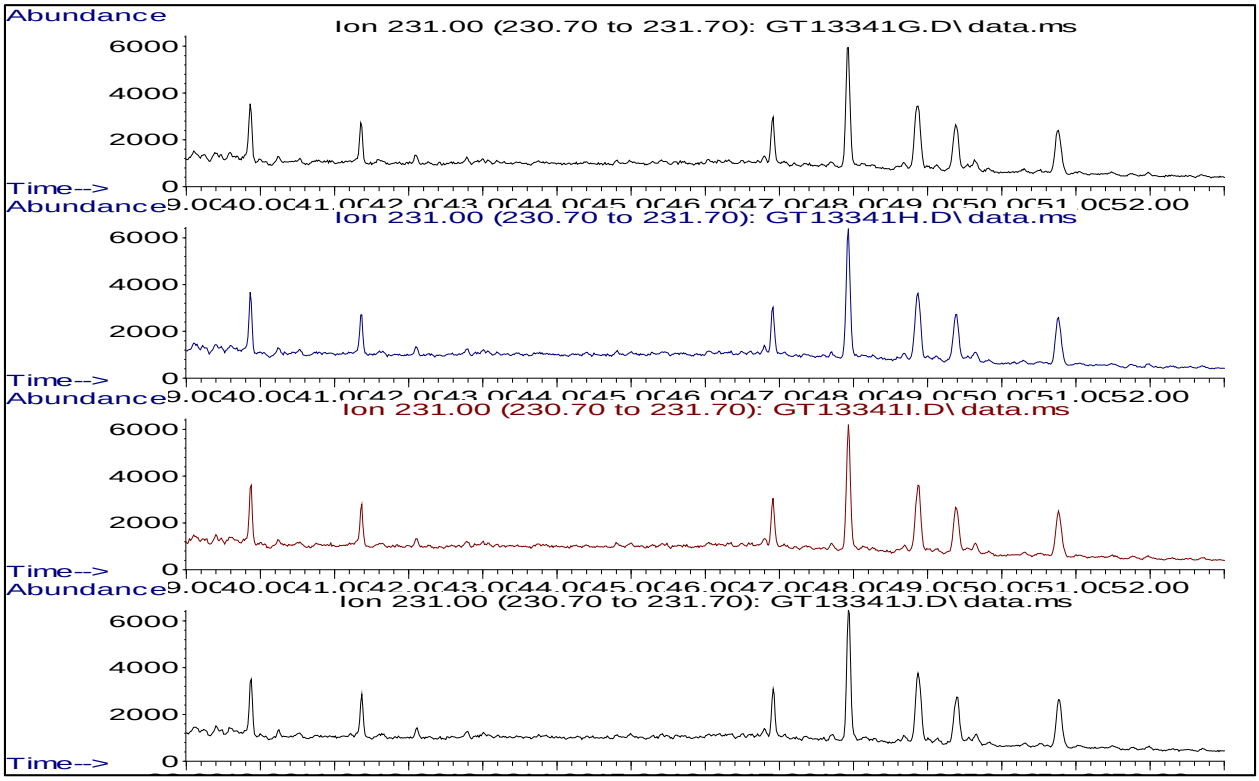

Exxon OCS – *m/z* 191

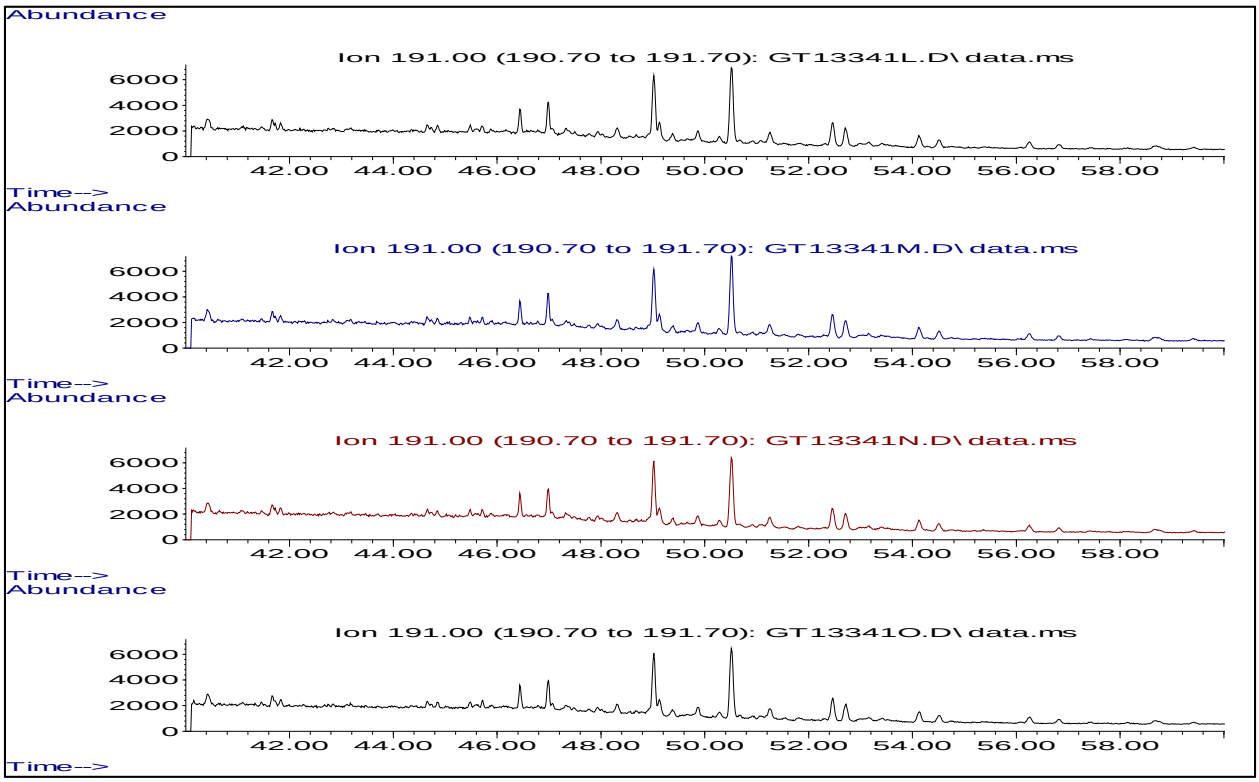


Exxon OCS – *m/z* 217

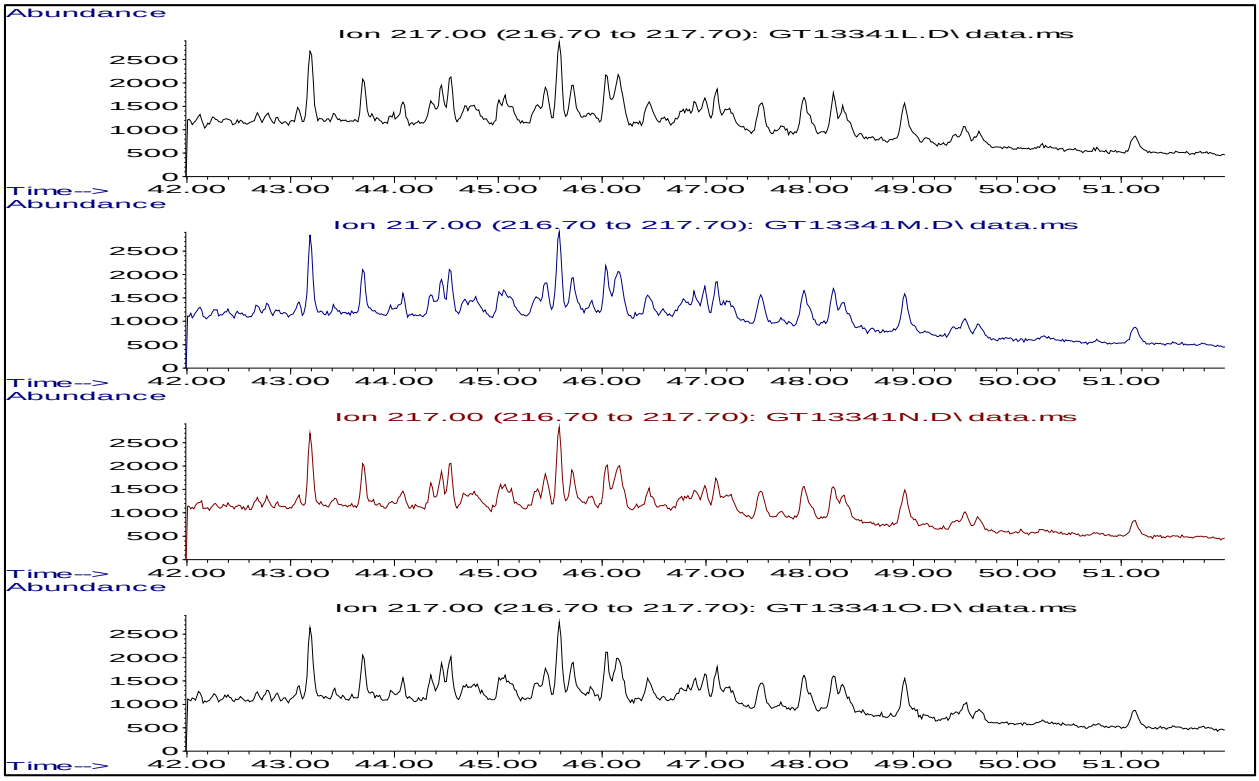

Exxon OCS – *m/z* 218

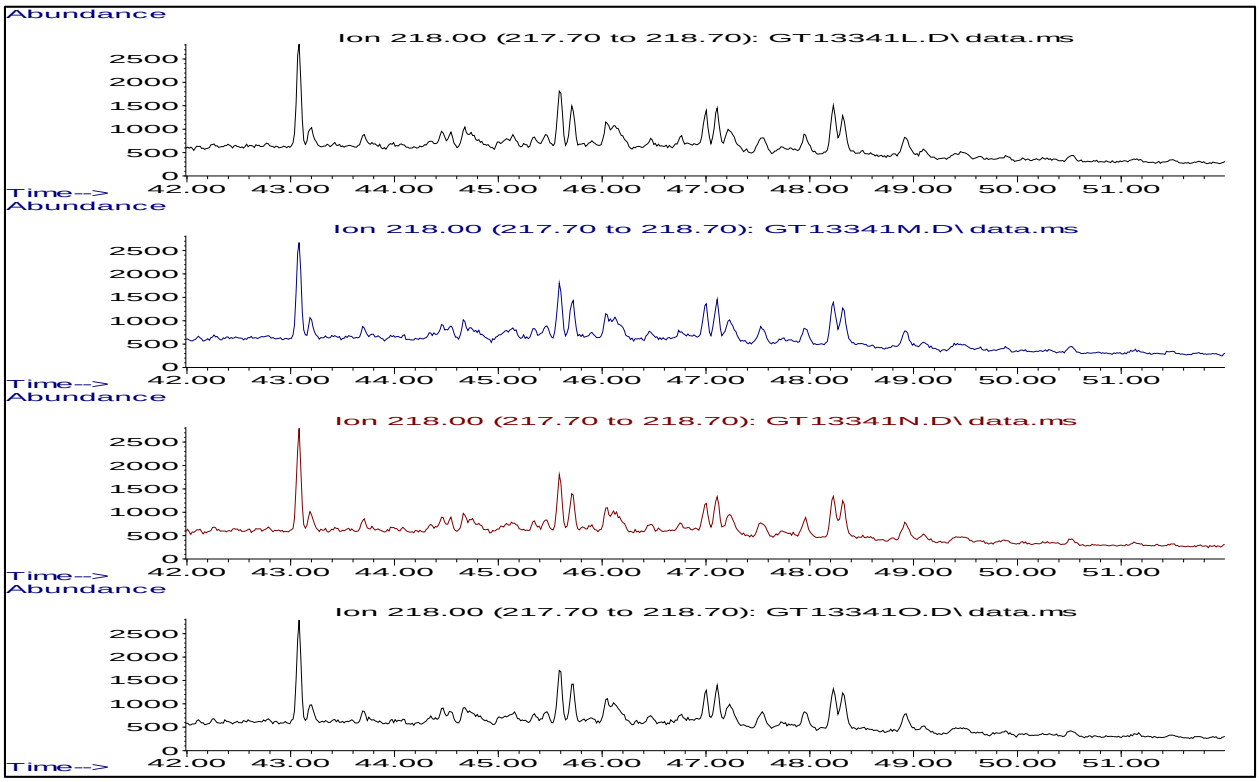


Exxon OCS – *m/z* 231

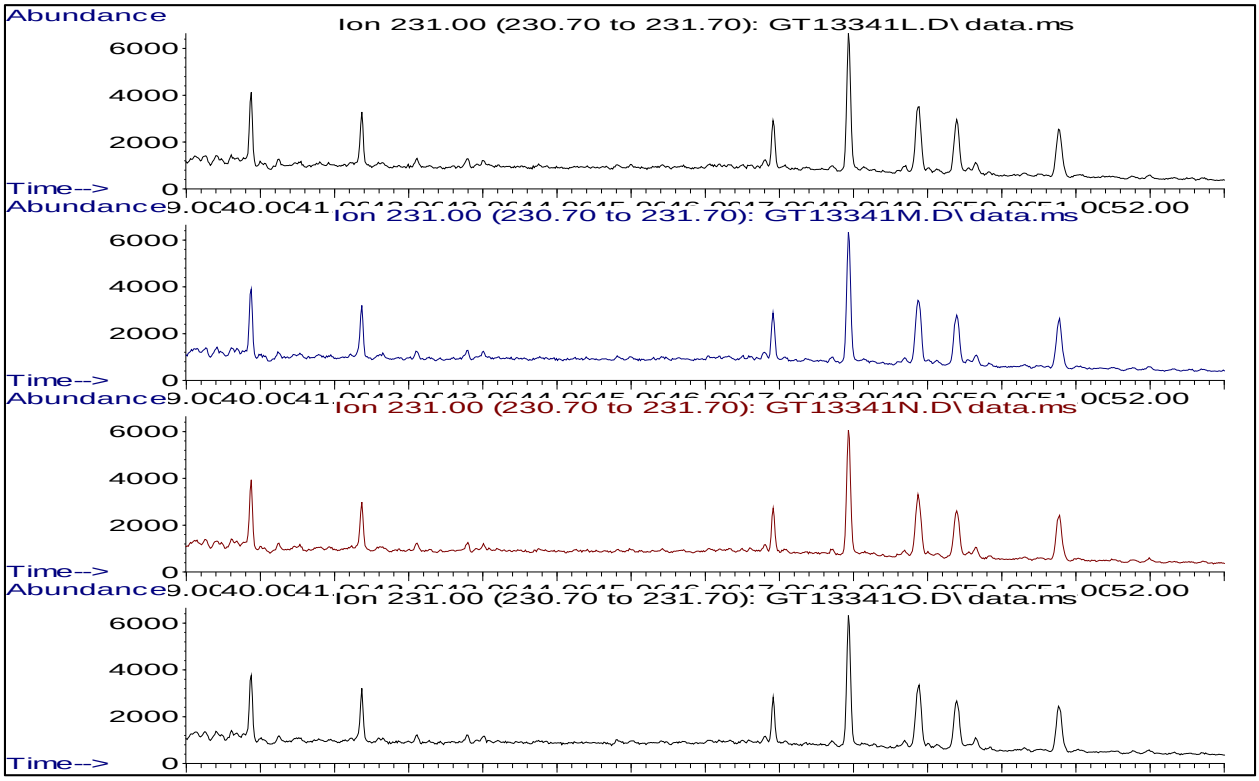

MC252 – *m/z* 191

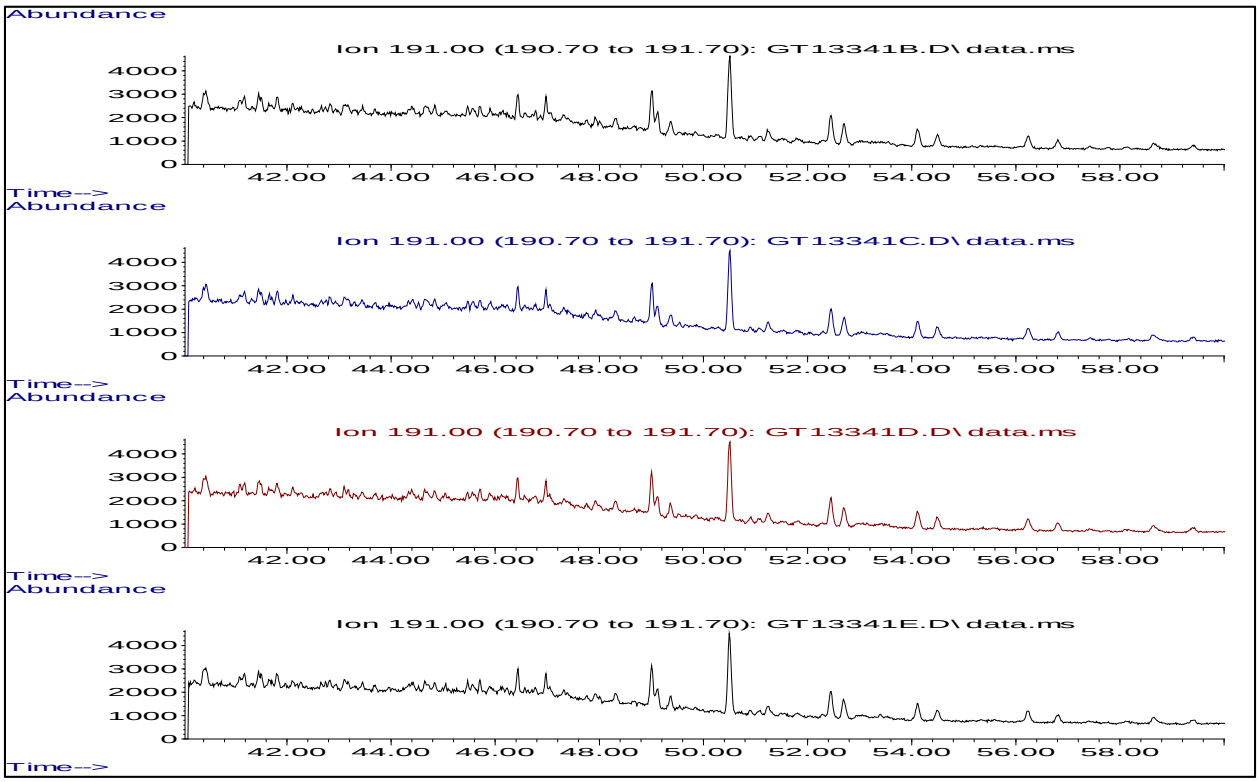


MC252 – *m/z* 217

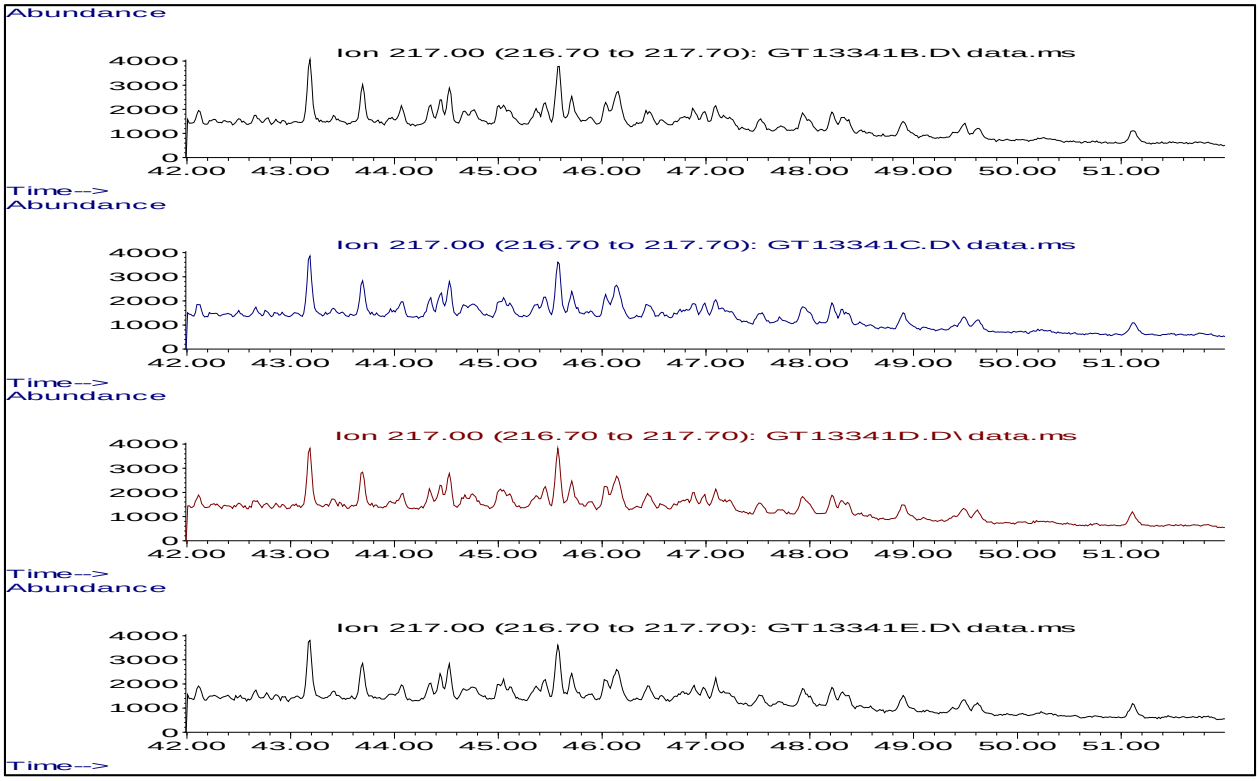

MC252 – *m/z* 218

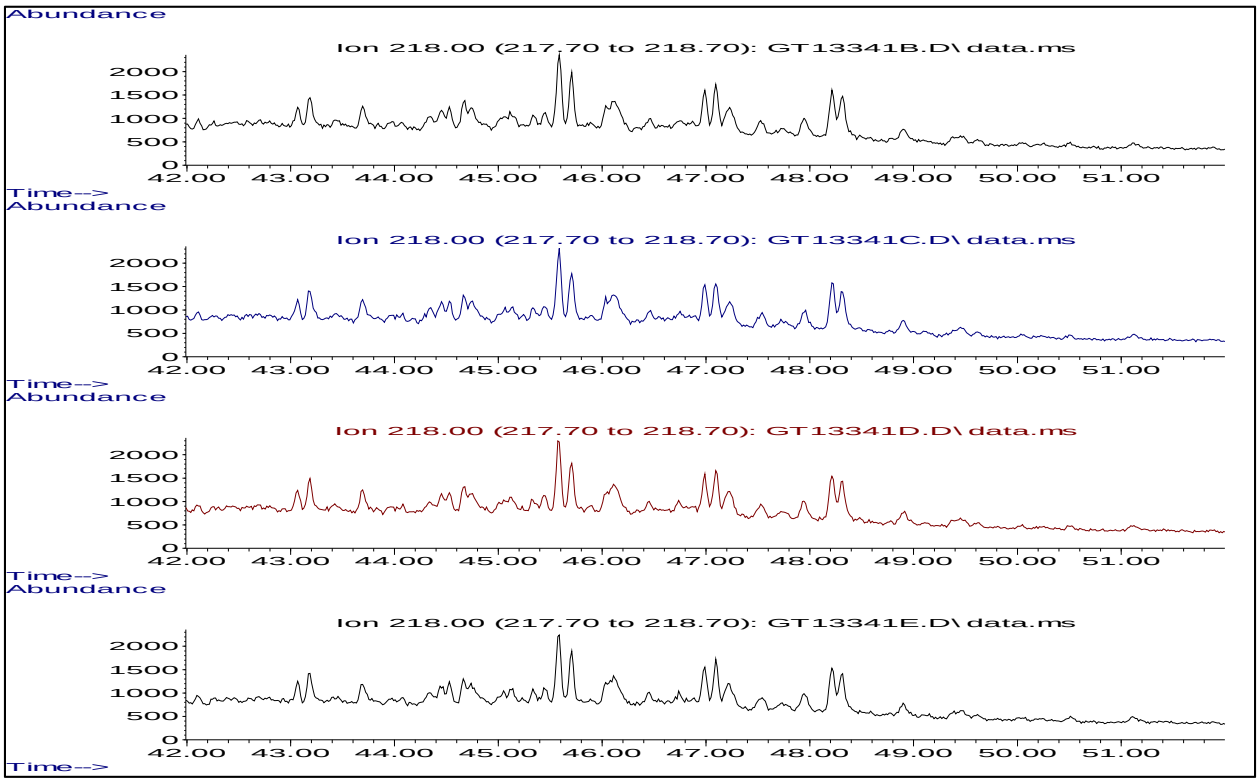


MC252 – *m/z* 231

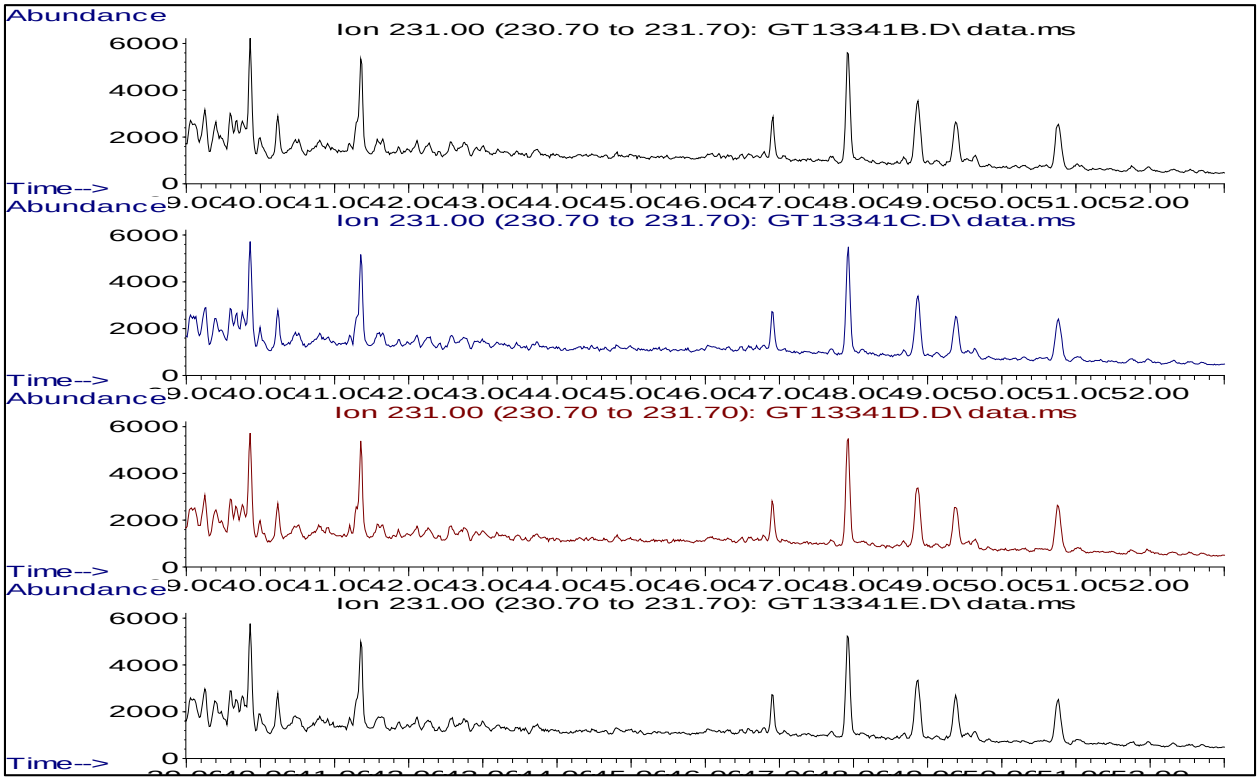

Pt. Coupee Crude – *m/z* 191

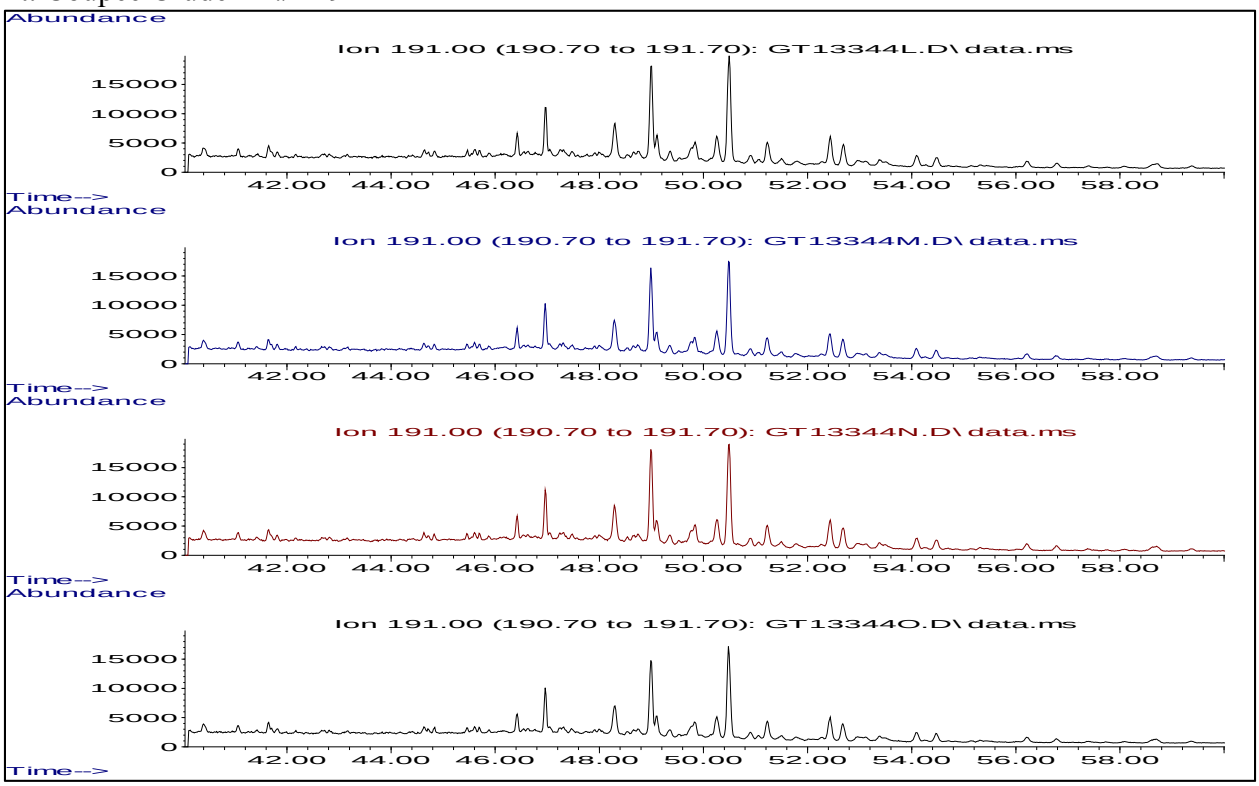


Pt. Coupee Crude – *m/z* 217

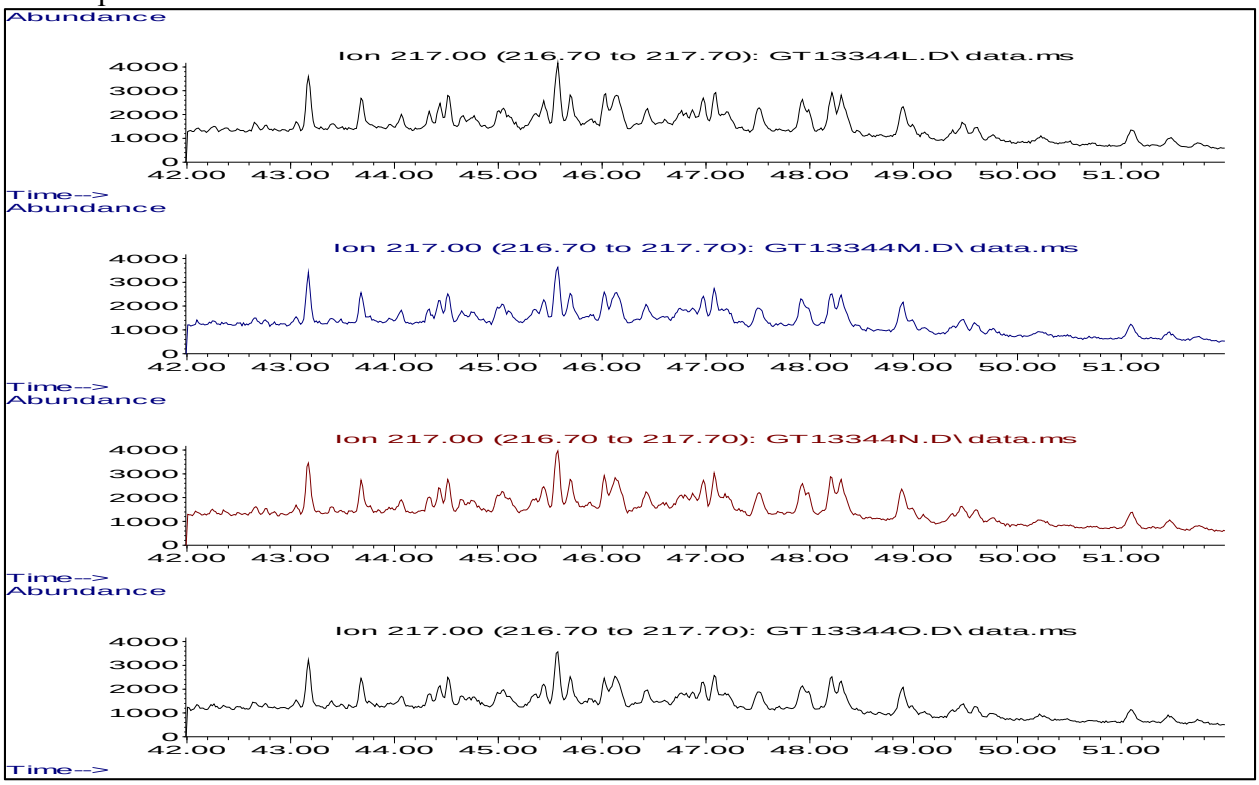

Pt. Coupee Crude – *m/z* 218

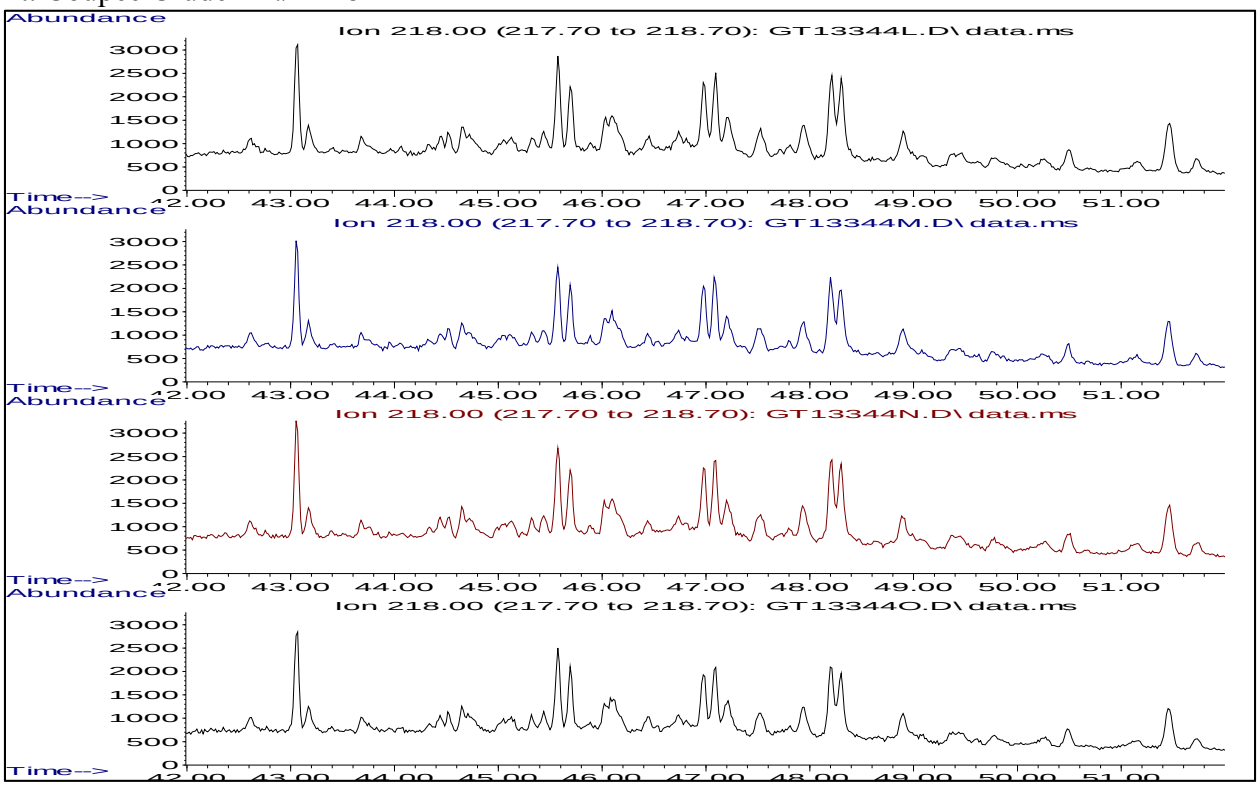


Pt. Coupee Crude – *m/z* 231

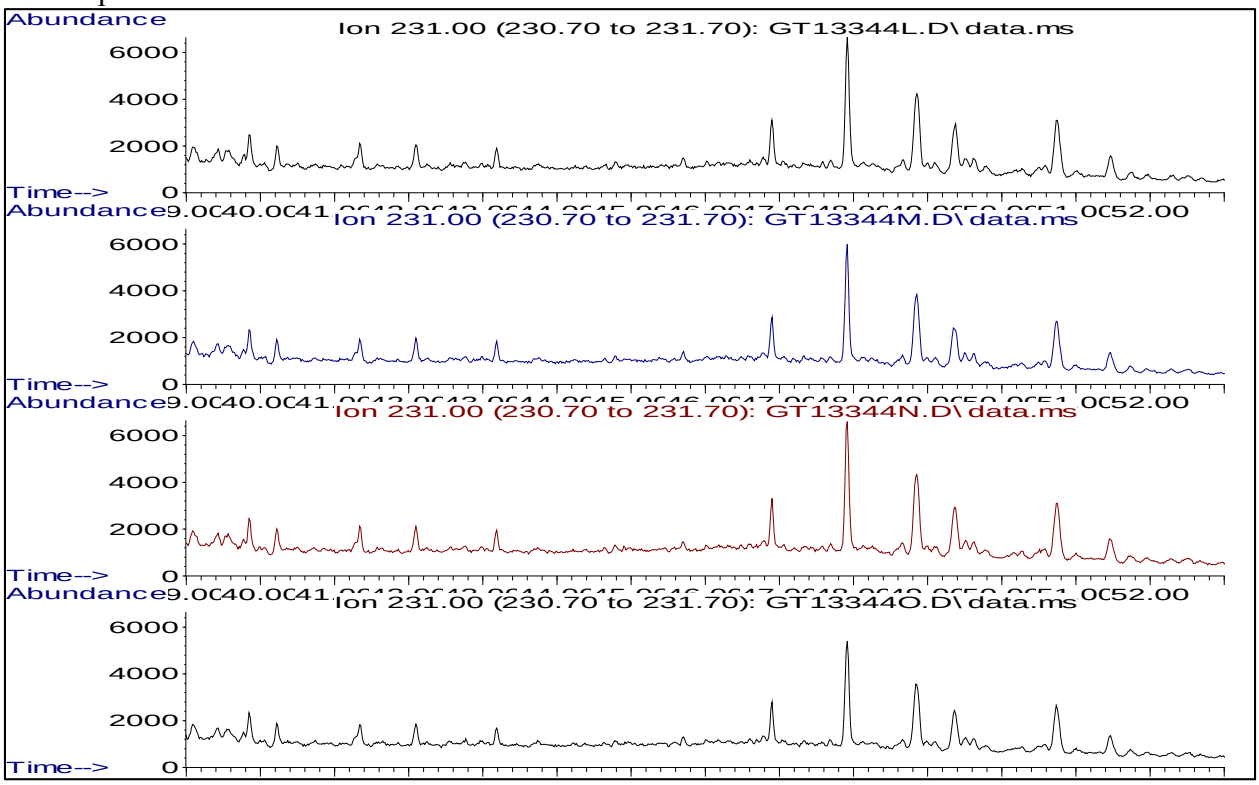

SLC Blend – *m/z* 191

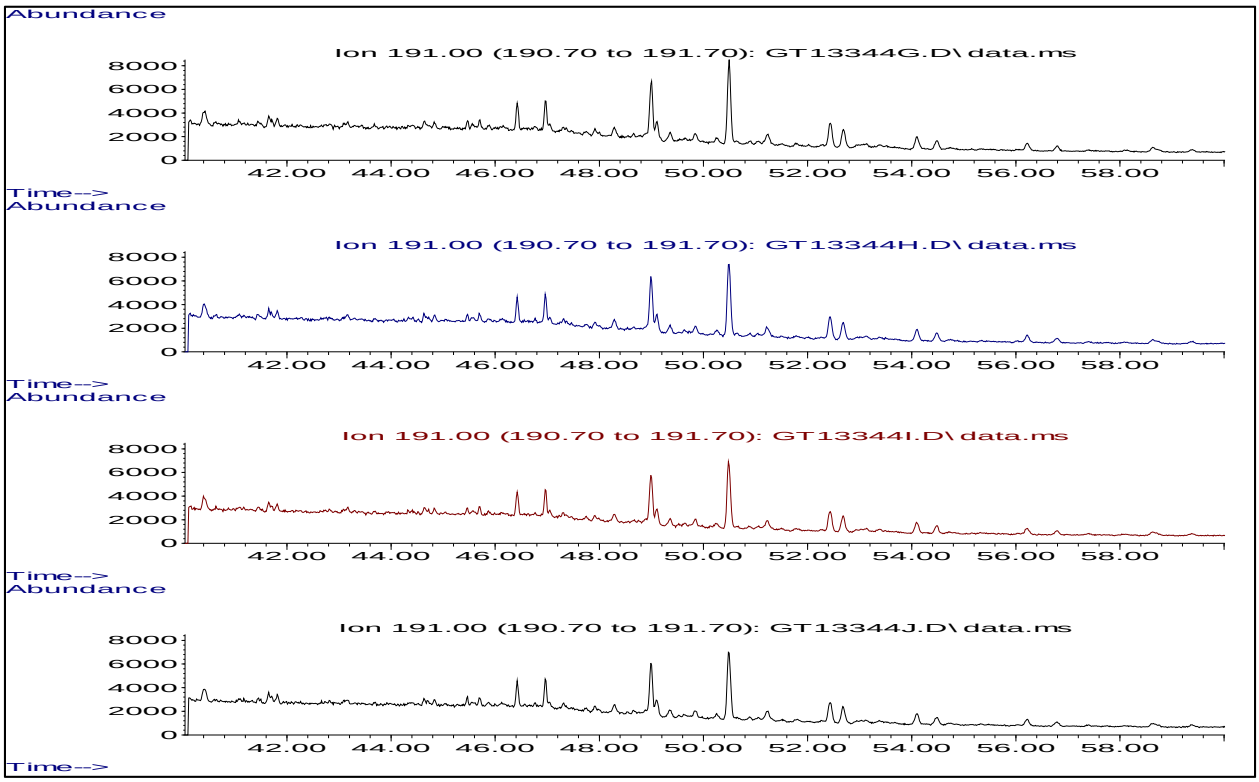


SLC Blend – *m/z* 217

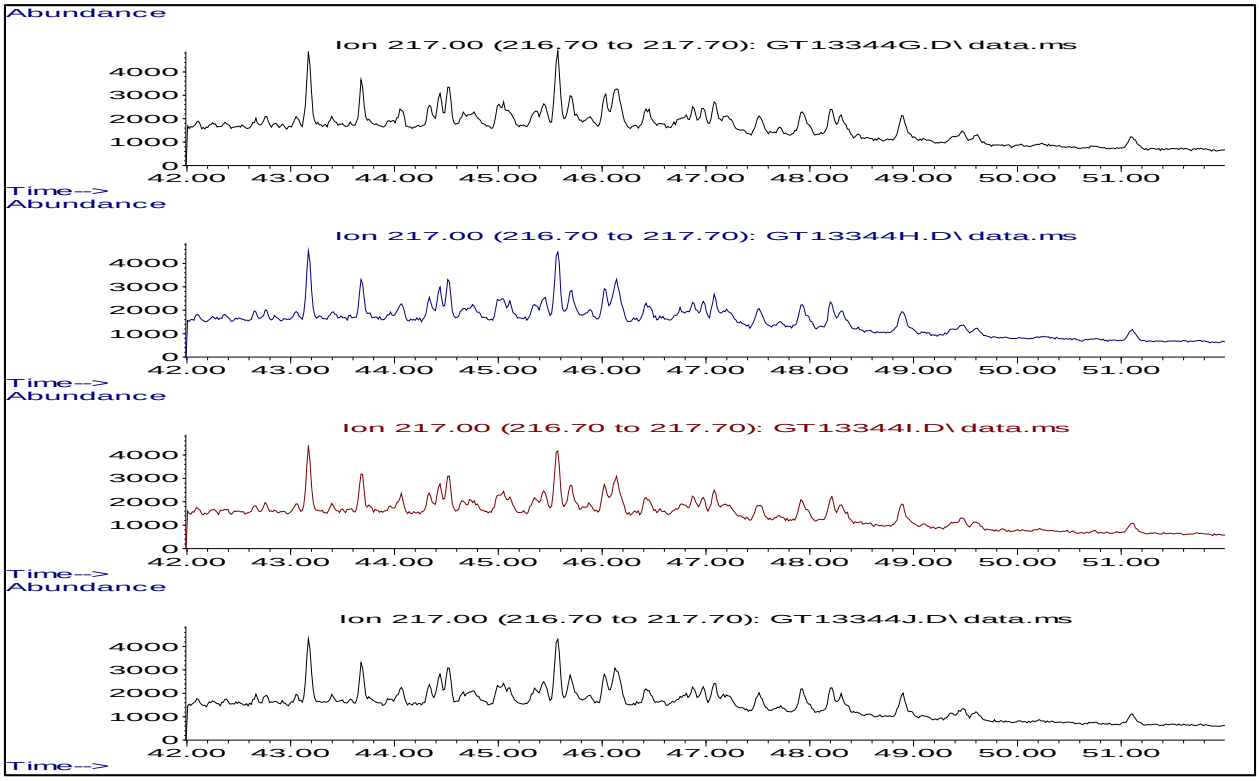

SLC Blend – *m/z* 218

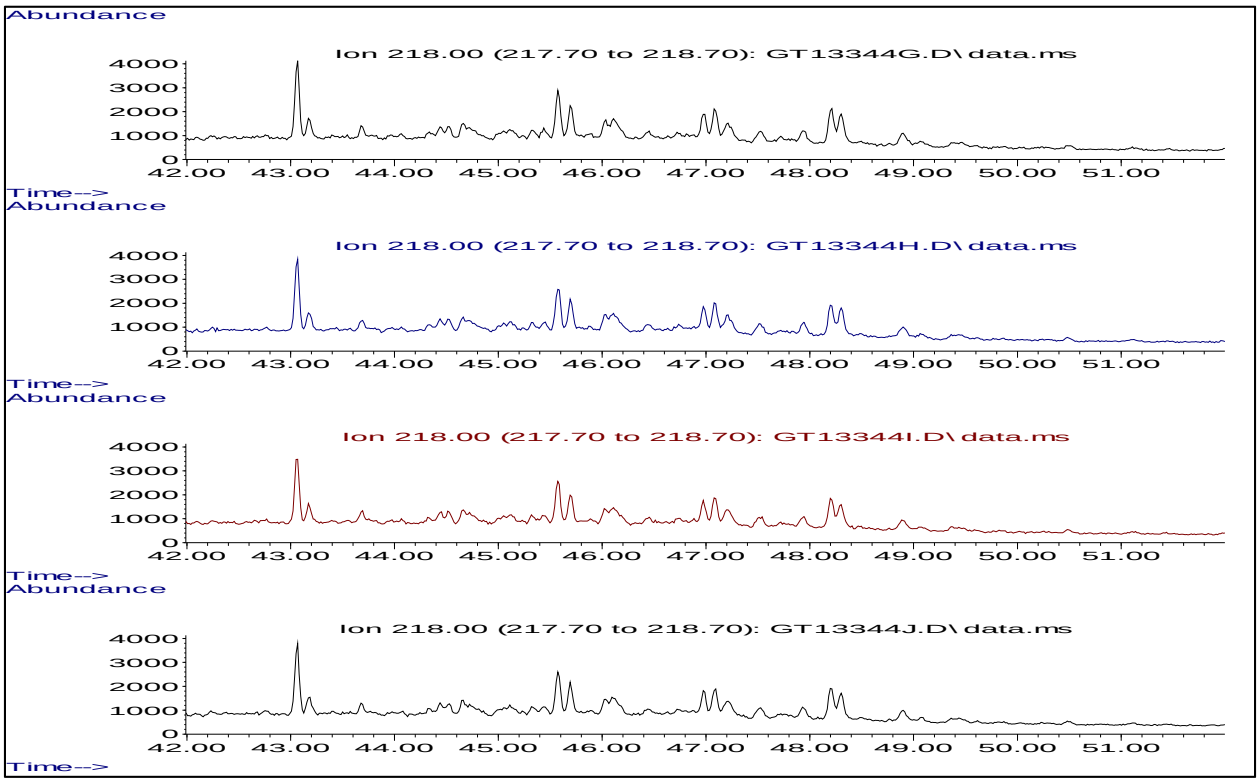


SLC Blend – *m/z* 231

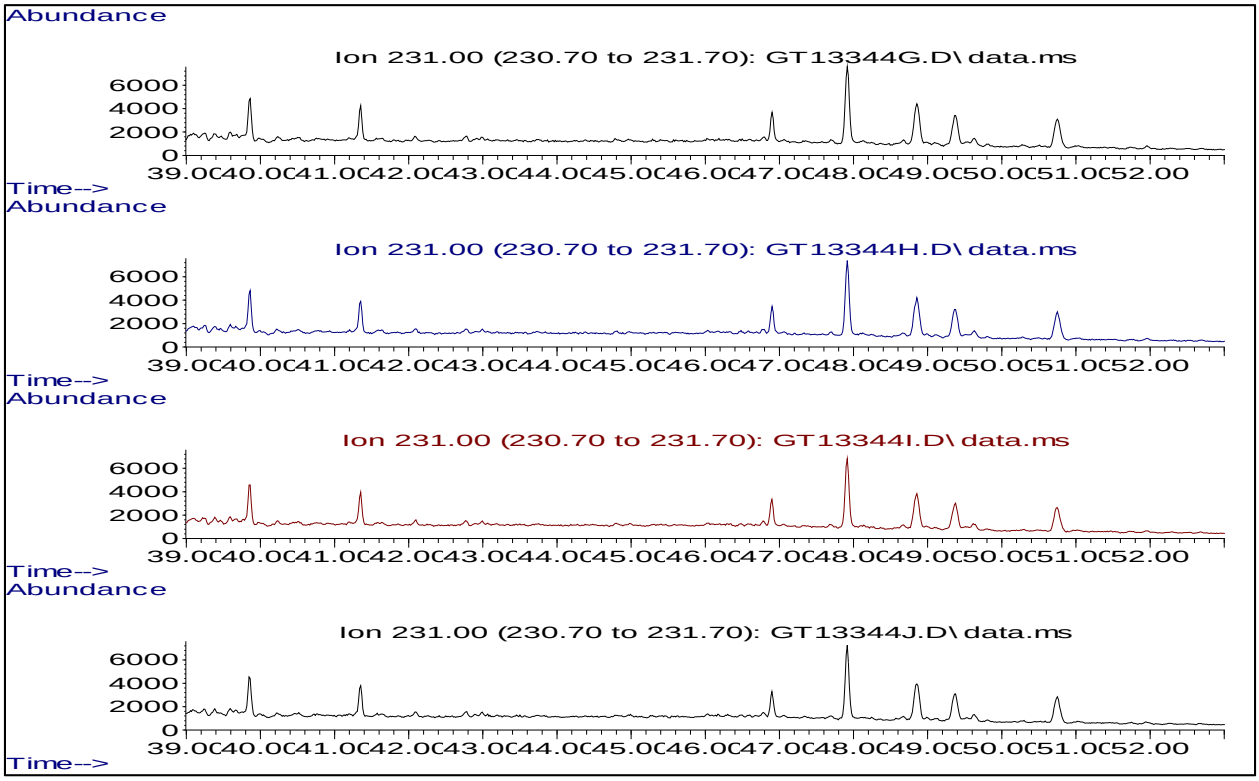

## APPENDIX C: EXTRACTED BIOMARKER CHROMATOGRAPHIC PROFILES OF SOURCE OILS

ANSC

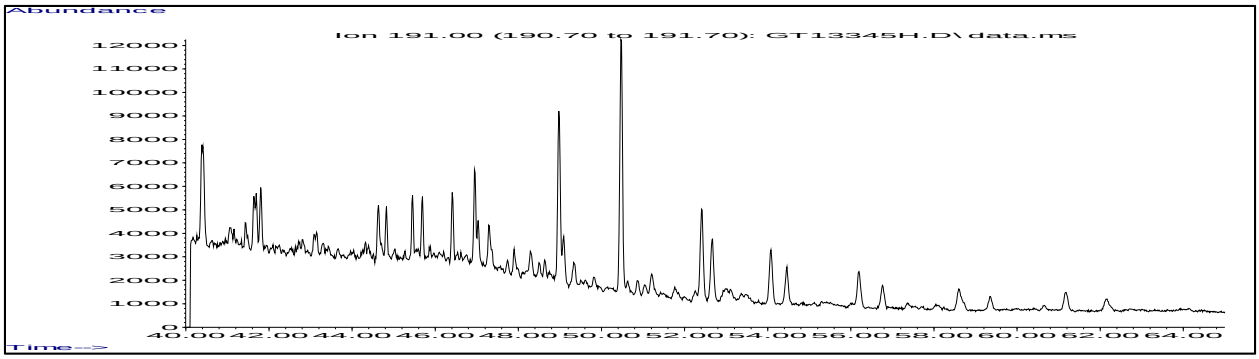


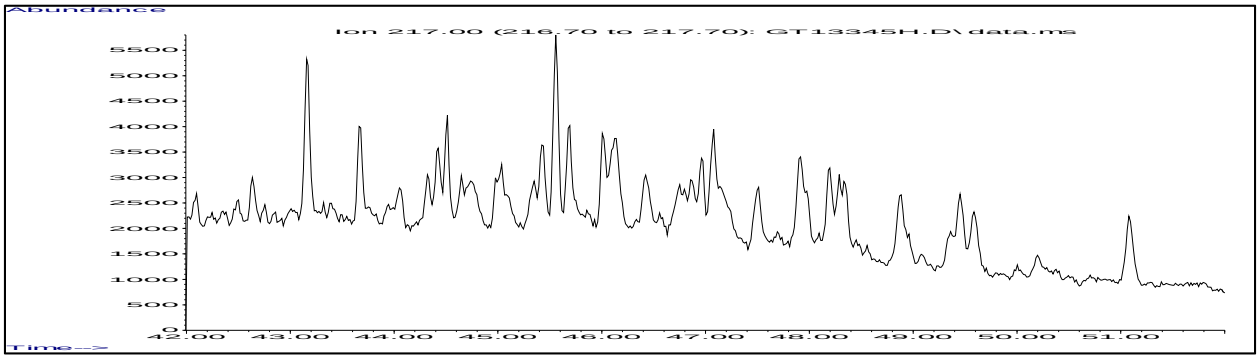


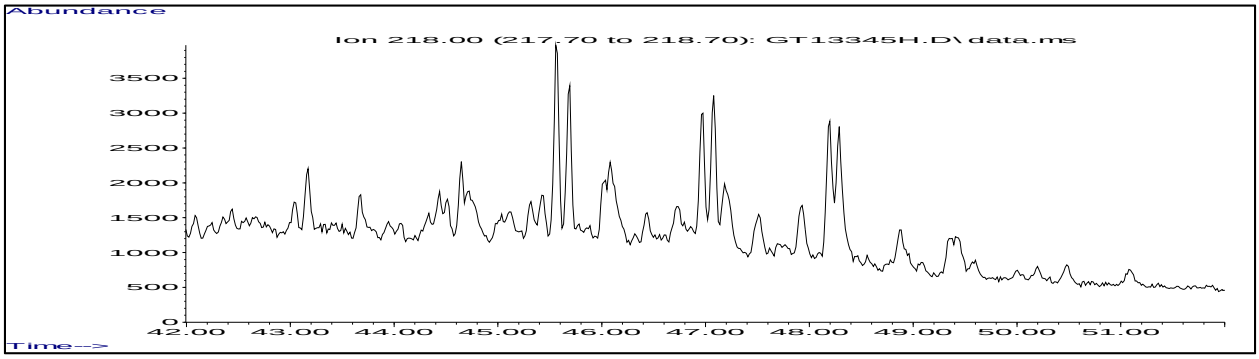


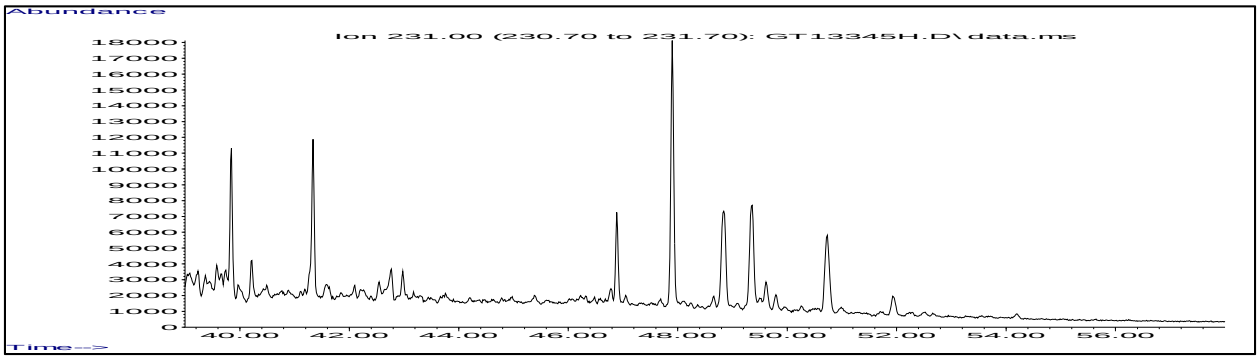

BP Surrogate Oil (Marlin Platform, VK915)

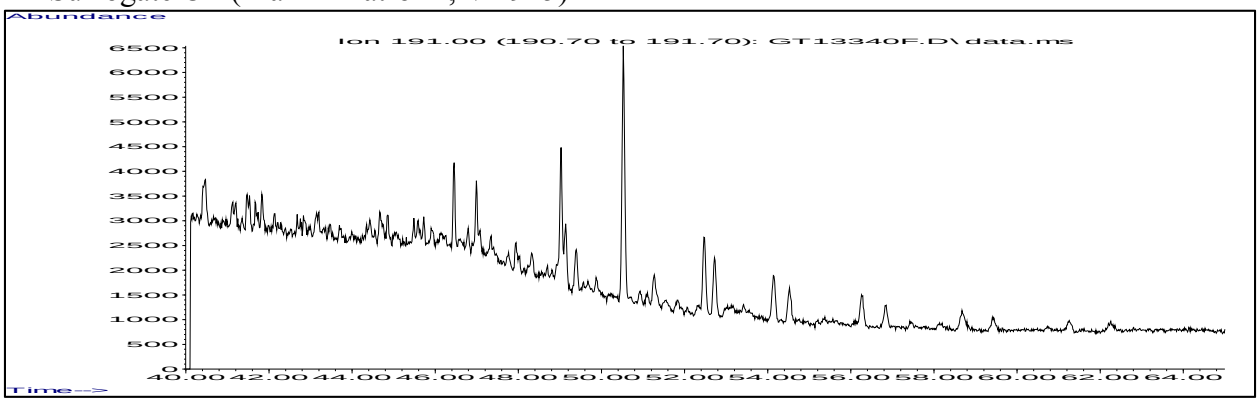


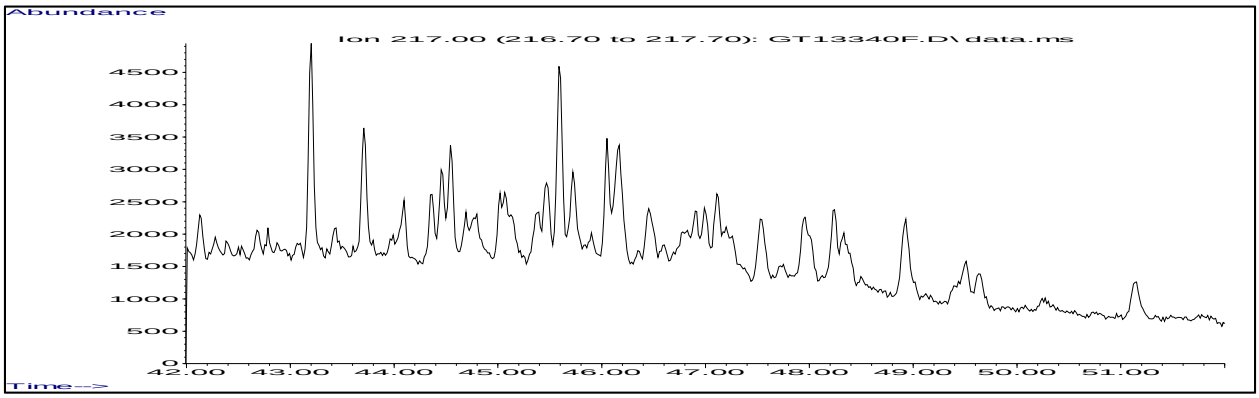


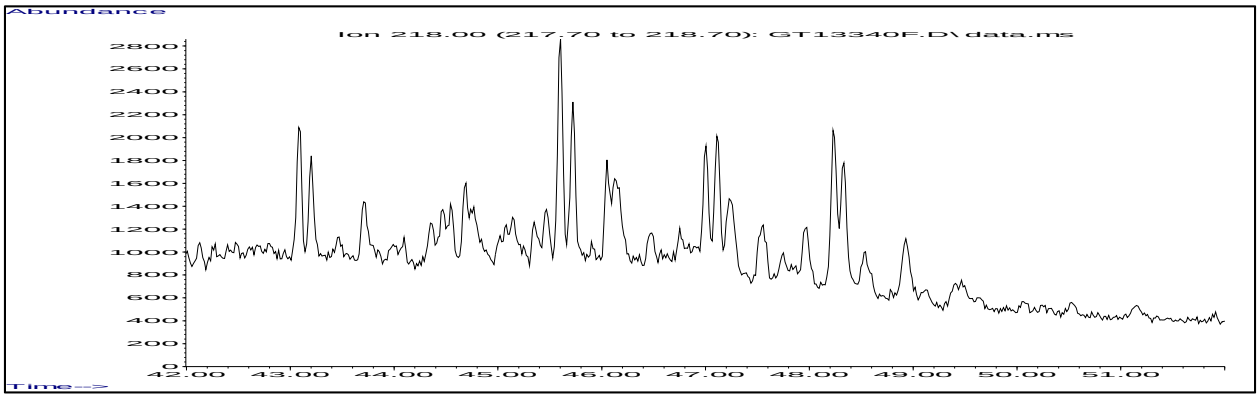


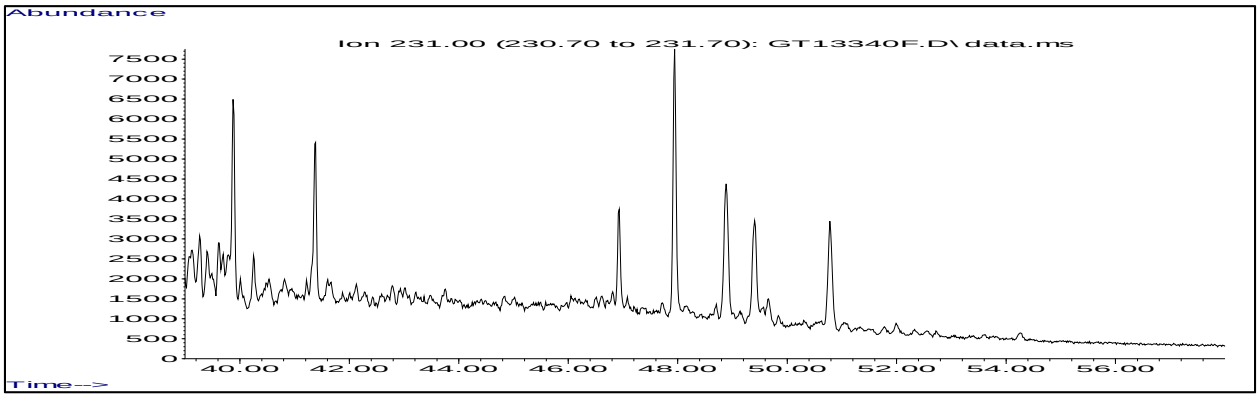

BP Surrogate Oil (Marlin Platform, VK915) – 15% Weathered

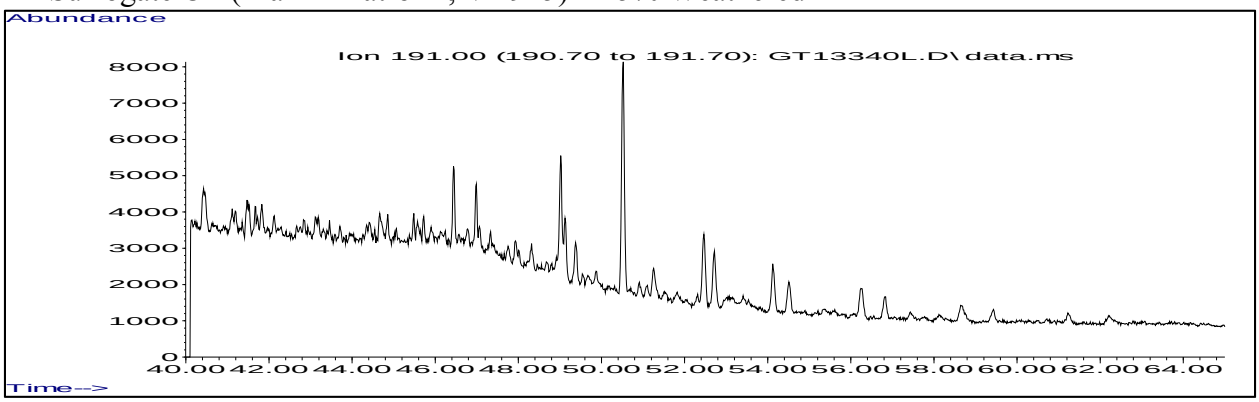


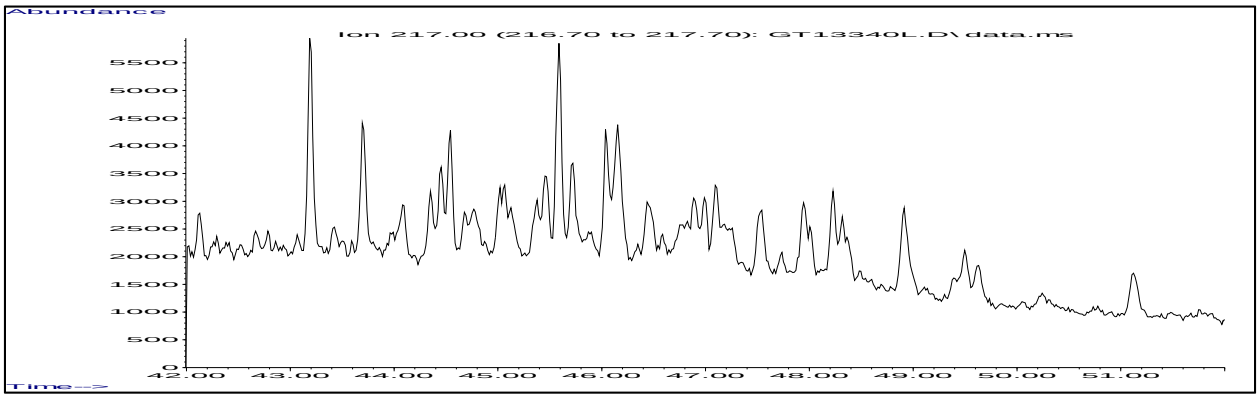


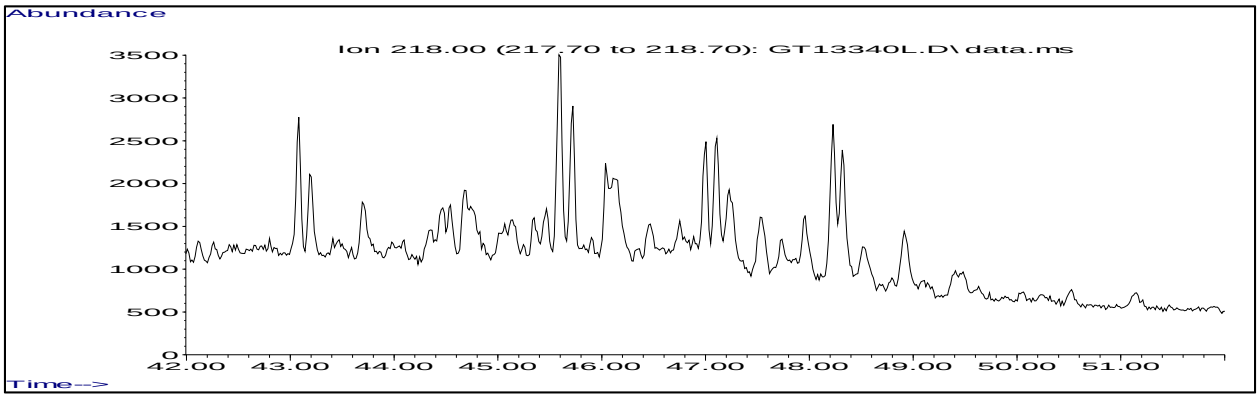


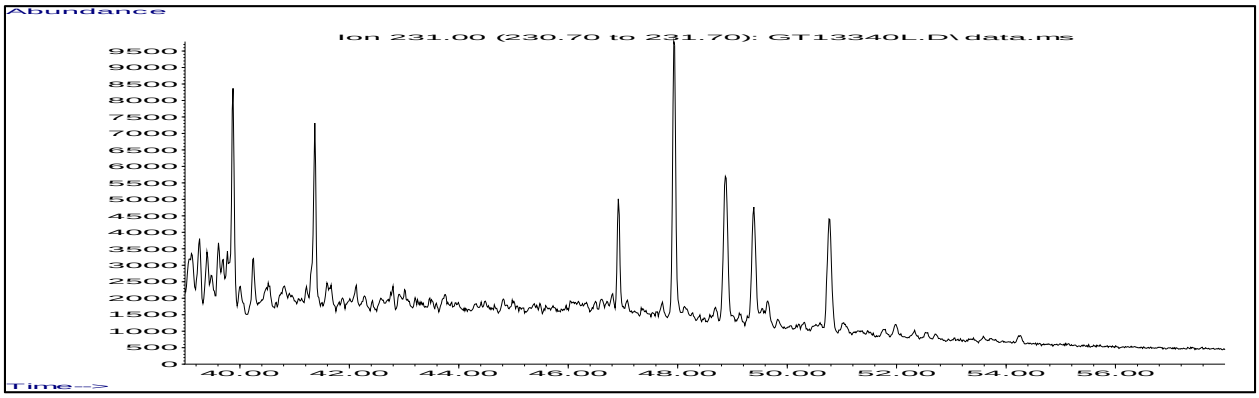

Cutoff, LA Pipeline

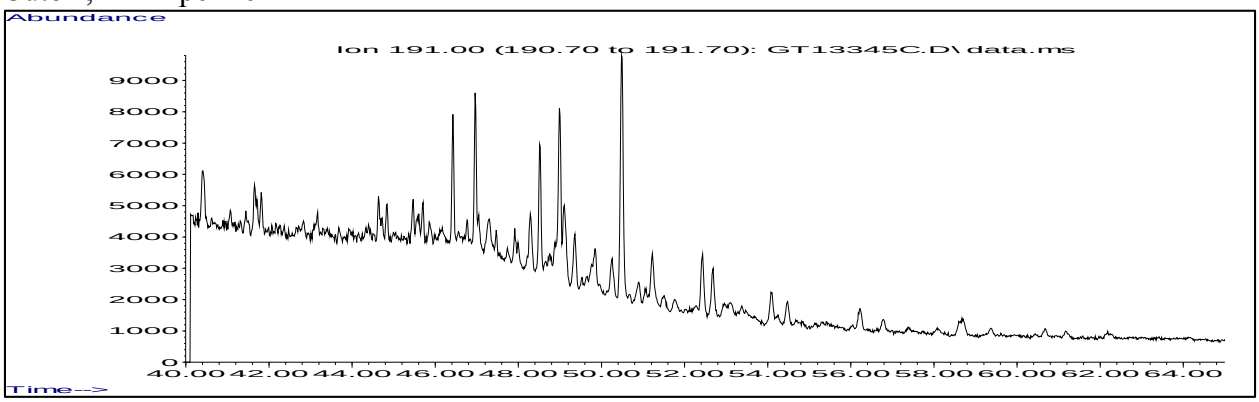


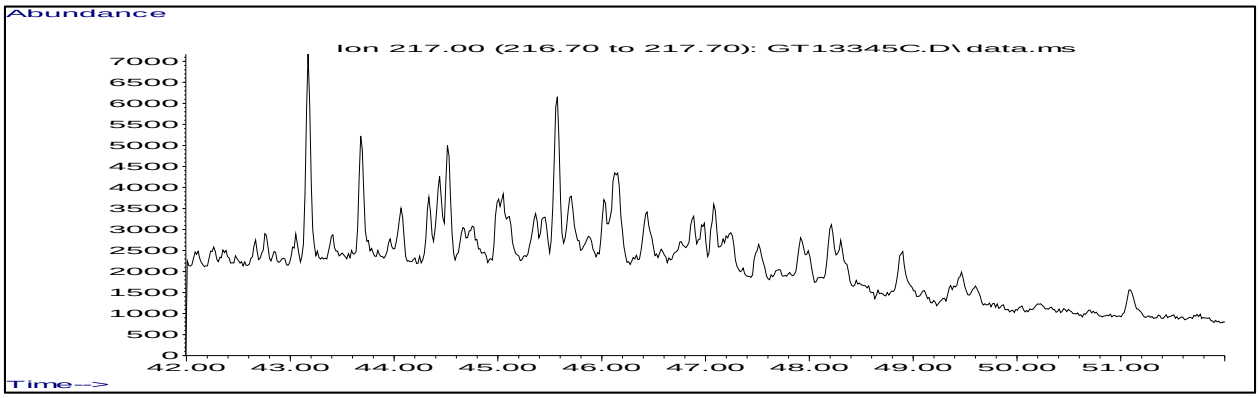


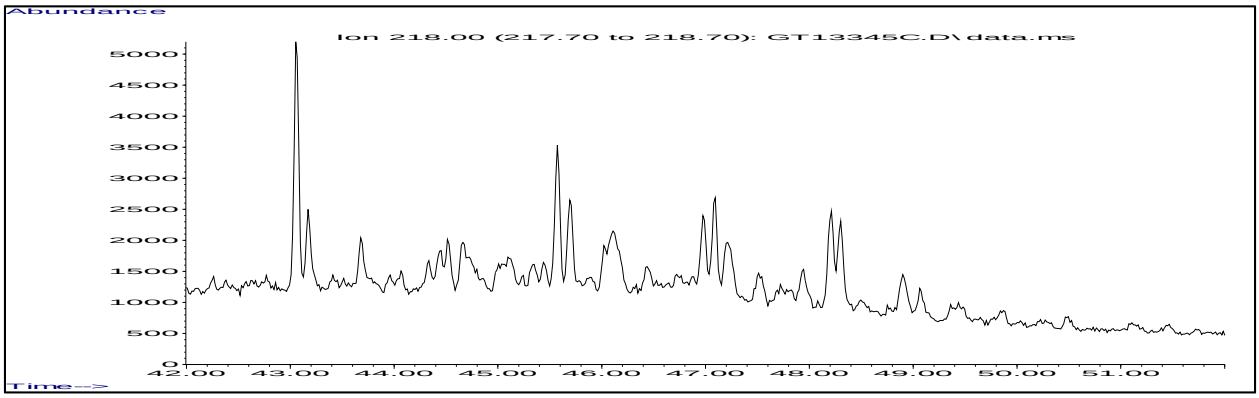


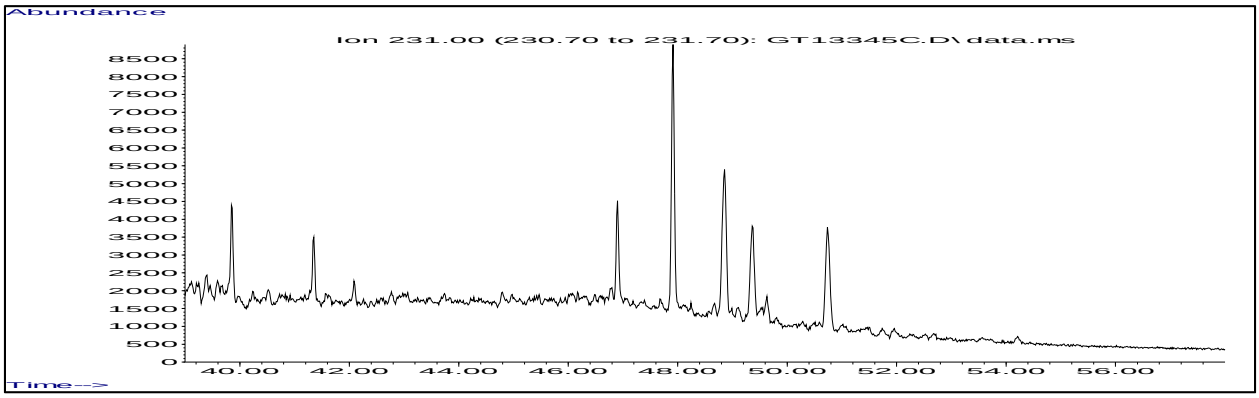

EPA South Louisiana Crude Oil

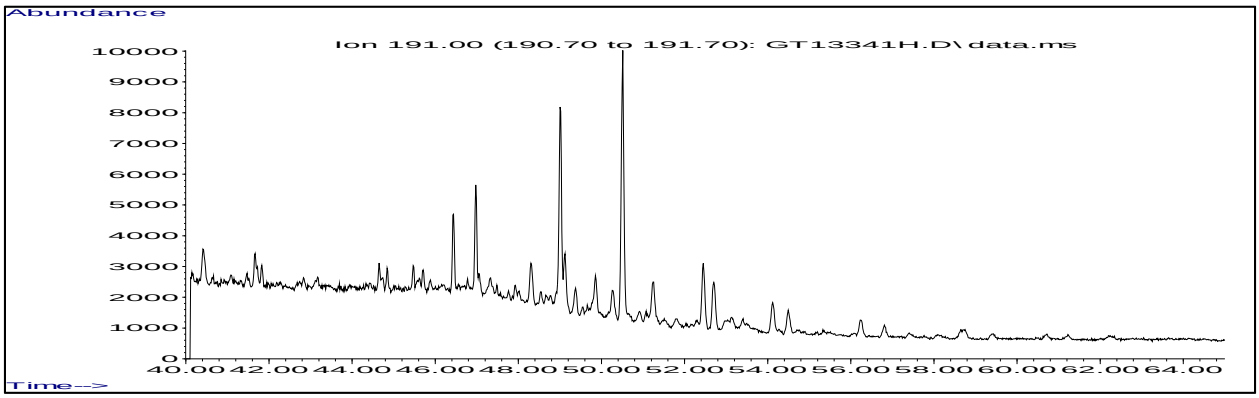


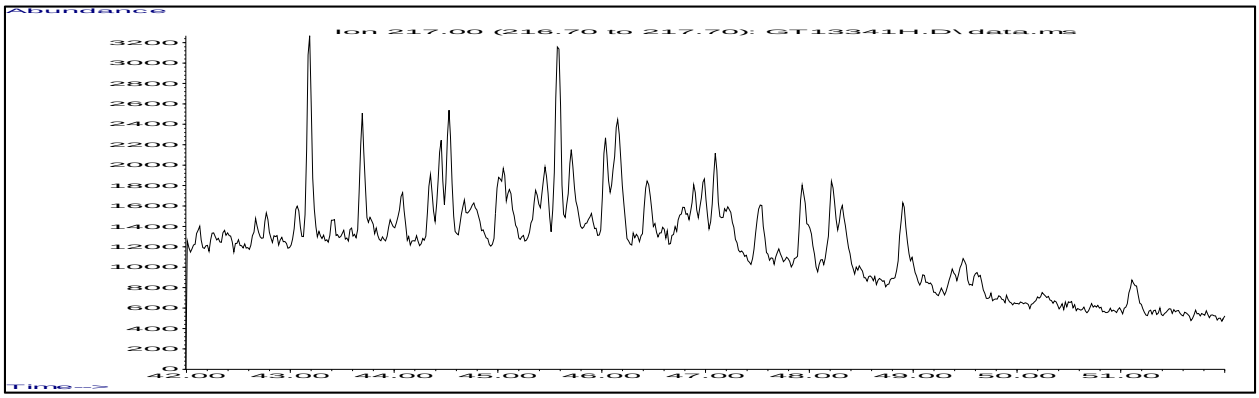


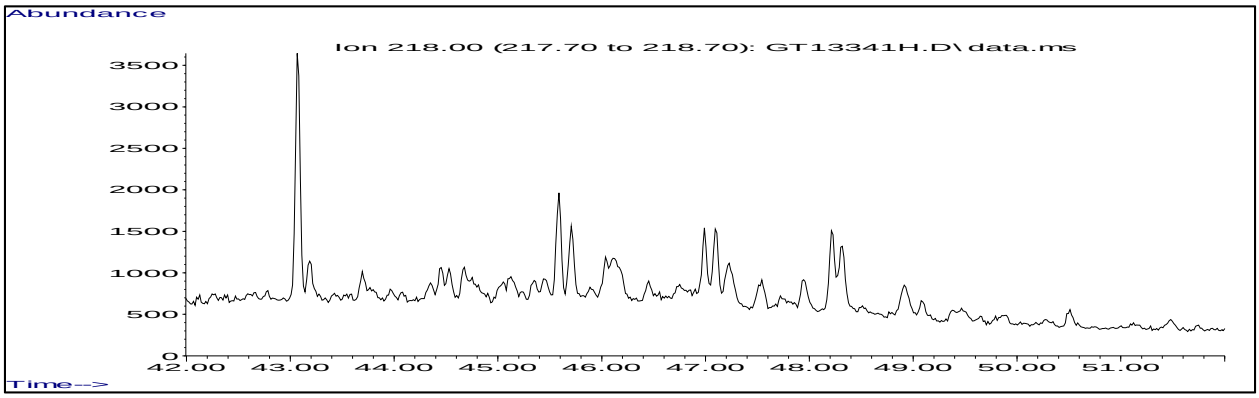


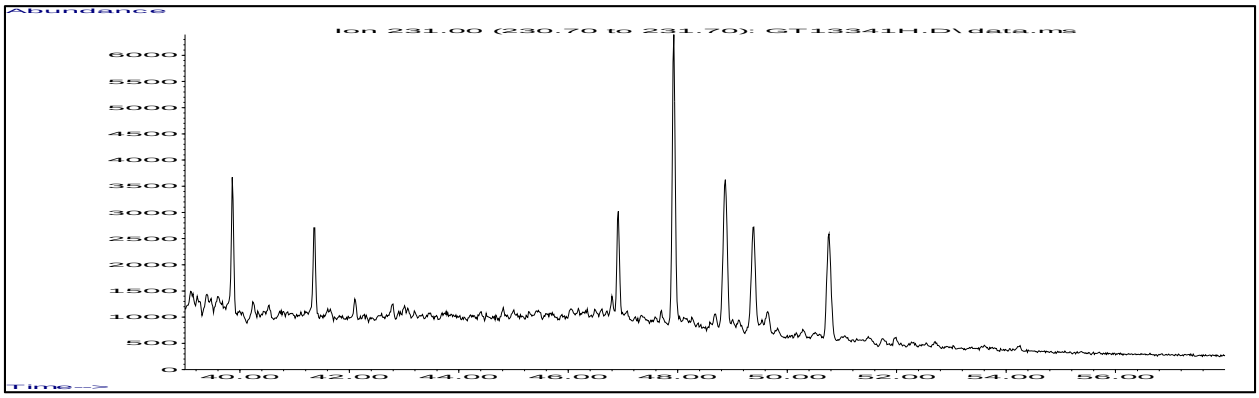

Exxon OCS

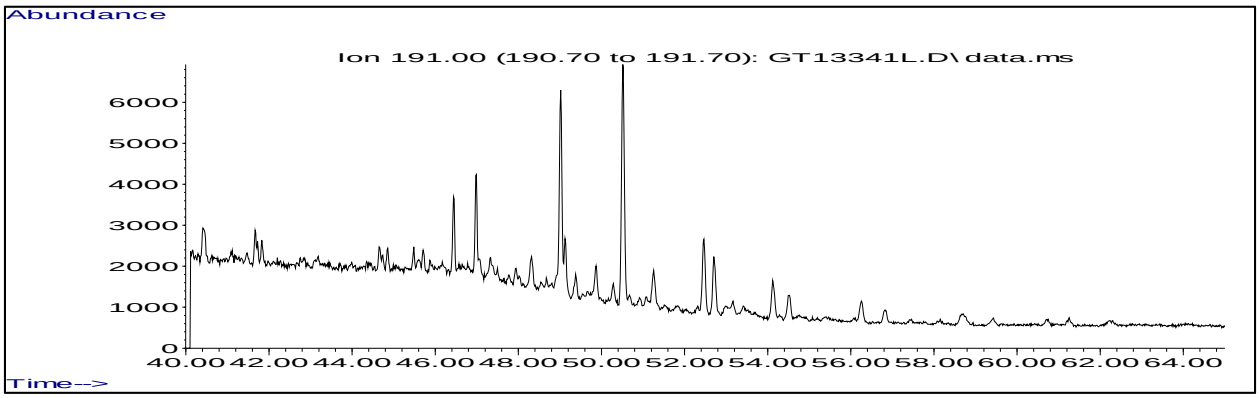
Abundance
Ion 191.00 (190.70 to 191.70): GT13341L.D\data.ms
6000
5000
4000
3000
2000
1000
0
40.00 42.00 44.00 46.00 48.00 50.00 52.00 54.00 56.00 58.00 60.00 62.00 64.00
Time-->

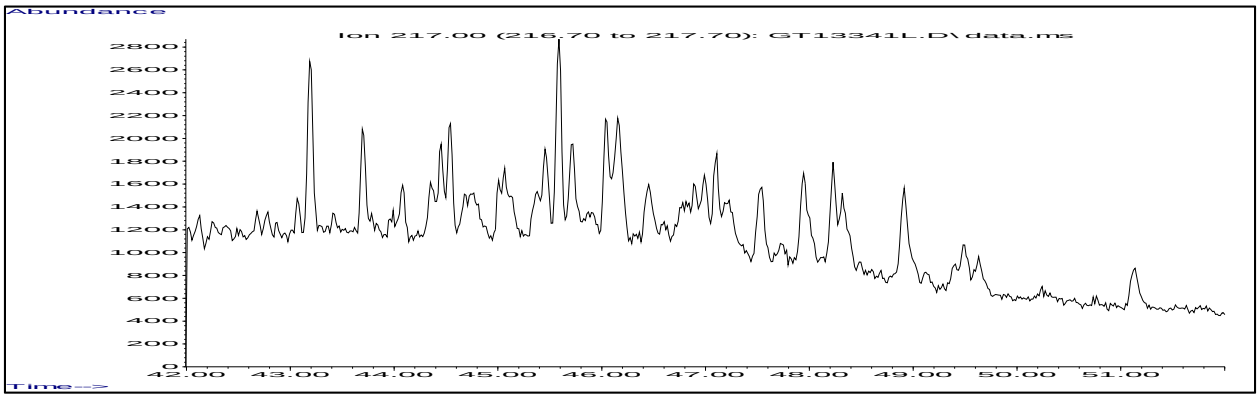
Abundance
Ion 217.00 (216.70 to 217.70): GT13341L.D\data.ms
2800
2600
2400
2200
2000
1800
1600
1400
1200
1000
800
600
400
200
0
42.00 43.00 44.00 45.00 46.00 47.00 48.00 49.00 50.00 51.00
Time-->

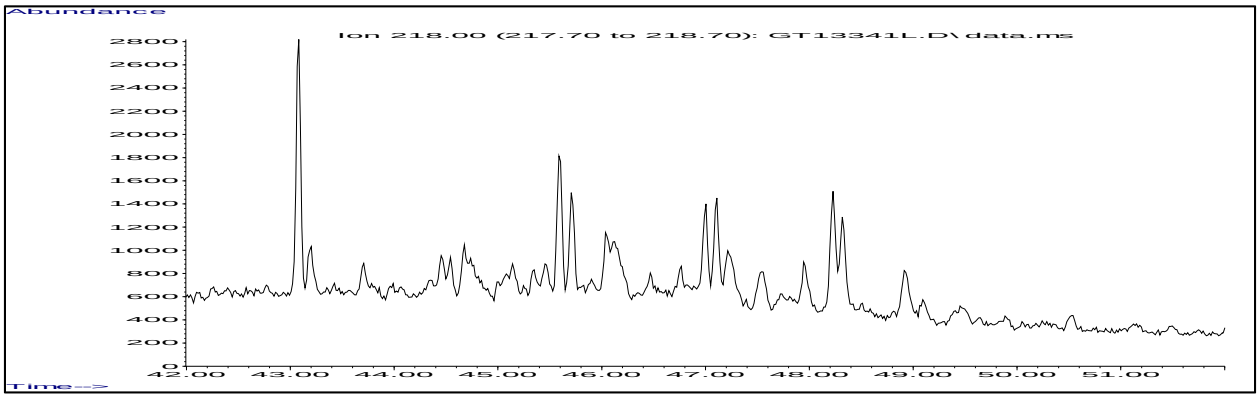
Abundance
Ion 218.00 (217.70 to 218.70): GT13341L.D\data.ms
2800
2600
2400
2200
2000
1800
1600
1400
1200
1000
800
600
400
200
0
42.00 43.00 44.00 45.00 46.00 47.00 48.00 49.00 50.00 51.00
Time-->

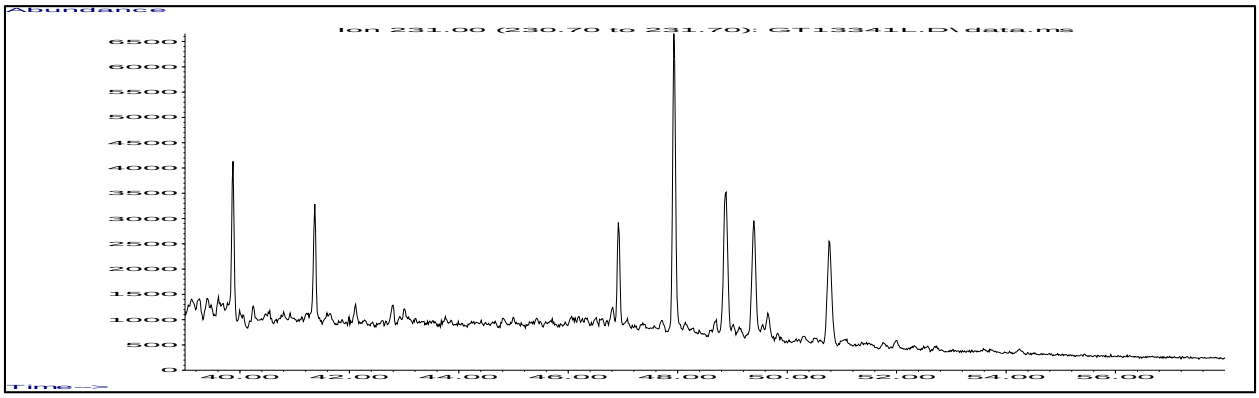
Abundance
Ion 231.00 (230.70 to 231.70): GT13341L.D\data.ms
6500
6000
5500
5000
4500
4000
3500
3000
2500
2000
1500
1000
500
0
40.00 42.00 44.00 46.00 48.00 50.00 52.00 54.00 56.00
Time-->

MC252

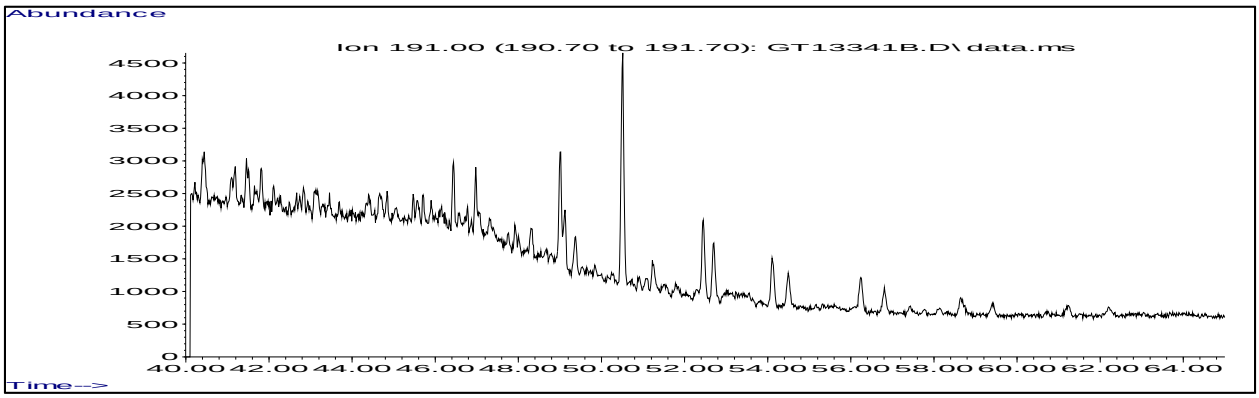
Abundance
Ion 191.00 (190.70 to 191.70): GT13341B.D\data.ms
4500
4000
3500
3000
2500
2000
1500
1000
500
0
40.00 42.00 44.00 46.00 48.00 50.00 52.00 54.00 56.00 58.00 60.00 62.00 64.00
Time-->

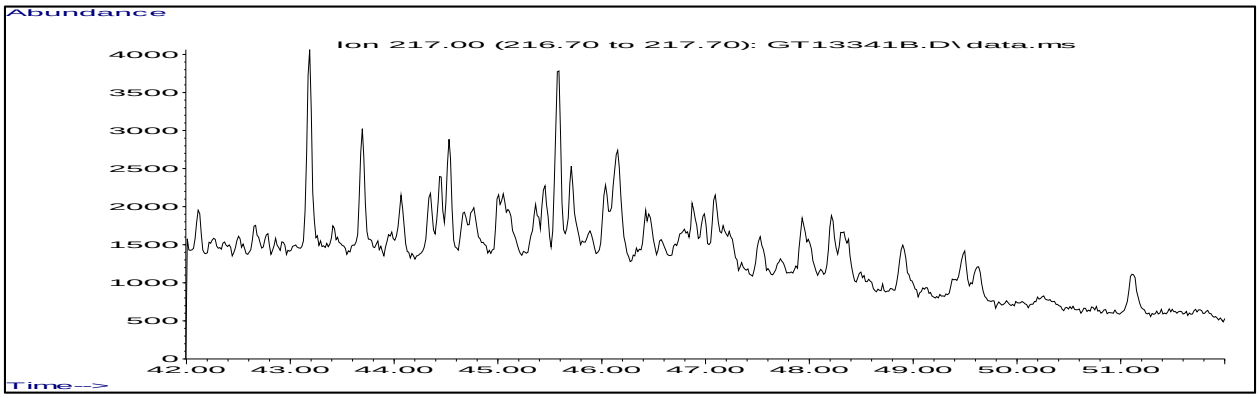
Abundance
Ion 217.00 (216.70 to 217.70): GT13341B.D\data.ms
4000
3500
3000
2500
2000
1500
1000
500
0
42.00 43.00 44.00 45.00 46.00 47.00 48.00 49.00 50.00 51.00
Time-->

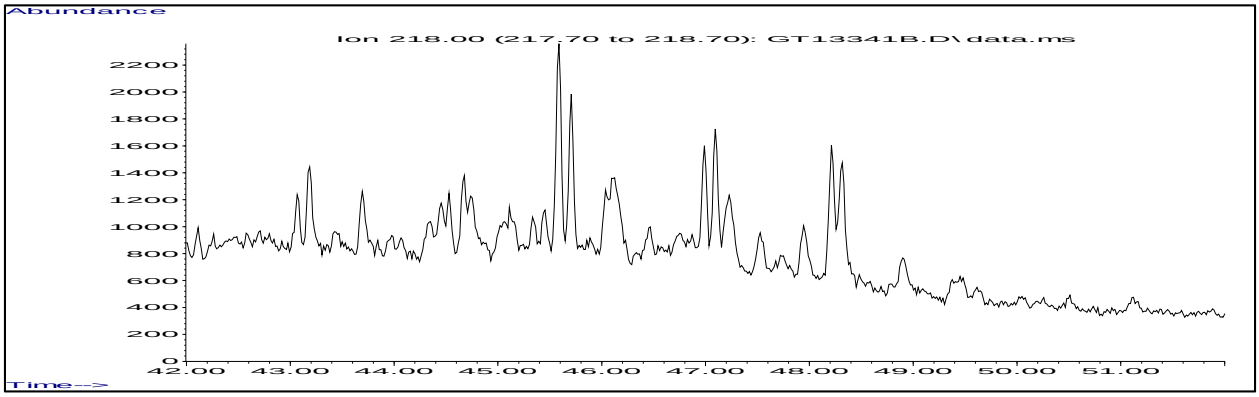
Abundance
Ion 218.00 (217.70 to 218.70): GT13341B.D\data.ms
2200
2000
1800
1600
1400
1200
1000
800
600
400
200
0
42.00 43.00 44.00 45.00 46.00 47.00 48.00 49.00 50.00 51.00
Time-->

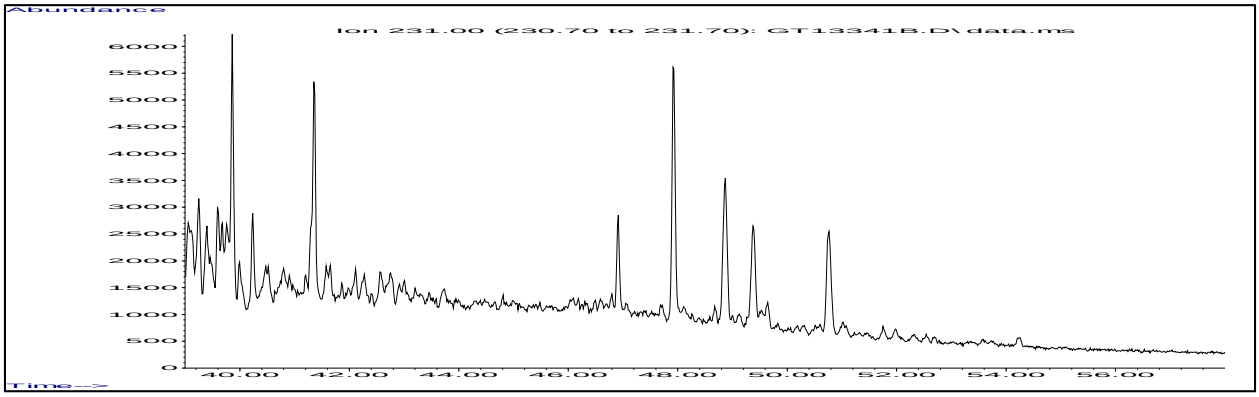
Abundance
Ion 231.00 (230.70 to 231.70): GT13341B.D\data.ms
6000
5500
5000
4500
4000
3500
3000
2500
2000
1500
1000
500
0
40.00 42.00 44.00 46.00 48.00 50.00 52.00 54.00 56.00
Time-->

Pt. Coupee Crude

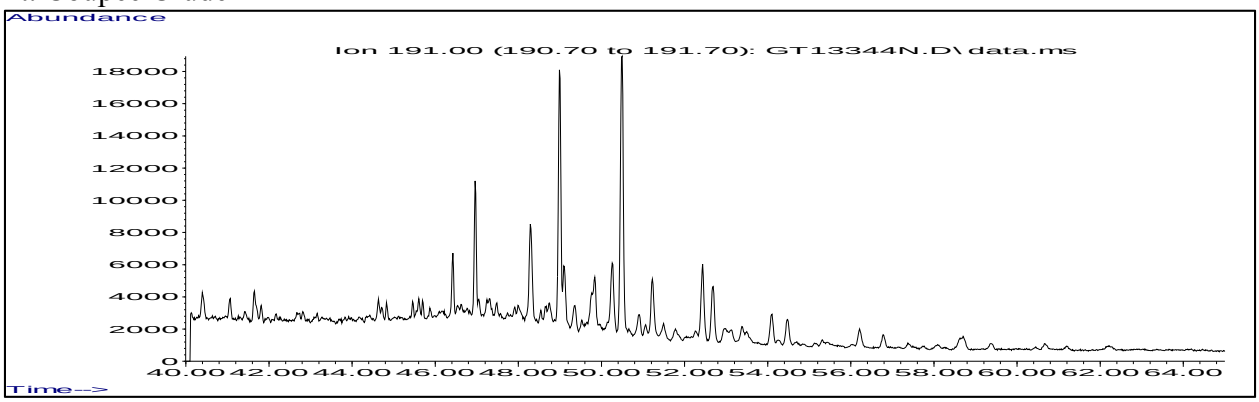


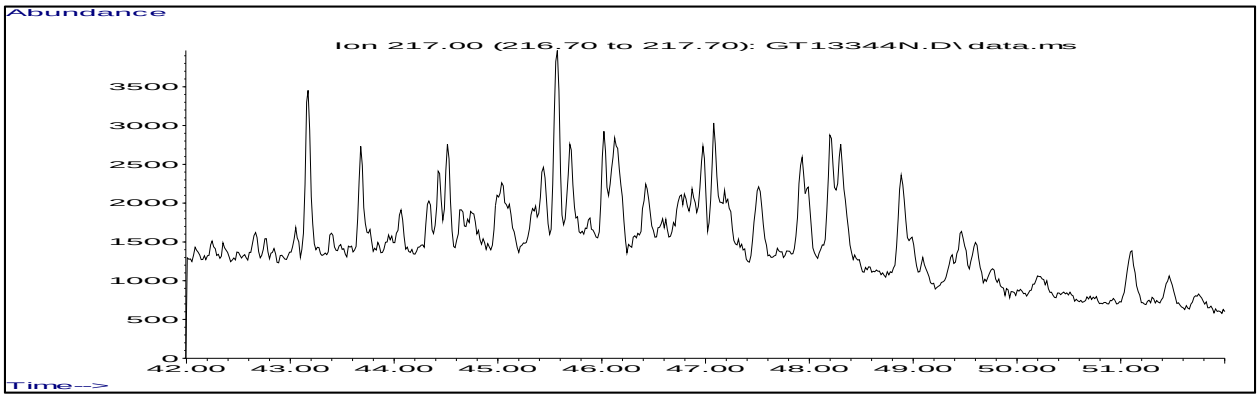


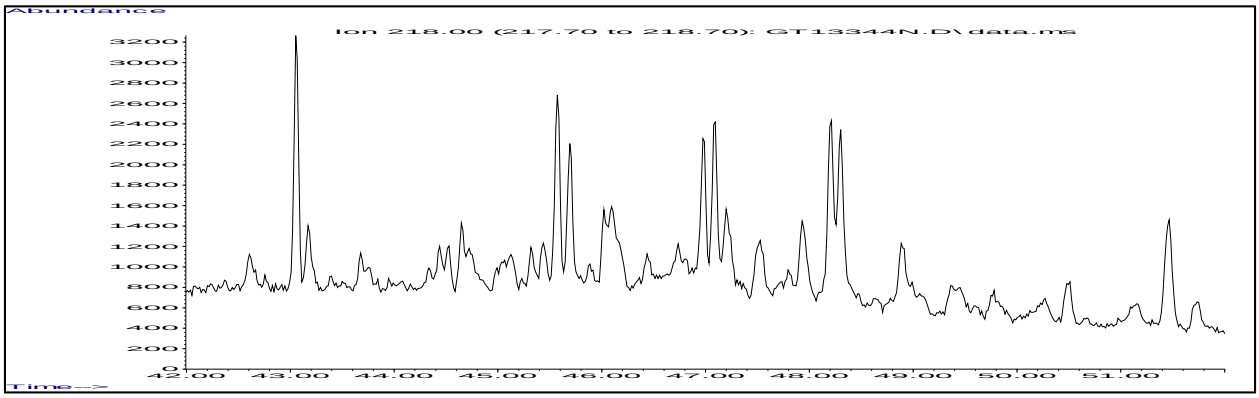


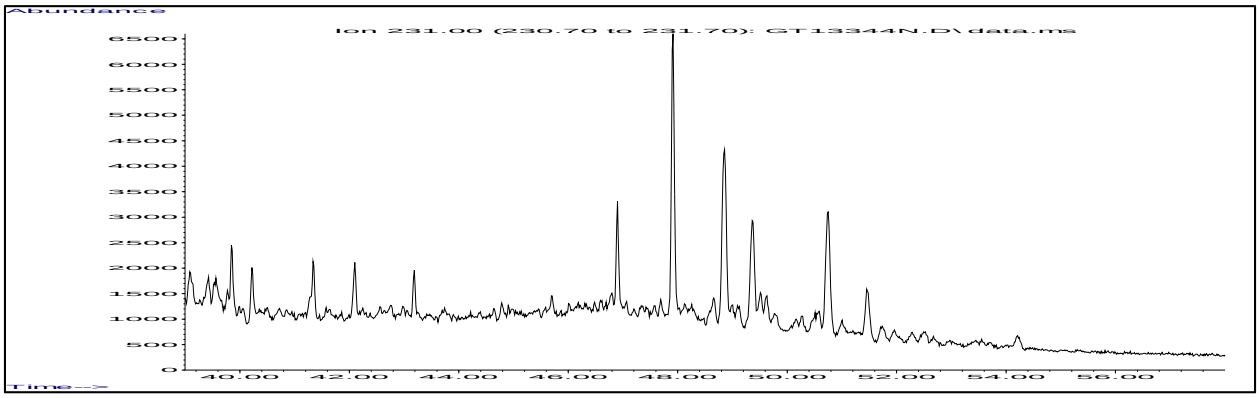

SLC Blend

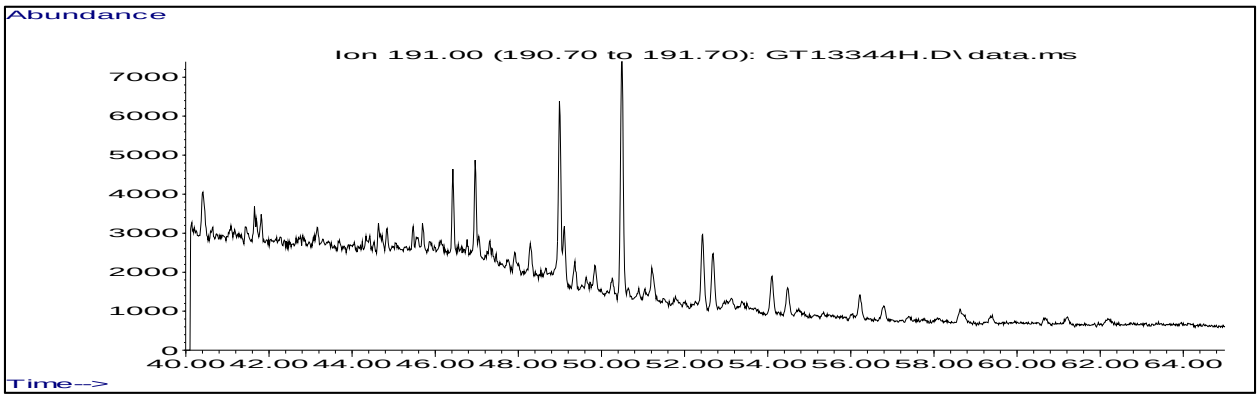
Abundance
Ion 191.00 (190.70 to 191.70): GT13344H.D\ data.ms
7000
6000
5000
4000
3000
2000
1000
0
40.00 42.00 44.00 46.00 48.00 50.00 52.00 54.00 56.00 58.00 60.00 62.00 64.00
Time-->

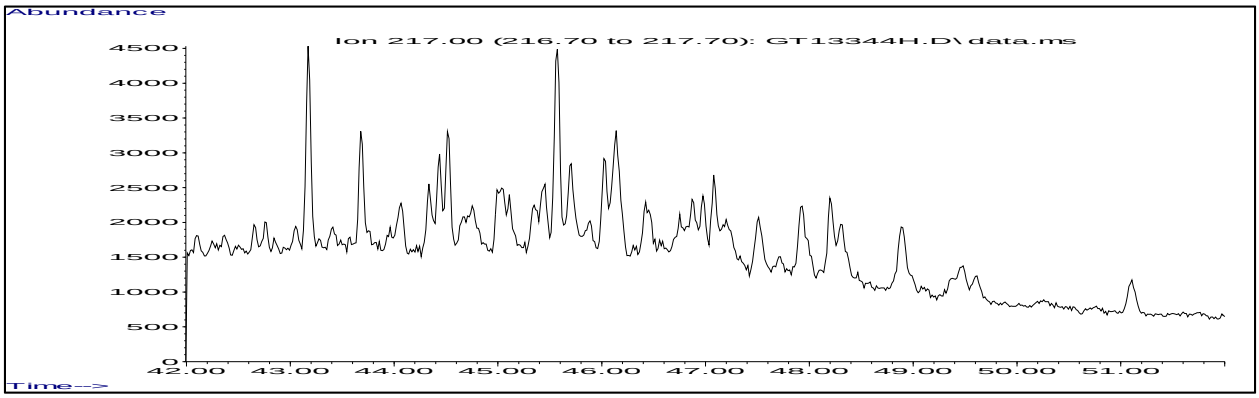
Abundance
Ion 217.00 (216.70 to 217.70): GT13344H.D\ data.ms
4500
4000
3500
3000
2500
2000
1500
1000
500
0
42.00 43.00 44.00 45.00 46.00 47.00 48.00 49.00 50.00 51.00
Time-->

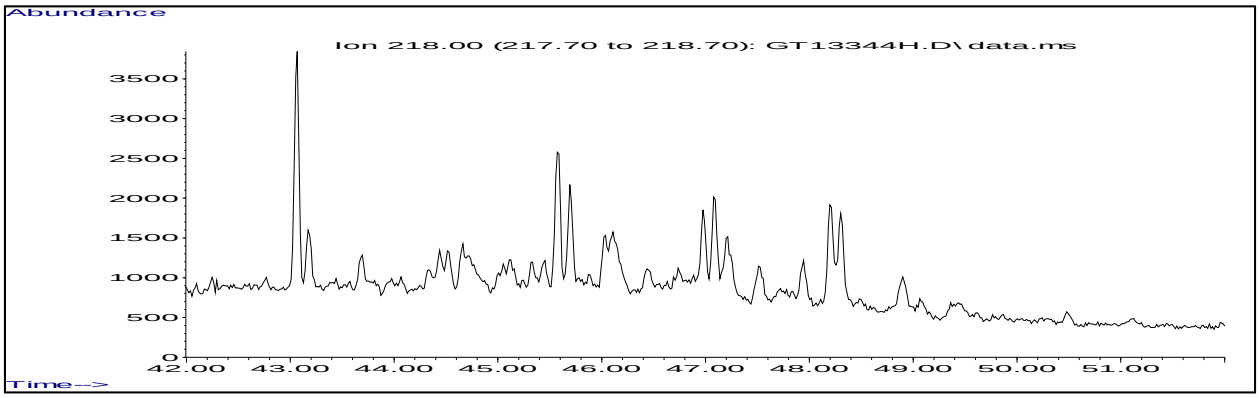
Abundance
Ion 218.00 (217.70 to 218.70): GT13344H.D\ data.ms
3500
3000
2500
2000
1500
1000
500
0
42.00 43.00 44.00 45.00 46.00 47.00 48.00 49.00 50.00 51.00
Time-->

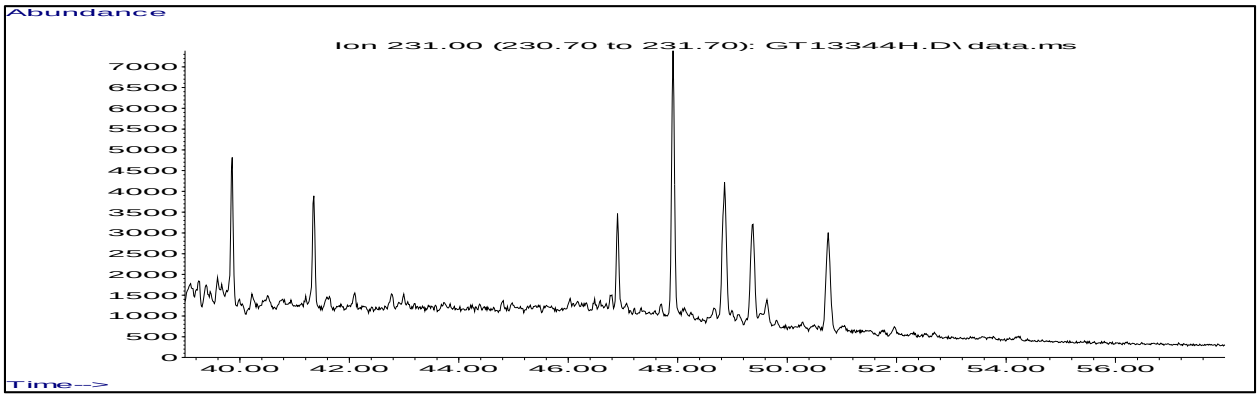
Abundance
Ion 231.00 (230.70 to 231.70): GT13344H.D\ data.ms
7000
6500
6000
5500
5000
4500
4000
3500
3000
2500
2000
1500
1000
500
0
40.00 42.00 44.00 46.00 48.00 50.00 52.00 54.00 56.00
Time-->

## APPENDIX D: PERMISSION REQUEST TO REPRINT

From: Buffy M Meyer [mailto:bashton@lsu.edu]
Sent: Friday, February 12, 2016 11:28 AM
To: Permissions Helpdesk
Subject: Permission for dx.doi.org/10.1016/j.marpolbul.2014.10.032

I am a co-author on the paper titled "Oil source-fingerprinting in support of polarimetric radar mapping of Macondo-252 oil in Gulf Coast marshes" published in Marine Pollution Bulletin, 89(2014):85-95, (dx.doi.org/10.1016/j.marpolbul.2014.10.032) and need to obtain permission to use portions of this publication as part of my dissertation. My university requires that I inform Elsevier that my dissertation will be available for viewing on the web. Can you please advise me on how to proceed in obtaining this permission, and receiving documentation of this permission to include in an appendix of my dissertation? Thank you in advance.

Buffy Meyer, Ph.D. Candidate
Research Associate V
Louisiana State University
Department of Environmental Sciences
1263 Energy, Coast & Environment Bldg, Baton Rouge, LA 70803

Dear Ms. Meyer:

As an Elsevier journal author, you retain the right to include the article in a thesis or dissertation (provided that this is not to be published commercially) whether in part or *in toto*, subject to proper acknowledgment; see http://www.elsevier.com/about/company-information/policies/copyright/personal-use for more information. As this is a retained right, no written permission from Elsevier is necessary.

If I may be of further assistance, please let me know. Best of luck with your dissertation and best regards,

Hop
Hop Wechsler
Permissions Helpdesk Manager
**Elsevier**
1600 John F. Kennedy Boulevard, Suite 1800
Philadelphia, PA 19103-2899
Tel: +1-215-239-3520
Mobile: +1-215-900-5674
Fax: +1-215-239-3805
E-mail: h.wechsler@elsevier.com
*Contact the Permissions Helpdesk:+1-800-523-4069 x 808 permissionshelpdesk@elsevier.com*

## APPENDIX E: CLUSTER DETAILS FOR COASTAL MARSH SEDIMENTS

2010 – Combined EICs, Background and Oiled Samples

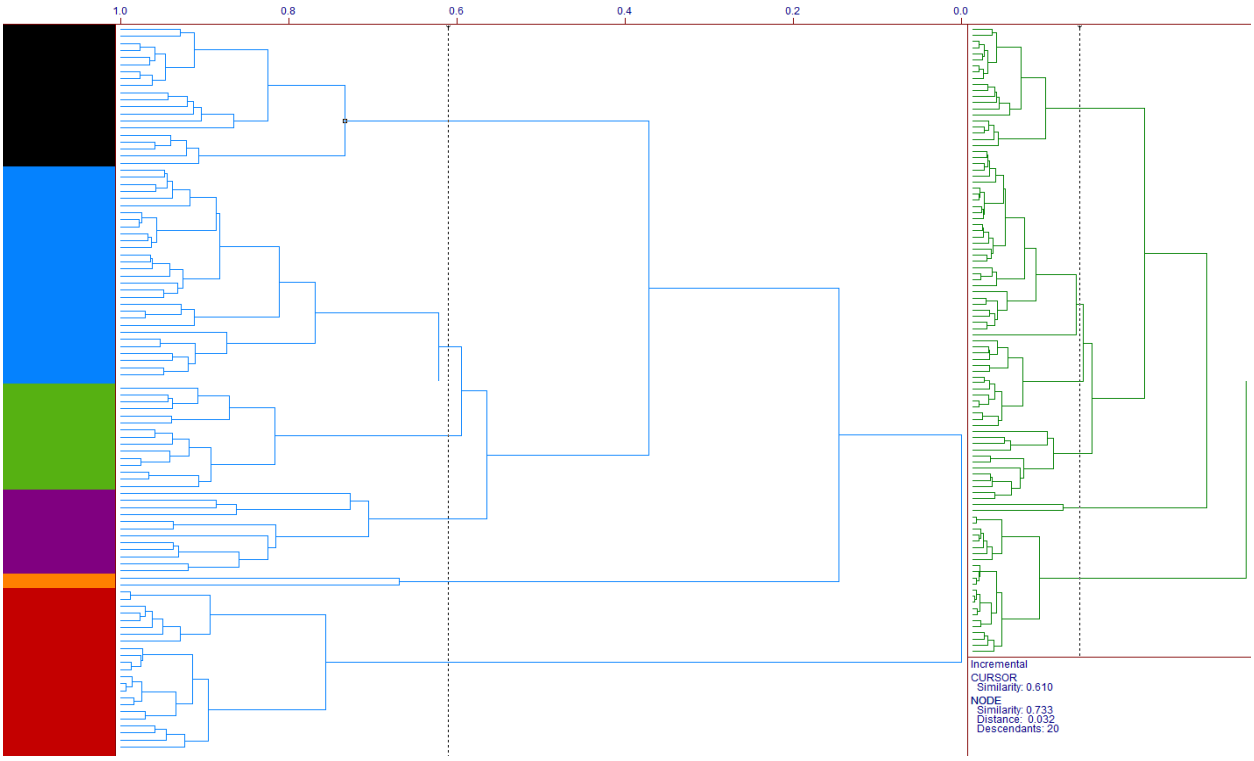


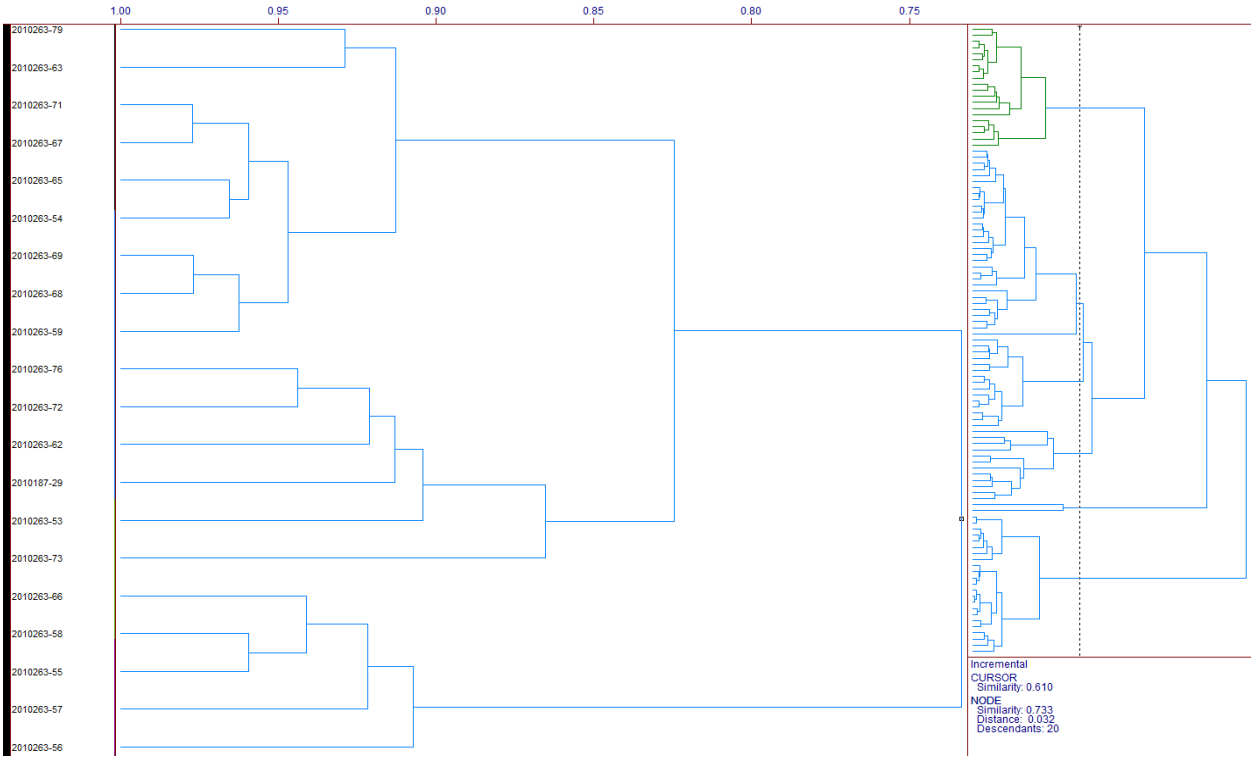

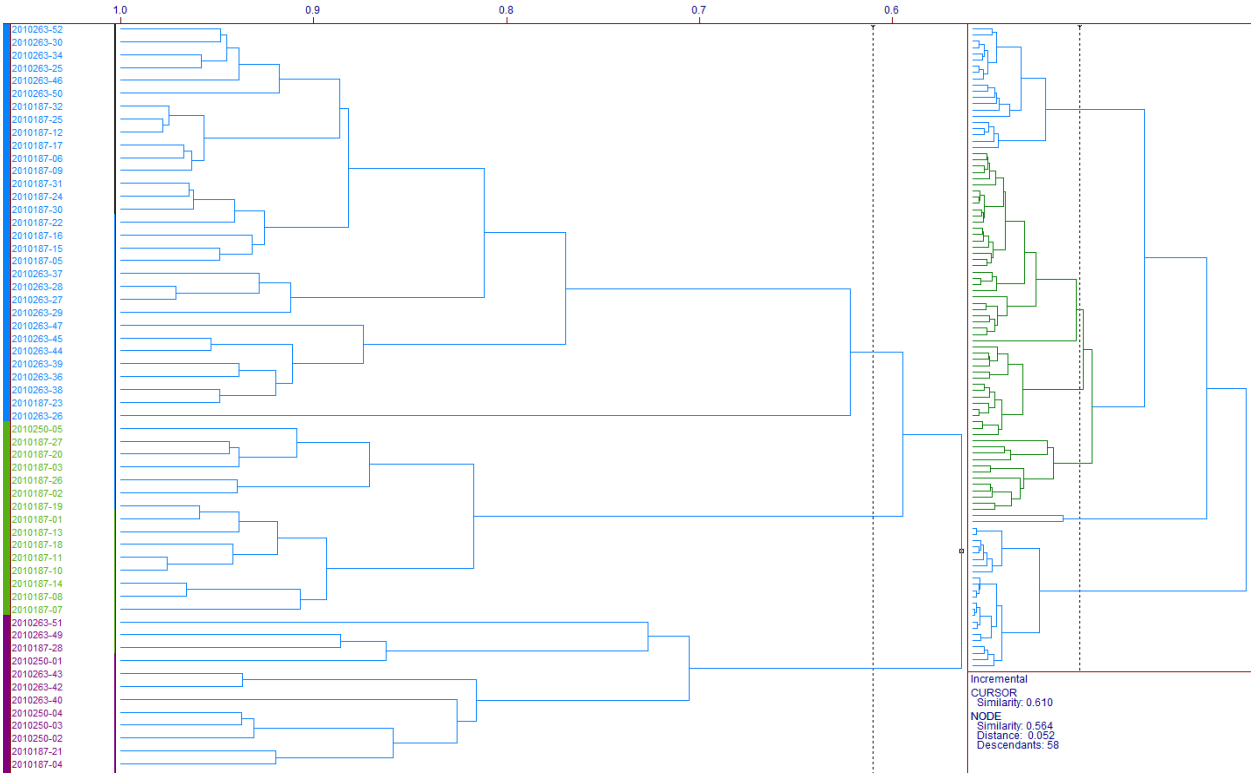
1.0
0.9
0.8
0.7
0.6
2010263-52
2010263-30
2010263-34
2010263-25
2010263-46
2010263-50
2010187-32
2010187-25
2010187-12
2010187-17
2010187-06
2010187-09
2010187-31
2010187-24
2010187-30
2010187-22
2010187-16
2010187-15
2010187-05
2010263-37
2010263-28
2010263-27
2010263-29
2010263-47
2010263-45
2010263-44
2010263-39
2010263-36
2010263-38
2010187-23
2010263-26
2010250-05
2010187-27
2010187-20
2010187-03
2010187-26
2010187-02
2010187-19
2010187-01
2010187-13
2010187-18
2010187-11
2010187-10
2010187-14
2010187-08
2010187-07
2010263-51
2010263-49
2010187-28
2010250-01
2010263-43
2010263-42
2010263-40
2010250-04
2010250-03
2010250-02
2010187-21
2010187-04
Incremental
CURSOR
Similarity: 0.610
NODE
Similarity: 0.564
Distance: 0.052
Descendants: 58


1.0
0.9
0.8
0.7
2010263-41
2010263-33
Incremental
CURSOR
Similarity: 0.610
NODE
Similarity: 0.668
Distance: 0.040
Descendants: 2

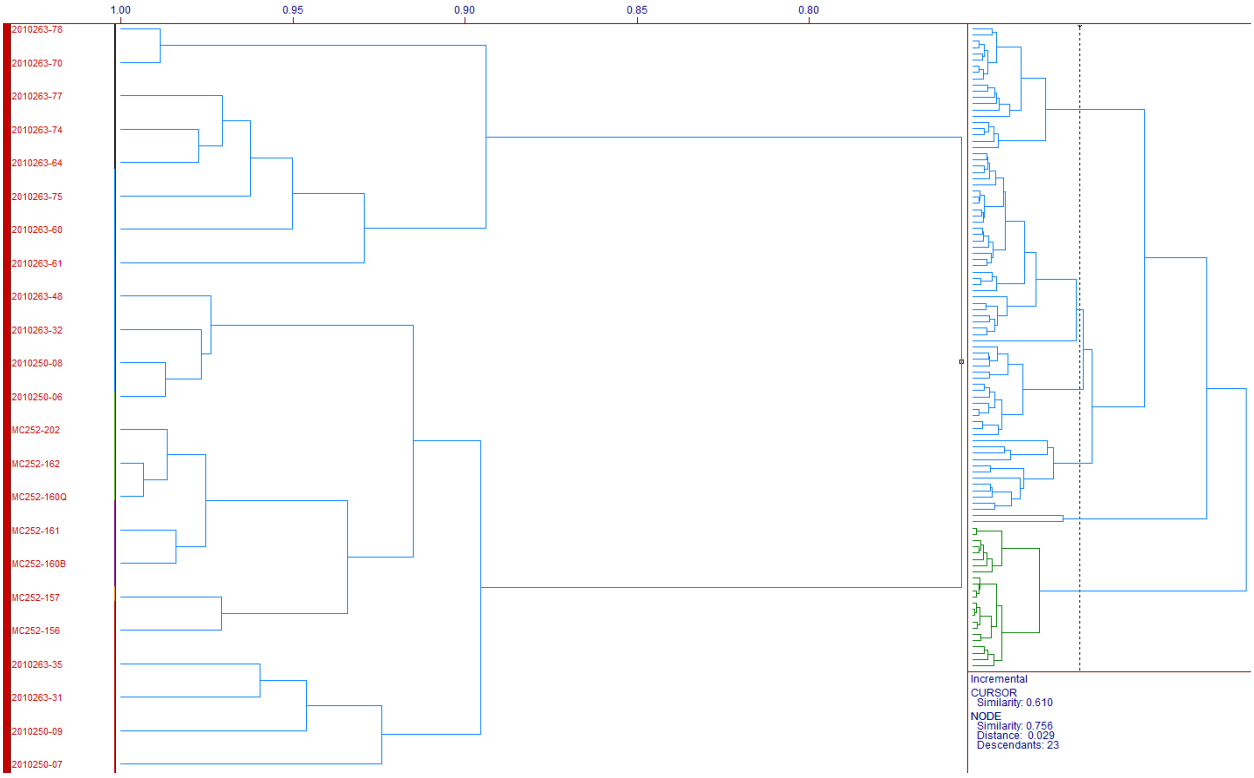


2011 – Combined EICs, Background and Oiled Samples

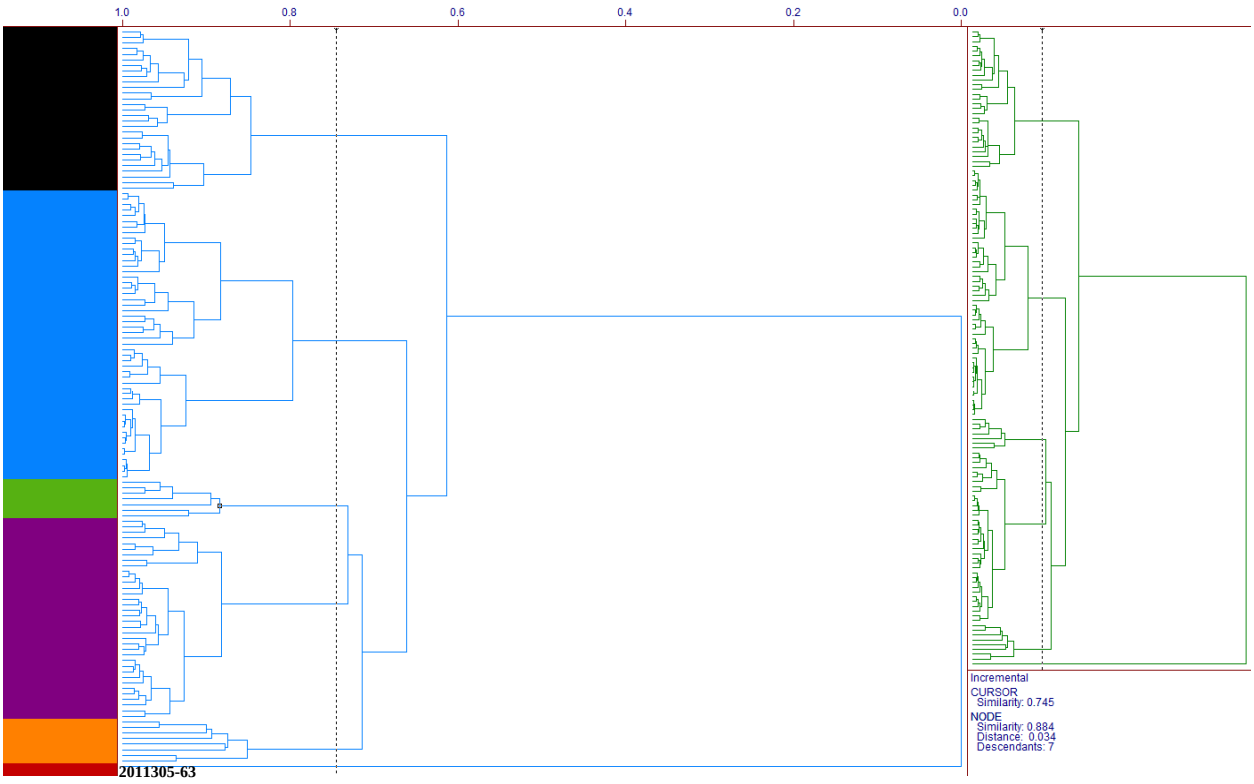

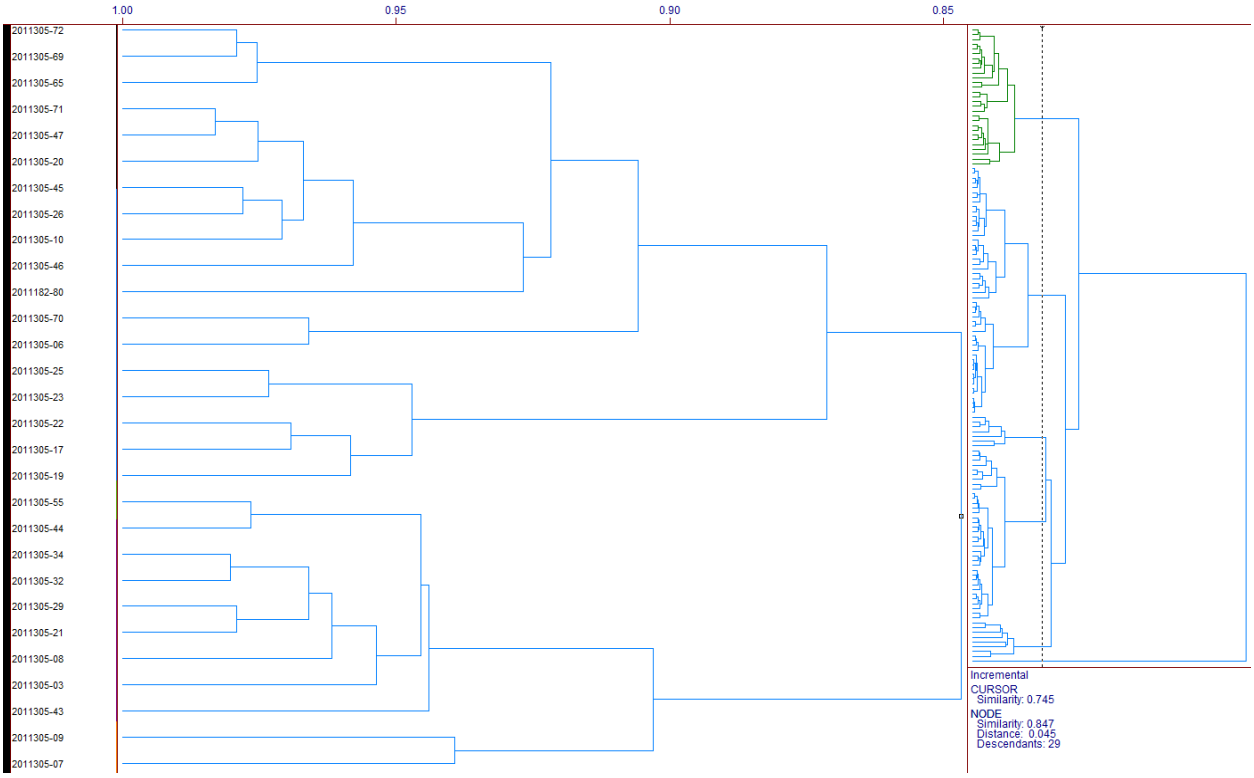
1.00
0.95
0.90
0.85
2011305-72
2011305-69
2011305-65
2011305-71
2011305-47
2011305-20
2011305-45
2011305-26
2011305-10
2011305-46
2011182-80
2011305-70
2011305-06
2011305-25
2011305-23
2011305-22
2011305-17
2011305-19
2011305-55
2011305-44
2011305-34
2011305-32
2011305-29
2011305-21
2011305-08
2011305-03
2011305-43
2011305-09
2011305-07
Incremental
CURSOR
Similarity: 0.745
NODE
Similarity: 0.847
Distance: 0.045
Descendants: 29

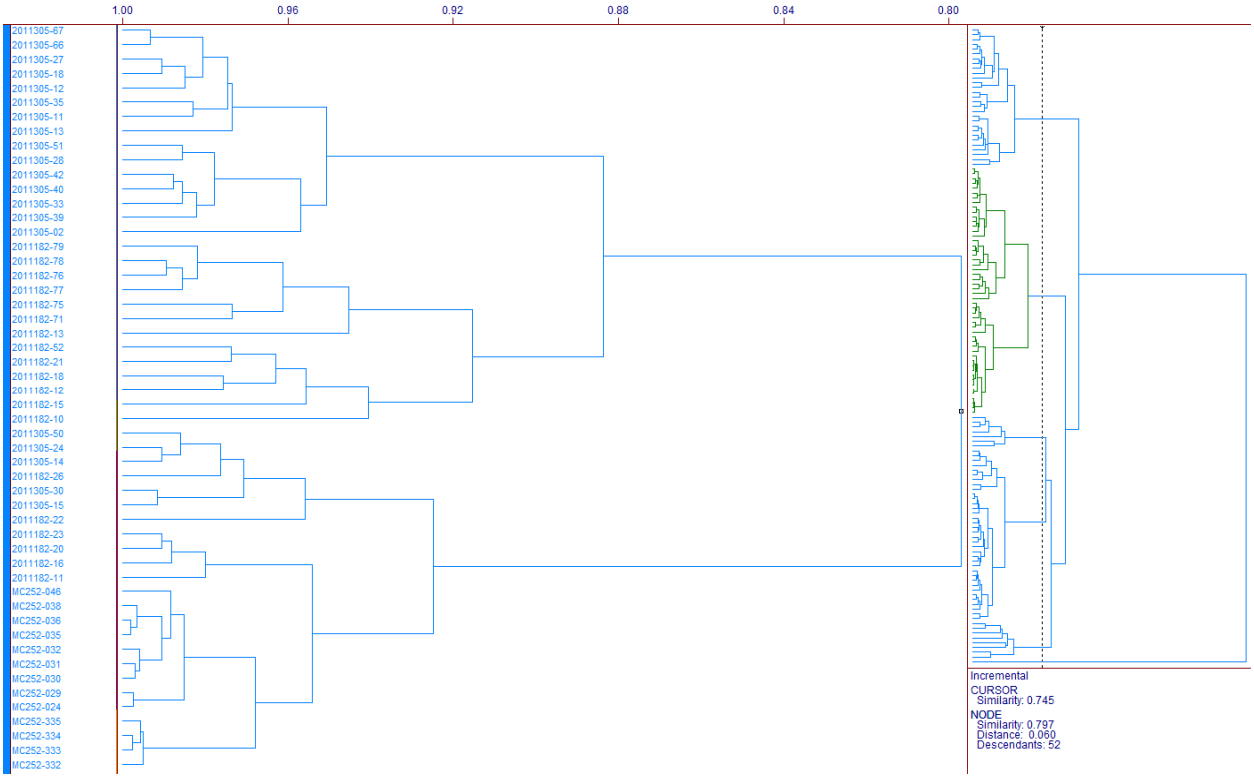
1.00
0.96
0.92
0.88
0.84
0.80
2011305-67
2011305-66
2011305-27
2011305-18
2011305-12
2011305-35
2011305-11
2011305-13
2011305-51
2011305-28
2011305-42
2011305-40
2011305-33
2011305-39
2011305-02
2011182-79
2011182-78
2011182-76
2011182-77
2011182-75
2011182-71
2011182-13
2011182-52
2011182-21
2011182-18
2011182-12
2011182-15
2011182-10
2011305-50
2011305-24
2011305-14
2011182-26
2011305-30
2011305-15
2011182-22
2011182-23
2011182-20
2011182-16
2011182-11
MC252-046
MC252-038
MC252-036
MC252-035
MC252-032
MC252-031
MC252-030
MC252-029
MC252-024
MC252-335
MC252-334
MC252-333
MC252-332
Incremental
CURSOR
Similarity: 0.745
NODE
Similarity: 0.797
Distance: 0.060
Descendants: 52

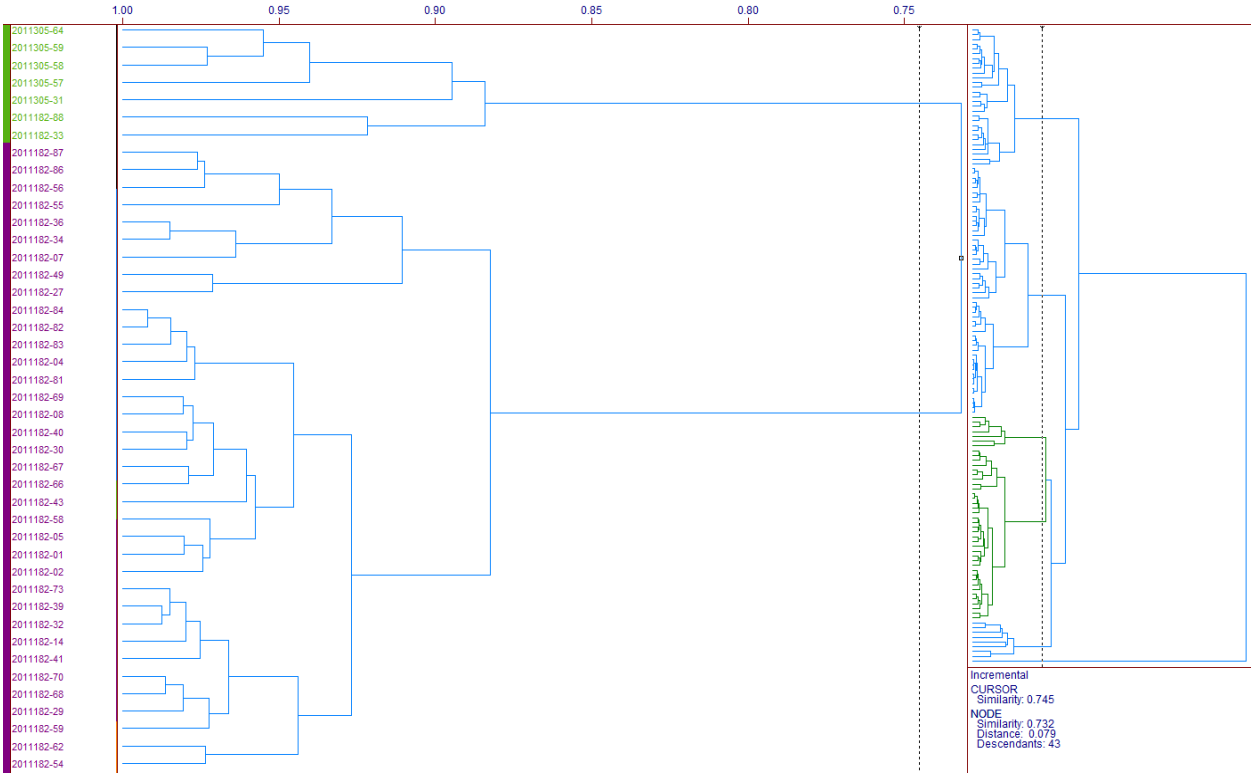
1.00
0.95
0.90
0.85
0.80
0.75
2011305-64
2011305-59
2011305-58
2011305-57
2011305-31
2011182-88
2011182-33
2011182-87
2011182-86
2011182-56
2011182-55
2011182-36
2011182-34
2011182-07
2011182-49
2011182-27
2011182-84
2011182-82
2011182-83
2011182-04
2011182-81
2011182-69
2011182-08
2011182-40
2011182-30
2011182-67
2011182-66
2011182-43
2011182-58
2011182-05
2011182-01
2011182-02
2011182-73
2011182-39
2011182-32
2011182-14
2011182-41
2011182-70
2011182-68
2011182-29
2011182-59
2011182-62
2011182-54
Incremental
CURSOR
Similarity: 0.745
NODE
Similarity: 0.732
Distance: 0.079
Descendants: 43

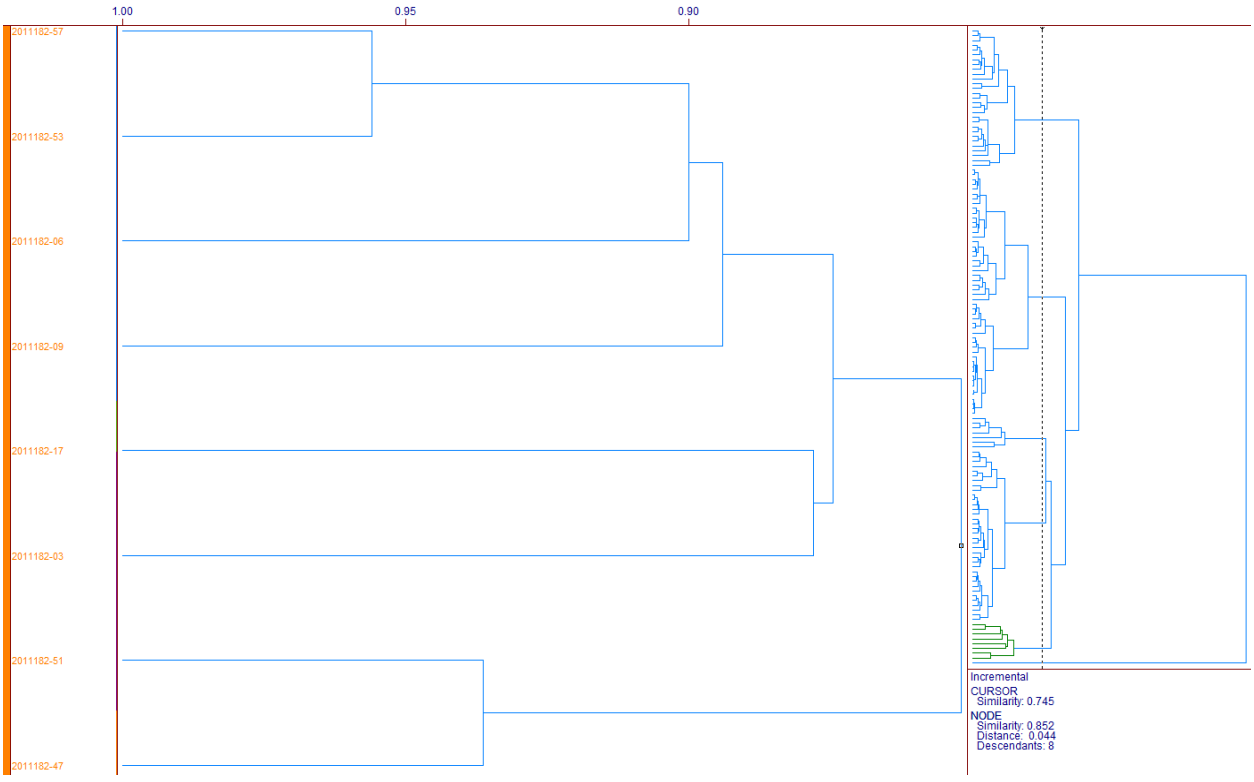
1.00
0.95
0.90
2011182-57
2011182-53
2011182-06
2011182-09
2011182-17
2011182-03
2011182-51
2011182-47
Incremental
CURSOR
Similarity: 0.745
NODE
Similarity: 0.852
Distance: 0.044
Descendants: 8

2012 – Combined EICs, Background and Oiled Samples

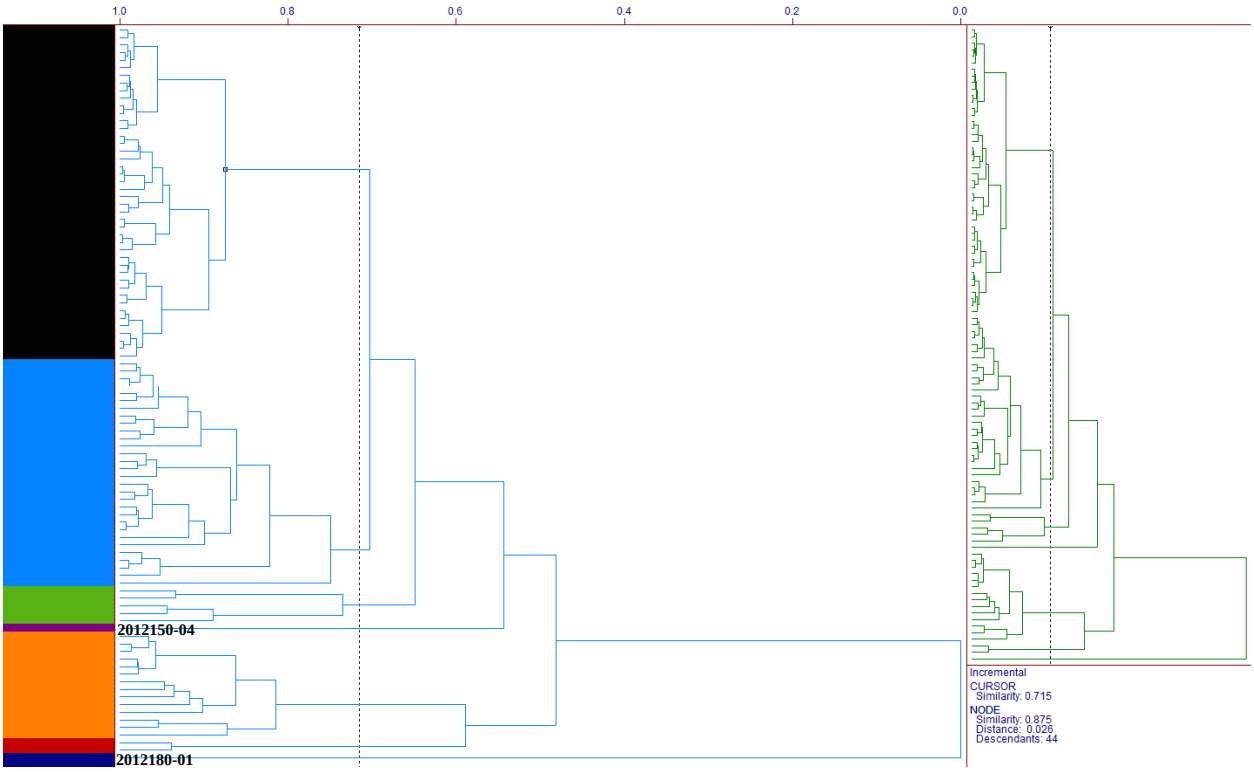


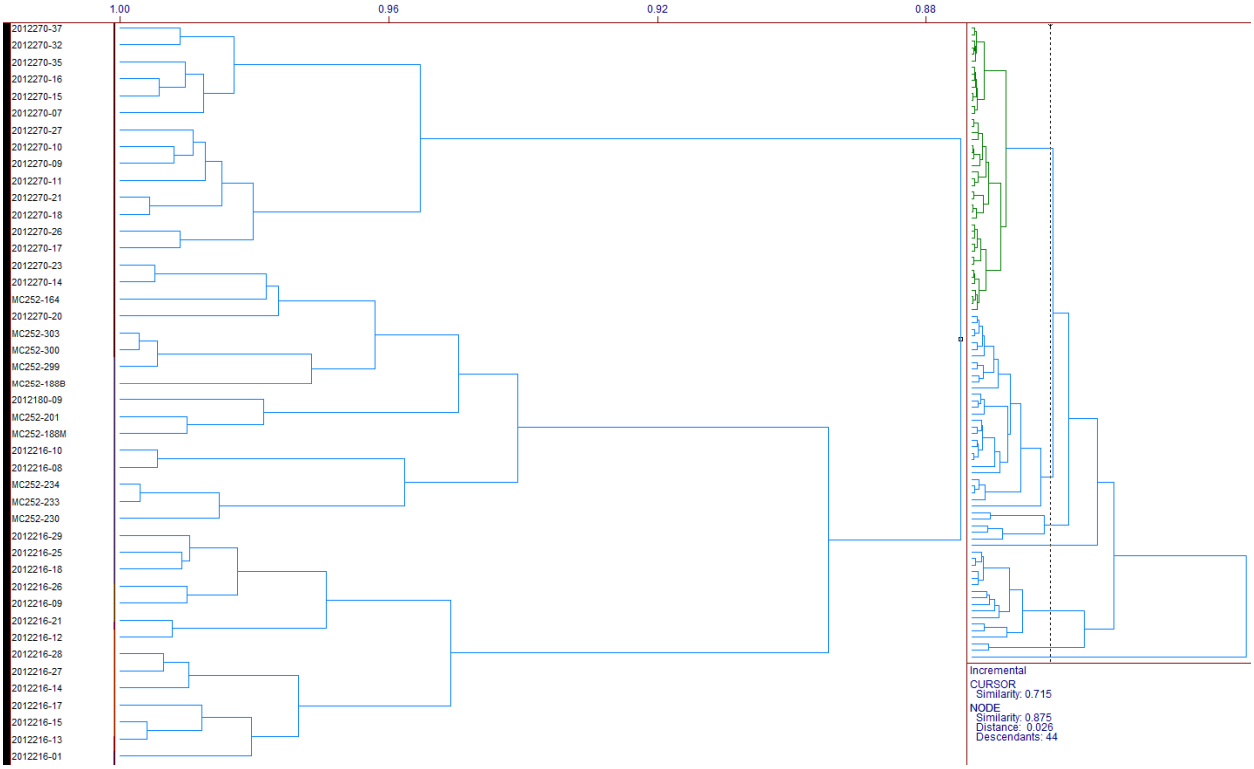

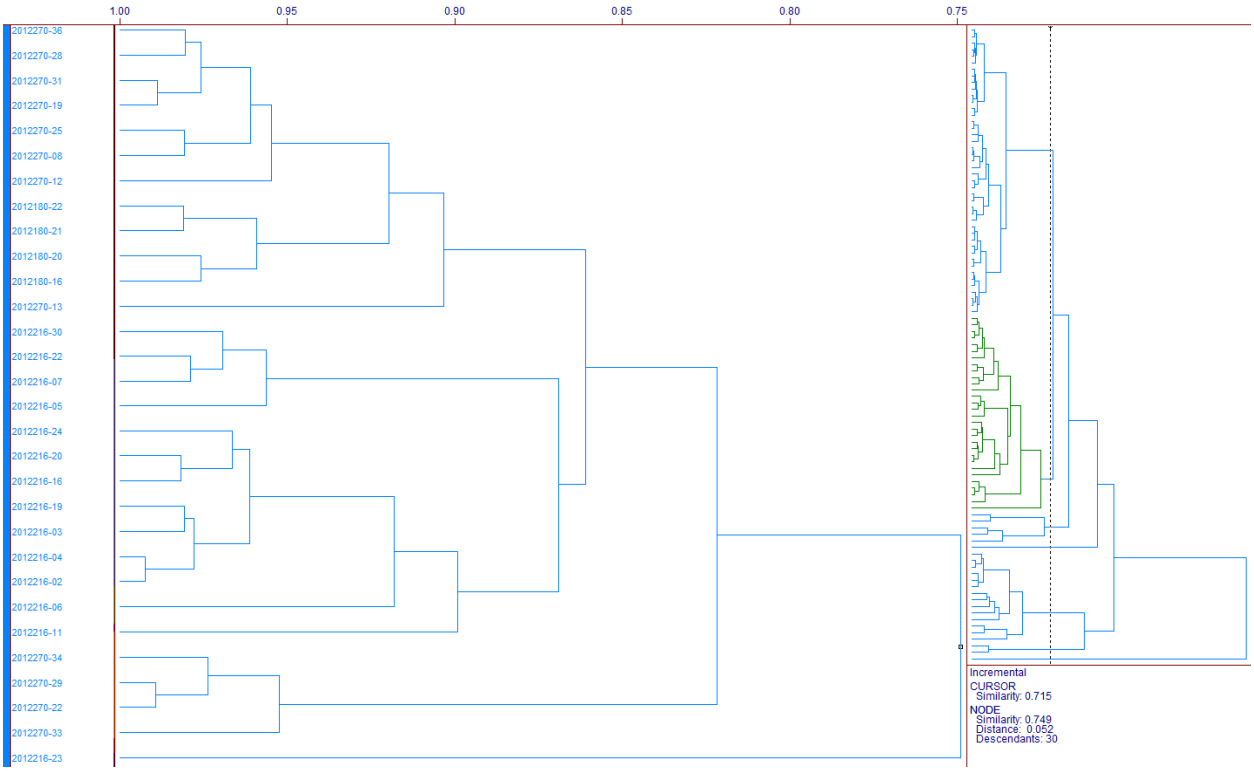
1.00
0.95
0.90
0.85
0.80
0.75
2012270-36
2012270-28
2012270-31
2012270-19
2012270-25
2012270-08
2012270-12
2012180-22
2012180-21
2012180-20
2012180-16
2012270-13
2012216-30
2012216-22
2012216-07
2012216-05
2012216-24
2012216-20
2012216-16
2012216-19
2012216-03
2012216-04
2012216-02
2012216-06
2012216-11
2012270-34
2012270-29
2012270-22
2012270-33
2012216-23
Incremental
CURSOR
Similarity: 0.715
NODE
Similarity: 0.749
Distance: 0.052
Descendants: 30

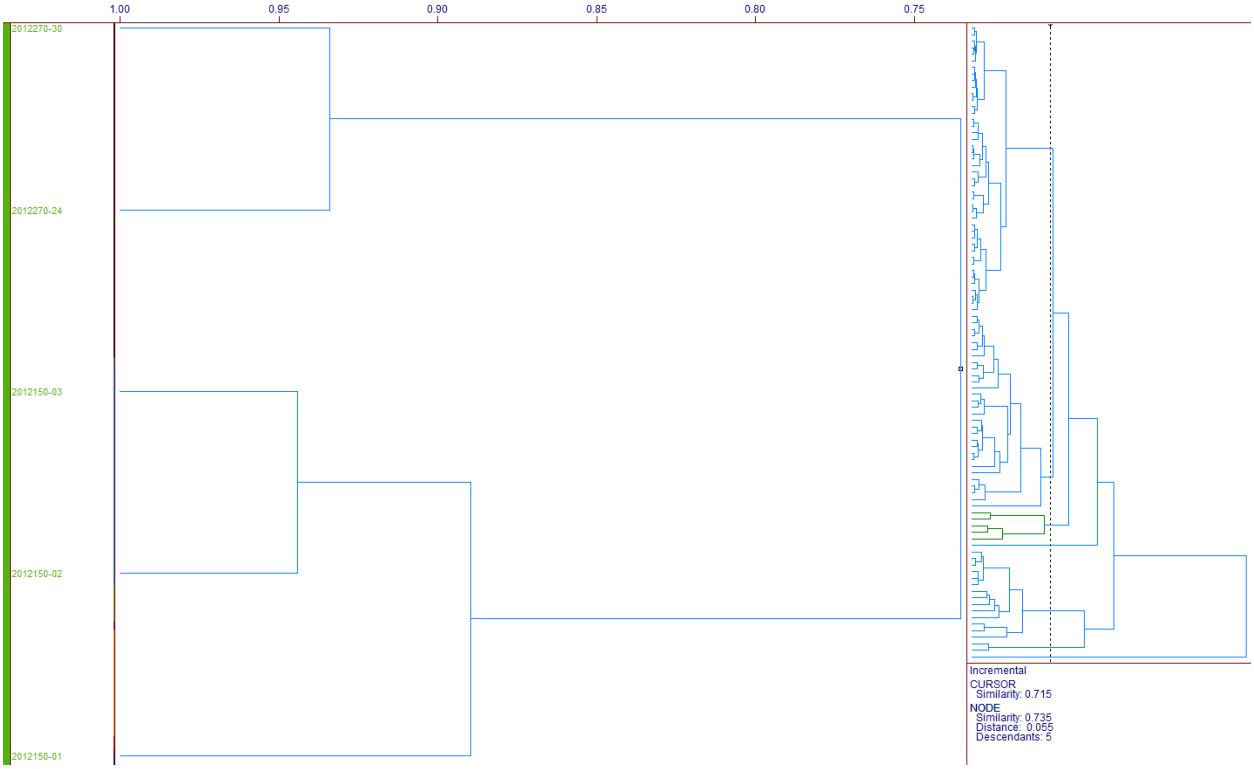
1.00
0.95
0.90
0.85
0.80
0.75
2012270-30
2012270-24
2012150-03
2012150-02
2012150-01
Incremental
CURSOR
Similarity: 0.715
NODE
Similarity: 0.735
Distance: 0.055
Descendants: 5

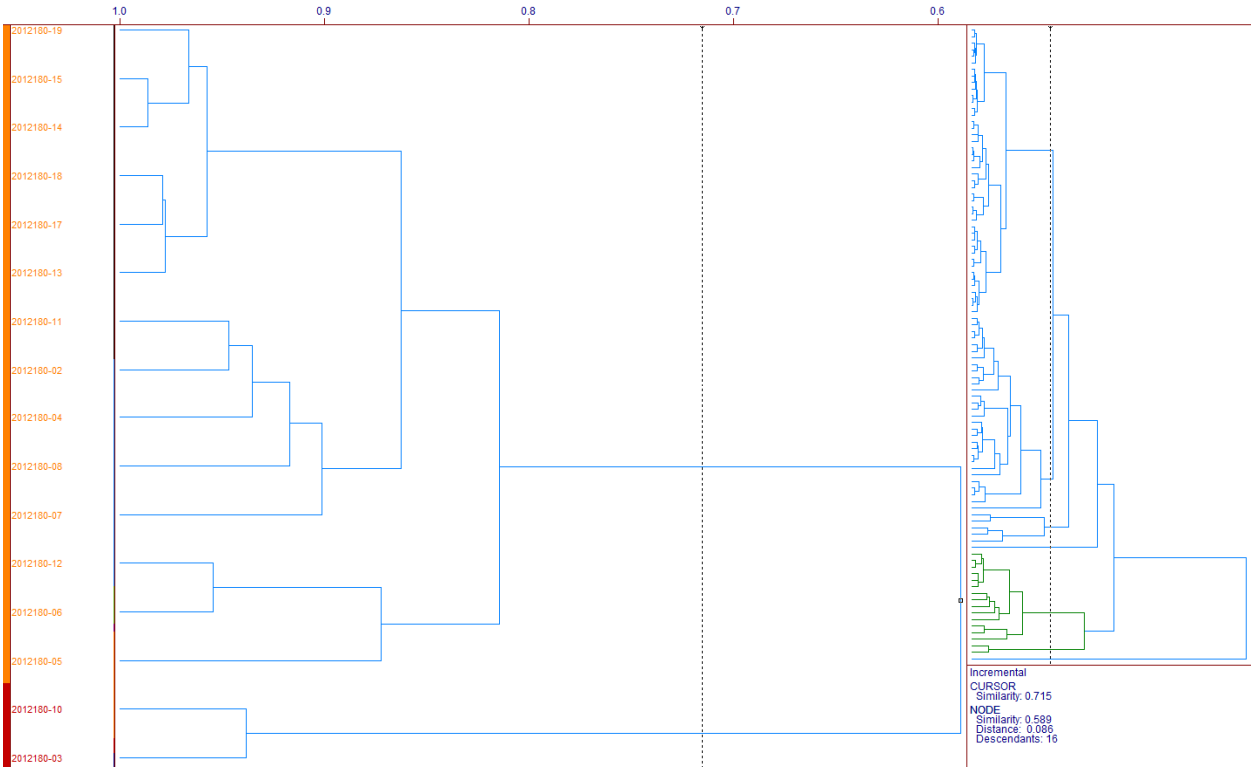
1.0
0.9
0.8
0.7
0.6
2012180-19
2012180-15
2012180-14
2012180-18
2012180-17
2012180-13
2012180-11
2012180-02
2012180-04
2012180-08
2012180-07
2012180-12
2012180-06
2012180-05
2012180-10
2012180-03
Incremental
CURSOR
Similarity: 0.715
NODE
Similarity: 0.589
Distance: 0.086
Descendants: 16

## APPENDIX F: *m/z* 217 CLUSTER DETAILS

**2010**

| BLACK CLUSTER | Date Collected | Ratio Score | Pattern | Field ID |
|---|---|---|---|---|
| 2010263-78 | 9/20/2010 | 11/11 | A | 77_COMAR_9/2010 |
| 2010263-70 | 9/20/2010 | 10/11 | AB | 63_COMAR_9/2010 |
| 2010263-77 | 9/20/2010 | 11/11 | AB | 76_COMAR_09/2010 |
| 2010263-74 | 9/20/2010 | 8/11 | AB | 68_COMAR_09/2010 |
| 2010263-64 | 9/20/2010 | 11/11 | A | 51_COMAR_09/2010 |
| 2010263-75 | 9/20/2010 | 11/11 | A | 70_COMAR_09/2010 |
| 2010263-60 | 9/20/2010 | 8/11 | A | 46_COMAR_09/2010 |
| 2010263-71 | 9/20/2010 | n/a | AB | 64 Edge_COMAR_09/2010 |
| 2010263-61 | 9/20/2010 | 9/11 | A | 48_COMAR_09/2010 |

| BLUE CLUSTER | Date Collected | Ratio Score | Pattern | Field ID |
|---|---|---|---|---|
| 2010263-52 | 9/20/2010 | n/a | A | 77 Edge_COMAR_09/2010 |
| 2010263-38 | 9/20/2010 | n/a | B | 53 Edge_COMAR_09/2010 |
| 2010187-23 | 7/6/2010 | 7/11 | C | C29_COMAR_07/06/2010 |
| 2010263-36 | 9/20/2010 | n/a | B | 51 Edge_COMAR_09/2010 |
| 2010263-45 | 9/20/2010 | n/a | AB | 66 Edge_COMAR_09/2010 |
| 2010263-44 | 9/20/2010 | n/a | AB | 65 Edge_COMAR_09/2010 |
| 2010263-47 | 9/20/2010 | n/a | AB | 68 Edge_COMAR_09/2010 |

| GREEN CLUSTER (MC252) | Date Collected | Ratio Score | Pattern | Field ID |
|---|---|---|---|---|
| 2010263-48 | 9/20/2010 | 11/11 | A | 69 Edge_COMAR |
| 2010263-32 | 9/20/2010 | 11/11 | A | 47_COMAR_09/2010 |
| 2010250-08 | 9/7/2010 | 10/11 | A | 8_09/07/2010 (Bay Batiste?) |
| 2010250-06 | 9/7/2010 | 10/11 | AB | 6_09/07/2010 (Bay Batiste?) |

| PURPLE CLUSTER (MC252) | Date Collected | Ratio Score | Pattern | Field ID |
|---|---|---|---|---|
| 2010263-35 | 9/20/2010 | 10/11 | A | 50 Edge_COMAR_09/2010 |
| 2010263-31 | 9/20/2010 | 9/11 | A | 46 Edge_COMAR_09/2010 |
| 2010250-09 | 9/7/2010 | 11/11 | A | 9_09/07/2010 (Bay Batiste?) |

| ORANGE CLUSTER (OUTLIER) | Date Collected | Ratio Score | Pattern | Field ID |
|---|---|---|---|---|
| 2010250-07 | 9/7/2010 | 10/11 | A | 7_09/07/2010 (Bay Batiste?) |

2010263-70 (Black Cluster)

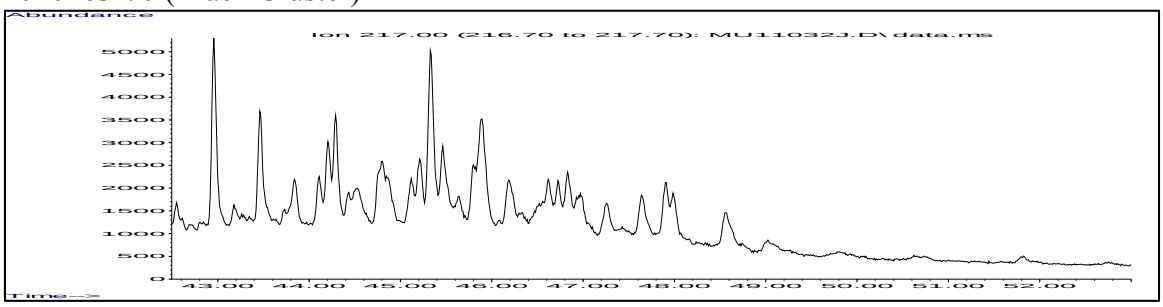


2010263-45 (Blue Cluster)

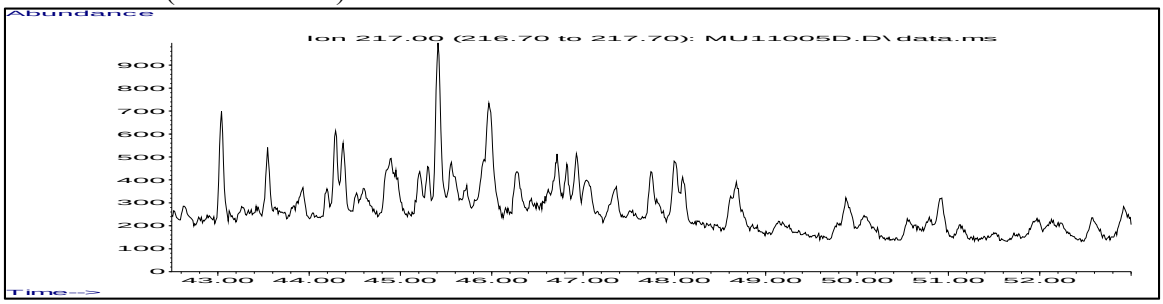


2010263-32 (Green Cluster including MC252)

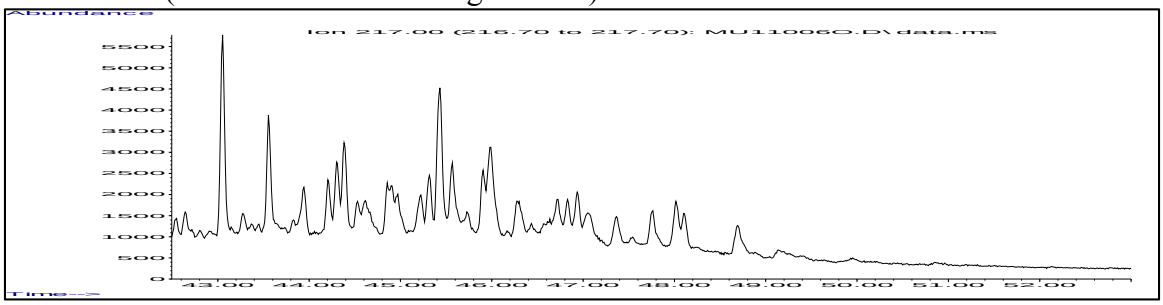


2010250-09 (Purple Cluster including MC252)

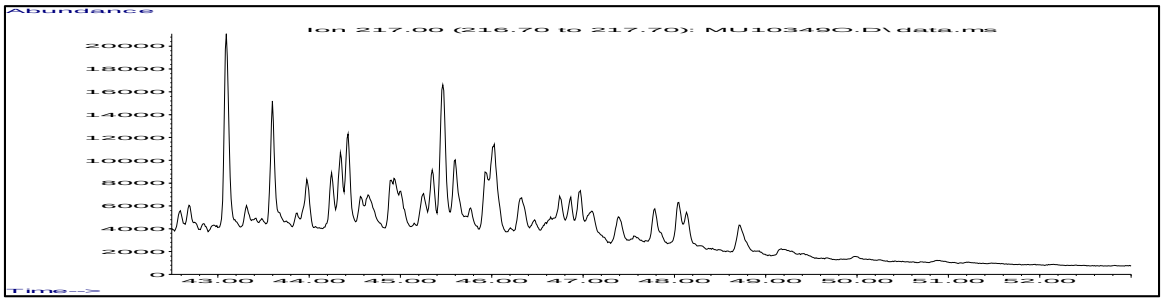


2010250-07 (Orange Cluster, Outlier)

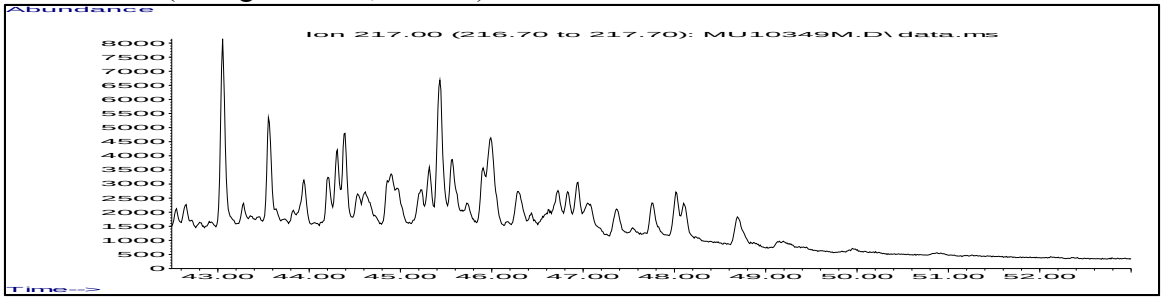

**LSU ID# 2011039**

| BLACK CLUSTER | Date Collected | Ratio Score | Pattern | Field ID |
|---|---|---|---|---|
| 2011039-29 | 2/5/2011 | 8/11 | AB | #39_RET 05 Feb 11 |
| 2011039-25 | 2/5/2011 | 9/11 | A | #35_RET 05 Feb 11 |
| 2011039-14 | 2/5/2011 | 10/11 | AB | #14_RET 05 Feb 11 |
| 2011039-08 | 2/5/2011 | 11/11 | A | #08_RET 05 Feb 11 |
| 2011039-16 | 2/5/2011 | 7/11 | B | #16_RET 05 Feb 11 |

| BLUE CLUSTER | Date Collected | Ratio Score | Pattern | Field ID |
|---|---|---|---|---|
| 2011039-27 | 2/5/2011 | 7/11 | B | #37_RET 05 Feb 11 |
| 2011039-23 | 2/5/2011 | 8/11 | B | #33_RET 05 Feb 11 |
| 2011039-24 | 2/5/2011 | 10/11 | AB | #34_RET 05 Feb 11 |
| 2011039-05 | 2/5/2011 | 10/11 | B | #05_RET 05 Feb 11 |

| GREEN CLUSTER | Date Collected | Ratio Score | Pattern | Field ID |
|---|---|---|---|---|
| 2011039-21 | 2/5/2011 | 11/11 | A | #31_RET 05 Feb 11 |
| 2011039-15 | 2/5/2011 | 11/11 | A | #15_RET 05 Feb 11 |
| 2011039-09 | 2/5/2011 | 11/11 | A | #09_RET 05 Feb 11 |

| PURPLE CLUSTER (MC252) | Date Collected | Ratio Score | Pattern | Field ID |
|---|---|---|---|---|
| 2011039-20 | 2/5/2011 | 11/11 | A | #20_RET 05 Feb 11 |
| 2011039-03 | 2/5/2011 | 11/11 | A | #03_RET 05 Feb 11 |
| 2011039-17 | 2/5/2011 | 11/11 | A | #17_RET 05 Feb 11 |
| 2011039-06 | 2/5/2011 | 11/11 | A | #06_RET 05 Feb 11 |
| 2011039-11 | 2/5/2011 | 11/11 | A | #11_RET 05 Feb 11 |
| 2011039-10 | 2/5/2011 | 11/11 | A | #10_RET 05 Feb 11 |
| 2011039-02 | 2/5/2011 | 11/11 | A | #02_RET 05 Feb 11 |
| 2011039-04 | 2/5/2011 | 11/11 | A | #04_RET 05 Feb 11 |
| 2011039-01 | 2/5/2011 | 11/11 | A | #01_RET 05 Feb 11 |

| ORANGE CLUSTER | Date Collected | Ratio Score | Pattern | Field ID |
|---|---|---|---|---|
| 2011039-18 | 2/5/2011 | 11/11 | A | #18_RET 05 Feb 11 |
| 2011039-13 | 2/5/2011 | 11/11 | AB | #13_RET 05 Feb 11 |
| 2011039-07 | 2/5/2011 | 11/11 | A | #07_RET 05 Feb 11 |
| 2011039-12 | 2/5/2011 | 11/11 | AB | #12_RET 05 Feb 11 |

2011039-16 (Black Cluster)

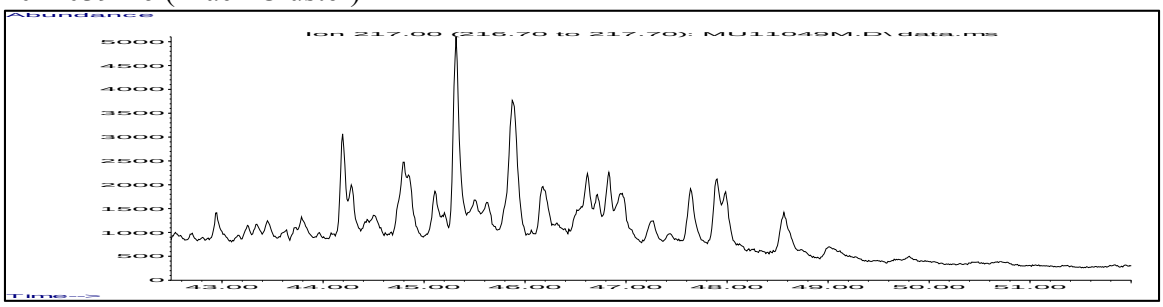


2011039-27 (Blue Cluster)

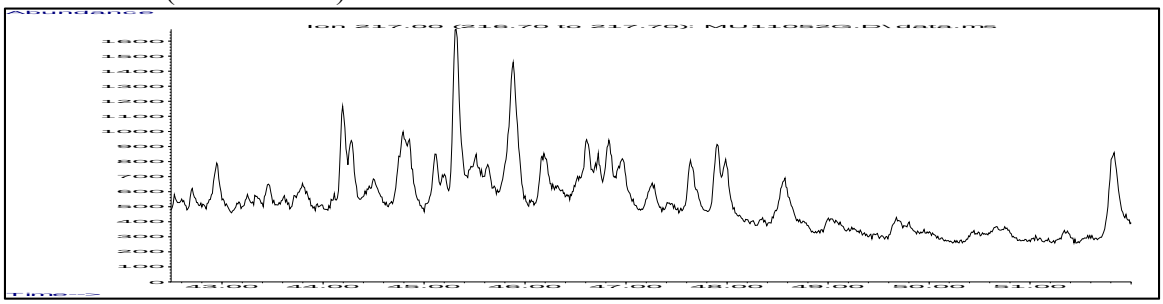


2011039-21 (Green Cluster)

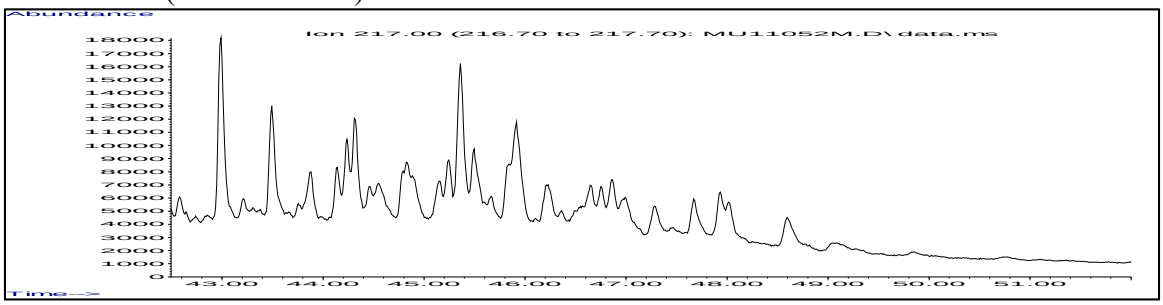


2011039-11 (Purple Cluster including MC252)

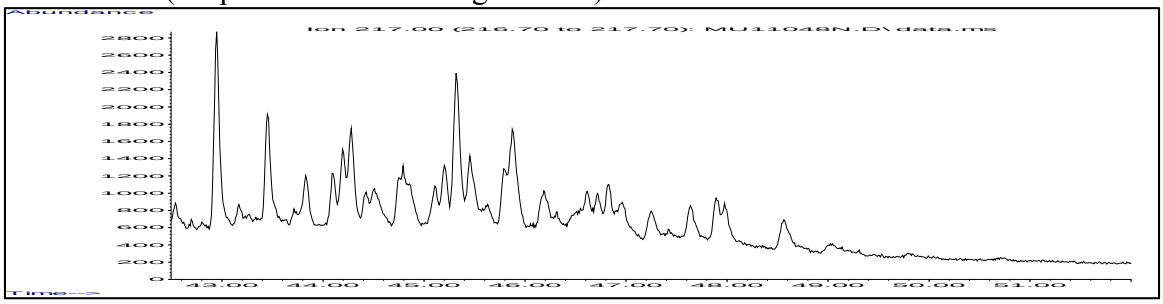


2011039-12 (Orange Cluster)

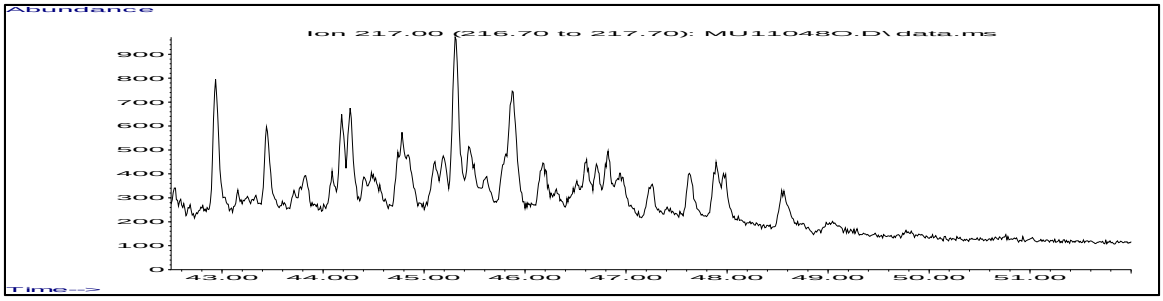

**2011**

| BLACK CLUSTER (MC252) | Date Collected | Ratio Score | Pattern | Field ID |
|---|---|---|---|---|
| 2011305-59 | 9/1/2011 | 18/20 | AB | 118, 20m_COMAR_01 Sep 2011 |
| 2011305-39 | 9/1/2011 | 20/20 | A | 115, 40m_COMAR_01 Sep 2011 |
| 2011305-28 | 9/1/2011 | 17/20 | AB | 113 Inland_COMAR_01 Sep 2011 |
| 2011305-30 | 9/1/2011 | 16/20 | AB | 114 Inland_COMAR_01 Sep 2011 |
| 2011305-24 | 9/1/2011 | 16/20 | AB | 111 Inland_COMAR_01 Sep 2011 |
| 2011305-15 | 9/1/2011 | 17/20 | AB | 107 Edge_COMAR_01 Sep 2011 |
| 2011305-50 | 9/1/2011 | 9/20 | B | 117 Edge_COMAR_01 Sep 2011 |

| BLUE CLUSTER | Date Collected | Ratio Score | Pattern | Field ID |
|---|---|---|---|---|
| 2011305-58 | 9/1/2011 | 18/20 | AB | 118 Inland_COMAR_01 Sep 2011 |
| 2011305-42 | 9/1/2011 | 16/20 | AB | 115, 100m_COMAR_01 Sep 2011 |
| 2011305-40 | 9/1/2011 | 19/20 | AB | 115, 60m_COMAR_01 Sep 2011 |
| 2011305-51 | 9/1/2011 | 11/20 | C | 117 Inland_COMAR_01 Sep 2011 |

| GREEN CLUSTER | Date Collected | Ratio Score | Pattern | Field ID |
|---|---|---|---|---|
| 2011182-62 | 7/1/2011 | 11/20 | A | 58, 10m_COMAR_01 Jul 2011 |
| 2011182-54 | 7/1/2011 | 15/20 | A | 98_COMAR_01 Jul 2011 |

| PURPLE CLUSTER | Date Collected | Ratio Score | Pattern | Field ID |
|---|---|---|---|---|
| 2011182-22 | 7/1/2011 | 17/20 | AB | 79_COMAR_01 Jul 2011 |

| ORANGE CLUSTER (MC252) | Date Collected | Ratio Score | Pattern | Field ID |
|---|---|---|---|---|
| 2011182-16 | 7/1/2011 | 19/20 | AB | 73_COMAR_01 Jul 2011 |

| RED CLUSTER | Date Collected | Ratio Score | Pattern | Field ID |
|---|---|---|---|---|
| 2011305-33 | 9/1/2011 | 7/10 | B | 2_COMAR_01 Sep 2011 |
| 2011305-14 | 9/1/2011 | 13/20 | AB | 106 Inland_COMAR_01 Sep 2011 |
| 2011182-26 | 7/1/2011 | 18/20 | AB | 81_COMAR_01 Jul 2011 |

| DK. BLUE CLUSTER | Date Collected | Ratio Score | Pattern | Field ID |
|---|---|---|---|---|
| 2011182-52 | 7/1/2011 | n/a | A | 97__July2011 |
| 2011182-23 | 7/1/2011 | 13/20 | B | 80 Edge_COMAR_01 Jul 2011 |

| | | | | |
|---|---|---|---|---|
| 2011182-21 | 7/1/2011 | 17/20 | AB | 79 Edge_COMAR_01 Jul 2011 |
| 2011182-12 | 7/1/2011 | 16/20 | AB | 59_COMAR_01 Jul 2011 |
| 2011182-11 | 7/1/2011 | 13/20 | C | 59 Edge_COMAR_01 Jul 2011 |
| 2011182-18 | 7/1/2011 | 19/20 | A | 74_COMAR_01 Jul 2011 |
| 2011182-10 | 7/1/2011 | 15/20 | AB | 58_COMAR_01 Jul 2011 |
| 2011182-15 | 7/1/2011 | 10/20 | C | 73 Edge_COMAR_01 Jul 2011 |

| GREY CLUSTER | Date Collected | Ratio Score | Pattern | Field ID |
|---|---|---|---|---|
| 2011182-79 | 7/1/2011 | 12/20 | A | 84, 90m_COMAR_01 Jul 2011 |
| 2011182-78 | 7/1/2011 | 16/20 | A | 84, 70m_COMAR_01 Jul 2011 |
| 2011182-76 | 7/1/2011 | 15/20 | A | 84, 30m_COMAR_01 Jul 2011 |
| 2011182-77 | 7/1/2011 | 18/20 | A | 84, 50m_COMAR_01 Jul 2011 |
| 2011182-75 | 7/1/2011 | 15/20 | A | 84, 10m_COMAR_01 Jul 2011 |
| 2011182-71 | 7/1/2011 | 13/20 | A | 79, 30m_COMAR_01 Jul 2011 |

2011305-39 (Black Cluster including MC252)

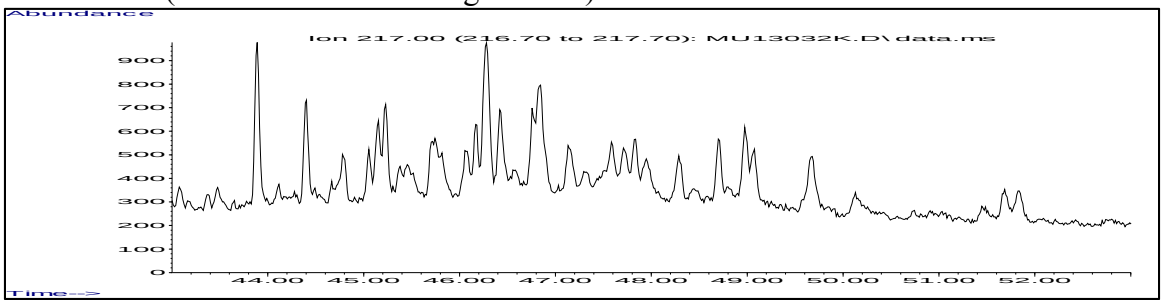


2011305-51 (Blue Cluster)

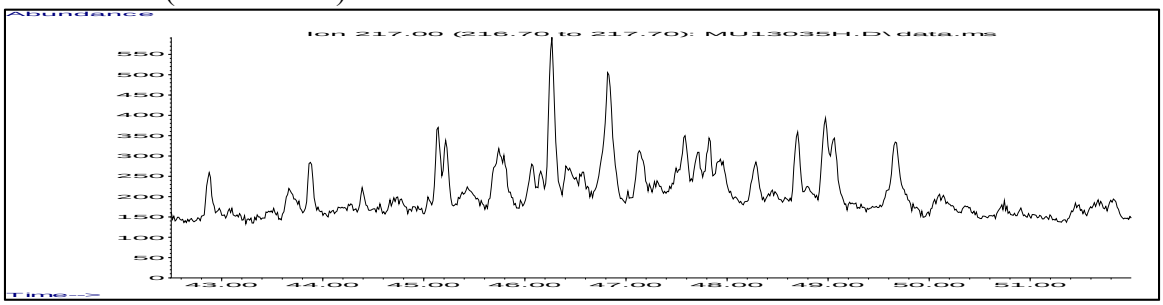


2011182-54 (Green Cluster)

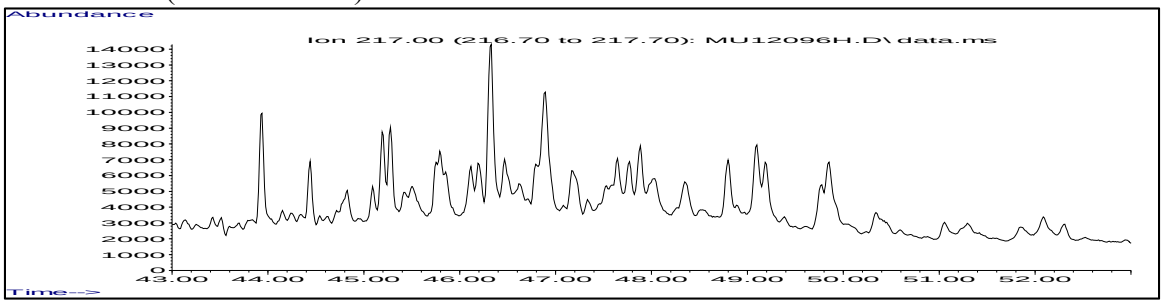

2011182-22 (Purple Cluster)

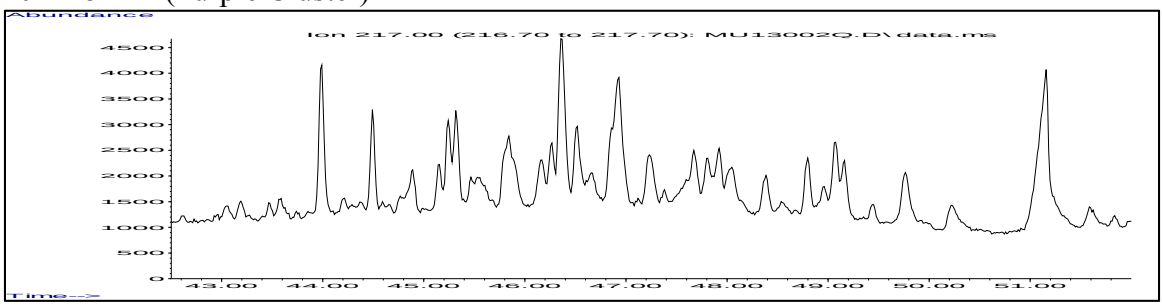


2011182-16 (Orange Cluster including MC252)

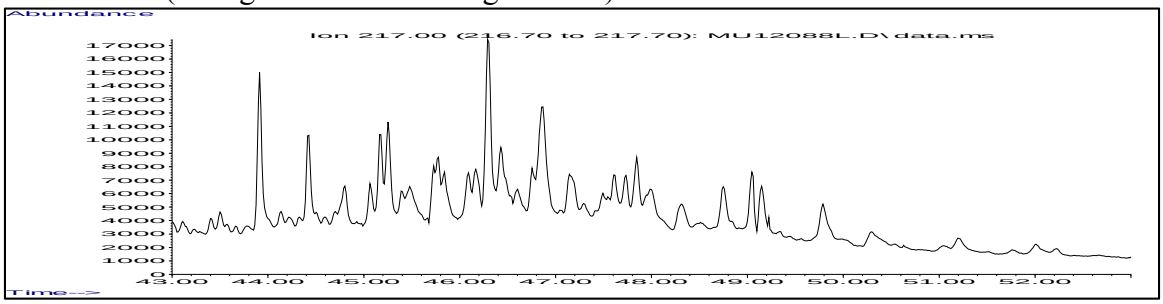


2011305-33 (Red Cluster)

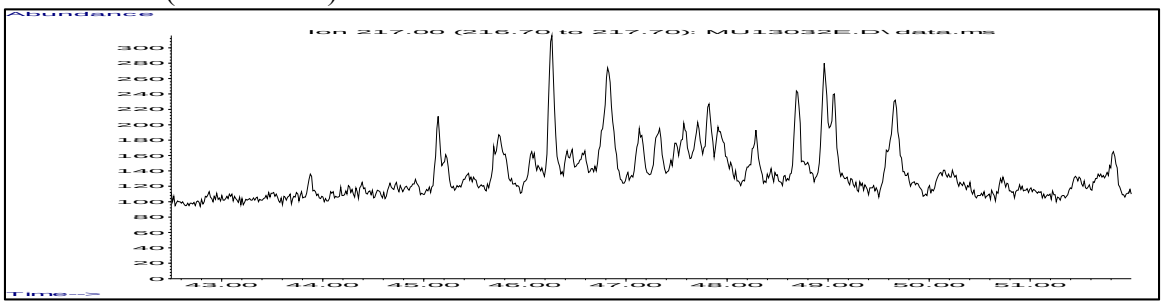


2011182-11 (Dk. Blue Cluster)

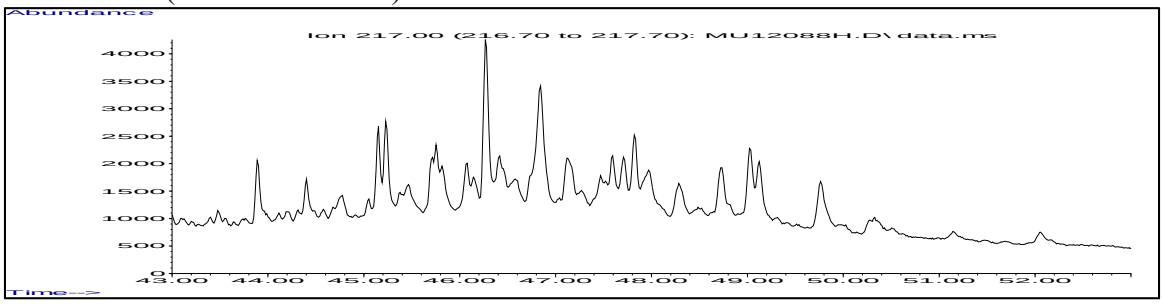


2011182-71 (Grey Cluster)

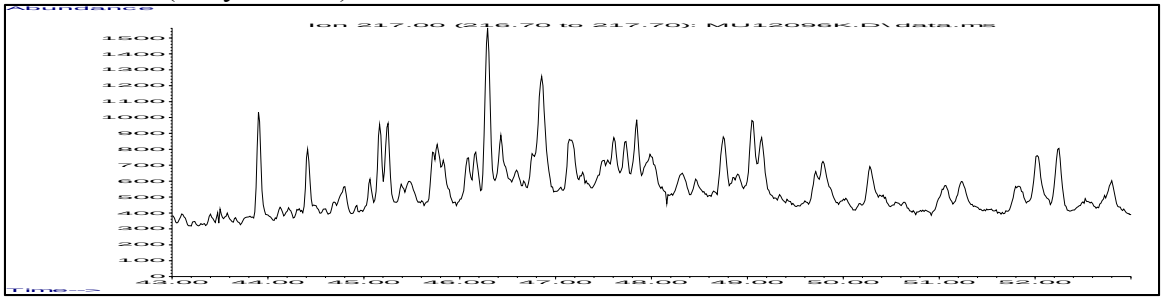

**2012**

| BLACK CLUSTER (MC252) | Date Collected | Ratio Score | Pattern | Field ID |
|---|---|---|---|---|
| 2012270-37 | 9/21/2012 | 19/20 | A | Bay Batiste_39 to 32, After Isaac |
| 2012270-23 | 9/21/2012 | 19/20 | A | Bay Batiste_17, After Isaac |
| 2012270-14 | 9/21/2012 | 17/20 | A | Bay Batiste_8, After Isaac |
| 2012270-35 | 9/21/2012 | 15/20 | AB | Bay Batiste_39, After Isaac |
| 2012270-32 | 9/21/2012 | 15/20 | AB | Bay Batiste_36, After Isaac |
| 2012270-15 | 9/21/2012 | 15/20 | AB | Bay Batiste_9, After Isaac |
| 2012270-16 | 9/21/2012 | 17/20 | A | Bay Batiste_10, After Isaac |

| BLUE CLUSTER | Date Collected | Ratio Score | Pattern | Field ID |
|---|---|---|---|---|
| 2012270-21 | 9/21/2012 | 10/20 | B | Bay Batiste_15, After Isaac |
| 2012270-18 | 9/21/2012 | 9/20 | B | Bay Batiste_12, After Isaac |
| 2012270-11 | 9/21/2012 | 10/20 | B | Bay Batiste_5, After Isaac |
| 2012270-10 | 9/21/2012 | 10/20 | B | Bay Batiste_4, After Isaac |
| 2012270-17 | 9/21/2012 | 12/20 | C | Bay Batiste_11, After Isaac |
| 2012270-09 | 9/21/2012 | 12/20 | C | Bay Batiste_3, After Isaac |
| 2012270-07 | 9/21/2012 | 15/20 | C | Bay Batiste_1, After Isaac |

| GREEN CLUSTER | Date Collected | Ratio Score | Pattern | Field ID |
|---|---|---|---|---|
| 2012270-31 | 9/21/2012 | 15/20 | C | Bay Batiste_35, After Isaac |
| 2012270-28 | 9/21/2012 | 16/20 | AB | Bay Batiste_32, After Isaac |
| 2012270-24 | 9/21/2012 | 15/20 | AB | Bay Batiste_18, After Isaac |
| 2012270-26 | 9/21/2012 | 13/20 | B | Bay Batiste_20, After Isaac |
| 2012270-25 | 9/21/2012 | 12/20 | B | Bay Batiste_19, After Isaac |
| 2012270-08 | 9/21/2012 | 12/20 | B | Bay Batiste_2, After Isaac |
| 2012150-01 | 5/29/2012 | 8/20 | B | Cat Island S1 |
| 2012216-24 | 8/3/2012 | 12/20 | C | Bay Batiste_34, Before Isaac |
| 2012216-16 | 8/3/2012 | 10/20 | B | Bay Batiste_16, Before Isaac |
| 2012216-04 | 8/3/2012 | 9/20 | B | Bay Batiste_4, Before Isaac |
| 2012216-02 | 8/3/2012 | 8/20 | B | Bay Batiste_2, Before Isaac |
| 2012216-03 | 8/3/2012 | 11/20 | B | Bay Batiste_33, Before Isaac |
| 2012216-15 | 8/3/2012 | 9/20 | B | Bay Batiste_15, Before Isaac |

| PURPLE CLUSTER (MC252) | Date Collected | Ratio Score | Pattern | Field ID |
|---|---|---|---|---|
| 2012270-20 | 9/21/2012 | 19/20 | A | Bay Batiste_14, After Isaac |

| | | | | |
|---|---|---|---|---|
| 2012180-22 | 6/28/2012 | 12/20 | B | PS-04 Inland |
| 2012180-21 | 6/28/2012 | 12/20 | B | PS-04 Edge |
| 2012180-20 | 6/28/2012 | 13/20 | AB | PS-03 Inland |
| 2012180-16 | 6/28/2012 | 14/20 | AB | PS-01 Inland |

| ORANGE CLUSTER (OUTLIER) | Date Collected | Ratio Score | Pattern | Field ID |
|---|---|---|---|---|
| 2012150-03 | 5/29/2012 | 9/20 | B | Cat Island N1 |

| RED CLUSTER (MC252) | Date Collected | Ratio Score | Pattern | Field ID |
|---|---|---|---|---|
| 2012216-29 | 8/3/2012 | 14/20 | AB | Bay Batiste_39, Before Isaac |
| 2012216-26 | 8/3/2012 | 16/20 | AB | Bay Batiste_36, Before Isaac |
| 2012216-25 | 8/3/2012 | 14/20 | AB | Bay Batiste_35, Before Isaac |
| 2012216-18 | 8/3/2012 | 12/20 | AB | Bay Batiste_18, Before Isaac |
| 2012216-09 | 8/3/2012 | 19/20 | A | Bay Batiste_9, Before Isaac |
| 2012216-10 | 8/3/2012 | 19/20 | A | Bay Batiste_10, Before Isaac |
| 2012216-08 | 8/3/2012 | 19/20 | A | Bay Batiste_8, Before Isaac |

| DK BLUE CLUSTER | Date Collected | Ratio Score | Pattern | Field ID |
|---|---|---|---|---|
| 2012216-28 | 8/3/2012 | 8/20 | B | Bay Batiste_38, Before Isaac |
| 2012216-27 | 8/3/2012 | 9/20 | B | Bay Batiste_37, Before Isaac |
| 2012216-14 | 8/3/2012 | 8/20 | B | Bay Batiste_14, Before Isaac |
| 2012216-21 | 8/3/2012 | 9/20 | B | Bay Batiste_32, Before Isaac |
| 2012216-12 | 8/3/2012 | 8/20 | B | Bay Batiste_12, Before Isaac |
| 2012216-20 | 8/3/2012 | 11/20 | B | Bay Batiste_20, Before Isaac |
| 2012216-19 | 8/3/2012 | 12/20 | C | Bay Batiste_19, Before Isaac |
| 2012216-17 | 8/3/2012 | 13/20 | B | Bay Batiste_17, Before Isaac |
| 2012216-01 | 8/3/2012 | 11/20 | B | Bay Batiste_1, Before Isaac |
| 2012180-15 | 6/28/2012 | 19/20 | A | PS-01 Edge |
| 2012216-13 | 8/3/2012 | 9/20 | B | Bay Batiste_13, Before Isaac |

2012270-14 (Black Cluster including MC252)

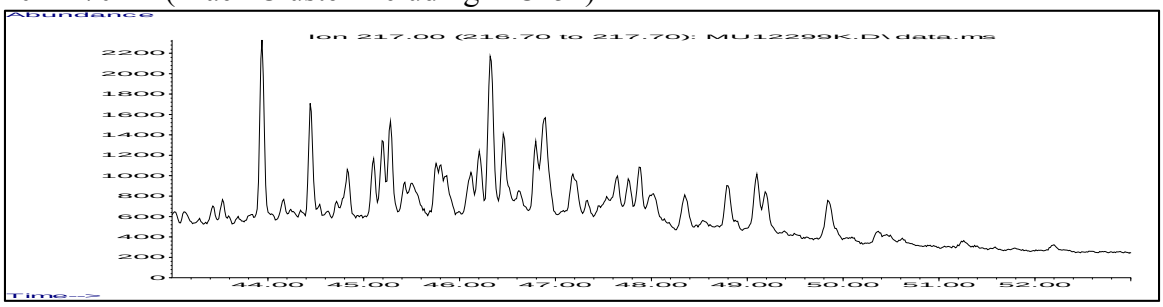


2012270-09 (Blue Cluster)

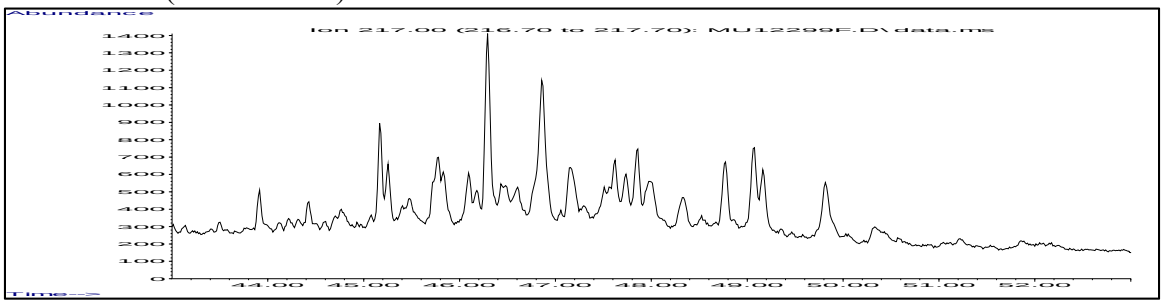


2012270-28 (Green Cluster)

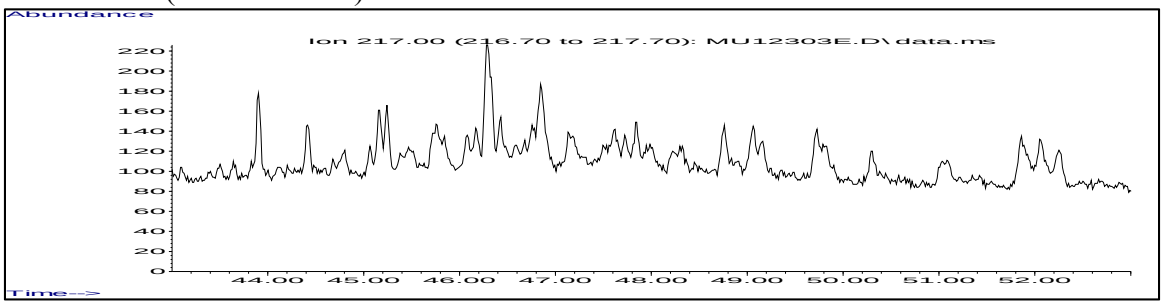


2012180-20 (Purple Cluster including MC252)

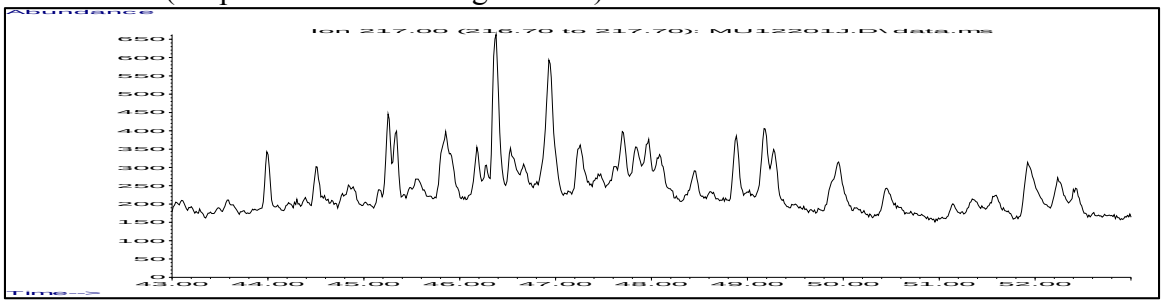


2012150-03 (Orange Cluster, Outlier)

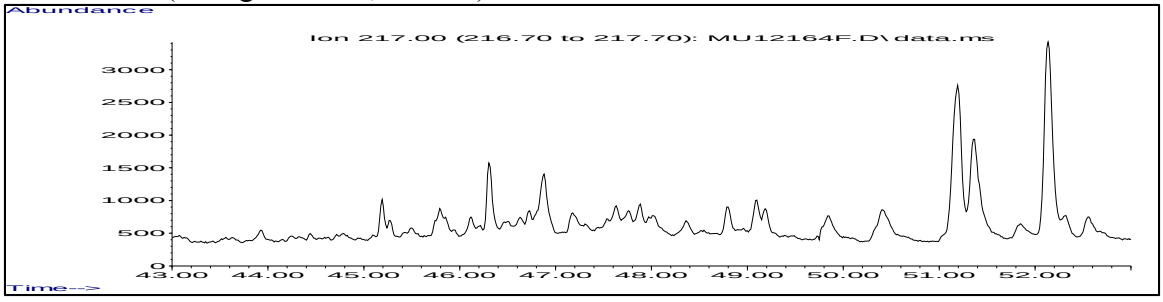

2012216-09 (Red Cluster including MC252)

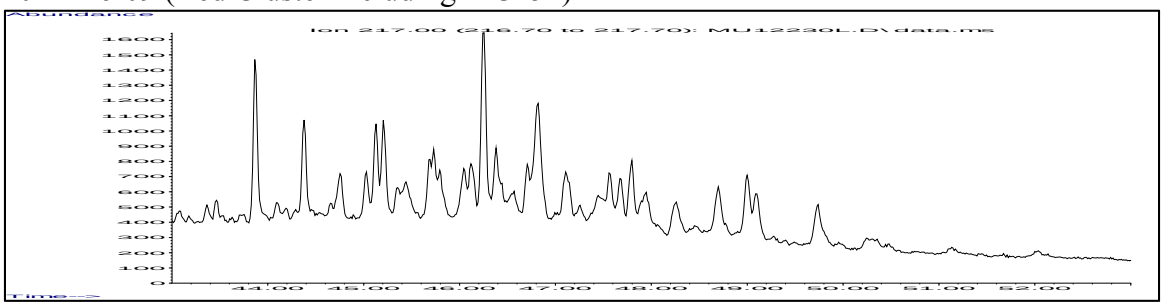


2012180-15 (Dark Blue Cluster)

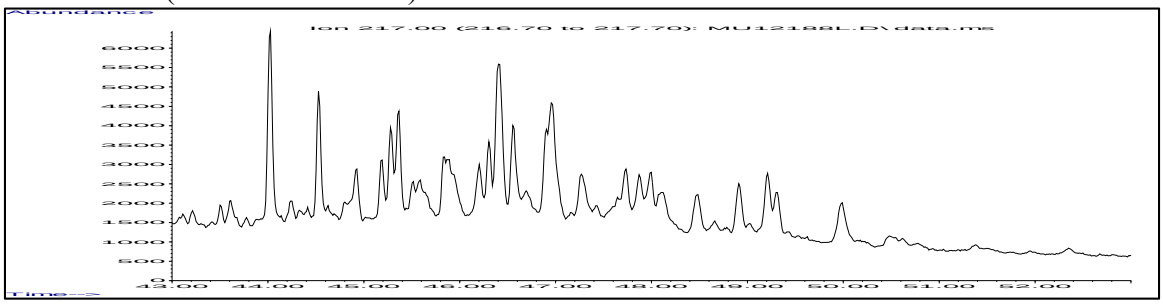

**2013 - GT**

| BLACK CLUSTER | Date Collected | Ratio Score | Pattern | Field ID |
|---|---|---|---|---|
| 2013289-36 | 10/1/2013 | 18/20 | A | PS-07 Inland, Oct 2013 |
| 2013289-32 | 10/1/2013 | 11/20 | AB | PS-06 Edge, Oct 2013 |
| 2013289-27 | 10/1/2013 | 13/20 | AB | PS-03A Inland, Oct 2013 |

| BLUE CLUSTER | Date Collected | Ratio Score | Pattern | Field ID |
|---|---|---|---|---|
| 2013289-15 | 10/1/2013 | n/a | B | GI-02 Inland, Oct 2013 |
| 2013289-12 | 10/1/2013 | 14/20 | AB | GI-01 Inland, Oct 2013 |
| 2013289-02 | 10/1/2013 | 8/20 | B | CO-03 Edge, Oct 2013 |
| 2013289-11 | 10/1/2013 | 9/20 | B | GI-01 Edge, Oct 2013 |

| GREEN CLUSTER (MC252) | Date Collected | Ratio Score | Pattern | Field ID |
|---|---|---|---|---|
| NO SAMPLES IN CLUSTER | | | | |

2013289-27 (Black Cluster)

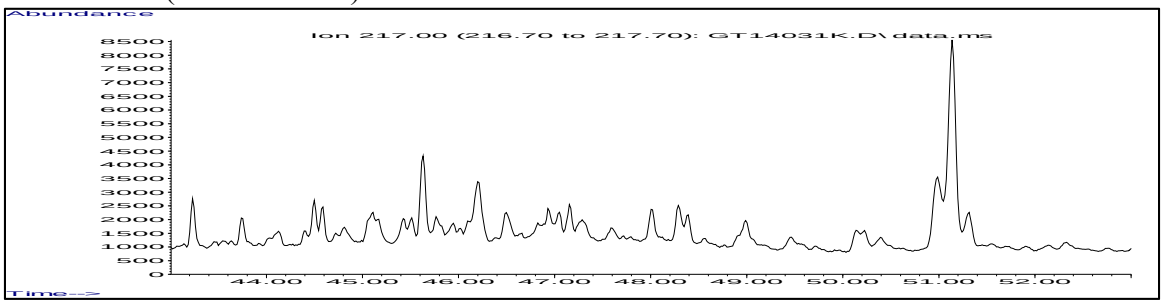


2013289-02 (Blue Cluster)

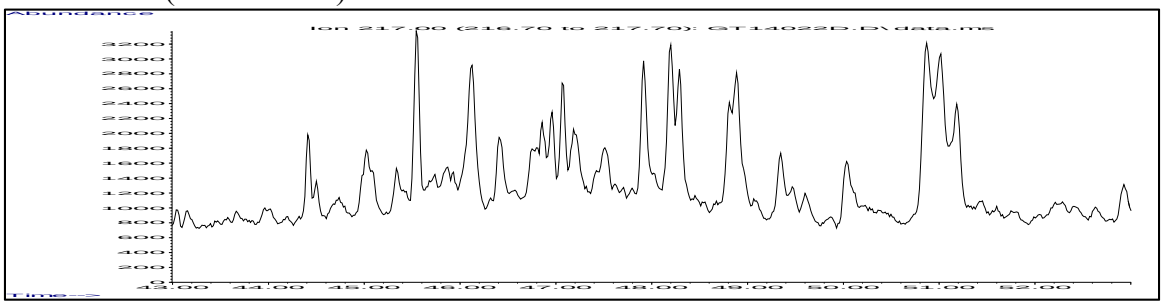

**2013 - MU**

| BLACK CLUSTER | Date Collected | Ratio Score | Pattern | Field ID |
|---|---|---|---|---|
| 2013212-09 | 6/27/2013 | 16/20 | AB | MK 6A 27 June 2013 |
| 2013176-05 | 5/2/2013 | 10/20 | B | GI-02 Edge Marsh, May 2013 |
| 2013156-29 | 5/23/2013 | 12/20 | AB | PS-07 Edge, May2013 |
| 2013156-20 | 5/23/2013 | 14/20 | AB | PS-03A Edge, May2013 |
| 2013156-14 | 5/23/2013 | 8/20 | B | CO-03Edge, May2013 |
| 2013175-24 | 6/20/2013 | 9/20 | B | 34_20 June 2013 |
| 2013156-27 | 5/23/2013 | 14/20 | AB | PS-06 Inland, May2013 |
| 2013156-25 | 5/23/2013 | 13/20 | B | PS-06 Edge Wat Bot, May2013 |
| 2013156-26 | 5/23/2013 | 12/20 | B | PS-06 Edge, May2013 |
| 2013175-20 | 6/20/2013 | 9/20 | B | 20_20 June 2013 |
| 2013156-21 | 5/23/2013 | 16/20 | AB | CO-03 Inland, May 2013 |
| 2013175-19 | 6/20/2013 | 10/20 | B | 19_20 June 2013 |
| 2013156-17 | 5/23/2013 | 9/20 | B | CO-04 Edge, May2013 |
| 2013156-15 | 5/23/2010 | 5/20 | B | CO-03 Inland, May 2013 |

| BLUE CLUSTER | Date Collected | Ratio Score | Pattern | Field ID |
|---|---|---|---|---|
| 2013175-18 | 6/20/2013 | 7/20 | B | 18_20 June 2013 |
| 2013175-14 | 6/20/2013 | 8/20 | B | 14_20 June 2013 |
| 2013175-04 | 6/20/2013 | 9/20 | B | 4_20 June 2013 |
| 2013156-05 | 5/23/2013 | 11/20 | B | Old 47 5 Edge, May2013 |
| 2013175-16 | 6/20/2013 | 7/20 | B | 16_20 June 2013 |
| 2013175-06 | 6/20/2013 | 16/20 | AB | 6_20 June 2013 |
| 2013156-02 | 5/23/2013 | 14/20 | B | 47a fish site, May2013 |

| GREEN CLUSTER (MC252) | Date Collected | Ratio Score | Pattern | Field ID |
|---|---|---|---|---|
| 2013212-08 | 6/27/2013 | 17/20 | AB | MK 5A 27 June 2013 |
| 2013212-07 | 6/27/2013 | 16/20 | AB | MK 4A 27 June 2013 |

| PURPLE CLUSTER | Date Collected | Ratio Score | Pattern | Field ID |
|---|---|---|---|---|
| 2013175-30 | 6/20/2013 | 13/20 | C | 40_20 June 2013 |
| 2013175-29 | 6/20/2013 | 14/20 | AB | 39_20 June 2013 |
| 2013175-23 | 6/20/2013 | 9/20 | C | 33_20 June 2013 |
| 2013175-25 | 6/20/2013 | 17/20 | AB | 35_20 June 2013 |
| 2013156-30 | 5/23/2013 | 15/20 | AB | CO-03 Inland, May 2013 |
| 2013175-28 | 6/20/2013 | 9/20 | B | 38_20 June 2013 |

| | | | | |
|---|---|---|---|---|
| 2013175-27 | 6/20/2013 | 10/20 | B | 37_20 June 2013 |
| 2013175-21 | 6/20/2013 | 8/20 | B | 31_20 June 2013 |
| 2013175-26 | 6/20/2013 | 10/20 | B | 36_20 June 2013 |

| ORANGE CLUSTER | Date Collected | Ratio Score | Pattern | Field ID |
|---|---|---|---|---|
| 2013175-17 | 6/20/2013 | 15/20 | AB | 17_20 June 2013 |
| 2013175-11 | 6/20/2013 | 13/20 | C | 11_20 June 2013 |
| 2013175-08 | 6/20/2013 | 14/20 | AB | 8_20 June 2013 |
| 2013175-15 | 6/20/2013 | 7/20 | B | 15_20 June 2013 |
| 2013175-13 | 6/20/2013 | 8/20 | B | 13_20 June 2013 |
| 2013175-12 | 6/20/2013 | 9/20 | B | 12_20 June 2013 |
| 2013175-05 | 6/20/2013 | 10/20 | B | 5_20 June 2013 |
| 2013175-01 | 6/20/2013 | 12/20 | B | 1_20 June 2013 |
| 2013175-02 | 6/20/2013 | 10/20 | B | 2_20 June 2013 |
| 2013175-09 | 6/20/2013 | 13/20 | B | 9_20 June 2013 |

2013156-25 (Black Cluster)

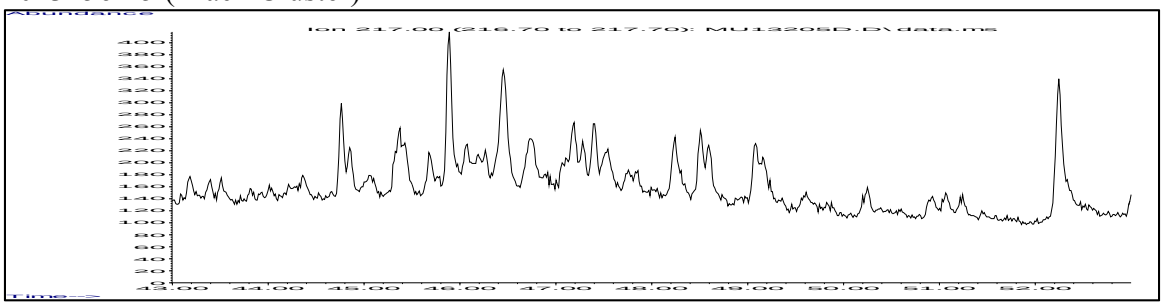


2013175-04 (Blue Cluster)

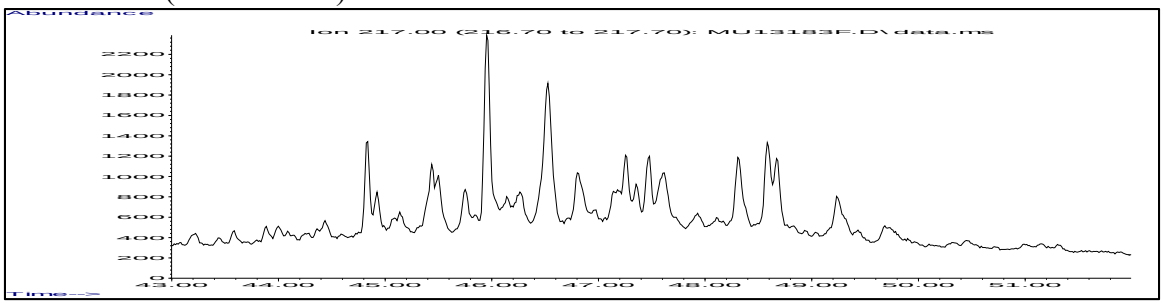

2013212-08 (Green Cluster including MC252)

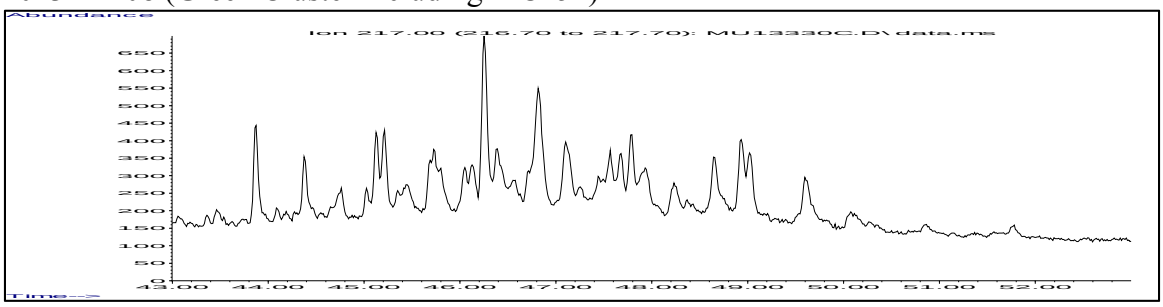


2013175-30 (Purple Cluster)

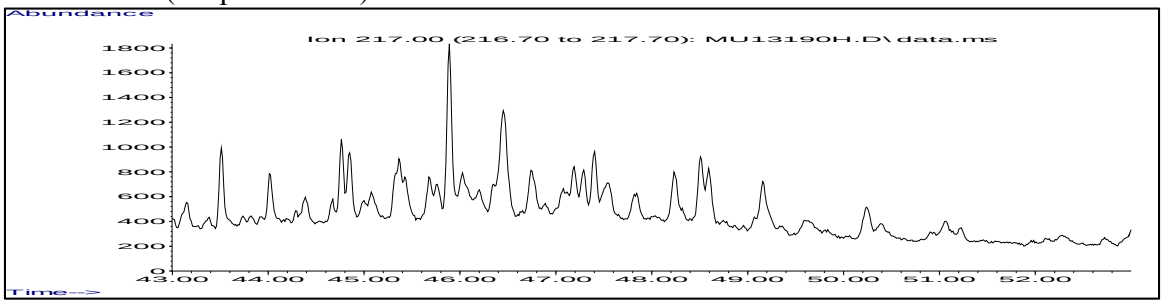


2013175-09 (Orange Cluster)

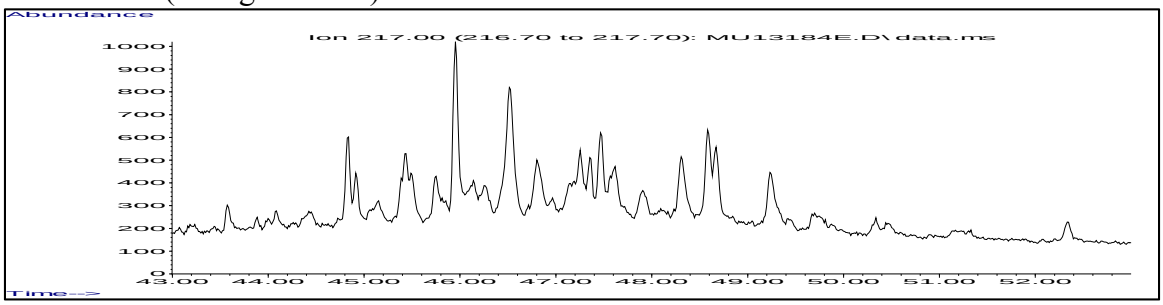

**2014 - GT**

| BLACK CLUSTER | Date Collected | Ratio Score | Pattern | Field ID |
|---|---|---|---|---|
| 2014227-59 | 8/14/2014 | 13/20 | C | 39_Aug 2014 |
| 2014227-53 | 8/14/2014 | 10/20 | B | 33_Aug 2014 |
| 2014227-51 | 8/14/2014 | 10/20 | B | 31_Aug 2014 |
| 2014227-52 | 8/14/2014 | 14/20 | AB | 32_Aug 2014 |
| 2014227-47 | 8/14/2014 | 12/20 | B | 17_Aug 2014 |
| 2014227-44 | 8/14/2014 | 8/20 | B | 14_Aug 2014 |
| 2014227-45 | 8/14/2014 | 14/20 | B | 15_Aug 2014 |
| 2014227-42 | 8/14/2014 | 11/20 | B | 12_Aug 2014 |
| 2014227-43 | 8/14/2014 | 8/20 | B | 13_Aug 2014 |

| BLUE CLUSTER | Date Collected | Ratio Score | Pattern | Field ID |
|---|---|---|---|---|
| 2014227-56 | 8/14/2014 | 13/20 | B | 36_Aug 2014 |
| 2014227-49 | 8/14/2014 | 9/20 | B | 19_Aug 2014 |
| 2014227-48 | 8/14/2014 | 9/20 | B | 18_Aug 2014 |
| 2014227-55 | 8/14/2014 | 12/20 | C | 35_Aug 2014 |
| 2014227-50 | 8/14/2014 | 12/20 | B | 20_Aug 2014 |
| 2014227-24 | 2/16/2014 | 15/20 | B | 34_Feb 2014 |
| 2014227-06 | 2/16/2014 | 16/20 | AB | 6_Feb 2014 |
| 2014227-01 | 2/16/2014 | 15/20 | AB | 1_Feb 2014 |

| GREEN CLUSTER | Date Collected | Ratio Score | Pattern | Field ID |
|---|---|---|---|---|
| 2014227-39 | 8/14/2014 | 12/20 | C | 39_Aug 2014 |
| 2014227-25 | 2/16/2014 | 10/20 | B | 35_Feb 2014 |
| 2014227-29 | 2/16/2014 | 13/20 | B | 39_Feb 2014 |
| 2014227-23 | 2/16/2014 | 13/20 | B | 33_Feb 2014 |
| 2014227-19 | 2/16/2014 | 11/20 | B | 19_Feb 2014 |
| 2014227-17 | 2/16/2014 | 10/20 | B | 17_Feb 2014 |
| 2014227-05 | 2/16/2014 | 13/20 | B | 5_Feb 2014 |
| 2014227-13 | 2/16/2014 | 11/20 | B | 13_Feb 2014 |
| 2014227-09 | 2/16/2014 | 15/20 | B | 9_Feb 2014 |
| 2014227-02 | 2/16/2014 | 11/20 | B | 2_Feb 2014 |

| PURPLE CLUSTER | Date Collected | Ratio Score | Pattern | Field ID |
|---|---|---|---|---|
| 2014227-41 | 8/14/2014 | 9/20 | B | 11_Aug 2014 |
| 2014227-26 | 2/16/2014 | 14/20 | C | 36_Feb 2014 |

| | | | | |
|---|---|---|---|---|
| 2014227-28 | 2/16/2014 | 11/20 | B | 38_Feb 2014 |
| 2014227-40 | 8/14/2014 | 16/20 | AB | 10_Aug 2014 |
| 2014227-27 | 2/16/2014 | 10/20 | B | 37_Feb 2014 |
| 2014227-21 | 2/16/2014 | 13/20 | C | 31_Feb 2014 |
| 2014227-11 | 2/16/2014 | 13/20 | B | 11_Feb 2014 |
| 2014227-10 | 2/16/2014 | 15/20 | AB | 10_Feb 2014 |
| 2014227-18 | 2/16/2014 | 10/20 | B | 18_Feb 2014 |
| 2014227-14 | 2/16/2014 | 8/20 | B | 14_Feb 2014 |
| 2014227-15 | 2/16/2014 | 10/20 | B | 15_Feb 2014 |
| 2014227-12 | 2/16/2014 | 12/20 | B | 12_Feb 2014 |

| ORANGE CLUSTER (MC252) | Date Collected | Ratio Score | Pattern | Field ID |
|---|---|---|---|---|
| 2014227-08 | 2/16/2014 | 19/20 | A | 8_Feb 2014 |

2014227-53 (Black Cluster)

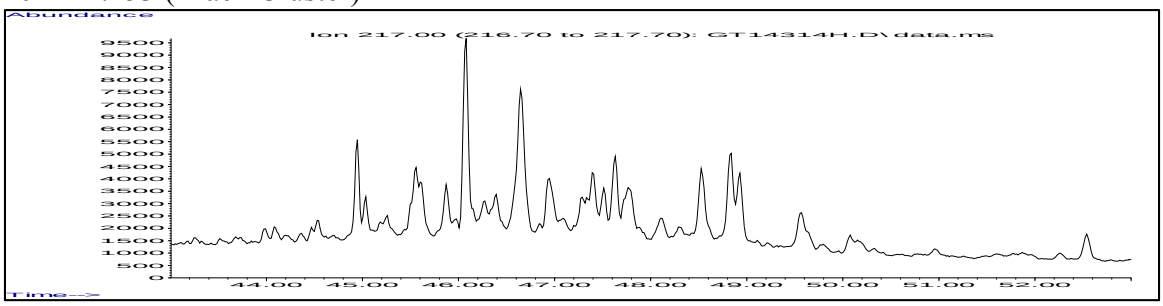


2014227-50 (Blue Cluster)

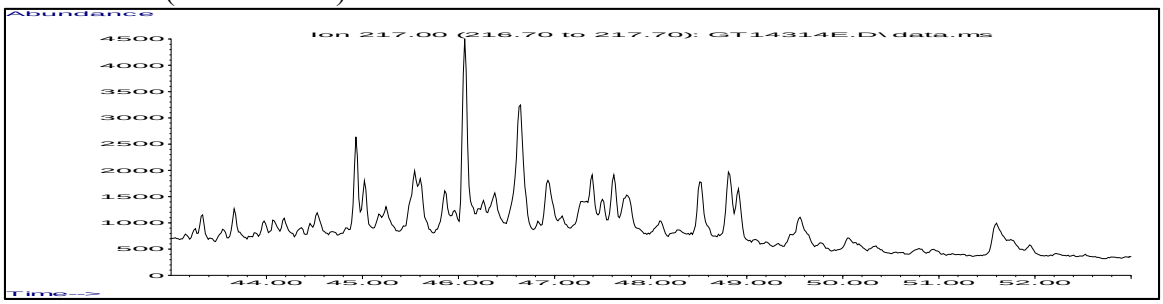


2014227-29 (Green Cluster)

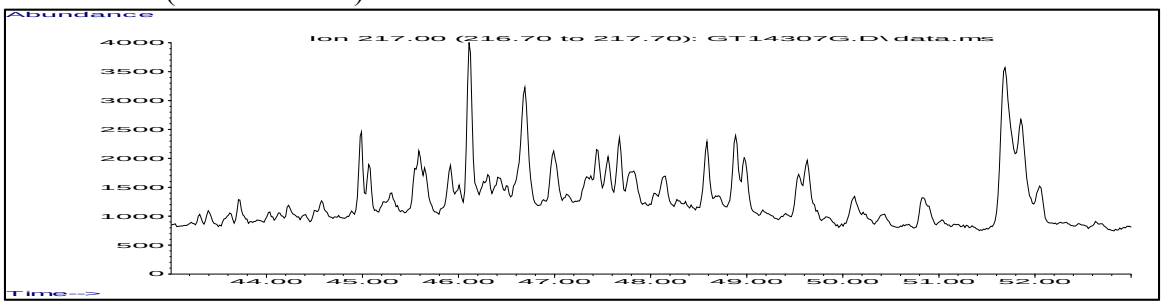

2014227-11 (Purple Cluster)

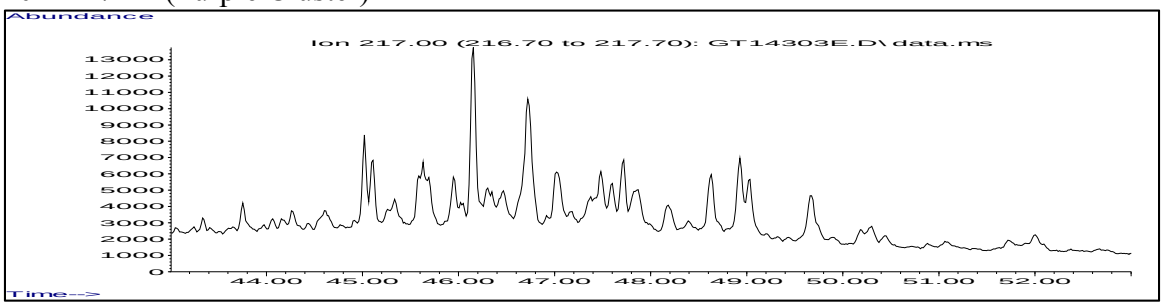


2014227-08 (Orange Cluster including MC252)

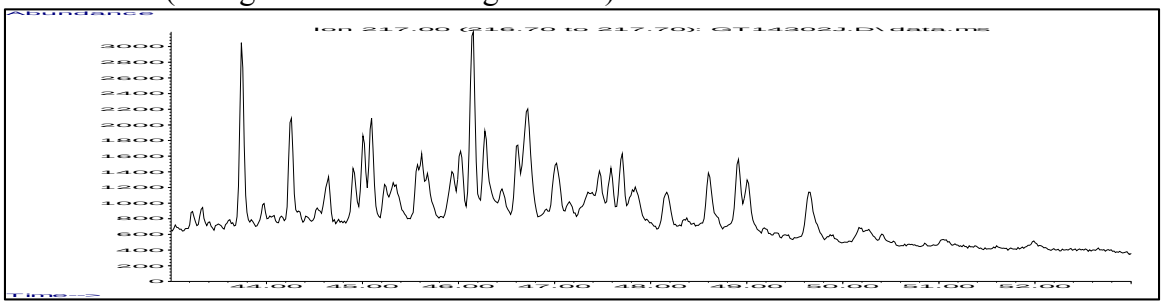

**2014 - MU**

| BLACK CLUSTER | Date Collected | Ratio Score | Pattern | Field ID |
|---|---|---|---|---|
| 2014276-29 | 10/3/2014 | 11/20 | AB | CO-04 Edge 1m, Fall 2014 |
| 2014153-05 | 5/1/2014 | 10/20 | C | CO-03 10m, May 2014 |
| 2014153-04 | 5/1/2014 | 11/20 | B | CO-03 1m, May 2014 |
| 2014276-09 | 10/3/2014 | 16/20 | AB | PS-06 Inland 10m, Fall 2014 |
| 2014276-03 | 10/3/2014 | 16/20 | AB | PS-03A Inland 10m, Fall 2014 |
| 2014181-04 | 5/1/2014 | 15/20 | AB | GI-01 10m, May 2014 |
| 2014181-01 | 5/1/2014 | 11/20 | C | GI-01 1m, May 2014 |

| BLUE CLUSTER | Date Collected | Ratio Score | Pattern | Field ID |
|---|---|---|---|---|
| 2014276-26 | 10/3/2014 | 9/20 | C | CO-03 Edge 1m, Fall 2014 |
| 2014276-25 | 10/3/2014 | 13/20 | C | CO-03 Wat Bot, Fall 2014 |
| 2014276-14 | 10/3/2014 | 10/20 | C | GI-01 Edge 1m, fall 2014 |
| 2014276-12 | 10/3/2014 | 15/20 | AB | PS-07 Inland 10m, Fall 2014 |
| 2014276-15 | 10/3/2014 | 14/20 | AB | GI-01 Inland 10m, Fall 2014 |
| 2014276-07 | 10/3/2014 | 16/20 | AB | PS-06 Wat Bot, Fall 2014 |
| 2014276-08 | 10/3/2014 | 12/20 | B | PS-06 Edge 1m, Fall 2014 |
| 2014153-22 | 5/1/2014 | 12/20 | C | PS-03A 1m, May 2014 |

| GREEN CLUSTER | Date Collected | Ratio Score | Pattern | Field ID |
|---|---|---|---|---|
| 2014276-17 | 10/3/2014 | 13/20 | C | GI-02 Edge 1m, Fall 2014 |
| 2014181-02 | 5/1/2014 | 14/20 | AB | GI-01 10m, May 2014 |

| PURPLE CLUSTER (MC252) | Date Collected | Ratio Score | Pattern | Field ID |
|---|---|---|---|---|
| NO SAMPLES IN CLUSTER | | | | |

2014153-04 (Black Cluster)

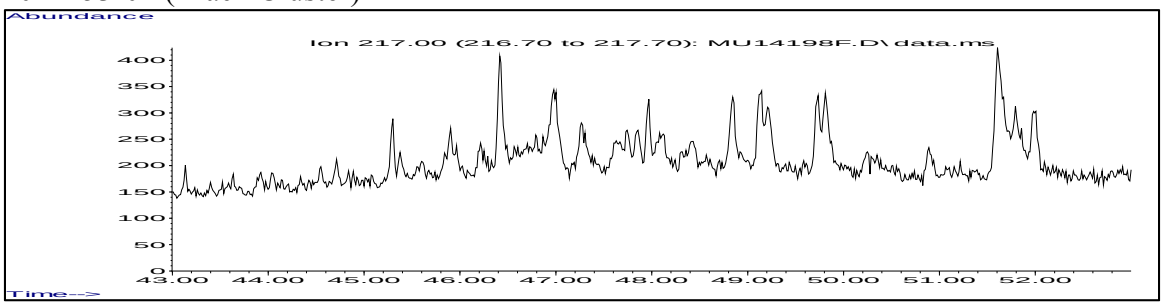

2014276-25 (Blue Cluster)

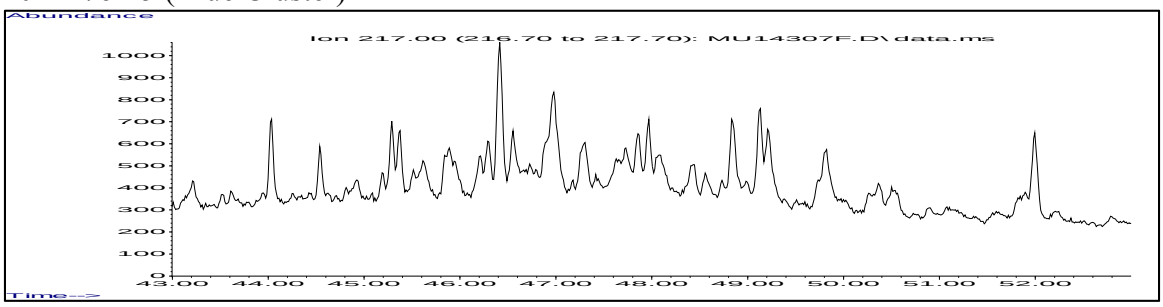


2014276-17 (Green Cluster)

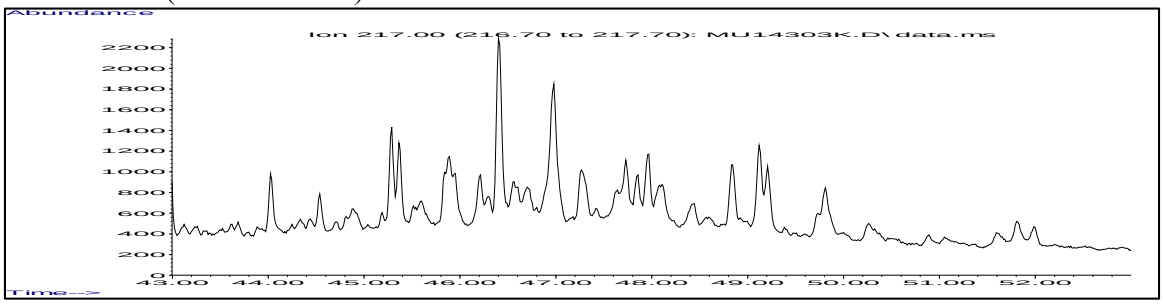

**2015 - GT**

| BLACK CLUSTER | Date Collected | Ratio Score | Pattern | Field ID |
|---|---|---|---|---|
| 2015134-36 | 5/14/2015 | 14/20 | AB | May 2015, PS-07 10m |
| 2015042-28 | 2/7/2015 | 12/20 | B | Bay Batiste-38 |
| 2015042-27 | 2/7/2015 | 13/20 | B | Bay Batiste-37 |
| 2015134-05 | 5/14/2015 | 10/20 | B | May 2015, CO-04 1m |
| 2015134-02 | 5/14/2015 | 7/20 | B | May 2015, CO-03 1m |
| 2015134-01 | 5/14/2015 | 10/20 | C | May 2015, CO-03 Wat Bot |

| BLUE CLUSTER | Date Collected | Ratio Score | Pattern | Field ID |
|---|---|---|---|---|
| 2015042-25 | 2/7/2015 | 9/20 | B | Bay Batiste-35 |
| 2015042-24 | 2/7/2015 | 13/20 | B | Bay Batiste-34 |
| 2015042-20 | 2/7/2015 | 9/20 | B | Bay Batiste-20 |
| 2015042-22 | 2/7/2015 | 13/20 | C | Bay Batiste-32 |
| 2015042-17 | 2/7/2015 | 9/20 | B | Bay Batiste-17 |
| 2015042-11 | 2/7/2015 | 8/20 | B | Bay Batiste-11 |
| 2015042-10 | 2/7/2015 | 11/20 | B | Bay Batiste-10 |
| 2015042-09 | 2/7/2015 | 11/20 | B | Bay Batiste-9 |
| 2015042-18 | 2/7/2015 | 9/20 | B | Bay Batiste-18 |
| 2015042-13 | 2/7/2015 | 9/20 | B | Bay Batiste-13 |

| GREEN CLUSTER | Date Collected | Ratio Score | Pattern | Field ID |
|---|---|---|---|---|
| 2015134-14 | 5/14/2015 | 14/20 | C | May 2015, GI-02 1m |
| 2015042-26 | 2/7/2015 | 8/20 | B | Bay Batiste-36 |
| 2015042-29 | 2/7/2015 | 10/20 | B | Bay Batiste-39 |

| PURPLE CLUSTER (MC252) | Date Collected | Ratio Score | Pattern | Field ID |
|---|---|---|---|---|

NO SAMPLES IN THIS CLUSTER

| ORANGE CLUSTER | Date Collected | Ratio Score | Pattern | Field ID |
|---|---|---|---|---|
| 2015134-31 | 5/14/2015 | 9/20 | B | May 2015, PS-06 Wat Bot |
| 2015134-11 | 5/14/2015 | 9/20 | B | May 2015, GI-01 1m |
| 2015042-21 | 2/7/2015 | 11/20 | B | Bay Batiste-31 |
| 2015042-12 | 2/7/2015 | 13/20 | B | Bay Batiste-12 |
| 2015042-08 | 2/7/2015 | 11/20 | B | Bay Batiste-8 |
| 2015134-12 | 5/14/2015 | 13/20 | AB | May 2015, GI-01 10m |

| | | | | |
|---|---|---|---|---|
| 2015134-10 | 5/14/2015 | 10/20 | AB | May 2015, GI-01 Wat Bot |
| 2015042-02 | 2/7/2015 | 13/20 | B | Bay Batiste-2 |
| 2015042-01 | 2/7/2015 | 14/20 | C | Bay Batiste-1 |

| RED CLUSTER (OUTLIER) | Date Collected | Ratio Score | Pattern | Field ID |
|---|---|---|---|---|
| 2015042-16 | 2/7/2015 | 10/20 | B | Bay Batiste-16 |
| 2015042-14 | 2/7/2015 | 15/20 | AB | Bay Batiste-14 |
| 2015042-15 | 2/7/2015 | 11/20 | B | Bay Batiste-15 |

2015042-28 (Black Cluster)

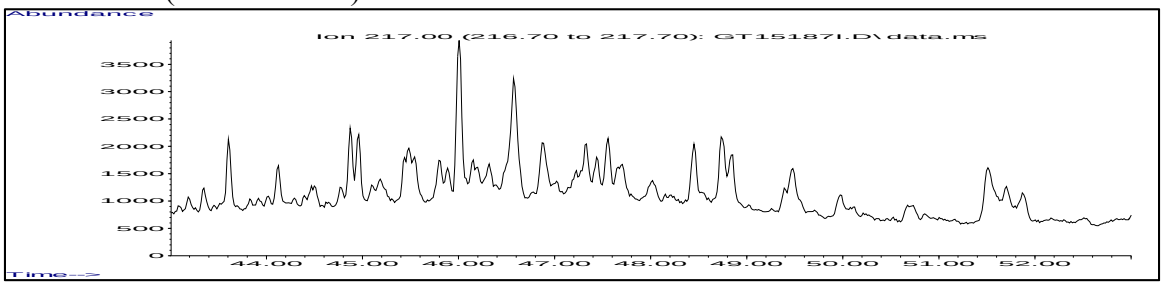


2015042-11 (Blue Cluster)

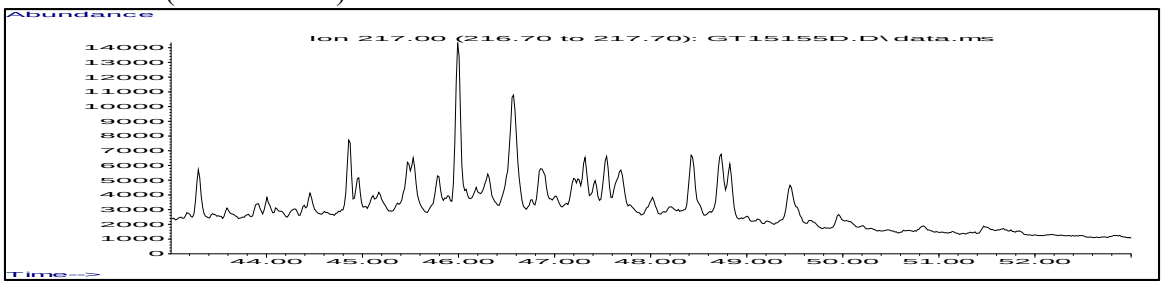


2015134-14 (Green Cluster)

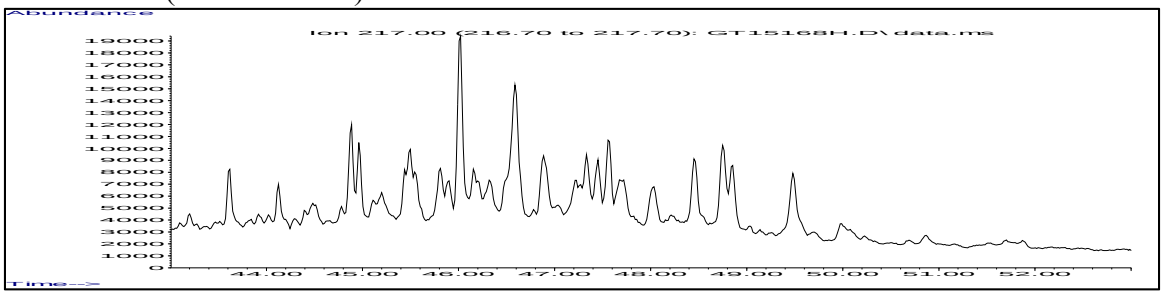


2015042-12 (Orange Cluster)

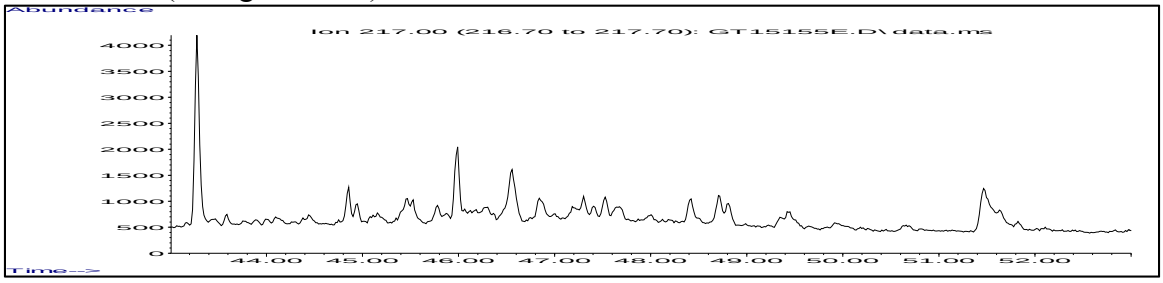

2015042-16 (Red Cluster, Outliers)

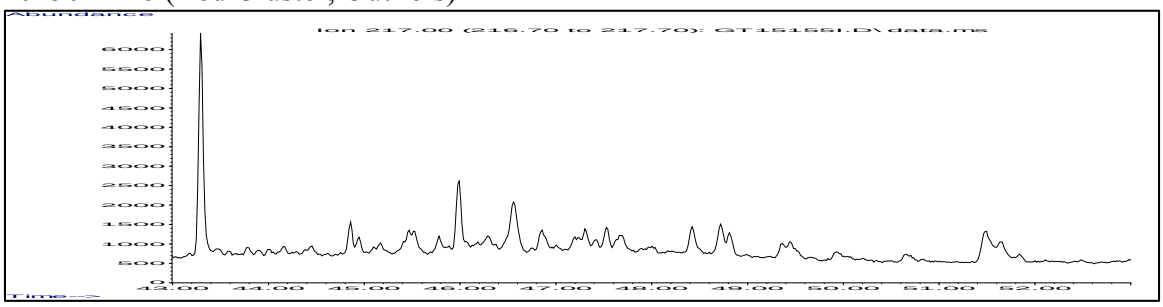

**2015 – MU**

| BLACK CLUSTER | Date Collected | Ratio Score | Pattern | Field ID |
|---|---|---|---|---|
| 2015342-12 | 12/8/2015 | 14/20 | C | PS-07 10m, Dec2015 |
| 2015342-11 | 12/8/2015 | 12/20 | B | PS-07 1m, Dec2015 |
| 2015342-03 | 12/8/2015 | 17/20 | AB | CO-03 10m, Oct 2015 |
| 2015294-06 | 10/21/2015 | 9/20 | B | CO-04 10m, Oct 2015 |
| 2015294-02 | 10/21/2015 | 7/20 | B | CO-03 1m, Oct 2015 |

| BLUE CLUSTER | Date Collected | Ratio Score | Pattern | Field ID |
|---|---|---|---|---|
| 2015251-17 | 9/4/2015 | 17/20 | AB | Sep 2015_32 |
| 2015251-12 | 9/4/2015 | 11/20 | B | Sep 2015_17 |
| 2015251-15 | 9/4/2015 | 11/20 | B | Sep 2015_20 |
| 2015251-01 | 9/4/2015 | 16/20 | AB | Sep 2015_1 |
| 2015251-11 | 9/4/2015 | 11/20 | B | Sep 2015_16 |
| 2015251-10 | 9/4/2015 | 13/20 | B | Sep 2015_15 |
| 2015251-08A | 9/4/2015 | 13/20 | B | Sep 2015_13A |
| 2015251-08B | 9/4/2015 | 13/20 | B | Sep 2015_13B |
| 2015251-07 | 9/4/2015 | 13/20 | B | Sep 2015_12 |

| GREEN CLUSTER (MC252) | Date Collected | Ratio Score | Pattern | Field ID |
|---|---|---|---|---|
| 2015294-01 | 10/21/2015 | 13/20 | C | CO-03 WatBot, Oct 2015 |
| 2015251-24 | 9/4/2015 | 16/20 | AB | Sep 2015_39 |
| 2015251-06 | 9/4/2015 | 15/20 | AB | Sep 2015_11 |

| PURPLE CLUSTER | Date Collected | Ratio Score | Pattern | Field ID |
|---|---|---|---|---|
| 2015251-23 | 9/4/2015 | 10/20 | B | Sep 2015_38 |
| 2015251-20 | 9/4/2015 | 11/20 | B | Sep 2015_35 |
| 2015251-13 | 9/4/2015 | 9/20 | B | Sep 2015_18 |
| 2015251-21 | 9/4/2015 | 11/20 | B | Sep 2015_36 |
| 2015251-22 | 9/4/2015 | 11/20 | B | Sep 2015_37 |
| 2015251-19 | 9/4/2015 | 9/20 | B | Sep 2015_34 |
| 2015251-14 | 9/4/2015 | 11/20 | B | Sep 2015_19 |
| 2015251-09 | 9/4/2015 | 11/20 | B | Sep 2015_14 |
| 2015251-18 | 9/4/2015 | 10/20 | B | Sep 2015_33 |

2015294-06 (Black Cluster)

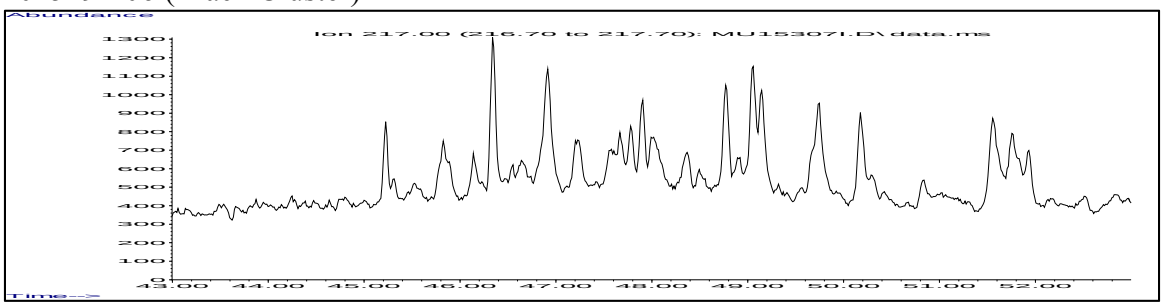


2015251-17 (Blue Cluster)

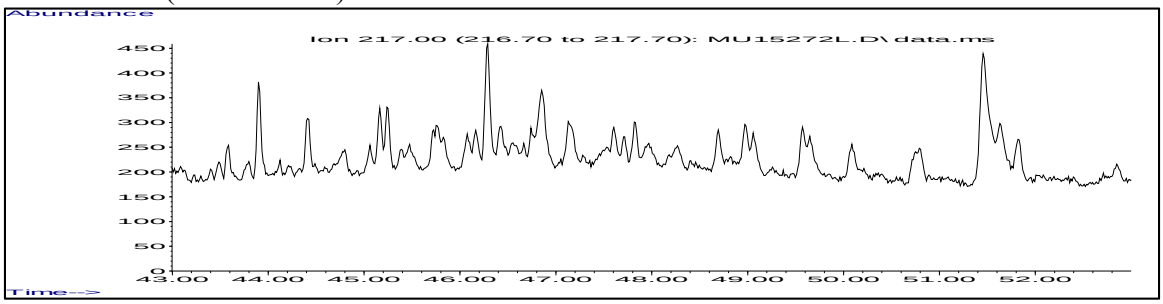


2015251-06 (Green Cluster including MC252)

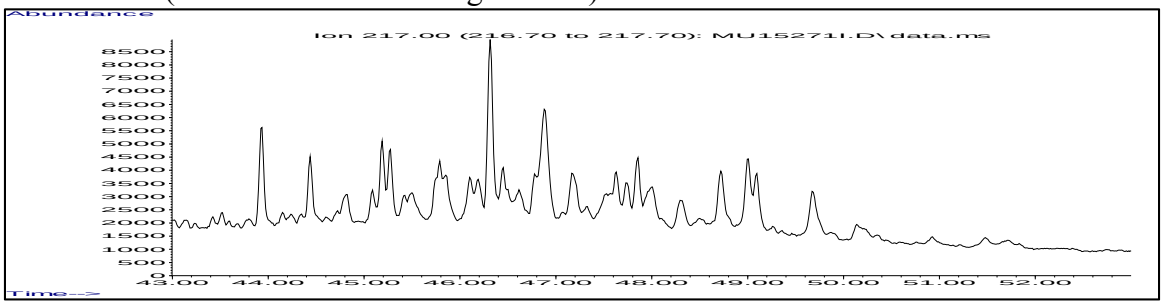


2015251-09 (Purple Cluster)

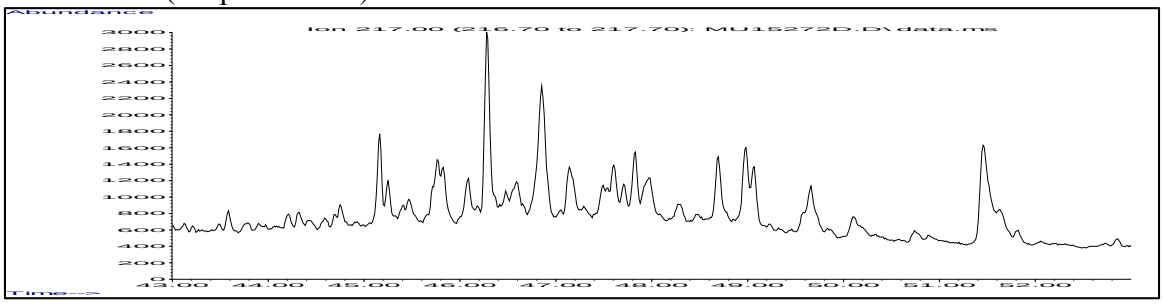

## VITA

Buffy Marie Ashton-Meyer is a native of Venice, Florida and is the only daughter of Ned and Janet Ashton. She received her Bachelor of Science in Environmental Sciences and graduated Cum Laude from Troy University, Troy, Alabama, in 1996. She carried on to complete her Master of Science in Environmental Sciences from Louisiana State University in 2000. Ms. Meyer is a Ph.D. candidate in Environmental Sciences at Louisiana State University, and has been a full-time Research Associate since May 2000 in the Louisiana State University, Department of Environmental Sciences, Response and Chemical Assessment Team laboratory that specializes in environmental and analytical chemistry. Ms. Meyer plans on continuing her oil source-fingerprinting research after receiving her Doctor of Philosophy degree.